NASA Contractor Report 165956 •

NASA-CR-165956 19830005227

Test and Analysis of Celion 3000 PMR-15, Graphite/ Polyimide Bonded Composite Joints

Data Report

J. B. Cushman, S. F. McCleskey and S. H. Ward

BOEING AEROSPACE COMPANY SEATTLE, WASHINGTON

CONTRACT NAS1-15644
JULY 1982



LIBRARY GOPY

OCT 28 1982

LANGLEY RESEARCH CENTER LIBRARY, NASA HAMPTON, VIRGINIA

National Aeronautics and Space Administration

Langley Research Center Hampton, Virginia 23665



# NASA Contractor Report 165956

Test and Analysis of Celion 3000 PMR-15, Graphite/ Polyimide Bonded Composite Joints

Data Report

J. B. Cushman, S. F. McCleskey and S. H. Ward

BOEING AEROSPACE COMPANY SEATTLE, WASHINGTON

**CONTRACT NAS1-15644 JULY 1982** 



Langley Research Center Hampton, Virginia 23665

1183-13498#

#### **FOREWORD**

This document was prepared by the Boeing Aerospace Company for the National Aeronautics and Space Administration, Langley Research Center in compliance with Contract NAS1-15644, "Design, Fabrication and Test of Graphite/Polymide Composite Joints and Attachments for Advanced Aerospace Vehicles."

This report is one of five that fully document contract results. It is the Data Report for the Task 2.0 "Bonded Joint Tests."

Dr. Paul A. Cooper was the contracting officer's technical representative for the full contract and Gregory Wichorek was the technical representative for design allowables testing of Celion 6000/PMR-15. Boeing performance was under the management of Mr. J. E. Harrison. Mr. D. E. Skoumal was the technical leader. Major participants in this program were Stephen H. Ward, Stephen F. McCleskey and James B. Cushman, Structural Development and Sylvester G. Hill, Materials and Processes.

Certain materials are identified in this publication in order to specify adequately which materials were investigated. In no case does such identification imply recommendation or endorsement of the material by NASA, nor does it imply that the materials are necessarily the only ones or the best ones available for the purpose.

## TABLE OF CONTENTS

	FORE	WORD		
	TABL	E OF CON	TENTS	
1.0	SUMM	1ARY		. 1
2.0	INTE	RODUCTION		3
3.0	LITE	RATURE S	URVEY AND PERFORMANCE TRENDS	, 6
4.0	TES1	F PLAN DE	VELOPMENT	9
	4.1	Standar	d Joint Test Matrices	9
	4.2	Joint To	est Procedures	10
5.0	MATE	RIALS	•	24
6.0	ADHE	SIVE CHA	RACTERIZATION	27
	6.1	Test Ma	trix	. 27
	6.2	Adhesiv	e Specimen Fabrication Procedures	27
	6.3	Adhesiv	e Test Procedures	29
	6.4	Ancilla	ry Laminate and Adhesive Test Results	<b>3</b> 3
7.0	STAN	IDARD BONI	DED JOINTS	44
	7.1	Standar	d Joint Specimen Fabrication	44
	7.2	Standard	d Joint Test Results	50
		7.2.1	Single Lap Joints	67
		7.2.2	Double Lap Joints	91
		7.2.3	Step-Lap Joints	120
		7.2.4	Trend Summaries	1.24
		7.2.5	Comparison of Single and Double Lap Joints	128
8.0	ADVA	NCED BON	DED JOINTS	134
	8.1	Advance	d Joint Test Matrices	134
	8.2	Specime	n Fabrication	135
	8.3	Test Pro	ocedures	137
	8.4	Advance	d Joint Test Results	150
		8.4.1	Preformed Adherends	169
		8.4.2	Scalloped Adherends	186
		8.4.3	Fabric Interfaces	195
		Ω Λ Λ	Quality Control Companison	202

# TABLE OF CONTENTS (Continued)

9.0	TEST/A	NALYS:	IS CORRELATION	211
	9.1 F	inite	Element Analaysis (Boeing IR&D)	211
	9	9.1.1	Study of Finite Element Modeling Techniques - Double Lap	211
	,	Jo	ints	
	9	9.1.2	Double Lap Joints	250
	9	9.1.3	Single Lap Joints	263
	9.2 S	Standar	d Joint Test/Analysis Correlation	268
	9	2.1	Single Lap Joints	270
	9	.2.2	Double Lap Joints	284
	9	.2.3	Step Lap Joints	293
10.0	CONCLU	SIONS	'RE COMMENDATATIONS	295
	APPEND	IX A	Adhesive Test Results Tables	297
	APPEND	IX B	Standard Bonded Joint Test Result Tables	302
	APPEND	IX C	Advanced Bonded Joint Test Result Tables	334
	REFERE	NCES		349

This report summarizes a test/analysis program of bonded composite joints conducted for NASA under Contract NAS1-15644. The objective of the program was to establish a limited data base describing the influence of variations in basic design parameters on the static strength and failure modes of graphite/polyimide (Gr/PI) bonded joints for use at elevated temperatures.

An initial literature search was conducted to seek experimental data and analyses concerned with standard bonded joints. While various research programs have dealt with epoxy bonded metal and epoxy bonded composite joints, few programs featuring polyimide materials and specifically bonded graphite/polyimide composites were found in the open literature.

A test plan was developed to investigate the effects of geometric and material parameters and elevated temperature on the static strength of "standard" joints. Single and double lap composite joints, and single, double, and step lap composite to metal joints were characterized. Tests were also conducted to measure shear strength, shear modulus and flatwise tension strength of the chosen adhesive system.

Finite element analyses were conducted to evaluate modeling techniques and to assess effects of lamina stacking sequence and adhesive filleting on single and double lap bonded composite joints.

Test specimens were fabricated from a Gr/PI system: Celion 3000 graphite fiber and PMR-15 polyimide resin. Joint bonding utilized a LARC-13 modified adhesive designated A7F. A total of 653 tests were conducted to evaluate effects of lap length, adherend thickness, adherend axial stiffness, lamina stacking sequence and adherend tapering. All specimens were subjected to a conditioning of 125 hours at 589K ( $600^{\circ}F$ ) prior to testing at 116K ( $-250^{\circ}F$ ), 294K ( $70^{\circ}F$ ) and 561K ( $550^{\circ}F$ ).

An additional test matrix of "advanced" joints was established based on the results of the "standard" tests. The advanced joints, consisting of preformed adherends, adherends with scalloped edges and joints with hybrid interface plies, were tested and compared to baseline single and double lap designs.

)

Test results indicated that single lap joints can be designed and fabricated that will carry from 123 to 385 kN/m (700 to 2200 lb/in) at 561 K ( $550^{0} \text{F}$ ) and double lap and symmetric step lap attachments would be effective in the 438 to 875 kN/m (2500-5000 lb/in) range at 561 K ( $550^{0} \text{F}$ ). The predominate failure mode was intralaminar shear and peel of the composite. The few adhesive failures that occurred were primarily on the high temperature tests of the composite-to-titanium joints.

The "advanced" joint tests indicated that a significant improvement in joint efficiency is available through geometric modifications and hybrid material additions at the adherend interfaces.

Correlation of test results for single lap composite-to-composite joints and to a limited degree for the titanium-step lap joints was achieved with closed form analytical models. Empirical correlations were developed for single and double lap joints.

#### 2.0 INTRODUCTION

Advanced designs for high-speed aircraft and space transportation systems require more efficient structures for operation in the 533K ( $500^{0}F$ ) to 589K ( $600^{0}F$ ) temperature range. Design data are needed for bonded and bolted composite joints to support advanced design concepts. An experimental program to develop several types of graphite/polyimide (Gr/PI) bonded and bolted joints was funded under NASA contract NAS1-15644.

The program was designed to extend the current epoxy-matrix composite technology in joint and attachment design to include high temperature polymide matrix composites. It provides an initial data base for designing and fabricating Gr/PI lightly loaded control surface structures for advanced space transportation systems and high speed aircraft. The objectives of this program were two-fold: first, to identify and evaluate design concepts for specific joining applications of built-up attachments which could be used at rib-skin and spar-skin interfaces; second, to explore concepts for joining simple composite-composite and composite-metallic structural elements, identify the fundamental parameters controlling the static strength characteristics of such joints, and compile data for design, manufacture, and test of efficient structural joints using the Gr/PI material system. The major technical activities followed two paths concurrently. TASK 1 consisted of design allowable testing and design and test of specific built-up attachments. TASK 2 evaluated standard and advanced Gr/PI and Gr/PI to titanium bonded joints. An overall program flow for the two tasks is shown in Figure 2-1.

This document presents the analysis and test results of TASK 2, shown enclosed in a dashed box in Figure 2-1. The primary objectives were to provide data useful for evaluation of standard bonded joint concepts and design procedures, to provide the designer with increased confidence in the use of bonded high-performance composite structures, and to evaluate possible modifications to the standard joint concepts for improved efficiency.

This is one of five reports that fully document the results of activities performed under NASA contract NAS1-15644. The other four reports are:

- "Design Allowables Test Program, Celion 3000/PMR-15 and Celion 6000/PMR-15 Graphite/Polyimide Composites," NASA CR-165840
- 2. "Design, Fabrication and Test of Graphite/ Polyimide Composite Joints and Attachments" - Summary, NASA CR-3601
- 3. "Design, Fabrication and Test of Graphite/ Polyimide Composite Joints and Attachments" - Data Report, NASA CR-165955
- 4. "Analysis and Test of Graphite/Polyimide Bonded Joints" -Summary, NASA CR-3602

#### Measurement Units

All measurement values in this report are expressed in the International System of Units and in U.S. Customary Units. Actual measurements and calculations were made in U.S. Customary Units.

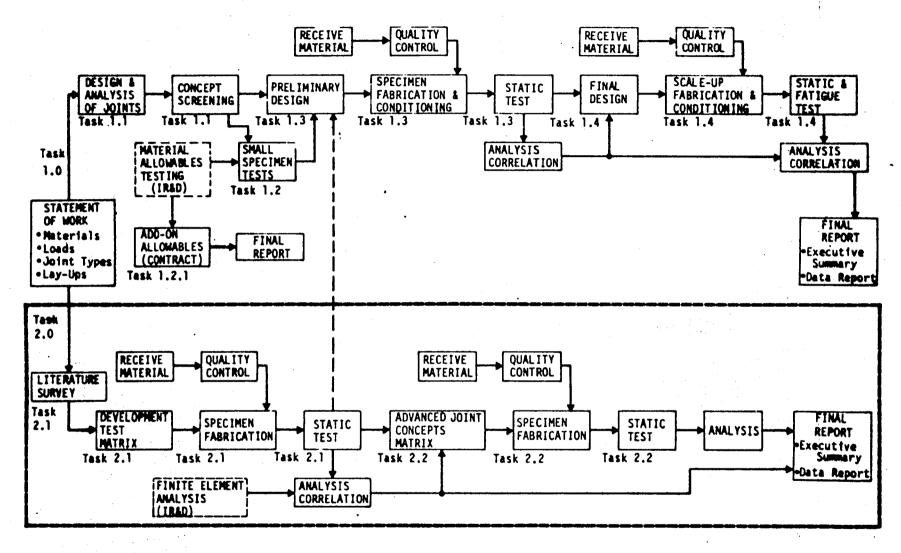


Figure 2-1: TASK 1 and TASK 2 PROGRAM FLOW

#### 3.0 LITERATURE SURVEY AND PERFORMANCE TRENDS

The initial phase of the design activities was to conduct a literature survey to obtain information on graphite/polyimide composites pertinent to this program. The search was not limited to graphite/polyimide composites since the available literature on this specific subject is limited and design guide methods and parameters for other composites would also be applicable to this program. The following sources were searched using a wide range of key words:

	SOURCE	TIME FRAME
0	NASA	1978-1979
0	NTIS	1964-1979
0	CHEM ABSTRACTS	1972-1978
0	ISMEC-MECH. ENGR.	1973-1977
0	ENGINEERING INDEX	1970-1978
0	SCISEARCH	1974-1978
0	BOEING COMPANY	1974-1979
	DOCUMENTS	
0	BOEING TECHNICAL	1974-1979
	LIBRARY	

A Defense Documentation Center (DDC) literature search was also conducted to obtain other references. This search used a narrow range of key words to avoid encountering a large quantity of miscellaneous references.

Approximately 1500 articles and reports were identified as potentially relevant and based on the abstracts about 200 were selected for further study. Brief summaries of each report reviewed are reported in NASA Contract Reports Numbers CR159108 through CR159115. Review of current literature was an "ongoing" process during the performance period of this program.

The following is a summary of the expected performance trends of bonded joints with respect to various parameters, resulting from the literature search and finite element analyses. Unless otherwise noted, these statements apply to both single and double lap joints:

- o Increasing the lap length increases joint strength towards an asymptote.
- o Increasing the axial and flexural stiffness of the adherends increases joint strength (because of peel stresses).
- o Increasing the adherend thicknesses increases joint strength towards an asymptote.
- O Stiffness balanced joints are stronger than unbalanced joints (because of reduced peel stresses).
- o Tapering the ends of the adherends increases joint strength (because of reduced peel stresses).
- o Placing a "softer" ply group at the joint interface ( $\pm 45^{\circ}$  vs.  $0^{\circ}$ ) results in a more uniform shear strain along the joint interface, thus increasing double lap joint strength.
- Single lap joints which have adherends with equal thermal expansion coefficients are stronger at 116K (-250°F) and 294K (70°F) than joints which have adherends that have thermal expansion imbalances. This is caused by increased moment and peel stresses in the adherend/adhesive resulting from the residual thermal stresses present in the joint. The effect of a thermal expansion imbalance is small at 561K (550°F) since this is close to the cure temperature (thermal stress free state).
- Composite (GR/PI) to metal (titanium) double lap joints have a thermal imbalance. This suggests that these joints would not be as strong as an "all-composite" joint. However, because the inner adherends are titanium and this is where the greatest peel stresses occur, these joints are stronger, since interlamina failures would occur in a composite inner adherend.

Increasing the temperature will reduce residual stresses, soften the resin, and slightly reduce the strength of the composite adherend. The net result is an increase in joint strength with increasing temperature because of a reduction in severity of stress concentrations. This assumes that the reduction in basic composite and adhesive material properties is small at the elevated temperature.

## 4.0 TEST PLAN DEVELOPMENT

#### 4.1 Standard Joint Test Matrices

The objective of the standard joint test program was to evaluate different types of bonded joints and the various parameters that affect joint performance. Standard bonded joints frequently used in industry are shown in Fig. 4-1. Single lap, double lap and symmetric step-lap joints as shown in Figure 4-2 were selected as the joint types to be evaluated. Analyses of these joint types are common in the literature and they represent types commonly used in aerospace structures. Test matrices were established to evaluate joint strength parameters of temperature, lap length, adherend thickness, adherend axial stiffness, laminate stacking sequence and adherend tapering. The baseline laminate was a quasi-isotrophic layup to be consistent with Task 1.0 joints. In addition, nominal joint strengths were selected to be in the range required for Task 1.0 joint designs. Typical design loads ranged from 227 kN/m (1300 lbs/in) to 2100 kN/m (12,000 lbs/in).

Test matrices and specimen configurations are given in Figures 4-3 through 4-10. All specimens were conditioned at  $589^{\circ}$ K ( $600^{\circ}$ F) in a one atmosphere environment (air) for 125 hrs. prior to test. A total of 186 single lap joints, 258 double lap joints, and 18 symmetric step-lap joints were tested. Test temperatures were 116K ( $-250^{\circ}$ F), 294K ( $70^{\circ}$ F) and 561K ( $550^{\circ}$ F).

Based on results from the standard bonded joint testing, several advanced joint concepts were defined. These concepts and the corresponding test matrix are described in Section 8.0.

To maintain consistency through the joint test program, the specimen numbering system given below was used.

3A	- 1	la -	. 2	-	1A
Test	Te	est	Cond.		Item
Matrix	No	o • '	Code		No .

The letter following the item number was a temperature code as defined below

- A Ambient Room Temperature
- $C 117K (-250^{\circ}F)$
- H  $561K (550^{\circ}F)$

A "data set" refers to all the test data for a specific test matrix and test number (i.e., data set 3A-1a) and includes data for all the temperatures tested.

#### 4.2 Joint Test Procedures

All bonded joint tests were performed in the Boeing materials test laboratories. Specimens were loaded to failure in a Baldwin universal test machine as shown in Figure 4-11. Load was applied at a load rate of 8.9 KN/min (2000 lbs/min).

Room temperature tests were conducted in the normal laboratory environment (nominally 294K  $(70^{\circ}F)$ ). No special environmental conditioning was used.

For the elevated temperature tests (561K ( $550^{\circ}$ )) the specimens were placed in an enclosure as shown in Figure 4-12 that was electrically heated using resistance heating elements. Temperatures were controlled to  $\pm 6K$  ( $\pm 10^{\circ}$ F) by placing thermocouples on the specimens which were connected to a Thermac Model 624A temperature controller.

For the  $116^{0}$ K (-250°F) tests, specimens were placed in an enclosure similar to that shown in Figure 4-12 but that was cooled by evaporating liquid nitrogen. Temperatures were controlled to  $\pm 6$ K ( $\pm 10^{0}$ F) by placing thermocouples on the specimens which were connected to an electro-pneumatic controller that pumped in the liquid/gaseous nitrogen.

All specimens were brought to temperature and then soaked for 10 minutes prior to test.

Specimen dimensions were measured and recorded prior to test. Specimen number, test temperature and ultimate failure load were recorded.

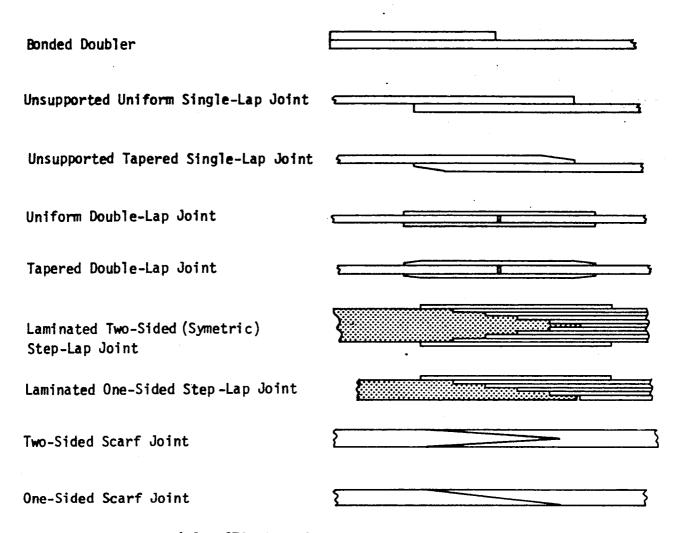


Figure 4-1: STANDARD BONDED JOINT CONFIGURATIONS

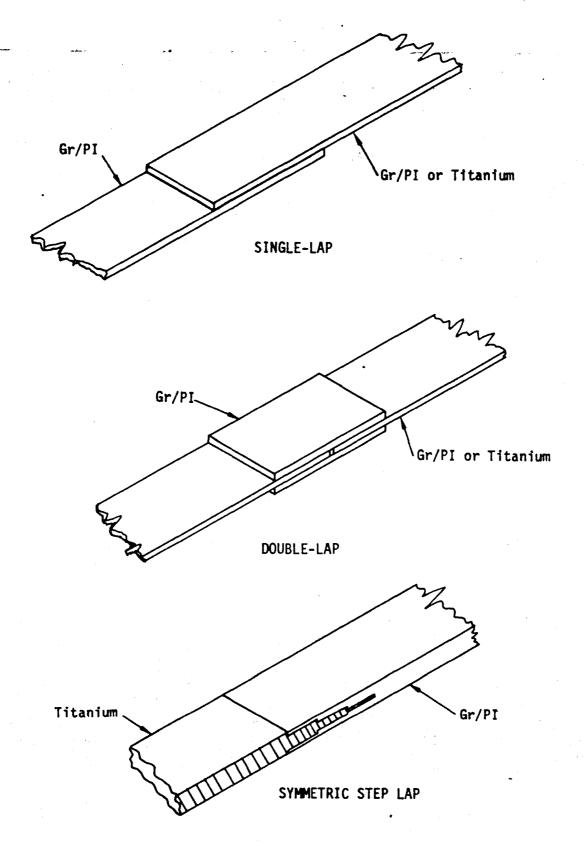
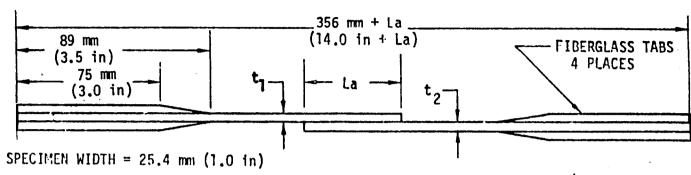


Figure 4-2: STANDARD BONDED JOINTS TESTED



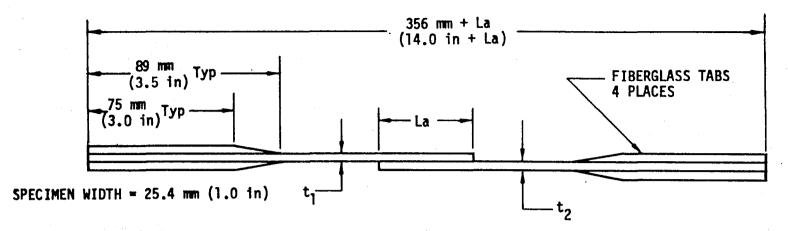
TEST HO	La nm (in)	t <sub>l</sub>	t <sub>2</sub> mmi(1n)	LAMINATE t <sub>1</sub> & t <sub>2</sub>	NUMBER 116K (-250°F)	OF TES	TS AT 561K (550°F)	TOTAL NUMBER OF SPECIMENS
la	25.4 (1.0)	1.52 (.06)	1.52 (.06)	(0,±45,90) <sub>3s</sub>	6	6	6	18
16	50.8 (2.0)	1.52 (.06)	1.52 (.06)	(0, <u>+</u> 45,90) <sub>3s</sub>	6	6	6	18
1c	76.2 (3.0)	1.52 (.06)	1.52 (.06)	(0, <u>+</u> 45,90) <sub>3s</sub>	6	6	6	18
2a	50.8 (2.0)	1.52 (.06)	1.52 (.06)	(0, <u>+</u> 45,0 <sub>3</sub> ) <sub>2s</sub>	6	6	6	18
3a	50.8 (2.0)	1.52 (.06)	1.52 (.06)	( <u>+</u> 45,0,90) <sub>3s</sub>		6		. 6
4a	50.8 (2.0)	1.52 (.06)	1.52 (.06)	$(0_3, \pm 45_3, 90_3)_s$		6		6
5a	50.8 (2.0)	1.02 (.04)	2.03 (.08)	(0,±45,90) <sub>2s</sub> /(0,±45,90) <sub>4s</sub> (t <sub>1</sub> /t <sub>2</sub> )	6	6	6	18
6a	50.8 (2.0)	2.54 (.10)	2.54 (.10)	(0,±45,90) <sub>5s</sub>		6		6
7a	12.7(0.5)	1.52(.06)	1.52(.06)	(0,+45,90) <sub>3s</sub>	6	6	6	18

**TOTAL 126** 

A7F (LARC-13, Amide-Imide modified) adhesive.

Condition specimens by soaking for 450 ks (125 hours) at 589K (600°F) in a one (1) atmosphere environment (air).

Figure 4-3: TEST MATRIX 3A, STANDARD JOINT, SINGLE LAP, GR/PI-GR/PI

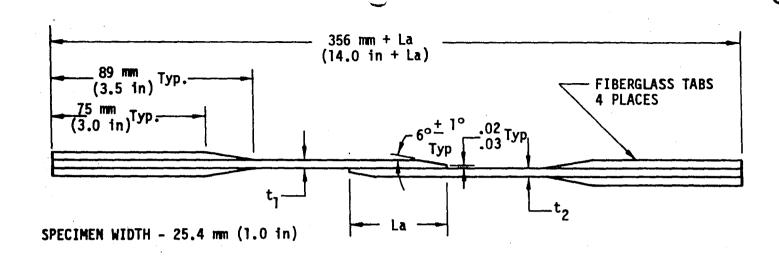


	EST NO	La . mm (in)	t <sub>l</sub> mm (in)	t <sub>2</sub> mm (in)	LAMINATE t <sub>1</sub>	t <sub>2</sub>	NUMBER 116K (-250°F)	-	TS AT 561K (550°F)	TOTAL NUMBER OF SPECIMENS
Г	la	25.4 (1.0)	1.52 (.06)	.76 (.03)	(0,±45,90) <sub>3s</sub>		6	6	· 6	18
1	16	50.8 (2.0)	1.52 (.06)	.76 (.03)	(0,±45,90) <sub>3s</sub>		6	6	6	18
	1c	76.2 (3.0)	1.52 (.06)	.76 (.03)	(0,±45,90) <sub>3s</sub>	<b>&gt;</b>	6	6	6	18

TOTAL 54

- Celion 3000 (NR150B2 Finish)/PMR-15 prepreg.
- A7F (LARC-13, Amide-Imide modified) adhesive.
- Condition specimens by soaking for 450 ks (125 hours) at 589K (600°F) in a one (1) atmosphere environment (air).
- Titanium 6Al-4V, Standard MIL-T-9046 Type III Annealed (or equivalent).

Figure 4-4: TEST MATRIX 3B, STANDARD JOINT, SINGLE LAP, GR/PI-T1

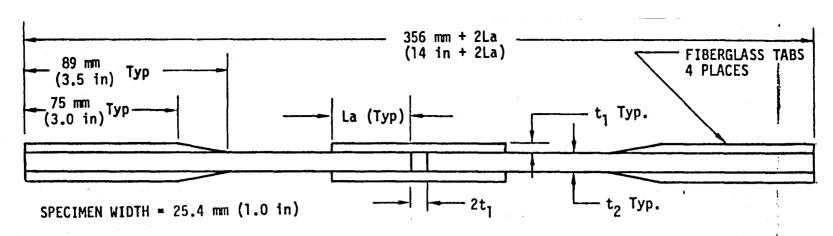


.ST 10	La www.(in)	t <sub>]</sub> mm (in)	t <sub>2</sub> mm (in)	LAMINATE t1 & t2	NUMBER 116 K (-250°F)		TOTAL NUMBER OF SPECIMENS
1a	50.8 (2.0)	2.54 (.10)	2.54 (.10)	(0, <u>+</u> 45,90) <sub>5s</sub>		6	6

A7F (LARC-13, Amide-Imide modified) adhesive.

Condition specimens by soaking for 450ks (125 hours) at 589K (600°F) in a one (1) atmosphere environment (air).

Figure 4-5: TEST MATRIX 3C, STANDARD JOINT, SINGLE LAP TAPERED ADHERENDS, GR/PI-GR/PI



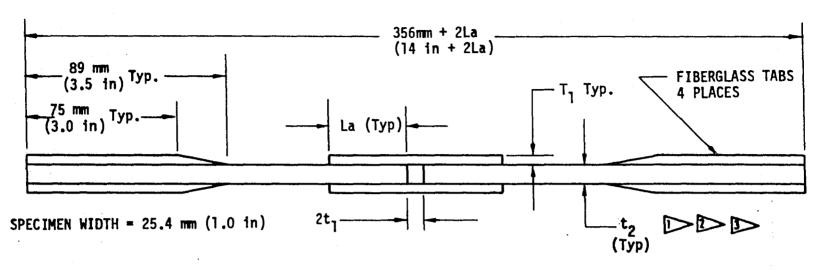
TEST	La	t <sub>1</sub>	t <sub>2</sub>	LAMIN	ATE .	NUMBER 116K		TS AT 561K	TOTAL NUMBER OF SPECIMENS
NO	mm (in)	mm (in)	mm (in)	լ՝ Հյ	t <sub>2</sub>	(-250°F)	RT	(550°F)	OF SPECIFICIAS
la	20.3 (.8)	1.02 (.04)		$(0,\pm 45,90)_{2s}$		6	6	6	18
1ь	33.0 (1.3)	1.02 (.04)	2.03 (.08)	(0,±45,90) <sub>2s</sub>	(0,+45,90) <sub>4s</sub>	6	6	6	· 18
-1c	45.7 (1.8)	1.02 (.04)	2.03 (.08)	(0,±45,90) <sub>2s</sub>	(0,+45,90) <sub>4s</sub>	6	6	6	18
2a	20.3 (.8)	1.52 (.06)	3.05 (.12)	(0, <u>+</u> 45,90) <sub>3s</sub>	(0, <u>+</u> 45,90) <sub>6s</sub>	6	6	6	18
2b	33.0 (1.3)	1.52 (.06)	3.05 (.12)	$(0,\pm 45,90)_{3s}$	$(0,\pm 45,90)_{65}$	6	6	6	18
2c	45.7 (1.8)	1.52 (.06)		(0, <u>+</u> 45,90) <sub>3s</sub>			6	6	18
3a	33.0 (1.3)	1.52 (.06)		(0,+45,0 <sub>2</sub> ,-45,0) <sub>2s</sub>			6	6	18
4a	33.0 (1.3)	1.52 (.06)	3.05 (.12)	(0 <sub>3</sub> , <u>+</u> 45 <sub>3</sub> ,90 <sub>3</sub> ) <sub>s</sub>	(0 <sub>3</sub> ,±45 <sub>3</sub> ,90 <sub>3</sub> ) <sub>2s</sub>	6	6	6	18
5a	33.0 (1.3)	1.52 (.06)	3.05 (.12)	$(\pm 45,0,90)_{3s}$	( <u>+</u> 45,0,90) <sub>6s</sub>	6	6	6	յ 18
6a	33.0 (1.3)	1.52 (.06)	2.03 (.08)	(0, <u>+</u> 45,90)3 <sub>5</sub>	(0, <u>+</u> 45,90) <sub>4s</sub>	6	6	6	18
7a	33.0 (1.3)	3.05 (.12)	6.10 (.24)	(0, <u>+</u> 45,90) <sub>6s</sub>	(0, <u>+</u> 45,90) <sub>12s</sub>		6	6	12

TOTAL 192

A7F (LARC-13, Amide-Imide modified) adhesive.

Condition specimens by soaking for 450 ks (125 hours) at 589K (600°F) in a one (1) atmosphere environment (air).

Figure 4-6: TEST MATRIX 3D, STANDARD JOINT, DOUBLE LAP, GR/PI-GR/PI

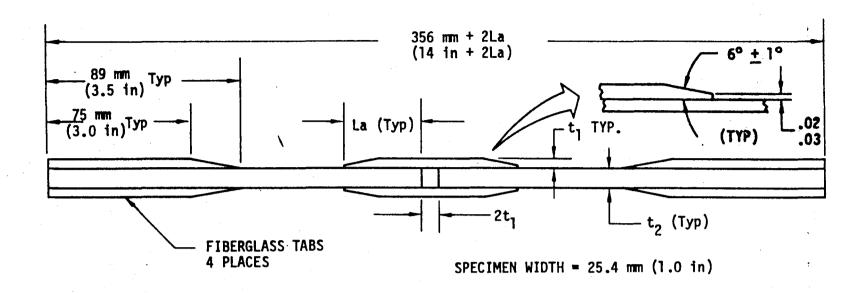


TEST NO	La mm (in)	t <sub>l</sub> mm (in)	t <sub>2</sub> rm (in)	LAMINATE t <sub>1</sub>	t <sub>2</sub>	NUMBER 116K (-250°F)	OF TES	TS AT 561 K (550°F)	TOTAL NUMBER OF SPECIMENS
la	20.3 (.8)	1.52 (.06)	1.52 (.06)	$(0, \pm 45, 90)_{35}$		6	6.	6	18
16	45.7 (1.8)	1.52 (.06)	1.52 (.06)	$(0, \pm 45, 90)_{3s}$		6	6	6	18
2a				( <u>+</u> 45,0,90) <sub>3s</sub>		6	6	6	18

TOTAL 54

- Celion 3000 (NR15082 Finish)/PMR-15 prepreg.
- A7F (LARC-13, Amide-Imide modified) adhesive.
- Condition specimens by soaking for 450 ks (125 hours) at 589K (600°F) in a one (1) atmosphere environment (air).
- Titanium 6A1-4V, Standard MIL-T-9046 Type III Annealed (or equivalent.

Figure 4-7: TEST MATRIX 3E, STANDARD JOINT, DOUBLE LAP, GR/PI-Ti



TEST NO	La mm (in)	t <sub>1</sub> t <sub>2</sub> mm (in) mm (in		LAMII t <sub>]</sub>	NUMBER OF TESTS AT 116K 561K (-250°F) RT (550°F)			TOTAL NUMBER OF SPECIMENS	
la	33.0 (1.3)	3.05 (.12)	6.10 (.24)	(0, <u>+</u> 45,90) <sub>6s</sub>	(0 <u>,+</u> 45,90) <sub>12s</sub>		6	. 6	12

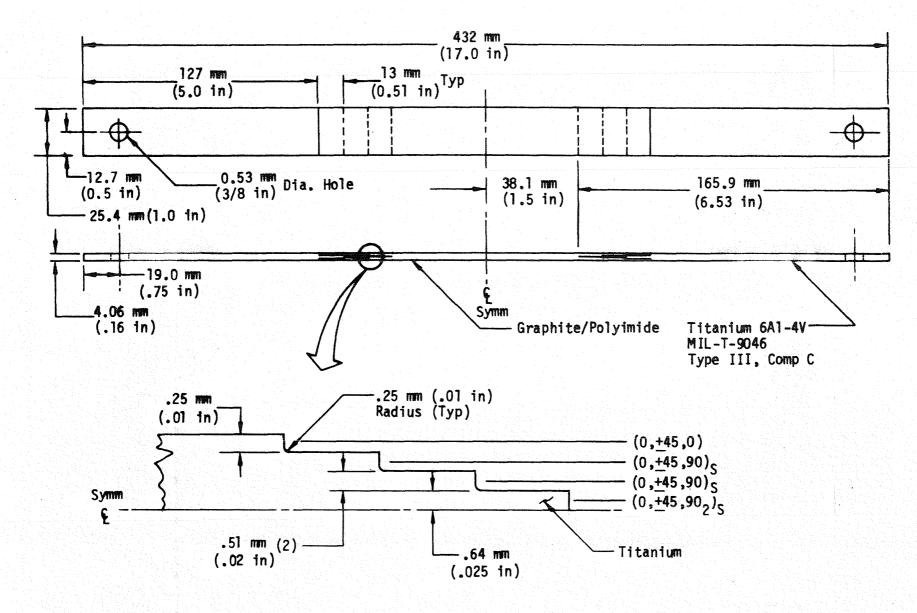
A7F (LARC-13, Amide-Imide modified) adhesive.

Condition specimens by soaking for 125 hours at 589K (600°F) in a one (1) atmospheric environment (air).

Figure 4-8: TEST MATRIX 3F, STANDARD JOINT, DOUBLE LAP, TAPERED ADHERENDS, GR/PI-GR/PI [ ]

					NUMBE	R OF TEST	S AT	TOTAL	
TEST NO.			NO. OF STEPS	SPECIMEN CONFIGURATION	116K (-250°F)	ROOM TEMP	561 K (550°F)	NO. OF SPECIMENS	
la	GR/PI 50% <u>+</u> 45°	TITANIUM 6AL-4V	3	See Figure 4-9	6	. 6	6	18	

Figure 4-9: TEST MATRIX 3G, STANDARD JOINT, SYM. STEP LAP, GR/PI - TITANIUM



NOTE: Joint Co-Cured With An Adhesive Primer Only

Figure 4-10: TEST MATRIX 3G, SPECIMEN CONFIGURATION

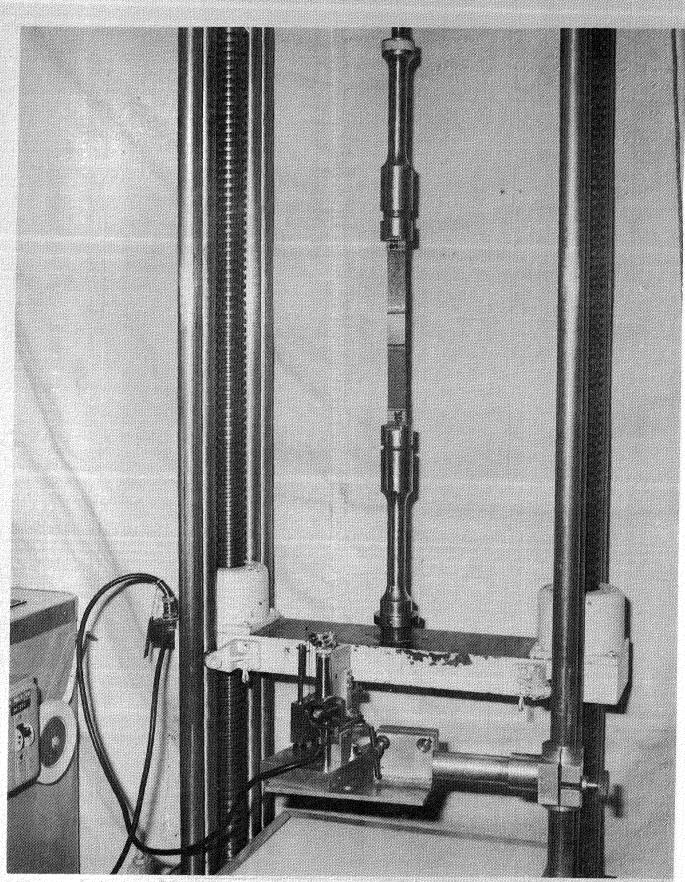
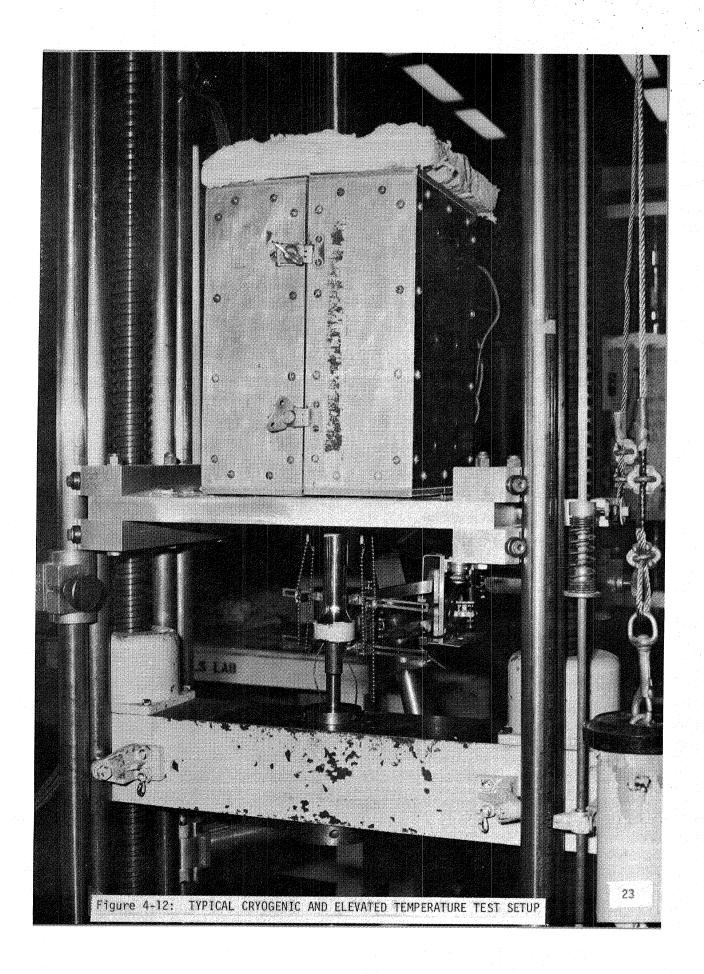


Figure 4-11: TYPICAL ROOM TEMPERATURE TEST SETUP



#### 5.0 MATERIALS

Graphite fibers, polyimide resin and the adhesive system used for this program were contractually specified by NASA/Langley. Following are descriptions of the principal materials used. Typical mechanical properties are listed in Table 5-1.

## Composites

The bonded composite joints characterized under this program were made from laminates of graphite fibers preimpregnated with polyimide resin. The graphite fibers were Celanese Corp. Celion 3000 with NR-150B2G polyimide sizing. The polyimide resin was PMR-15, processed according to the procedures developed under Contract NAS1-15009. PMR-15 is an addition-type, thermosetting polyimide system originated by NASA/Lewis and further studied by Boeing under NASA/LaRC sponsored "CASTS"\* studies. Material was procured from U.S. Polymeric Inc., Santa Ana, CA to the material specification in Reference 1. Quality control test results for the Celion 3000 prepreg lots used are given in Sections 7.1 and 8.1 for the standard and advanced joints respectively. Chemical characterization tests of the resin system were also conducted, using high pressure liquid chromatography, gas chromatography, mass spectroscopy, infrared spectroscopy, and thermal gravametric analysis.

The advanced joint fabric interfaces were made from graphite/polyimide and S-glass/polyimide fabrics. The Celion 3000 181 style graphite fabric was preimpregnated in the Boeing Materials Technology laboratory using U.S. Polyimeric's PMR-15 resin. The S-glass 181 style fabric prepreg was procured from U.S. Polymeric.

\*Composites for Advanced Space Transportation Systems (Contracts NAS1-15009 and NAS1-15644)

Fiberglass/polyimide prepreg used in making specimen load tabs was 7781 style E-glass with F174-1 polyimide resin. Material was procured from Hexcel Corp. in Livermore, CA 94550.

## Adhesive

The high temperature adhesive system tested under this program was designated A7F. This adhesive system is a 50:50 resin solids copolymer blend of NASA LaRC supplied LARC-13 adhesive (supplied by NASA Langley) (Ref. 2) and AMOCO's AI-1130 L Amide-Imide. Sixty percent by weight aluminum powder was added to improve high temperature performance. Five percent by weight Cab-o-sil was added as a thickening agent. The material was blended to a uniform consistency and spread on 6 mil 112 style E-glass cloth with A-1100 finish to make an adhesive film for bonding operations.

## <u>Titanium</u>

Titanium used was 6A1-4V (Standard) purchased to MIL-T-9046, Type III Comp. C.

Table 5-1: TYPICAL ROOM TEMPERATURE MATERIAL PROPERTIES

MATERIAL		tu (kai)	CD-/1	FT OF STATE	Su (ksi)	MO :	G <sub>xy</sub> ı (ksi)	cm/	TE CM-K
CELION 3000/PMR-15* (51.4% FV) 00 90 <sup>0</sup> (0/ <u>+</u> 45/90) <sub>45</sub>		(187) (6,6)	130 8.3	(18.8) (1,2) (7.3)		-			
ADHESIVE* A7F TITANIUM 6A1-4V	924			(16)	 		(11.6)	17.5	(9.7)

<sup>\*</sup> Aged 125 Hrs at 589K (600°F)

#### 6.0 ADHESIVE CHARACTERIZATION

To support design and analysis of bonded joints it was necessary to characterize the adhesive system being used. Adhesive used in this program, designated A7F (LARC-13 Amide-Imide modified), is described in section 5.0. This section describes the test matrix, specimen fabrication procedures, test procedures, and presents test results of testing conducted to characterize A7F high temperature adhesive.

#### 6.1 Test Matrix

The A7F adhesive test matrix, Matrix 2, is shown in Table 6.1. Specimen configurations are shown in Figures 6.1 through 6-3.

Test 4 of Matrix 2 was subcontracted to the University of Delaware (U of D), Dr. J. R. Vinson; however, the test specimens were fabricated by Boeing.

6.2 Adhesive Specimen Fabrication Procedures

### Titanium Single Lap Shear Bonding

Titanium 12.7 mm (0.5 inch) single lap shear specimens were fabricated using 6A1-4V titanium finger panels and A7F adhesive. The finger panels were stamped out of 1.07 mm (.042 in) sheet titanium using a standard ST8813 blanking die, milled on the bonding edge and deburred.

Panels were surface treated for bonding with a chromic acid anodize process. This process consisted of solvent wiping and alkaline cleaning, hot water rinsing followed by anodization in a chromic acid solution, cold water rinsing and drying in a forced air oven at  $339 \text{ K} (150^{\circ}\text{F})$ .

The anodized parts were then primed with a dilute solution of A7F adhesive (containing 30% aluminum powder) and baked at  $464 \text{ K}(375^{\circ}\text{F})$  for 30 minutes to remove solvents.

Primed titanium panels were assembled with a 19.0 mm x 152 mm (.75 in x 6 in) strip of A7F adhesive film between the faying surfaces of the titanium adherends. The panels were placed on standard bonding tools designed to maintain the 12.7 mm (.5 in) overlap, vacuum bagged and cured in an autoclave at 602 K  $(625^{\circ}F)$  using the conventional high temperature bagging materials outlined in Reference 2. The cured lap shear panels were post-cured in an oven at 589 K  $(600^{\circ}F)$  for six hours.

The titanium panels were then cut into individual lap shear specimens using a band saw equipped with a carbide tipped blade. After the bonded panels were cut into individual specimens, specimens were conditioned per the test matrix prior to testing.

## "Thick Adherend" Shear Specimens

)

)

"Thick Adherend" lap shear specimens were fabricated from 6.4 mm (.25 in) thick 6Al-4V titanium plate bond with A7F adhesive. Two 305 mm x 762 mm (12 in x 30 in) plates were surface treated using the chromic acid process and bonded together with A7F adhesive film using the same processing procedures as for the lap shear specimens. The bonded plate was C-scanned for voids. No apparent voids were detected. The bonded panel was sawed into strips approximately 26.7 mm (1.05 in) wise and 305 mm (12 in) long. The strips were milled on both sawed surfaces to produce smooth and parallel edges on the specimens. The titanium bars then had slots milled in them to make the machined lap shear specimens with 25.4 mm (1.0 in) overlap as shown in Figure 6-2.

## Flatwise Tension Specimens

Flatwise tension specimens were fabricated using 31.8 mm (1.25 in) diameter 6A1-4V titanium load blocks bonded together with A7F adhesive film. The load blocks were bonded using the same surface treatment, priming, bonding, curing and post curing procedures used for the titanium single lap shear tests. To align the blocks during the bonding cycle, aluminum right angle extrusions were cut approximately 7.6 mm (0.3 in) shorter than the assembled tension

specimen (two blocks + adhesive). The assembled tension specimens were positioned in the V area of the extrusion so that at least 2.5 mm (0.1 in) was extended beyond the angle blocks to insure adequate pressure on the blocks when curing. The angle assemblies were envelope bagged, and the adhesive cured in an autoclave using the A7F cure cycle as outlined in Reference 1. These specimens were conditioned per the test matrix prior to testing.

Two prior attempts to bond the flatwise tension specimens were made using standard laboratory stainless steel load blocks. The aged specimens failed in conditioning, leaving most of the adhesive in a white powdery state. The cause of this problem was not determined. A change to titanium adherends was made and produced good bonds which subsequently failed cohesively.

#### 6.3 Adhesive Test Procedures

Adhesive tests conducted at Boeing, tests 3 and 5, were performed in the Boeing materials test laboratories. Specimens were loaded to failure in a Baldwin universal test machine. Load was applied at a crosshead travel rate of  $2.1 \times 10^{-2}$  mm/sec (.05 in/min).

Room temperature tests were conducted in the normal laboratory environment (nominally 294K  $(70^{\circ}F)$ ). No special environmental conditioning was used.

For the elevated temperature tests (561K ( $550^{O}F$ )) the specimens were placed in an enclosure as shown in Figure 4-12 that was electrically heated using resistance heating elements. Temperatures were controlled to  $\pm 6K$  ( $\pm 10^{O}F$ ) by placing thermocouples on the specimens which were connected to a Thermac Model 624A temperature controller.

For the 116K ( $-250^{\circ}F$ ) tests, specimens were placed in an enclosure similar to that shown in Figure 4-12 but that was cooled by evaporating liquid nitrogen. Temperatures were controlled to  $\pm 6K$  ( $\pm 10^{\circ}F$ ) by placing thermocouples on the specimens which were connected to an electro-pneumatic controller that pumped in the liquid/gaseous nitrogen.

All specimens were brought to temperature and then soaked for 10 minutes prior to test. Specimen dimensions were measured and recorded prior to test. Specimen number, test temperature and ultimate failure load were recorded.

)

)

)

Specimens tested at the University of Delaware, test 4, were tested under tensile load using an Instron Model TTC test machine. Tensile load was applied at a constant rate of .005 cm/min. (.002 inches/min.) in all cases. Applied load and elongation were plotted on an x-y plotter. The tests were performed at three different temperatures; 116K (- $250^{\circ}F$ ), ambient, and 561K ( $550^{\circ}F$ ). The temperatures were measured by direct contact of a thermocouple on the bond test section and monitored throughout the test.

High temperature tests were performed in an "Applied Test Systems" oven capable of 589K ( $600^{O}F$ ). The warm-up time was approximately 1-1/2 hrs. for each test.

For the 116K (-250°F) tests, a simple cooling box was built of plywood and lined with polyurethane foam. Liquid nitrogen was used as a cooling agent, and the air in the box was circulated with a small fan. To prevent condensation and thus ice from forming on the specimen and the extensometer, several coils of copper tubing were placed across the bottom of the chamber. By allowing the liquid nitrogen to flow slowly through the coils first, the moisture in the chamber would condense on the coils and freeze, thus keeping the specimen and extensometer dry. The average cool-down time was approximately 1/2 hr. The temperature was then controlled using a needle type flow control valve to regulate the liquid nitrogen flow. A ribbon type heating element was hung into the test chamber to greatly reduce the time required to bring the box and specimen back to room temperature after the test.

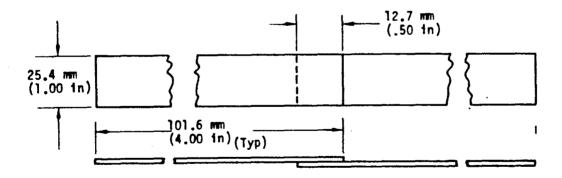
Table 6-1: TEST MATRIX 2 - A7F (LARC-13 Amide-Imide Modified) ADHESIVE

TEST		NUMBER OF TESTS AT				TOTAL		
NO.	TYPE	CONDITIONING	116K (-250"F)	RT	561 K (550°F)	MIMBER	TEST PROCEDURES	SPECIMEN CONFIGURATION
3	SHEAR	1 2 3	3 3 3	3 3 3	3 3 3	9 9 9	ASTM D1002	FIGURE 6-1
4	SHEAR	1 2	3 3	3 3	3	9 9	U of D* Thick Adherend	F IGURE 6-2
5	TENSION	1 2	3 3	3 3	3	9 9	ASTM D2095	F IGURE 6-3

CONDITION CODE

\*U of D ~ University of Delaware

- 1 As cured/postcured
- 2 Soaked for 125 hours at 589K (600°F) in a one (1) atmosphere environment (air)
- 3 Thermally cycled 125 times in a temperature range from 116K to 589K (-250°F to 600°F) and in a one (1) atmosphere environment (air)



MATERIAL: TITANIUM 6AT-4V ANNEALED 1.07 mm (.042 in) NOM. BOND WITH LARC-13 (A7F) .254 mm (.01 in) THICK

(ASTM D1002 STANDARD)

Figure 6-1: TITANIUM SINGLE LAP SHEAR SPECIMEN

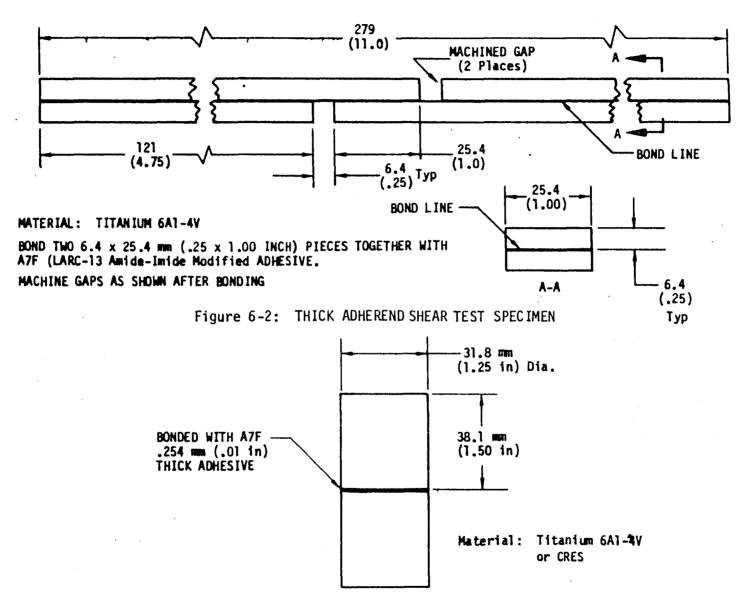


Figure 6-3: FLATWISE TENSION ADHESIVE TEST SPECIMEN

### 6.4 Adhesive Test Results

Adhesive test results are summarized and discussed in this section. Complete test results, by specimen, are located in Appendix A.

Attempts to compression mold a "neat" adhesive (A7F) tension test specimen for Matrix 2, Test 1 were unsuccessful. The molds experienced some leakage during resin B-staging; however, the major problem was fracture of the brittle adhesive during cool-down and subsequent removal from the mold. The molded sheet would have to have undergone additional machining and handling after removal from the mold. Because of the brittle nature of the adhesive, there was a high probability there would be significant breakage during these operations. It was decided not to expend additional resources because of the low probability of success. Program schedules and cost prevented trying an alternate test procedure. Flatwise tension ultimate of the A7F under a constrained condition, Matrix 2 Test 5, were used for analysis purposes.

Test results of the standard 12.7 mm (0.5 in) single lap titanium-to-titanium shear tests (Matrix 2, Test 3) are shown in Figure 6-4. The data indicate a significant drop in shear strength due to aging and thermal cycling. Cured/post-cured specimens showed a significant drop in shear strength at elevated temperature. The aged specimens, however, exhibited essentially the same shear strength over the entire temperature range. The thermally cycled specimens failed adhesively with a characteristic silver/gray color on the adherends. This indicates a possible deterioration of the aluminum powder in the adhesive formulation or its interaction with other constituents.

The thick adherend tests (Matrix 2, Test 4) were conducted by Dr. J. R. Vinson at the University of Delaware. A summary of the test results is given in Figures 6-5 through 6-7. Since the thick adherend tests reduce peel stresses, it was expected that ultimate shear strengths would be higher than shown. Also, shear modulus and strain to failure data indicate an adhesive significantly more ductile than had been anticipated.

From Figure 6-5, it is seen that at room temperature the ultimate strength values of the cured/post-cured adhesive are very consistent, the standard deviation being only 1.58% of the mean value. It is also seen that statistically there is no difference between the ultimate strength of the cured/post-cured and the aged adhesive at room temperature. However, the ultimate strength of the cured/post-cured adhesive diminishes by 47% at 561K ( $550^{\circ}F$ ) compared to room temperature; but the ultimate strength of the aged adhesive is reduced only by 17% at 561K ( $550^{\circ}F$ ) from the room temperature value.

It is also seen that the ultimate strength of the cured/post-cured adhesive at 116K ( $-250^{\circ}F$ ) is 35% higher than the room temperature values, while there is a corresponding 32% increase in the value of the aged adhesive. Again, at 116K ( $-250^{\circ}F$ ) there is no statistical difference between the ultimate strengths of the cured/post-cured and the aged adhesive.

As shown in Figure 6-6, at 294K ( $70^{0}F$ ) the aged adhesive appears to have two distinct shear moduli (a bimodulus material). It therefore is difficult to draw conclusions between the cured/post-cured and aged adhesive at room temperature.

)

Concerning the cured/post-cured adhesive, it is seen that at 561K ( $550^{0}F$ ) the shear modulus has been reduced by 35% from the room temperature value, and is very consistent, the standard deviation being less than 1% of the mean value at 561K ( $550^{0}F$ ).

As for the aged adhesive, the shear modulus at 561K ( $550^{O}F$ ) is almost identical to the secondary modulus at room temperature. Furthermore, the shear modulus at 561K ( $550^{O}F$ ) is statistically not significantly different from the primary modulus at room temperature, because the standard deviations are so large. It is difficult to rationalize the low values for the 116K ( $-250^{O}F$ ) shear moduli compared to those of room temperature.

From Figure 6-7, it is seen that the repeatability of the shear strain to failure is excellent at all temperatures. It is seen that at 294K ( $70^{\circ}F$ ) and

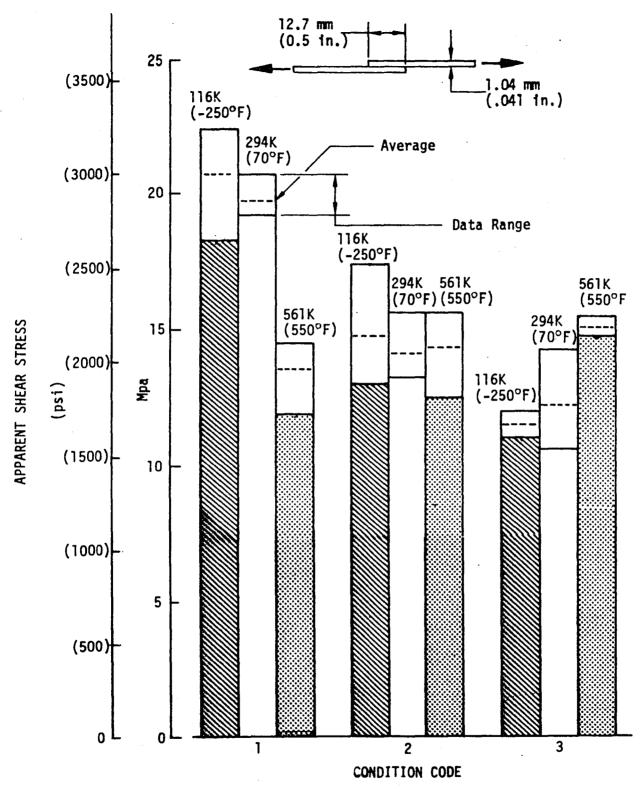
561K ( $550^{O}F$ ) the aged adhesive is more ductile than the cured/post-cured adhesive, but the values at both room temperature and 561K ( $550^{O}F$ ) are surprisingly close. Again, it is surprising that the A7F adhesive appears to be more ductile at 116K ( $-250^{O}F$ ) compared to 294K ( $70^{O}F$ ) and 561K ( $550^{O}F$ ).

A comparison of the room temperature values of the A7F adhesive with several lower temperature epoxy adhesives obtained by Flaggs and Vinson (Ref. 3) shows that the ultimate strengths of the A7F adhesives at room temperature fall in the same range as the epoxy adhesives. However the A7F adhesives are much stiffer and less ductile at room temperature.

A comparison has also been made of single-lap shear test results for A7F adhesive using ASTM D 1002 procedures and "Thick Adherend" procedures (See Figure 6-8). Data are shown in Table 6-2. Results for cured/post cured specimens at 294K ( $70^{\circ}$ F) and 561K ( $550^{\circ}$ F) are higher for the ASTM D 1002 procedure than for the "Thick Adherend" procedure. This is contrary to what was expected because of peel stresses in the ASTM D 1002 specimens. ASTM D 1002 results for aged specimens were only slightly higher than "Thick Adherend" results at 561K ( $550^{\circ}$ F). There is really no explanation for these apparent anomalies other than possible material and processing variations. Adhesive thicknesses could have been different for the two specimen configurations. Also there may have been some edge effects during the curing or aging. The "Thick Adherend" specimens were conditioned as a single plate approximately 762mm (30 inches) wide and then cut into specimens. The ASTM D 1002 specimens were made from standard titanium "finger" blanks 25.4mm (1.0 inch) wide which may have contributed to edge effects.

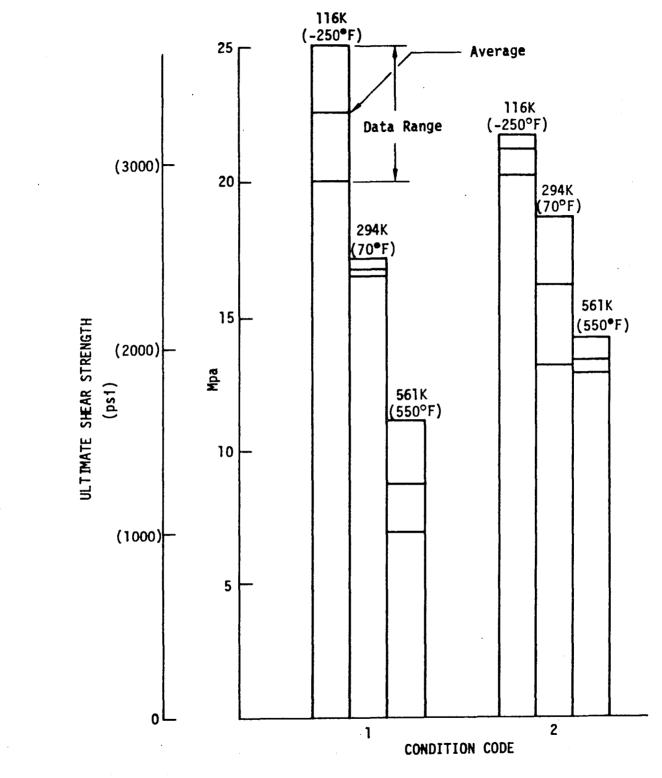
Tension test results of A7F adhesive bonding 31.8 mm (1.25 in) diameter bars end-to-end (Matrix 2, Test 5) are shown in Figure 6-9. All of the specimens failed cohesively. Cured/post-cured specimens had stainless steel bars, while aged specimens used titanium bars.

Coefficient of thermal expansion (CTE) tests on A7F adhesive were performed under contract Task 1.2.1 and are reported in Ref. 4. Test results are shown in Figure 6-10 and are included here for completeness.



- Cured/Post Cured
- 2. Aged 125 hrs @ 589K (600°F)
- 3. Cycled 125 times 116K (-250°F) to 589K (600°F)

Figure 6-4: Matrix 2, Test 3, 12.7mm (0.50 in), Single Lap Titanium/Titanium, 1.04 mm (.041 in) Adherends A7F Adhesive



)

)

- Cured/Post Cured
- 2. Aged 125 hrs @ 589K (600°F)

Figure 6-5: ULTIMATE SHEAR STRENGTH OF "A7F" ADHESIVE "THICK ADHEREND" TESTS

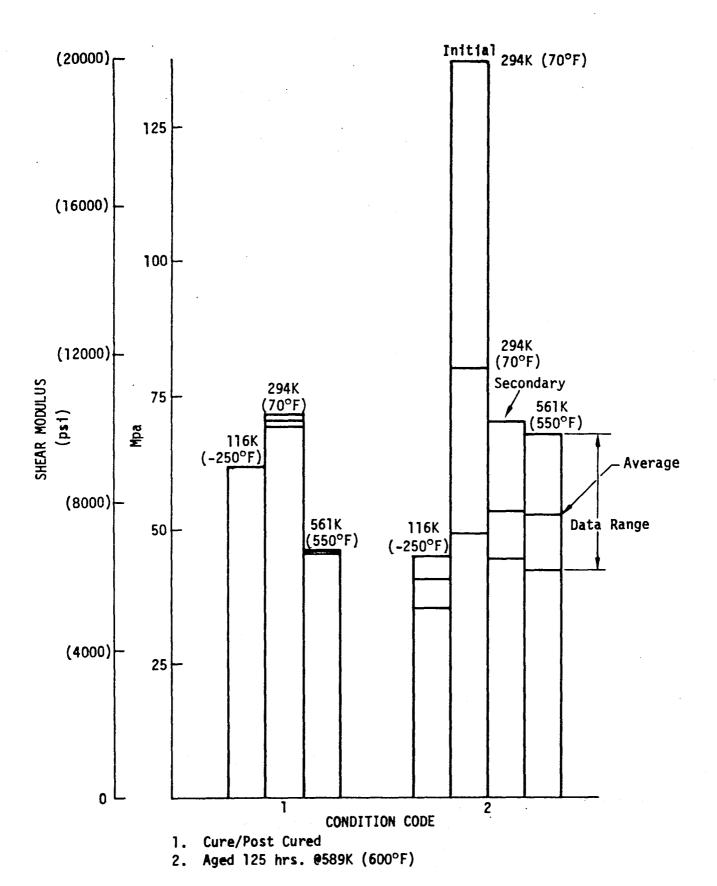


Figure 6-6: SHEAR MODULUS OF "A7F" ADHESIVE "THICK ADHEREND" TESTS

.80 116K (-250°F) 116K (-<u>250°F</u>) .60 294K (70°F) 561K Average (550°F) ULTIMATE SHEAR STRAIN 294K 561K (70°F)(550°F) Data Range .40 .20 0 1 2 CONDITION CODE

- Cured/Post Cured
- 2. Aged 125 hrs. @ 589K (600°F)

Figure 6-7: ULTIMATE SHEAR STRAIN OF "A7F" ADHESIVE "THICK ADHEREND" TESTS

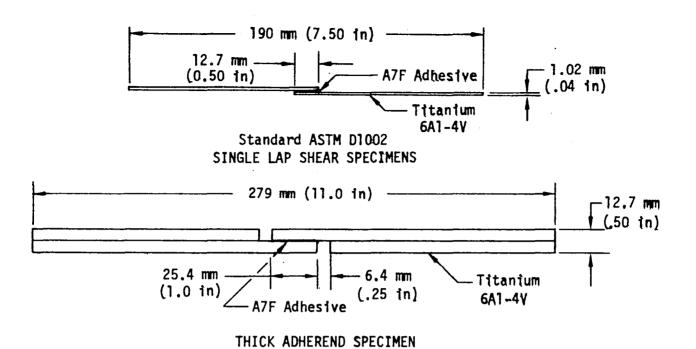
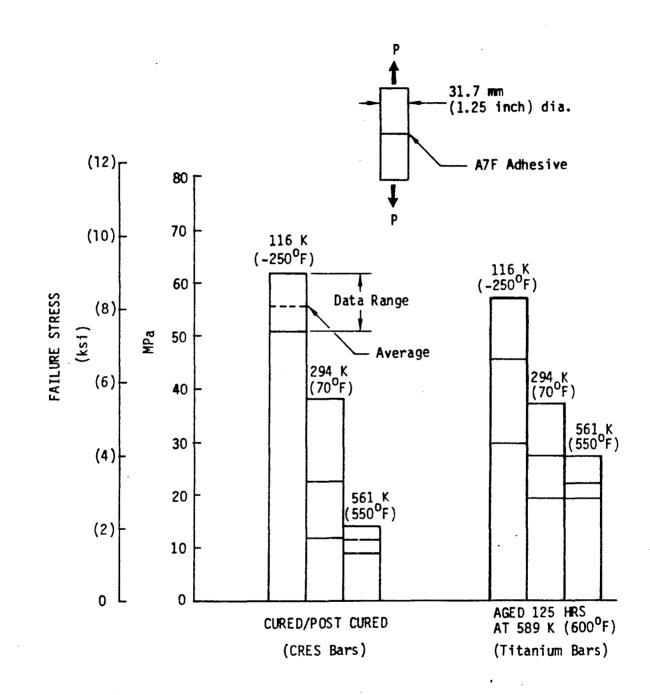


Figure 6-8: COMPARISON OF ASTM D1002 SINGLE LAP SHEAR AND "THICK ADHEREND" SPECIMEN CONFIGURATIONS

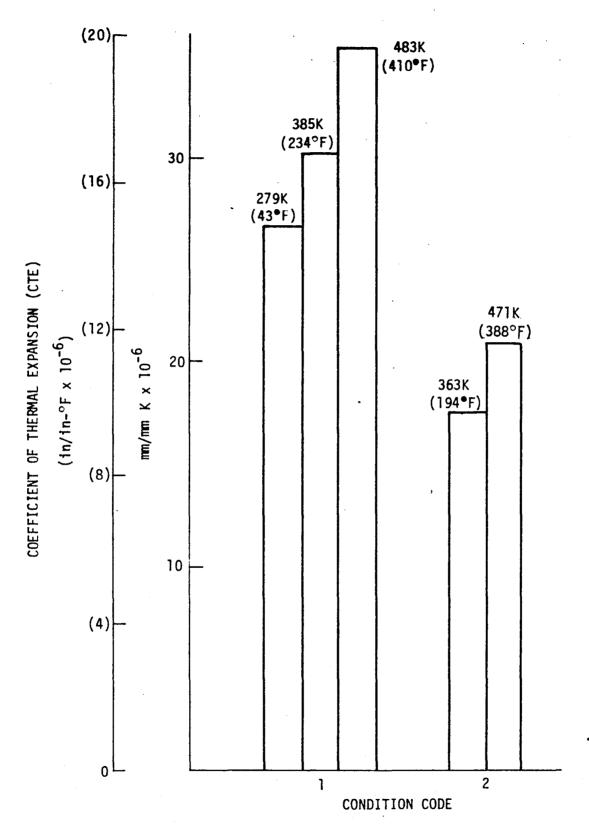
Table 6-2: COMPARISON OF ASTM D1002 SINGLE-LAP SHEAR AND "THICK ADHEREND" SINGLE-LAP SHEAR TEST RESULTS-- "A7F" ADHESIVE

	TEMPERATURE	AVERAGE SHEAR STRESS						
CONDITIONING	K (*F)	ASTM D1002 Mpa (psi)	THICK ADHEREND Mpa (psi)					
	116 (-250)	20.7 (3003)	22.6 (3274)					
Cured/Post-Cured	294 (70)	19.7 (2853)	16.7 (2425)					
	561 (550)	13.5 (1963)	8.8 (1275)					
	116 (-250)	14.8 (2140)	21.2 (3076)					
Aged 125 hrs. 9 589K (600°F)	294 (70)	14.1 (2047)	16.1 (2333)					
	561 (550)	14.3 (2080)	13.3 (1933)					



)

Figure 6-9: FLATWISE TENSION STRENGTH-- "A7F" ADHESIVE



Cured/Post Cured

2. Aged 125 hrs. @ 589K (600)°F

Figure 6-10: COEFFICIENT OF THERMAL EXPANSION-- "A7F" ADHESIVE

## 7.0 STANDARD BONDED JOINTS

## 7.1 Standard Joint Specimen Fabrication

Standard bonded joint test specimens were fabricated using Celion 3000/PMR-15 graphite/polyimide prepreg, 6A1-4V tianium, A7F adhesive, and E-glass polyimide prepreg for load tabs. Graphite/polyimide material lot numbers used for the various test sets are given in Tables 7-1 through 7-3. Table 7-4 is a summary of the quality control test results for each prepreg lot used.

Figure 7-1 shows the bonded joint fabrication flow. The Gr/PI prepreg was laid up per the test matrices and cured on a large flat tool per the procedures in Reference 1. The cured laminates were C-scannned for voids and checked against the control standard for acceptance or rejection of the laminates. A large number of the laminates were remade because of voids, surface porosities, and/or delaminations between plies.

To minimize the number of autoclave cycles, more than one laminate was cured on the tool in each autoclave run when space was available. This procedure was later determined to be part of the curing problem which caused porosities and delaminations. The application of pressure during the autoclave came too late for proper curing unless the temperature was monitored from the thinnest laminate. Normally, pressure is applied when the thickest portion of a part reaches temperature. This curing problem was not resolved until much later in the program.

Gr/PI adherend panels were trimmed, adherends tapered where applicable, and doublers cut to the proper sizes in preparation for bonding. The panels were lightly sandblasted and wiped with reagent grade MEK solvent to remove residues from the sanding and trimming operations. Laminate doublers, for double lap joints, were primed with A7F on the faying surfaces only and the panels baked in an oven at  $339 \text{ K} (150^{\circ}\text{F})$  for 30 minutes.

The titanium panels were surface treated using the chromic acid anadize process as described in Section 6.2. The titanium was then primed with A7F adhesive primer applied with a brush, and the panels baked using the above cure cycle.

The primed adherends were assembled for bonding with a strip of A7F adhesive film between the faying surfaces, using soft aluminum pins in the trim areas of the panels to hold the assemblies together for bonding. Titanium for the Gr/PI-titanium joints was received as 25.4 mm (1.0 inch) wide strips. A special bonding jig was used to align the titanium strips to allow the required number to be bonded simultaneously to a single laminate. The panel assemblies were envelope bagged and cured using the A7F cure cycle as given in Reference 1.

The A7F adhesive film used to bond the panels for this test matrix was prepared in the Boeing Material Technology Laboratories. The 112 E-glass cloth with A-1100 finish was stretched over a frame and the A7F adhesive brushed on. The adhesive was dried and the process repeated until the desired thickness, .254 mm (.010 in), was achieved.

The bonded panels were then conditioned per the test matrix. Following conditioning, the bond areas were C-scanned for disbonds. Assemblies were sawed into individual specimens using a band saw equipped with a carbide blade. Edges of each specimen were sanded after cutting to assure uniformity.

To fabricate the symmetric step-lap specimens the titanium adherends were milled to the desired dimension using maskant and chemical milling solutions. The titanium was then chromic acid anodized and primed with A7F adhesive per the same procedure as described previously. The Gr/PI prepreg was layed-up on the titanium steps, and the assemblies bagged and co-cured per NASA CR 159182. No adhesive scrim was used. Both the "3-step" and "5-step" panels were cured in the same bag.

The cured panels were C-scanned to detect voids, delaminations, etc. The "3-step" panels showed clear C-scans. The "5-step" panels had clear C-scans in the Gr/PI laminate and in the first two or three steps away from the center Gr/PI portion. The last two steps had extensive voids, with disbonds to the titanium visually noticeable in some places.

The "5-step" panels were remade using the previous procedure except a coat of liquid A7F adhesive was applied over the cured primer on the titanium. C-scans of the cured panels showed no improvement from the previous panels.

Fabrication of the "5-step" panels a third time was made using the above procedures except that the liquid A7F adhesive was dried 30 minutes at 339 K  $(150^{\circ}F)$  and another 5 minutes at 464 K  $(375^{\circ}F)$  to remove solvents. C-scans of the cured panels indicated that there was a slight improvement in bonding, but the panels were still unsatisfactory.

Because of time and money constraints, and the lack of a good process, the "5-step" lap joints were deleted from the test matrix. Subsequently, work on this program indicated that the bonding problem with these joints may have been due to the uneven heating of the titanium and the composite. Uneven temperatures were caused by the titanium being a good thermal conductor whereas the Gr/PI is only a fair conductor. The prepreg that was laid up on the titanium steps had cured or advanced past the gell stage when the pressure was applied during the cure cycle. Thus, the outer two steps were never bonded well onto the titanium because the PMR-15 resin and A7F primer were cured or partially cured when the pressure was applied.

Table 7-1: SUMMARY OF MATERIAL LOTS USED FOR SPECIMEN FABRICATION, SINGLE LAP JOINTS

TEST SET NUMBER	MATERIAL LOT NUMBER
3A - 1A	2 <b>W4</b> 604
3A - 1B	2W4582
3A - 1C	2W4604
.3A - 2A	2W4604
3A - 3A	2W4582
3A - 4A	2W4651
3A - 5A	3W2O2O, 2W46O4
3A - 6A	3W2O2O
3A - 7A	2W4632
3B - la	2W4604
3B - 1b	2W4604
3B - 1c	2W4604
3C - 1a	3W2020

Table 7-2: SUMMARY OF MATERIAL LOTS USED FOR SPECIMEN FABRICATION, DOUBLE-LAP JOINTS

TECT CET MUMBED	MATERIAL L	OT NUMBER
TEST SET NUMBER	Inner Adherend	Outer Adherend
3D - 1A	2W4632	3W2O2O
3D - 1B	2W4632	3 <b>W2</b> 020
3D - 1C	2W4632	3W2O2O
3D - 2A	2 <b>W</b> 4651	3W2020
3D - 2B	2 <b>W45</b> 82	3W2O2O
3D - 2C	2W4632	3W2020
3D - 3A	2W4632	3W2020
3D - 4A	2W4632	3W2020
3D - 5A	3W2O2O	2W4632
3D - 6A	2W4632	3W2O2O
3D - 7A	2W4632 2W4643	2W4632
3E - 1A	Titanium	2W4604
3E - 1B	Titanium	2W4604
3E - 2A	Titanium	2W4632
3F - 1A	2W4643 3W2020	2W4651

Table 7-3: SUMMARY OF MATERIAL LOTS USED FOR SPECIMEN FABRICATION, SYMMETRIC STEP-LAP JOINTS

TEST SET NUMBER	MATERIAL LOT NUMBER
3G - 1A	2W4781

Table 7-4: SUMMARY OF QUALITY CONTROL TEST RESULTS - CELION 3000/PMR-15

Р	ROPERTY	REQUIREMENTS	2W4582*	2W4604	2W4632	2W4643	2W4651	3W2020**	2W4781
Resin C Specifi	olume, % (Volume) ontent, % (Weight) c Gravity g/cc ntent, %	58 +2 30 +3 1.54	51.4 41.3 1.54 < 1	58.5 34.4 1.57 < 1	57.2 35.4 1.56 < 1	57.8 33.9 1.54 1.9	57.5 34.6 1.56 1.1	58.7 33.6 1.57 1	41.5
At Ambient Flexural		1515 (220)	1489 (216)	1282 (186)	1544 (224)	1537 (223)	1517 (220)	1378 (200)	1489 (216)
Strength	At 589K (600°F)	757 (110)	958 (139)	807 (117)	889 (129)	862 (125)	772 (112)	855 (124)	634 (92)
MPa (ksi)	Aged, at 589K (600°F)	757 (110)	958 (139)	896 (130)	951 (138)	1000 (145)	862 (125)	862 (125)	
Flexural	At Ambient	117 ( 17)	119 (17.2)	113 (16.4)	113 (16.4)	122 (17.7)	118 (17.1)	115 (16.7)	135 (19.6)
Modulus	At 589K (600°F)	103 ( 15)	105 (15.3)	112 (16.2)	128 (18.3)	114 (16.5)	105 (15.2)	109 (15.9)	110 (16)
GPa (msi)	Aged, at 589K (600°F)	103 ( 15)	109 (15.9)	127 (18.4)	137 (19.8)	114 (16.5)	107 (15.5)	104 (15.1)	
Short Beam	At Ambient	96 ( 14)	99 (14.4)	98 (14.2)	105 (15.2)	94 (13.7)	95 (13.8)	96 (14.0)	93 (13.5)
Shear Strength	At 589K (600°F)	41 . ( 6 )	66 ( 9.6)	56 (8.1)	50 ( 7.2)	52 ( 7.5)	50 ( 7.2)	57 ( 8.3)	48 (6.9)
MPa (ksi)	Aged, at 589K (600°F)	41 ( 6)	63 ( 9.2)	56 (8.1)	54 ( 7.9)	52 ( 7.5)	52 ( 7.5)	56 (8.1)	

<sup>\*</sup> Average of Two Rolls
\*\* Average of Four Rolls

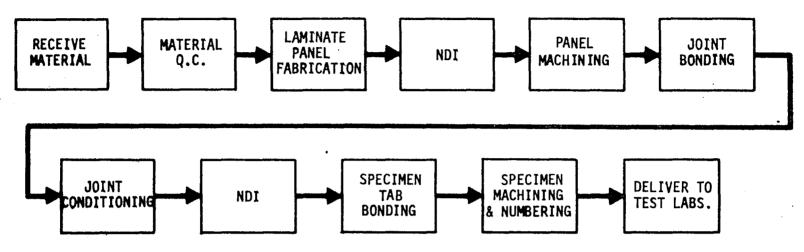


Figure 7-1: BONDED JOINT FABRICATION FLOW

## 7.2 Standard Joint Test Results

The test results obtained for the single and double-lap joints had a significant amount of data scatter. Normally large scatter can be attributed to processing and manufacturing variables. However, since all adherend laminates received strict process control no conclusive explanation was found for the data scatter. To establish a feel for the quality of the data, standard deviations and coefficients of variation were calculated for all the test results. Coefficients of variation for the single lap joints range from 0.047 to 0.410 and for the double lap joints from 0.023 to 0.355. The "3-step" symmetric step lap joints had very little data scatter with coefficients of variation from 0.032 to 0.087.

In an attempt to find an explanation for the large standard deviations, scanning-electron microscope (SEM) photos were taken of the failure surfaces of four specimens. Photos were taken of two single lap joints and two double lap joints. Each pair was the same joint configuration and consisted of one specimen which had failed at a high load and one which had failed at a low load (See Figures 7-2 and 7-3). Three photos of each specimen were taken near the end of the overlap region. Comparing the specimens in Figure 7-2 (single lap) and the specimens in Figure 7-3 (double lap), there is no obvious difference between the failure surfaces for the specimens with the high failure load and those with the low failure load. Based on this and because of the data scatter, it was decided to make comparisons between joint types and perform analysis/correlations based on average failure loads only. It is possible that the data scatter may have masked the effect of parameter changes and thus affected the conclusions drawn from the test results.

Actual thicknesses of the adherends varied from the nominal thickness by up to 27%. Most of the variation was on the high side. These thickness variations complicated the task of analyzing the test results by introducing another variable. This is more critical for the single-lap joints than the double-lap joints. The single-lap joint's strength is more dependent on the flexural

stiffness of the adherends, which varies with the cube of the adherend thickness, than the double lap joints strength. Flexural stiffnesses for the single lap joints, based on actual measured thicknesses are given in Table 7-5. Stiffness were calculated using the average "per ply" thickness obtained by dividing the total thickness by the number of plies.

In most cases, the all composite (Gr/PI-Gr/PI) joints exhibited an intralimina failure mode. This failure mode consists of a failure within a ply, as opposed to an interlamina failure where the failure occurs between the plies. In most cases, for both single and double lap joints, the intralamina failure occurred in the ply nearest the joint interface, with the failure occurring for the double lap joints in the inner adherends. Figure 7-4 shows a typical specimen exhibiting this failure mode. Some of the exceptions to this failure mode were the specimens with a  $\pm$  45° plies at the joint interface and the tapered adherend specimens. Both of these had intralamina and interlamina failures in the first few plies.

The "Gr/PI-titanium" joints had adhesive failures over a portion of the joint for some specimens at all test temperatures. The majority of the 561 K (550°F) specimens experienced this type of failure. The remaining specimens exhibited intralamina and/or interlamina failures in the Gr/PI plies near the joint interface. Figure 7-5 shows a typical adhesive failure, while Figure 7-6 shows a typical interlamina failure.

Tables 7-6 through 7-10 summarize the test data for the single, double and step-lap joints. Shown are the average failure loads (nominally of 6 data points) with corresponding standard deviations and coefficients of variation, and average joint stress (avg load/(lap length\*width). To give an indication of how well the joint is performing the joint structural efficiency and weight coefficient are also given. The structural efficiency is defined as the average failure load divided by the adherend ultimate strength as given below.

Structural Efficiency = P/F<sup>tu</sup>t

P = Average Failure Load

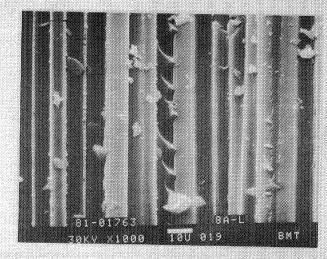
F<sup>tu</sup> = Ultimate Stress of Adherend

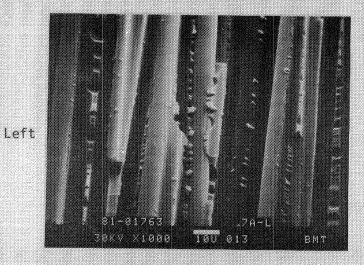
t = thickness of Adherend

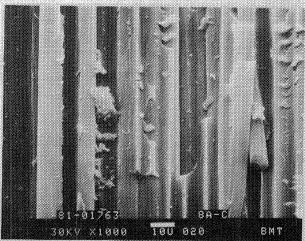
The weight coefficient is an efficiency type of parameter and is defined in Figure 7-7. It is desirable to maximize this parameter, achieving the greatest load for the least added weight.

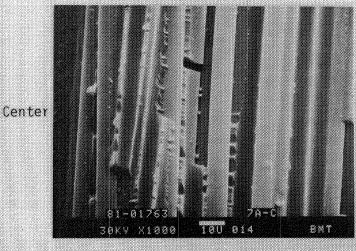
Average test results shown include all the test data. No data have been censored from any data set. There are some cases where deletion of test results for specimens that had different failure modes than others from the same set resulted in an improved correlation of the data. Such areas are noted and discussed as applicable in the following sections.

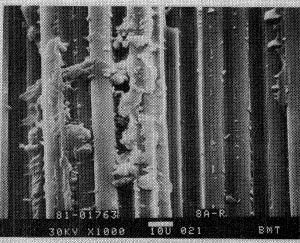
A complete set of test results, by specimen, is given in Appendix B. It should be noted that the average joint stress has little meaning, due to the highly nonlinear distribution of the shear stresses at the joint interface. It is included here for completeness, as much of the literature surveyed reports joint strength results in terms of the average shear stress in the joint.

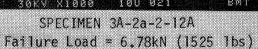


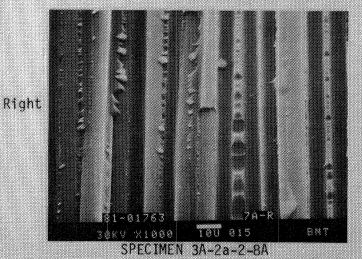








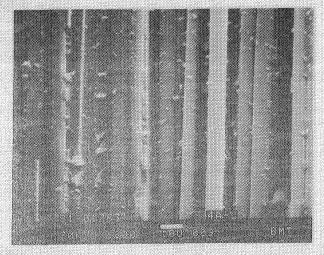




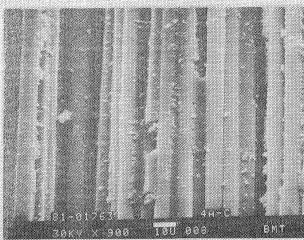
Failure Load = 5.00kN (1125 1bs)

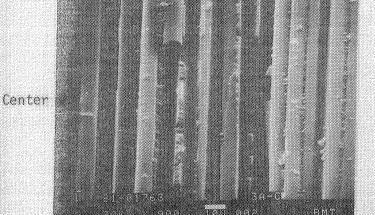
Lap Length = 50.8mm (2.0in)
Room Temperature

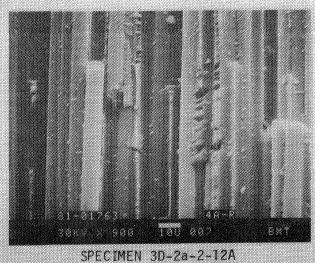
Figure 7-2: SEM PHOTOS OF SINGLE LAP JOINT FAILURE SURFACES



Left

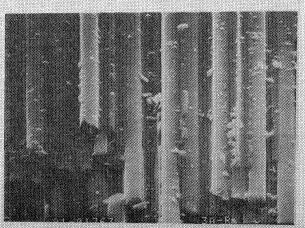






Failure Load = 16.1kN (3615 1bs)





SPECIMEN 3D-2a-2-10A

Failure Load = 8,67kN (1950 lbs)

Lap Length = 20.3mm (0.8in)
Room Temperature

Figure 7-3: SEM PHOTOS OF DOUBLE LAP JOINT FAILURE SURFACES

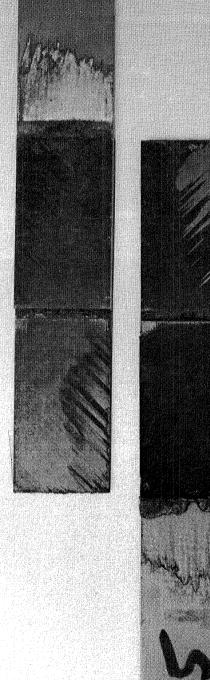
Table 7-5: ADHEREND FLEXURAL STIFFNESSES FOR SINGLE LAP JOINTS (Based on Actual Thicknesses)

TECT	ACTUAL	FLEXURAL STIFE	FNESS - D11	LAYUP	
TEST SET	THICKNESS mm (in)	294K (70°F) N-m (1b-in)	561K (550°F) N-m (1b-in)		
3A-7A	1.70 (.067	29.27 (259.1)	29.97 (265.3)	(0/ <u>+</u> 45/90) <sub>3S</sub>	
3A-1A	1.75 (.069	32.20 (285.0)	32.97 (291.8)	(0/ <u>+</u> 45/90) <sub>35</sub>	
3A-1B	1.93 (.076	42.93 (380.0)	43.84 (388.0)	(0/ <u>+</u> 45/90) <sub>35</sub>	
3A-1C	1.88 (.074	39.38 (348.5)	40.32 (356.9)	(0/ <u>+</u> 45/90) <sub>35</sub>	
3A-2A	1.75 (.069	46.82 (414.4)	48.03 (425.1)	(0/ <u>+</u> 45/0 <sub>3</sub> ) <sub>2S</sub>	
3A-3A	1.60 (.063	19.55 (173.0)		( <u>+</u> 45/0/90) <sub>35</sub>	
3A-4A	1.50 (.059	24.22 (214.4)		(0 <sub>3</sub> / <u>+</u> 45 <sub>3</sub> /90 <sub>3</sub> ) <sub>S</sub>	
3A-6A	2.95 (.116	140.0 (1239.6)		(0/ <u>+</u> 45/90) <sub>5S</sub>	
3C-1A	2.95 (.116	140.0 (1239.6)		(0/ <u>+</u> 45/90) <sub>5S</sub>	

MATRIX 3A- TEST NUMBER 1c, Gr/Pi - Gr/Pi SINGLE LAP

561 K (550°F)

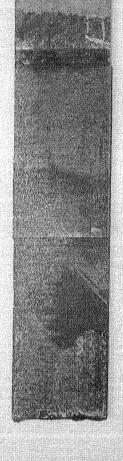
Figure 7-4: TYPICAL INTRALAMINA FAILURE SURFACES, TEST 3A-1C, 561K (550°F)



# MATRIX 3E-TEST NUMBER 2a, Gr/Pi - Titanium DOUBLE LAP

## 116 K (-250°F)

Figure 7-5: TYPICAL ADHESIVE FAILURE SURFACE, TEST 3E-2A, 561K (550°F)





## MATRIX 3E-TEST NUMBER 2a, Gr/Pi - Titanium DOUBLE LAP

561 K (550°F)

Figure 7-6: TYPICAL INTERLAMINA FAILURE SURFACE, TEST 3E-2A, 116K (-250°F)

TABLE 7-6 SUMMARY OF BONDED SINGLE LAP JOINT TEST RESULTS - GR/P! TO GR/P!

(A) SI UNITS

TEST SET	TEMPERATURE K	LAP LENGTH MM	AVERAGE FAILURE LOAD KN	STANDARD DEVIATION KN	COEFFICIENT OF VARIATION	AVERAGE JOINT STRESS MPA	AVERAGE JOINT EFFICIENCY	ADDED JOINT WEIGHT N/M	AVERAGE WEIGHT COEFFICIENT
3A-1A	116.	25.70	2.33	. 40	.173	3.56	.100	.71	1.29E5
3A-1A	294.	25.95	3.65	. 68	.185	5.53	.156	.72	2.00
3A-1A	561.	25.87	4.91	. 68	.138	7.45	.210	.71	.2.71
3A-1B	116.	52.15	3.47	. 18	.052	2.59	.134	1.59	.86
3A-1B	294.	52.24	3.56	. 24	.068	2.67	.138	1.58	.89
3A-1B	561.	52.32	3.89	. 46	.118	2.89	.150	1.59	.96
3A-1C	116.	77.55	5.30	.54	.102	2.64	. 208	2.29	.91
3A-1C	294.	77.47	5.33	.93	.174	2.66	. 209	2.28	.92
3A-1C	561.	77.30	6.41	1.37	.214	3.24	. 254	2.30	1.10
3A-2A	116.	51.16	5.67	.79	.140	4.35	.131	1.41	1.58
3A-2A	294.	51.05	5.26	.79	.150	4.06	.122	1.41	1.47
3A-2A	561.	51.29	9.71	1.08	.111	7.42	.224	1.42	2.70
3A-3A	294.	51.02	5.30	.57	.108	4.07	. 248	1.29	1.62
3A-4A	294.	51.56	5.35	2.19	.410	4.02	. 264	1.22	1.73
3A-5A	116.	51.56	2.47	.15	.062	1.87	.161	1.41	.89
3A-5A	294.	51.39	2.90	.75	.259	2.20	.188	1.39	.82
3A-5A	561.	51.51	4.14	1.44	.347	3.14	.270	1.40	1.16
3A-6A	294.	51.48	5.03	.39	.077	3.77	.126	2.38	.83
3A-7A	116.	13.42	2.94	. 44	.148	8.62	.130	.36	3.22
3A-7A	294.	13.38	2.67	. 27	.101	7.87	.118	.36	2.92
3A-7A	561.	13.29	3.22	. 53	.165	9.55	.142	.36	3.56
3C-1A	294.	51.27	6.22	. 8 2	.132	4.69	.156	1.54	1.33

TABLE 7-6 CONCLUDED
(B) US CUSTOMARY UNITS

TEST SET	TEMPERATURE F	LAP LENGTH IN	AVERAGE FAILURE LOAD LBS	STANDARD DEVIATION LBS	COEFFICIENT OF VARIATION	AVERAGE JOINT STRESS PSI	AVERAGE JOINT EFFICIENCY	ADDED JOINT WEIGHT LB/IN	AVERAGE WEIGHT COEFFICIENT
3A-1A	-250.	1.012	524.	91.	.173	517.	.100	4.06E-3	1.29E5
3A-1A	70.	1.022	821.	152.	.185	802.	.156	4.10	2.00
3A-1A	550.	1.018	1103.	152.	.138	1080.	.210	4.07	.2.71
3A-1B	-250.	2.053	780.	41.	.052	376.	.134	9.07	. 86
3A-1B	70.	2.057	805.	54.	.068	387.	.138	9.04	. 89
3A-1B	550.	2.060	874.	103.	.118	419.	.150	9.10	. 96
3A-1C	-250.	3.053	1192.	121.	.102	383.	.208	13.10	.91
3A-1C	70.	3.050	1199.	208.	.174	385.	.209	13.03	.92
3A-1C	550.	3.043	1442.	308.	.214	470.	.254	13.11	1.10
3A-2A	-250.	2.014	1274.	178.	.140	631.	.131	8.06	1.58
3A-2A	70.	2.010	1183.	178.	.150	588.	.122	8.05	1.47
3A-2A	550.	2.019	2184.	243.	.111	1077.	.224	8.09	2.70
3A-3A	70.	2.009	1191.	128.	. 108	590.	.248	7.35	1.62
3A-4A	70.	2.030	1203.	493.	.410	583.	. 264	6.95	1.73
3A-5A	-250.	2.030	556.	34.	.062	272.	.161	8.06	. 69
3A-5A	70.	2.023	653.	169.	.259	319.	.188	7.96	. 82
3A-5A	550.	2.028	930.	323.	.347	455.	.270	8.02	1 . 16
3A-6A	70.	2.027	1130.	88.	.077	547.	. 126	13.61	.83
3A-7A	-250.	. 528	661.	98.	.148	1250.	.130	2.05	3.22
3A-7A	70.	. 527	599.	61.	.101	1141.	.118	2.05	2.92
3A-7A	550.	. 523	724.	119.	.165	1385.	.142	2.03	3.56
3C-1A	70.	2.018	1398.	185.	. 132	680.	. 156	10.51	1.33

TABLE 7-7 SUMMARY OF BONDED SINGLE LAP JOINT TEST RESULTS - GR/PI TO TITANIUM

(A) SI UNITS

TEST SET	TEMPERATURE K	LAP LENGTH MM	AVERAGE FAILURE LOAD KN	STANDARD DEVIATION KN	COEFFICIENT OF VARIATION	AVERAGE JOINT STRESS MPA	AVERAGE JOINT EFFICIENCY	ADDED JOINT WEIGHT N/M	AVERAGE WEIGHT COEFFICIENT
3B-1A	116.	25.61	2.47		. 131	3.85	. 135	. 80	1.22E5
3B-1A	294.	25.74	2.90	42	.144	4.48	.159	. 80	1.42
3B-1A	561.	25.74	4.96	1.46	. 294	7.66	. 271	. 80	2.44
3B-1B	116.	51.10	3.41	. 48	. 140	2.65	. 186	1.60	. 84
3B-1B	294.	51.14	4.84	. 5 5	.113	3.79	. 266	1.59	1.20
3B-1B	561.	51.10	6.98	. 33	. 047	5.44	.382	1.59	1.73
3B-1C	116.	76.88	2.75	. 22	. 081	1.42	. 150	2.40	. 45
3B-1C	294.	76.83	3.44	.75	. 219	1.78	.188	2.37	. 57
3B-1C	561.	76.79	6.44	.89	.134	3.45	. 365	2.34	1.09

TEST SET	TEMPERATURE F	LAP LENGTH IN	AVERAGE FAILURE LOAD LBS	STANDARD DEVIATION LBS	COEFFICIENT OF VARIATION	AVERAGE JOINT STRESS PSI	AVERAGE JOINT EFFICIENCY	ADDED JOINT WEIGHT LB/IN	AVERAGE WEIGHT COEFFICIENT
3B-1A	-250.	1.008	556.	73.	.131	588.	.135	4.56E-3	1.22E5
3B-1A	70.	1.013	651.	94.	.144	650.	.159	4.58	1.42
3B-1A	550.	1.013	1115.	328.	. 294	1111.	. 271	4.57	2.44
3B-1B	-250.	2.012	766.	107.	.140	385.	. 186	9.12	.84
3B-1B	70.	2.013	1089.	123.	.113	549.	. 266	9.08	1.20
3B-1B	550.	2.012	1570.	74.	.047	788.	.382	9.08	1.73
3B-1C	-250.	3.027	618.	50.	.081	207.	.150	13.73	.45
3B-1C	70.	3.025	773.	169.	.219	258.	.188	13.56	. 57
3B-1C	550.	3.023	1493.	200.	.134	501.	. 365	13.70	1.09

TABLE 7-8 SUMMARY OF BONDED DOUBLE LAP JOINT TEST RESULTS - GR/PI TO GR/PI

(A) SI UNITS

TEST SET	TEMPERATURE K	LAP LENGTH MM	AVERAGE FAILURE LOAD KN	STANDARD DEVIATION KN	COEFFICIENT OF VARIATION	AVERAGE JOINT STRESS MPA	AVERAGE JOINT EFFICIENCY	ADDED JOINT WEIGHT N/M	AVERAGE WEIGHT COEFFICIENT
3D-1A	116.	20.8	11.19	1.82	.162	10.51	.359	1.53	2.88E5
3D-1A	294.	20.7	9.01	.38	.042	8.54	.289	1.51	2.34
3D-1A	561.	21.3	11.28	2.05	.182	10.59	.361	1.53	2.90
3D-1B	116.	32.8	10.48	.67	.064	6.24	.344	2.37	1.74
3D-1B	294.	32.7	9.87	1.28	.130	5.88	.324	2.37	1.64
3D-1B	561.	33.0	11.62	2.22	.191	6.86	.381	2.40	1.91
3D-1C	116.	45.6	9.13	1.79	. 196	3.94	.297	3.30	1.09
3D-1C	294.	45.5	8.93	1.53	. 172	3.84	.290	3.29	1.07
3D-1C	561.	45.6	9.96	3.09	. 311	4.29	.323	3.29	1.19
3D-2A	116.	20.8	9.88	3.50	.355	9.35	.221	2.14	1.82
3D-2A	294.	20.3	10.56	3.17	.301	10.10	.237	2.12	1.96
3D-2A	561.	20.2	12.91	3.73	.289	12.40	.290	2.12	2.40
3D-2B	116.	33.9	16.19	1.08	.067	3.37	.312	4.11	1.55
3D-2B	294.	34.0	14.89	.73	.049	8.60	.287	4.13	1.42
3D-2B	561.	34.1	14.01	2.03	.145	8.11	.270	4.12	1.34
3D-2C	116.	46.1	15.15	3.24	. 214	6.47	.329	5.01	1.19
3D-2C	294.	46.1	15.64	3.37	. 216	6.68	.340	4.96	1.24
3D-2C	561.	46.1	17.87	2.45	. 139	7.54	.384	5.01	1.39
3D-3A	116.	33.7	16.01	1.29	. 08 1	9.36	.193	3.54	1.78
3D-3A	294.	34.0	16.34	.76	. 04 6	9.55	.197	3.53	1.82
3D-3A	561.	33.9	24.64	2.22	. 09 0	14.40	.297	3.54	2.74
3D-4A	116.	33.6	11.28	.87	.077	6.60	.266	3.36	1.32
3D-4A	294.	33.6	13.02	2.19	.169	7.61	.307	3.37	1.52
3D-4A	561.	33.3	16.15	3.10	.192	9.49	.382	3.38	1.88
3D-5A	116.	32.7	16.10	.72	.045	9.57	.328	3.82	1.66
3D-5A	294.	32.2	14.89	1.49	.100	8.82	.302	3.81	1.54
3D-5A	561.	32.9	20.91	1.19	.057	12.39	.424	3.81	2.16
3D-6A	116.	33.5	9.58	2.09	.218	5.60	.310	3.63	1.04
3D-6A	294.	33.7	8.73	1.57	.180	5.11	.283	3.66	.94
3D-6A	561.	33.5	9.82	1.78	.182	5.76	.319	3.85	1.06
3D-7A	294.	33.7	15.70	3.34	. 213	9.15	.178	7.02	.88
3D-7A	561.	33.6	17.73		. 107	10.30	.200	6.98	1.00
3F-1A 3F-1A	294. 561.	34.4	19.21 19.02	2.20 .44	.115 .023	11.14 10.95	.216	5.14 5.20	1.47 1.44

TABLE 7-8 CONCLUDED

TEST SET	TEMPERATURE F	LAP LENGTH IN	AVERAGE FAILURE LOAD LBS	STANDARD DEVIATION LBS	COEFFICIENT OF VARIATION	AVERAGE JOINT STRESS PSI	AVERAGE JOINT EFFICIENCY	ADDED JOINT WEIGHT LB/IN	AVERAGE WEIGHT COEFFICIENT
3D-1A	-250.	.82	2516.	409.	.162	1524.	.359	8.74E-3	2.88E5
3D-1A	70.	.81	2025.	85.	.042	1239.	.289	8.65	2.34
3D-1A	550.	.84	2535.	462.	.182	1537.	.361	8.74	2.90
3D-1B	-250.	1.29	2356.	150.	.064	906.	.344	13.54	1.74
3D-1B	70.	1.29	2219.	288.	.130	852.	.324	13.53	1.64
3D-1B	550.	1.30	2613.	499.	.191	996.	.381	13.83	1.91
3D-1C	-250.	1.79	2053.	402.	.196	571.	.297	18.83	1.09
3D-1C	70.	1.79	2008.	345.	.172	557.	.290	18.77	1.07
3D-1C	550.	1.79	2238.	696.	.311	622.	.323	18.80	1.19
3D-2A	-250.	. 82	2220.	788.	.355	1352.	. 221	12.20	1.82
3D-2A	70.	. 80	2373.	713.	.301	1465.	. 237	12.10	1.96
3D-2A	550.	. 80	2902.	839.	.289	1798.	. 290	12.09	2.40
3D-2B	-250.	1.34	3639.	243.	.067	1359.	.312	23.48	1.55
3D-2B	70.	1.34	3347.	165.	.049	1248.	.287	23.57	1.42
3D-2B	550.	1.34	3150.	456.	.145	1176.	.270	23.51	1.34
3D-2C	-250.	1.81	3405.	728.	.214	938.	.329	28.61	1.19
3D-2C	70.	1.81	3515.	759.	.216	968.	.340	28.35	1.24
3D-2C	550.	1.82	3972.	551.	.139	1094.	.384	28.58	1.39
3D-3A	-250.	1.33	3598.	290.	.081	1358.	.193	20.21	1.78
3D-3A	70.	1.34	3673.	170.	.046	1385.	.197	20.18	1.82
3D-3A	550.	1.34	5540.	499.	.090	2059.	.297	20.22	2.74
3D-4A	-250.	1.32	2535.	196.	.077	958.	.266	19.20	1.82
3D-4A	70.	1.32	2927.	493.	.169	1104.	.307	19.26	1.52
3D-4A	550.	1.31	3632.	698.	.192	1377.	.382	19.32	1.88
3D-5A	-250.	1.29	3618.	161.	.045	1388.	.328	21.80	1.66
3D-5A	70.	1.31	3347.	336.	.100	1279.	.302	21.73	1.54
3D-5A	550.	1.30	4702.	268.	.057	1797.	.424	21.77	2.16
3D-6A	-250.	1.32	2153.	470.	.218	813.	.310	20.70	1.04
3D-6A	70.	1.33	1963.	353.	.180	741.	.283	20.88	.94
3D-6A	550.	1.32	2208.	401.	.182	836.	.319	20.83	1.06
3D-7A	70.	1.33	3529.	752.	.213	1327.	.178	40.10	.88
3D-7A	550.	1.32	3985.	426.	.107	1494.		39.85	1.00
3F-1A 3F-1A	70. 550.	1.36 1.36	4318. 4275.	495. 100.	.115	1615. 1588.	.216	29.37 29.69	1.47 1.44

TABLE 7-9 SUMMARY OF DOUBLE LAP JOINT TEST RESULTS - GR/PI TO TITANIUM

(A) SI UNITS

TEST SET	TEMPERATURE K	LAP LENGTH MM	AVERAGE FAILURE LOAD KN	STANDARD DEVIATION KN	COEFFICIENT OF VARIATION	AVERAGE JOINT STRESS MPA	AVERAGE JOINT EFFICIENCY	ADDED JOINT WEIGHT N/M	AVERAGE WEIGHT COEFFICIENT
3E-1A	116.	20.6	12.37	1.22	.099	12.94	.344	1.95	2.50E5
3E-1A	294.	20.2	18.24	.61	.033	17.90	.487	1.95	3.68
3E-1A	561.	20.2	17.52	.67	.038	17.26	.472	1.95	3.54
3E-1B	116.	45.6	8.85	1.60	.181	3.87	.238	4.36	.80
3E-1B	294.	45.6	14.35	2.42	.169	6.23	.383	4.34	1.30
3E-1B	561.	45.6	23.25	1.18	.051	10.08	.619	3.89	.2.35
3E-2A	116.	45.7	16.08	1.41	.088	6.97	.430	4.40	1.44
3E-2A	294.	45.7	17.04	1.73	.102	7.39	.455	4.36	1.54
3E-2A	561.	45.7	21.29	1.18	.049	9.18	.640	4.96	1.91

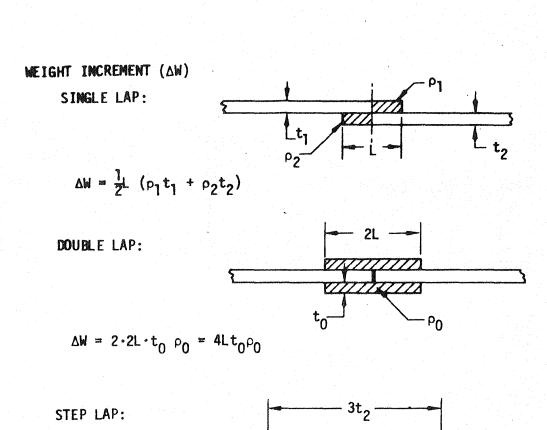
TEST SET	TEMPERATURE F	LAP LENGTH IN	AVERAGE FAILURE LOAD LBS	STANDARD DEVIATION LBS	COEFFICIENT OF VARIATION	AVERAGE JOINT STRESS PSI	AVERAGE JOINT EFFICIENCY	ADDED JOINT WEIGHT LB/IN	AVERAGE WEIGHT COEFFICIENT
3E-1A	-250.	.80	2780.	275.	.099	1775.	.334	11.12E-3	2.50E5
3E-1A	70.	.80	4100.	137.	.033	2596.	.487	11.14	3.68
3E-1A	550.	.80	3938.	151.	.038	2504.	.472	11.12	3.54
3E-1B	-250.	1.79	1990.	359.	.181	562.	. 238	24.88	.80
3E-1B	70.	1.79	3225.	545.	.169	903.	. 383	24.81	1.30
3E-1B	550.	1.79	5227.	265.	.051	1462.	. 619	22.24	2.35
3E-2A	-250.	1.80	3615.	317.	.088	1011.	.430	25.10	1.44
3E-2A	70.	1.80	3830.	389.	.102	1072.	.455	24.87	1.54
3E-2A	550.	1.80	5410.	266.	.049	1504.	.640	28.32	1.91

TABLE 7-10 SUMMARY OF BONDED STEPPED LAP JOINT TEST RESULTS - GR/PI TO TITANIUM

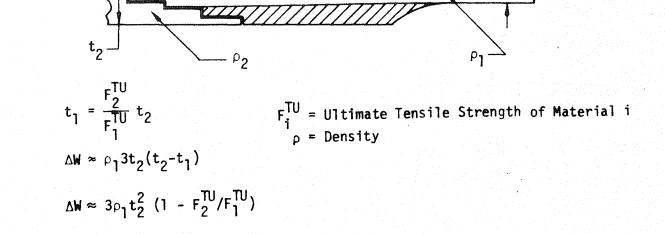
(A) SI UNITS

TEST SET	TEMPERATURE K	AVERAGE FAILURE LOAD KN	STANDARD DEVIATION KN	COEFFICIENT OF VARIATION	AVERAGE JOINT STRESS MPA	AVERAGE JOINT EFFICIENCY	ADDED JOINT WEIGHT N/M	AVERAGE WEIGHT COEFFICIENT
3G-1A	116.	14.07	1.22	.087	7.274	.263	.94	5.9E5
3G-1A	294.	18.28	.95	.052	9.446	.343	.93	7.7
3G-1A	561.	22.89	.73	.032	11.83	.429	.93	9.7

TEST SET	TEMPERATURE F	AVERAGE FAILURE LOAD LBS	STANDARD DEVIATION LBS	COEFFICIENT OF VARIATION	AVERAGE JOINT STRESS PSI	AVERAGE JOINT EFFICIENCY	ADDED JOINT WEIGHT LB/IN	AVERAGE WEIGHT COEFFICIENT
3G-1A	-250.	3164.	275.	.087	1055.	.263	5.36E-3	5.9E5
3G-1A	70.	4110.	214.	.052	1370.	.343	5.34	7.7
3G-1A	550.	5147.	165.	.032	1716.	.429	5.31	9.7



)



AVERAGE WEIGHT COEFFICIENT =  $\frac{AVERAGE}{WEIGHT}$  FAILURE LOAD =  $\frac{P}{\Delta W}$ 

Figure 7-7: CALCULATION OF WEIGHT INCREMENT & AVERAGE WEIGHT COEFFICIENT

## 7.2.1 Single-Lap Joints

Single-lap joint test results have been plotted showing the average failure loads with the plus/minus one standard deviation range for each data set. Some of the data points were shifted slightly in the abscissa direction to eliminate overlap of the vertical standard deviation lines.

Failure load versus lap length of "Gr/PI-Gr/PI" single-lap joints is shown in Figure 7-8 for the three temperatures tested. As expected there was a general increase in load with increasing temperature. The load also increases with lap length and appears to be leveling off as expected. The data shown for the 50.8mm (2.0 inch) lap length (data set 3A-1B) seem to be low based on the other test results; however, post test examination of the specimens did not show any apparent failure anomalies. These specimens were made from material lot 2W4582 which had a low fiber volume of 51.4% as compared to 55.8% for lot 2W4604 which was used for the other specimens. This may have been contributed to the apparent low failure loads. The "weight coefficient" versus lap length is shown in Figure 7-9 and shows that the 12.7mm (0.5 inch) lap length is the most weight efficient. Figures 7-10 through 7-12 show typical failed specimens for the 25.4 mm (1.0 in) to 76.2 mm (3.0 in) lap lengths.

Failure load versus lap length of "Gr/PI-titanium" single-lap joints is shown in Figure 7-13. For these joints the effect of temperature is much greater, due to the difference in thermal expansions of the Gr/PI and titanium adherends. There was an increase in load going from the 25.4mm (1.0 inch) to 50.8mm (2.0 inch) lap length; however, the load dropped slightly at all temperatures going from a 50.8mm (2.0 inch) to a 76.2mm (3.0 inch) lap length. Figure 7-14 shows the "weight coefficient" for the "Gr/PI-titanium" joints. As for the "Gr/PI-Gr/PI" joints, this figure shows that the shortest lap length, 25.4mm (1.0 inch), is the most weight efficient. Typical failed specimens for these configurations are shown in Figures 7-15 through 7-17.

The effect of increasing the axial stiffness of the adherends with the same adherend thickness, is demonstrated in Figure 7-18. The increased stiffness

configuration (3A-2A) had a 9% increase in flexural stiffness and a 100% increase in axial stiffness over the baseline configuration (3A-1B). The increased stiffness configuration shows a 50% increase in failure load at  $116K(-250^{\circ}F)$  and  $294K(70^{\circ}F)$  and a 150% increase at  $561K(550^{\circ}F)$ . The reason for the large jump from  $294K(70^{\circ}F)$  to  $561K(550^{\circ}F)$  is not apparent, though it is suspected that the results for the  $294K(70^{\circ}F)$  test are somewhat low. Also it should be noted that the data for the baseline data set (3A-1B) may be on the low side as discussed above (See Figure 7-8.)

An increase in axial stiffness can also be obtained by increasing the adherend thickness; however, this also increases the flexural stiffness. Tests at 294K  $(70^{\circ}\ \text{F})$  show an increase in strength of 40% going from nominal 1.52 mm (.06 inch) to 2.54 mm (.10 inch) adherends of the same lay-up. This increse is primarily attributed to the 400% increase in flexural stiffness as opposed to the 67% increase in axial stiffness.

The results of testing unbalanced joints (different adherend thicknesses) shows a reduction in joint strength at 116K ( $-250^{O}$ ) and 394K ( $70^{O}$  F) as was expected. (See Figure 7-19.) There was no significant difference at 561K ( $550^{O}$  F). This may be due to the data for the baseline configuration (3A-1B) being low (See 50.8mm (2.0 inch) data on Figure 7-8).

The other single lap joint parameters investigated, laminate stacking sequence and tapered adherend ends, were only tested at 294K ( $70^{\circ}$  F). Results are compared to baseline data in bar graph form in Figures 7-20 and 7-21 and are discussed below.

The baseline single-lap joint (3A-1B) had adherends of  $(0/\pm45/90)_{3S}$  laminates. To evaluate the effect of ply stacking sequence at the bondline interface two other laminate layups were tested, data set (3A-3A) with  $(\pm45/0/90)_{3S}$  laminates and data set 3A-4A with  $(0_3/\pm45_3/90_3)_S$  laminates. Both layups exhibited failure loads 50% greater than the baseline. As discussed previously, however, test results for data set (3A-1B) may be low and therefore, the increase in performance may not be as great as indicated.

These changes in lay-up were expected to improve the joint performance; however, results of finite element analysis shown in Figures 9-44 and 9-45 indicate that test set (3A-3A) should fail at a lower load than (3A-4A) because of higher peel stresses. Test set (3A-3A) and (3A-4A) each had two specimens that had apparent adhesive failures rather than interlaminar failures. If data for these specimens are ignored the average failure loads become 5.58KN (1254 lbs) and 6.60KN (1484 lbs) respectively. Since failures are attributed primarily to peel stresses, this brings the test data into agreement with the finite element analysis results.

Tapering the 2.5mm (0.10 inch) nominal thick adherends gave a 24% increase in strength over the untapered configuration (See Figure 7-21).

Typical failed specimens for the baseline, increased stiffness, altered stacking sequence and tapered adherend configurations are shown in Figures 7-22 and 7-23. The average weight coefficients for the joint configurations in Figures 7-20 and 7-21 are shown in Figure 7-24. This shows that the  $(0_3/+45_3/90_3)_S$  lay-up (set 3A-4A) is the most weight efficient.

Figures 7-25, 7-26 and 7-27 are comparisons of the "Gr/PI-Gr/PI" joints with "Gr/PI-titanium" joints for 25.4, 50.8 and 76.2mm (1, 2 and 3 inch) lap lengths respectively. Because of thermal stresses it was expected that the "Gr/PI-Gr/PI" joints would be stronger at 116K ( $-250^{\circ}$  F) and 294K ( $70^{\circ}$  F), and would be approximately the same strength as the "Gr/PI-titanium" joints at 561K ( $550^{\circ}$  F). For the 25.4mm (1 inch) lap length the two joint types showed equal failure loads at 116K ( $-250^{\circ}$  F) and 561K ( $550^{\circ}$ F) while at 294K ( $70^{\circ}$  F) the "Gr/PI-Gr/PI" joints were 24% stronger than the "Gr/PI-titanium" joints.

For the 50.8mm (2 inch) lap length case the "Gr/PI-Gr/PI" joints and "Gr/PI-titanium" joints had equal strengths at 116K ( $250^{\circ}F$ ). However the "Gr/PI-titanium" joints were 35% and 80% stronger at 294K ( $70^{\circ}F$ ) and 561K ( $550^{\circ}F$ ) respectively. As noted before the results for data set (3A-1B) appear to be lower than what would be expected from the results of the other test sets. Thus the comparisons here may not be valid.

The results for the 76.2mm (3 inch) lap lengths were as expected. The "Gr/PI-Gr/PI" joints were 93% and 55% stronger at 116K (- $250^{O}F$ ) and 294K ( $70^{O}F$ ) respectively, while at 561K ( $550^{O}F$ ) the "Gr/PI-Gr/PI" joints and "Gr/PI-titanium" joints had approximately equal strengths.

# GR/PI TO GR/PI (0/+-45/90) 33 SINGLE LEP JOINTS

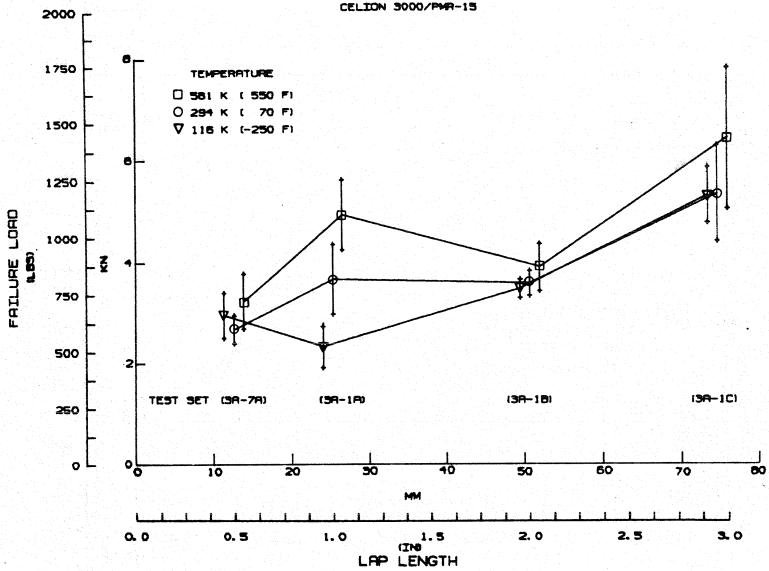


Figure 7-8: EFFECT OF LAP LENGTH

## WEIGHT COEFFICIENT FOR INCREASING LAP LENGTH GR/PI TO GR/PI (0/+-45/90) 35 SINGLE LAP JOINTS

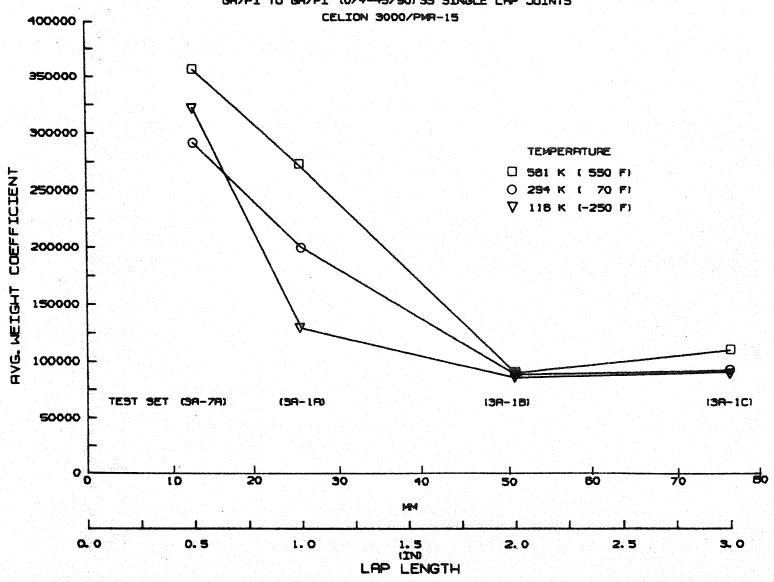
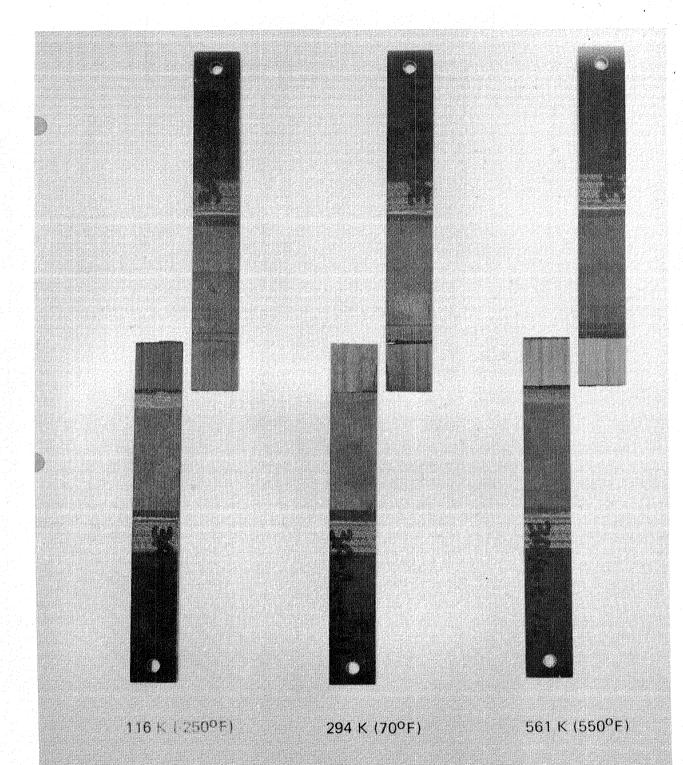


Figure 7-9: WEIGHT COEFFICIENT FOR INCREASING LAP LENGTH



MATRIX 3A Gr/Pi - Gr/Pi - SINGLE LAP

TEST No. 1a

73

Figure 7-10: GR/PI SINGLE LAP, TEST 3A-1A, 25.4 MM (1.0 IN) LAP LENGTH - FAILED SPECIMENS

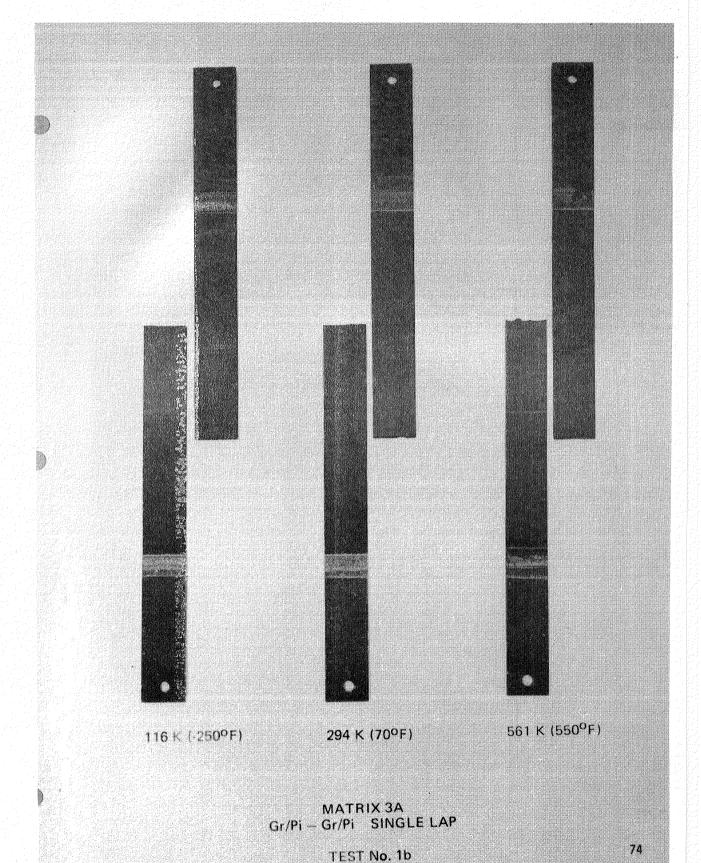
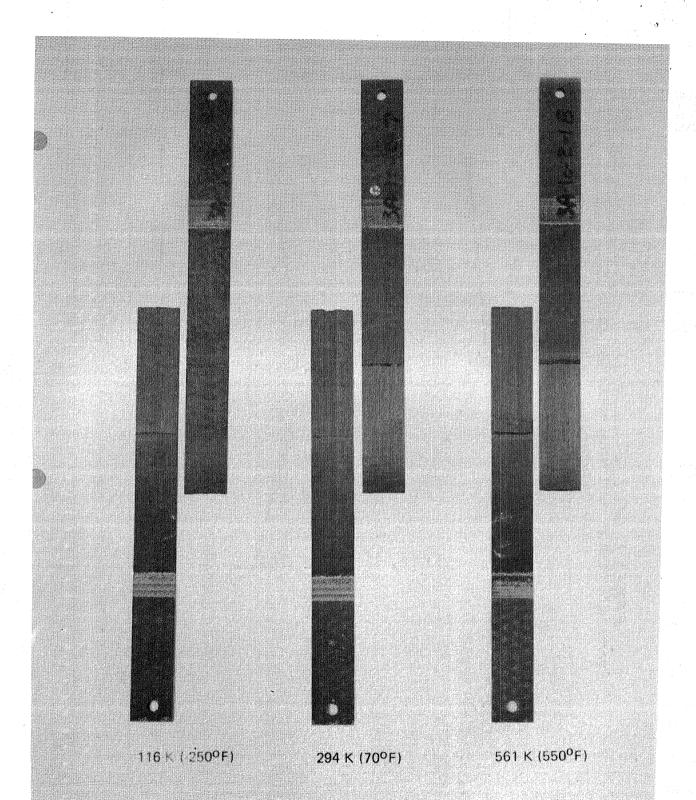


Figure 7-11: GR/PI SINGLE LAP, TEST 3A-1B, 50.8 MM (2.0 IN) LAP LENGTH - FAILED SPECIMENS



MATRIX 3A Gr/Pi — Gr/Pi SINGLE LAP

TEST No. 1c

75

## EFFECT OF LAP LENGTH GR/PI (0/+-45/90) 35 TO TITANIUM SINGLE LAP JOINTS 2000 1750 TEMPERATURE V 118 K (-250 F) 1500 5 1250 FAILURE LOAD (LBS) 1000 750 500 (38-1C) TEST SET (38-1A) (38-18) 250 o L 20 30 50 10 MM 3. 0 0. 5 1.0 LAP LENGTH 0.0 2. 0 2. 5

Figure 7-13: EFFECT OF LAP LENGTH

# WEIGHT COEFFICIENT FOR INCREASING LAP LENGTH GR/PI (0/+-45/90) 99 TO TITRIUM SINGLE LAP JOINTS

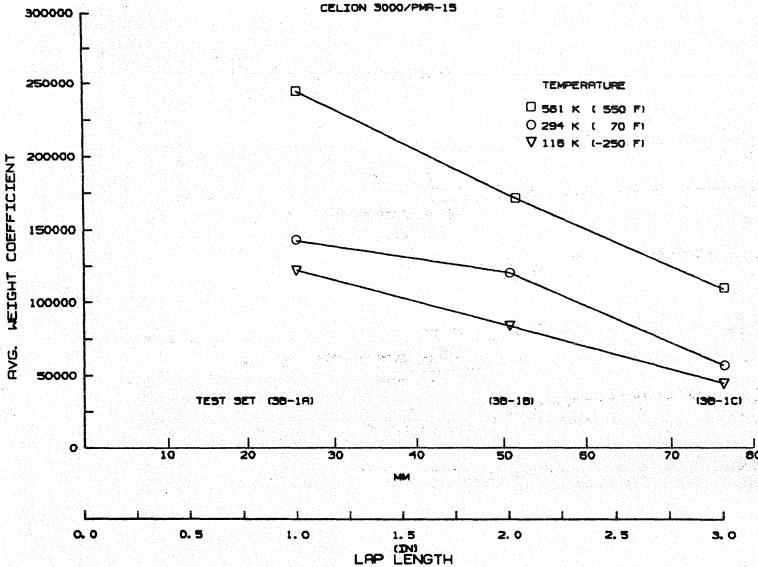


Figure 7-14: WEIGHT COEFFICIENT FOR INCREASING LAP LENGTH

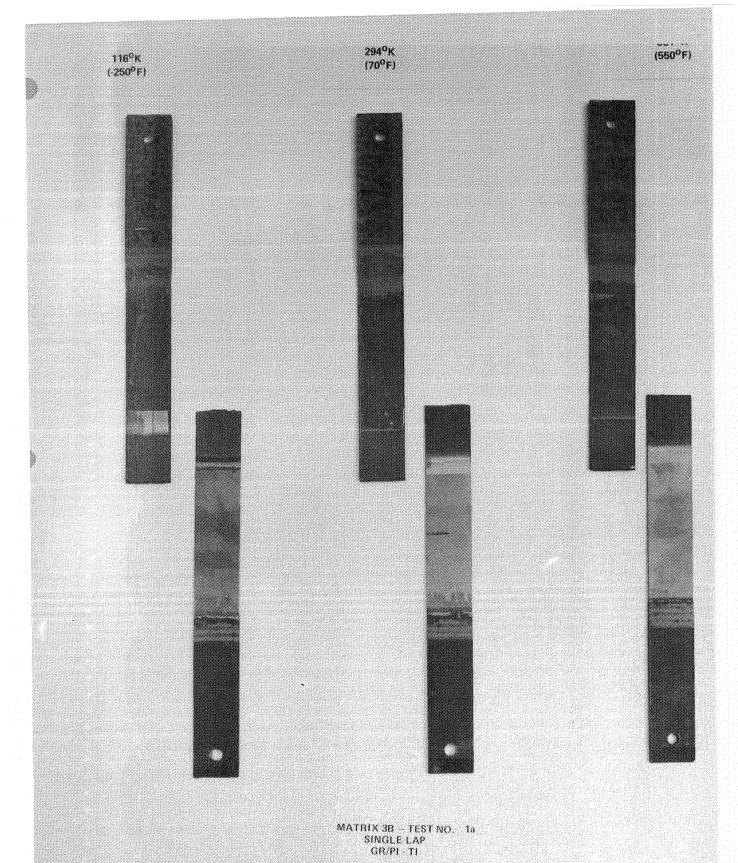
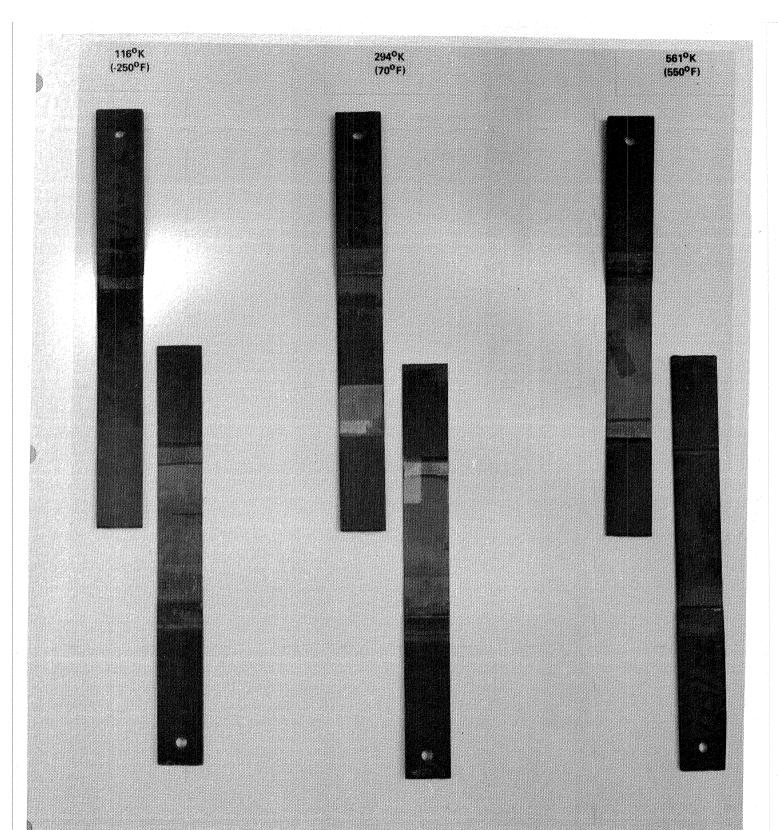
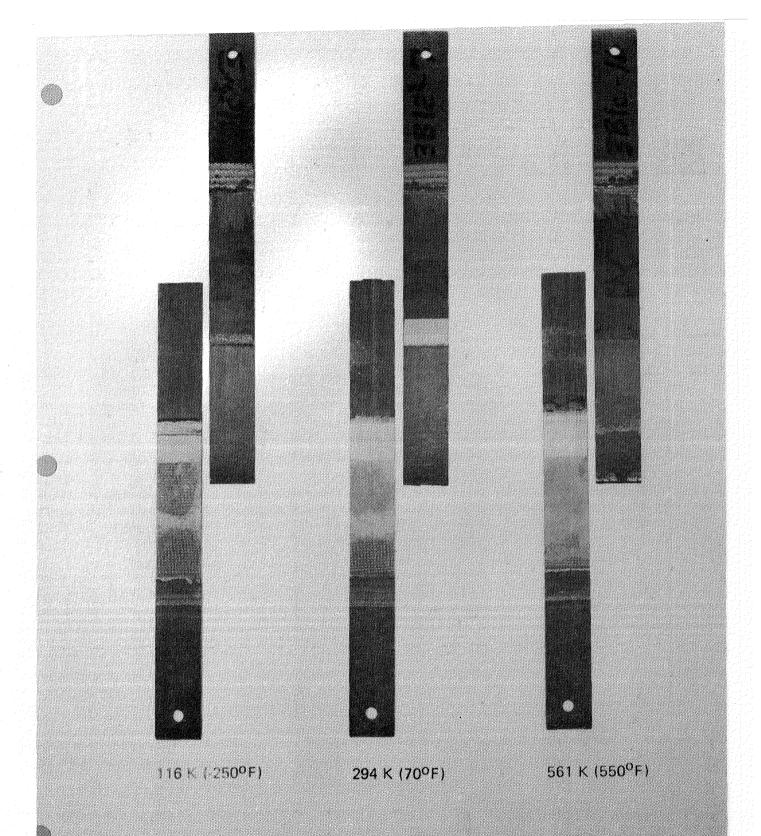


Figure 7-15: GR/PI-Ti SINGLE LAP, TEST 3B-1A, 25.4 MM (1.0 IN) LAP LENGTH - FAILED SPECIMENS



MATRIX 38 — TEST NO. 16 SINGLE LAP GR/PI - TI

Figure 7-16: GR/PI-Ti SINGLE LAP, TEST 3B-1B, 50.8 MM (2.0 IN) LAP LENGTH - FAILED SPECIMENS



MATRIX 3B Gr/Pi — Titanium SINGLE LAP

TEST No. 1c

80

Figure 7-17: GR/PI-Ti SINGLE LAP, TEST 3B-1C, 76.2 MM (3.0 IN) LAP LENGTH - FAILED SPECIMENS

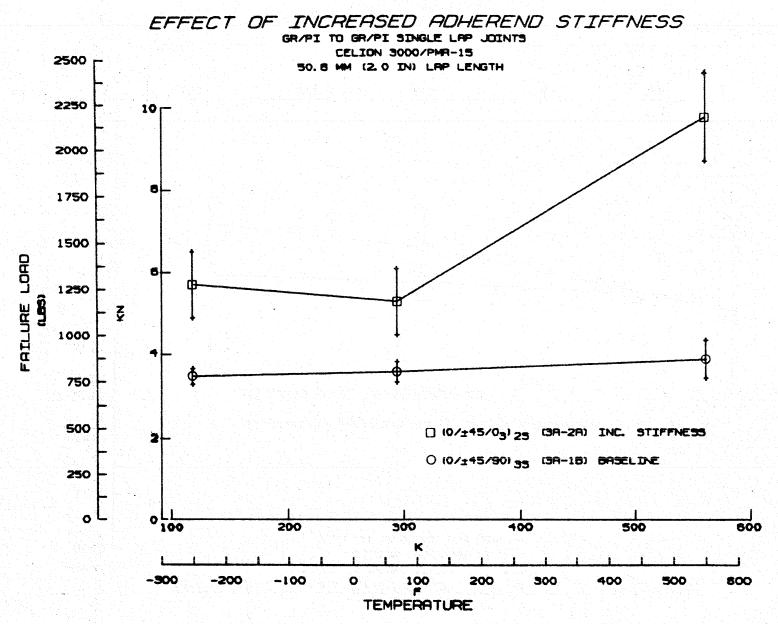


Figure 7-18: EFFECT OF INCREASED ADHEREND STIFFNESS

#### EFFECT OF ADHEREND STIFFNESS IMBALANCE

50. 8 MM (2. 0 IN) LAP LENGTH □ (0/±45/90) 25/ (0/±45/90) 45 (3R-5A) UNBALANCED O 10/±45/901 35 (3A-18) BALANCED FAILURE LOGO 100 2 TEMPERATURE -300 -200 -100 

Figure 7-19: EFFECT OF ADHEREND STIFFNESS IMBALANCE

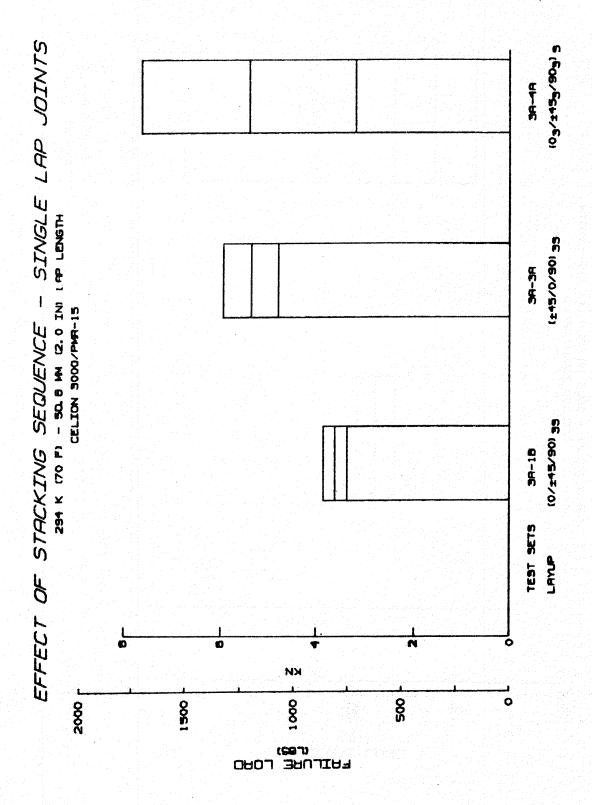


Figure 7-20: EFFECT OF LAMINATE STACKING SEQUENCE - SINGLE LAP JOINTS

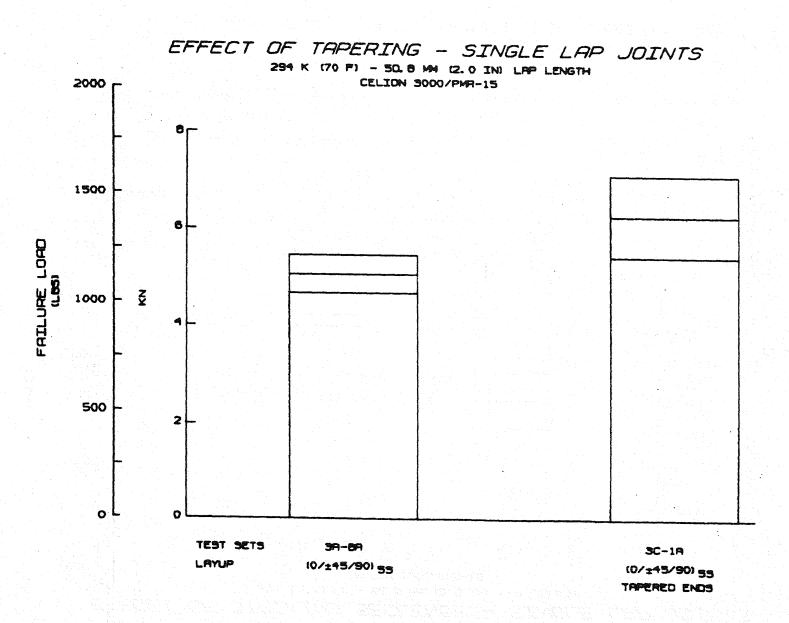
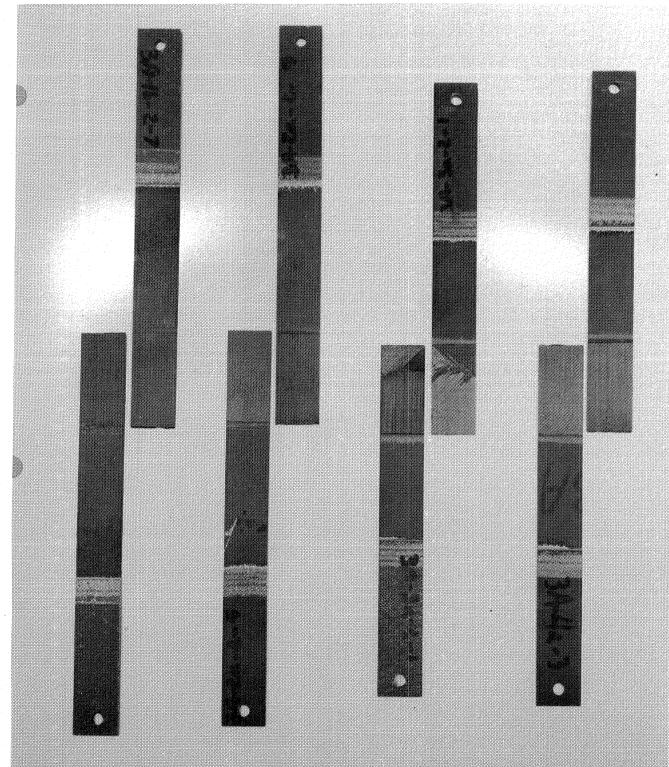


Figure 7-21: EFFECT OF TAPERING - SINGLE LAP JOINTS

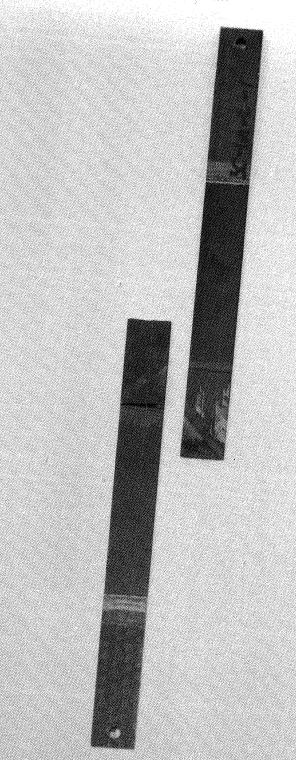


TEST No. 1b TEST No. 2a TEST No. 3a TEST No. 4a

MATRIX 3A Gr/Pi - Gr/Pi SINGLE LAP

294 K (70°F)

Figure 7-22: GR/PI SINGLE LAP, TESTS 3A-1B, 2A, 3A, 4A, 294K (70°F) - FAILED SPECIMENS



MATRIX 3C TEST NO 1a SINGLE LAP, TAPERED ADHERENDS GR/PLGR/PI

Figure 7-23: GR/PI SINGLE LAP, (TAPERED), TEST 3C-1A, 25.4 MM (1.0 IN) LAP LENGTH -

# WEIGHT COEFFICIENT - SINGLE LAP JOINTS 294 K (70 F) - 50.8 MM (2.0 IN) LRP LENGTH 200000 CELION 3000/PMR-15 150000 WEIGHT COEFFICIENT 100000 AVG. 50000 TEST SET 3C-1A LAYUP (0/±45/90) 35 (±45/0/90) 35 (03/±453/903) 5 (0/±45/90) 35 10/145/90 55 TAPERED ENDS

Figure 7-24: WEIGHT COEFFICIENT - SINGLE LAP JOINTS

## COMPARISON OF GR/PI-GR/PI AND GR/PI-TITANIUM JOINTS SINGLE LAP JOINTS - 25.4 MM (1.0 IN) LAP LENGTH

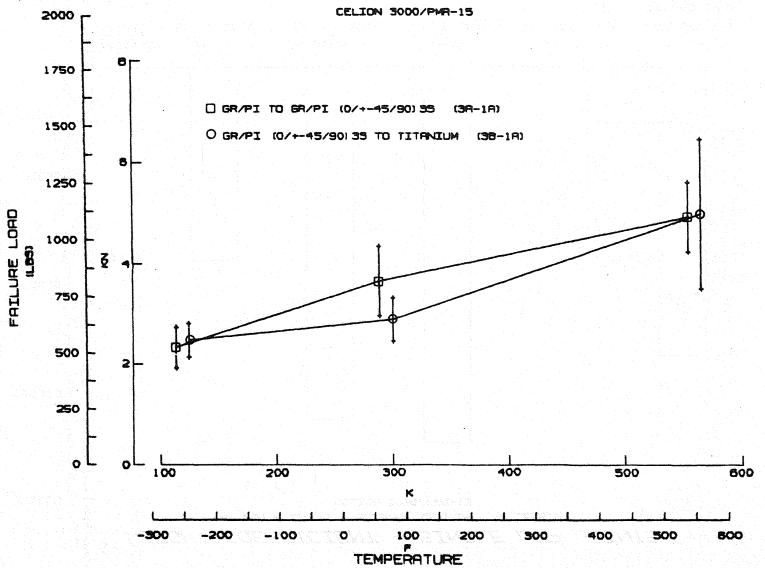


Figure 7-25: COMPARISON OF GR/PI-GR/PI AND GR/PI-TITANIUM JOINT

## COMPARISON OF GR/PI-GR/PI AND GR/PI-TITANIUM JOINTS SINGLE LAP JOINTS - 50.8 MM (2.0 IN) LAP LENGTH FAILURE LOAD ☐ GR/PI TO GR/PI (0/+-45/90) 33 O GR/PI (0/+-45/90) 35 TO TITANIUM -200 -100 TEMPERATURE

Figure 7-26: COMPARISON OF GR/PI-GR/PI AND GR/PI-TITANIUM JOINT

## COMPARISON OF GR/PI-GR/PI AND GR/PI-TITANIUM JOINTS

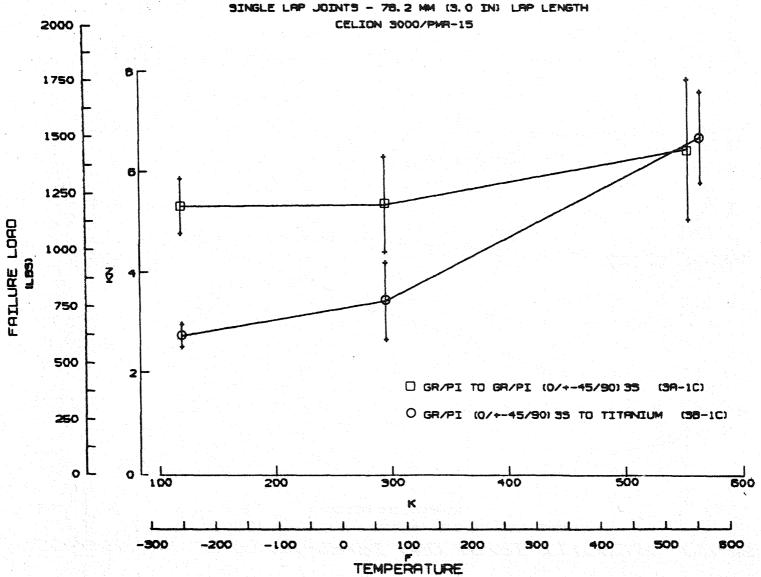


Figure 7-27: COMPARISON OF GR/PI-GR/PI AND GR/PI-TITANIUM JOINT

#### 7.2.2 Double-Lap Joints

Double-lap joint test results have also been plotted showing average failure loads with the plus/minus one standard deviation range for each data set. As done for the single-lap joints, some of the data points are shifted slightly in the abscissa direction to prevent overlap of the vertical standard deviation lines.

Figures 7-28 and 7-29 show load versus lap length for the "Gr/PI-Gr/PI" double-lap joints for the three temperatures tested. Results are shown for the 2.03mm (.08 inch) and 3.05mm (.12 inch) nominal thickness inner adherend configurations respectively. For the 2.03mm (.08 inch) case there is little variation in failure load with lap length over the range of the lengths tested. This suggests that the optimum lap length for 2.03mm (.08 inch) thick adherends is less than 20.3mm (.8 inch). The effect of temperature is quite small with the 116K ( $-250^{\circ}$ F) results being slightly greater than the 294K ( $70^{\circ}$ F). In contrast, the results for the 3.05mm (.12 inch) thick adherend case show a greater dependence on lap length. The failure load increases for all temperatures when going from a 20.3mm (.8 inch) to a 33.0mm (1.3 inch) lap length; however, the failure load levels out when the lap length is increased to 45.7mm (1.8 inch). This indicates that increasing the adherend thickness also increases the optimum lap length. The effect of temperature is not consistent. The 20.3mm (.8 inch) and 45.7mm (1.8 inch) lap lengths show an increase in failure load with temperature while the 33.0mm (1.3 inch) lap length is the opposite. There is no explanation why the results for the 33.0mm (1.3 inch) lap length are the reverse.

The average weight coefficients versus lap length for the 2.03mm (.08 inch) and 3.05mm (.12 inch) thick adherend configurations are shown in Figures 7-30 and 7-31. Like the single-lap joints, the shortest lap lengths are the most weight efficient. Figures 7-32 through 7-34 show typical failed specimens for the three lap lengths tested for the 3.05 mm (.12 inch) thick configuration.

The effect of increasing the adherend thickness of double lap joints for a 33mm (1.3 inch) lap lengths is presented in Figures 7-35 and 7-36. Shown are the average failure loads, structural joint efficiencies and average weight coefficients for 116K (-250°F), 294K (70°F) and 561K (550°F). As expected the failure load appears to level off with increasing thickness, while the joint efficiency and weight coefficients decline.

)

)

The effect of a stiffness imbalance between the inner and outer adherends of a double-lap joint is presented in Figure 7-37. This effect can be evaluated in three ways. A balanced joint (3D-2B) can be compared to an unbalanced joint (3D-6A) with the same outer adherend thickness and thinner inner adherend. Compared this way the unbalanced joints fail at a much lower load (about 40%) than the balanced joints. However this is not a good comparison as the inner adherend thicknesses are not the same, and a lower load would be expected for the joint with a smaller inner adherend thickness, even if balanced. Another comparison involves a balanced joint (3D-1B) and an unbalanced joint (3D-6A) with the same inner adherend thickness and a thicker outer adherend. In this case the balanced joints are only about 10% stronger than the unbalanced joints. The third possible comparison would be to compare balanced and unbalanced joints with the same inner adherend thickness and a thinner outer adherend on the unbalanced joint. No tests were conducted to make this latter comparison.

Increasing the axial and flexural stiffness of the adherends was expected to increase the failure load. Results of increasing the stiffness are shown in Figure 7-38. There was no change in failure load from the baseline at 116K ( $-250^{\circ}F$ ) and only a slight increase in load at 294K ( $70^{\circ}F$ ). At 561K ( $550^{\circ}F$ ) the increased stiffness configuration was 76% stronger than the baseline. Typical failed specimens are shown in Figure 7-39.

The effect of the laminate stacking sequence is shown in Figure 7-40. At 116K (-250°F) and 294K ( $70^{\circ}$ F) the ( $0/\pm45/90$ ) and ( $\pm45/0/90$ ) laminates have roughly equal strengths while the ( $0_3/\pm45_3/90_3$ ) laminate is 30% and 10% weaker. However, at 561K ( $550^{\circ}$ F) the ( $\pm45/0/90$ ) laminate is 50% stronger and the

 $(0_3/\pm45_3/90_3)$  laminate 15% stronger than the  $(0/\pm45/90)$  laminate. Typical failed specimens for the baseline, and altered stacking sequence configurations are shown in Figure 7-39. It should be noted that the results for the  $(0/\pm45/90)$  (3D-2B) configuration appear to be suspect, as the failure load declines with temperature. (These specimens were made from material lot 2W4582 which had only 51.4% fiber volume as discussed in Section 7.2.1.) This is in contrast to the trend of increasing load with increasing temperature shown by most of the other test sets. As stated before there is no apparent explanation for this anomaly.

Finite element analyses were performed on the above adherend lay-ups as discussed in Section 9.1.2. Results of the analyses showed ±5% type changes in peak adhesive shear stresses and inner adherend peel stresses from the baseline (0/±45/90) lay-ups. These differences are too small to pick up by the test results because of the large data scatter. The analyses do show, however, that the peak peel stresses occur in the inner adherend and therefore, interlaminar peel failures should initiate on the inner adherend. Examination of the specimens showed that all the "Gr/PI-Gr/PI" double-lap joints had intralaminar peel failures on the inner adherend. All specimens also had intralaminar failures on the doubler splice plate interface. These were probably secondary failure modes although it is impossible to tell from the specimens which failure occurred first.

Figure 7-41 shows the effect of tapering the ends of the outer adherends in order to reduce the peel stresses in the inner adherend. Tapering resulted in an 18% increase in load at 294K ( $70^{O}F$ ) and a 7% increase at 561K ( $550^{O}$  F). Figure 7-42 shows typical failed specimens for the tapered adherend joints.

Figures 7-43 and 7-44 show load versus lap length and temperature of "Gr/PI-titanium" double-lap joints. The data show the effect of lap length is temperature dependent. Increasing the lap length resulted in increased failure loads at 561K ( $550^{O}F$ ) and decreased loads at 294K ( $70^{O}F$ ) and 116K ( $-259^{O}F$ ). Because of residual stresses in these joints due to the differences in coefficients of thermal expansion of Gr/PI and titanium, the failure load

was expected to increase with temperature (i.e. as the stress free state was approached). This was not the case with the 20.3mm (.8 inch) lap length configuration (See Figure 7-44). The reason for this may be found by examining the failure mode of the joints. Unlike the rest of the joints tested, all of the elevated temperature 561K (550°F) Gr/PI-titanium double-lap joints showed significant amounts of cohesive failures, up to one-third of the total bond area. The shorter lap length joints exhibited adhesive failures over a greater percentage of the bond area than the longer lap length joints. This explains why the failure load for the 20.3mm (.8 inch) lap length joints was approximately the same at 294K (70°F) and 561K (550°F). At the elevated temperature the ultimate average adhesive shear stress was exceeded resulting in a different failure mode. Although the room temperature specimens showed an intralaminar failure, adhesive failure may have been imminent. Figures 7-45 through 7-47 show typical failed specimens for the three lap lengths tested.

)

)

The average weight coefficient versus lap length is shown in Figure 7-48 for the "Gr/PI-titanium" double-lap joints. This indicates that there is a large "weight penalty" in increasing the lap length from 20.3mm (.8 inch) to 45.7mm (1.8 inch).

The effect of putting  $\pm$  45° plies at the titanium interface for the "Gr/PI-titanium" joints is shown in Figure 7-49. The effect is most pronounced at 116K (-250°F) and lessens as the temperature increases. The ( $\pm$ 45/0/90) laminate is consistently stronger than the (0/ $\pm$ 45/90) baseline laminate, but the difference at 561K (550°F) is small. The reason for the higher strength of the ( $\pm$ 45/0/90) laminate may be due to the  $\pm$ 45° plies at the joint interface reducing the thermal stresses because of a lower tension modulus than a 0° ply.

Figures 7-50 and 7-51 are comparisons of "Gr/PI-Gr/PI"and "Gr/PI-titanium" double-lap joints as a function of temperature. The results of the comparison are inconsistent. With the shorter lap lengths, 20.3mm (.8 inch), the Gr/PI-titanium joints are stronger at all temperatures than the "Gr/PI-Gr/PI"

joints. However with a longer lap length, 45.7mm (1.8 inch), the "Gr/PI-Gr/PI" joints are stronger at 116K (- $250^{O}F$ ) and 294K  $70^{O}F$ ) while the "Gr/PI-titanium" joints are stronger at 561K ( $550^{O}F$ ).

## EFFECT OF LAP LENGTH

GR/PI TO GR/PI (0/+-45/90) 25. 45 DOUBLE LAP JOINTS

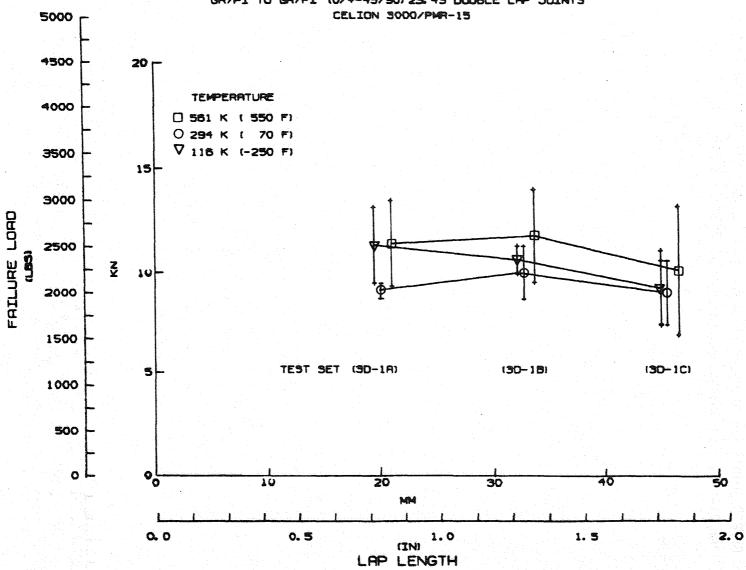


Figure 7-28: EFFECT OF LAP LENGTH

### EFFECT OF LAP LENGTH

## GR/PI TO GR/PI (0/+-45/90) 35.65 DOUBLE LAP JOINTS

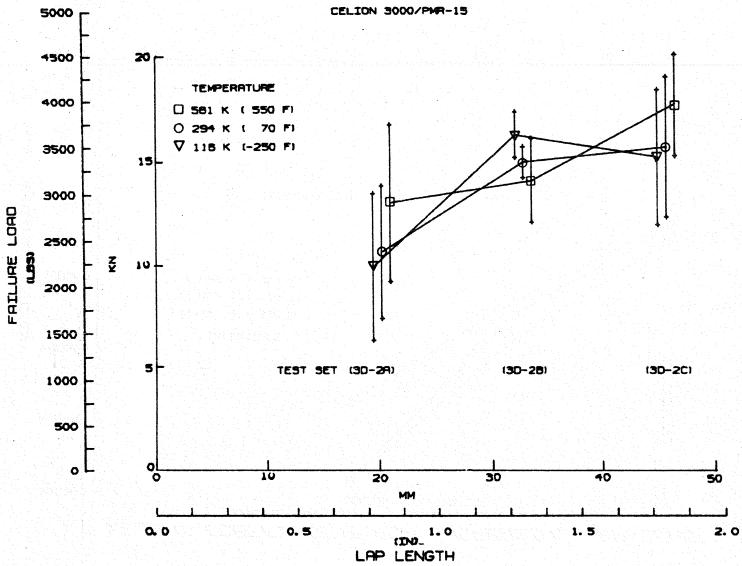


Figure 7-29: EFFECT OF LAP LENGTH

## WEIGHT COEFFICIENT FOR INCREASING LAP LENGTH

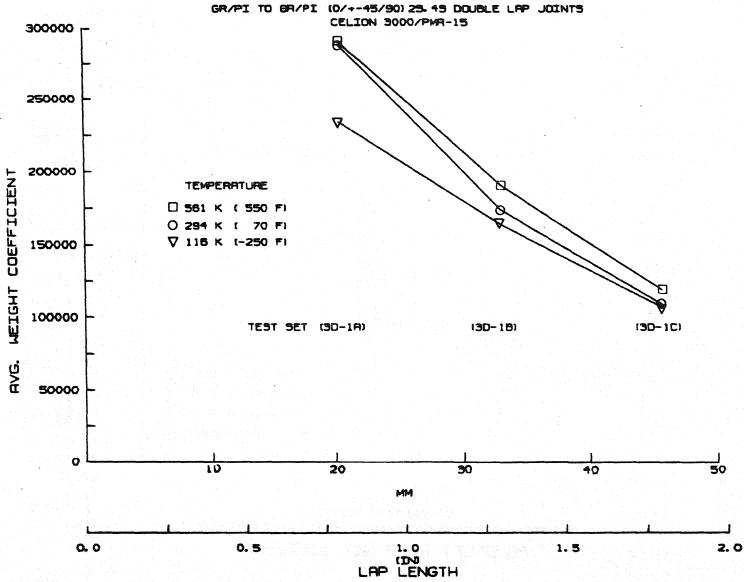


Figure 7-30: WEIGHT COEFFICIENT FOR INCREASING LAP LENGTH

## WEIGHT COEFFICIENT FOR INCREASING LAP LENGTH

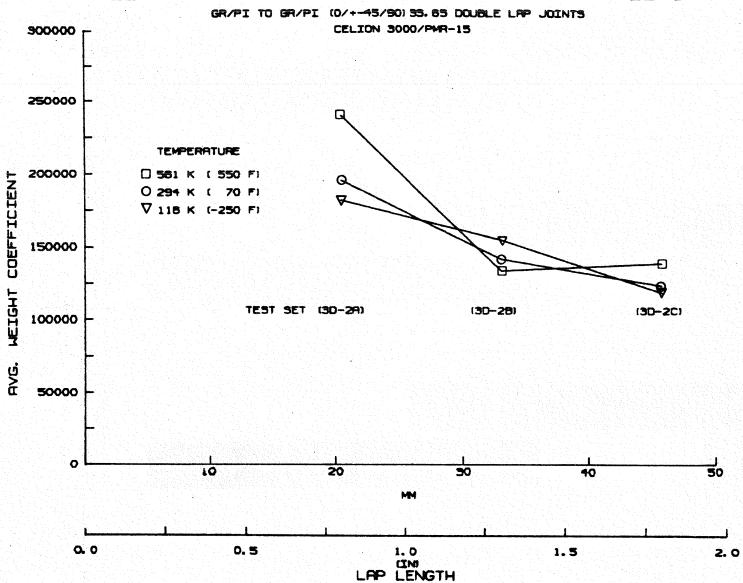
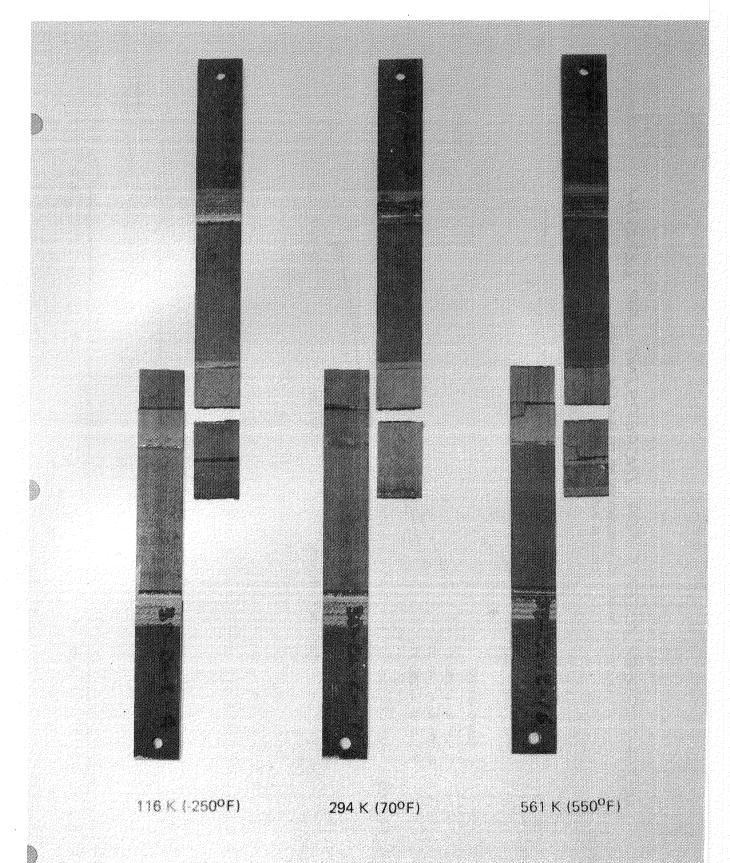


Figure 7-31: WEIGHT COEFFICIENT FOR INCREASING LAP LENGTH

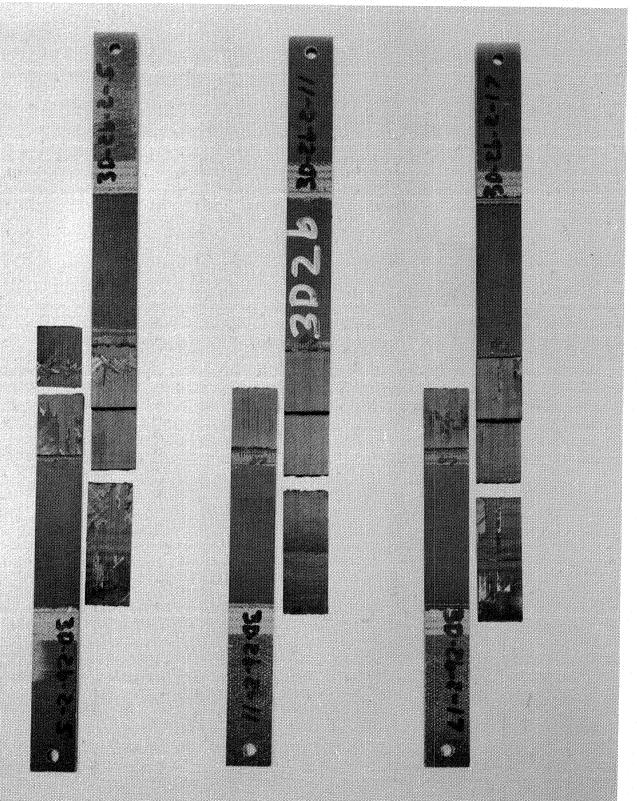


MATRIX 3D Gr/Pi – Gr/Pi DOUBLE LAP

TEST No. 2a

100

Figure 7-32: GR/PI DOUBLE LAP, TEST 3D-2A, 20.8 MM (.8 IN) LAP LENGTH - FAILED SPECIMENS



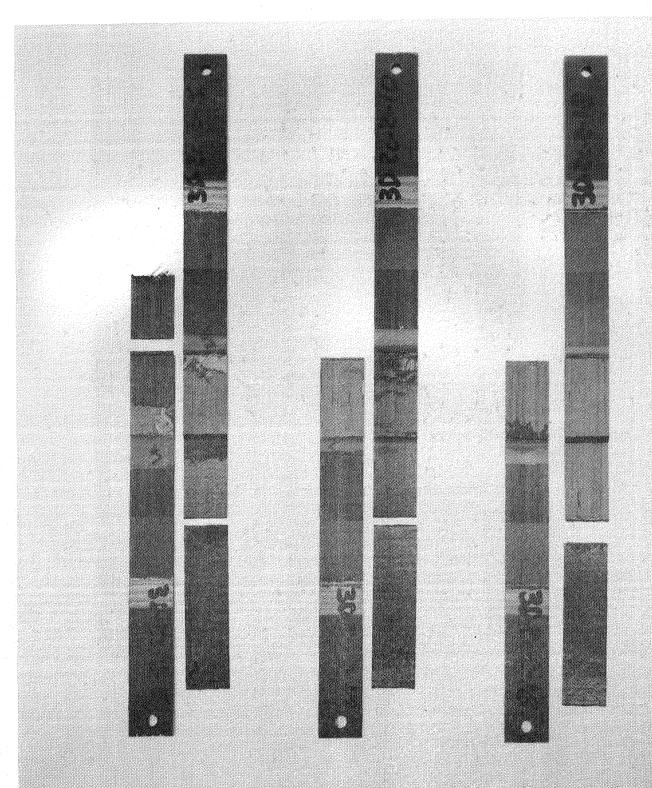
116 K (-250°F)

294 K (70°F)

561 K (550<sup>0</sup>F)

Figure 7-33: GR/PI DOUBLE LAP, TEST 3D-2B, 33.0 MM (1.3 IN) LAP LENGTH - FAILED SPECIMENS

MATRIX 3D Gr/Pi – Gr/Pi DOUBLE LAP



116 K ( 250°F) 294 K (70°F) 561 K (550°F)

MATRIX 3D Gr/Pi – Gr/Pi DOUBLE LAP

TEST No. 2c

102

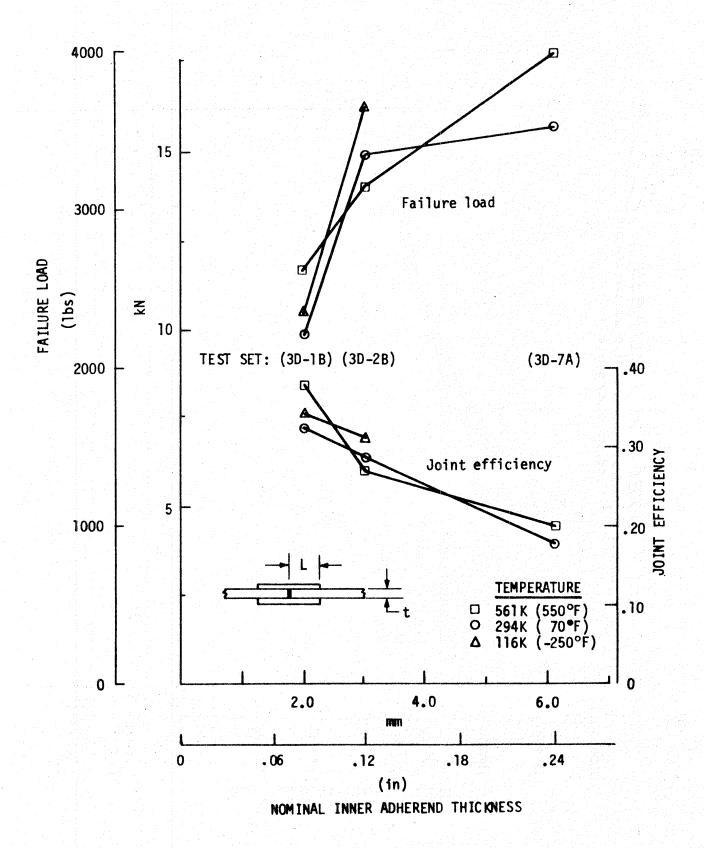


Figure 7-35: EFFECT OF ADHEREND THICKNESS - DOUBLE LAP JOINTS LAP LENGTH = 33.0 mm (1.3 in)

103

# EFFECT OF THICKNESS CELION 3000/PMR-15 200000 175000 150000 WEIGHT COEFFICIENT TEMPERATURE 125000 □ 581 K ( 550 F) O 294 K ( 70 F) V 118 K (-250 F) 100000 TEST SET (90-18) 130-281 (3D-7A) 75000 50000 25000

NOMINAL INNER ADHEREND THICKNESS

Figure 7-36: EFFECT OF THICKNESS

IN

0. 15

0. 20

0. 25

0.10

0.05

0.00

# EFFECT OF ADHEREND STIFFNESS IMBALANCE

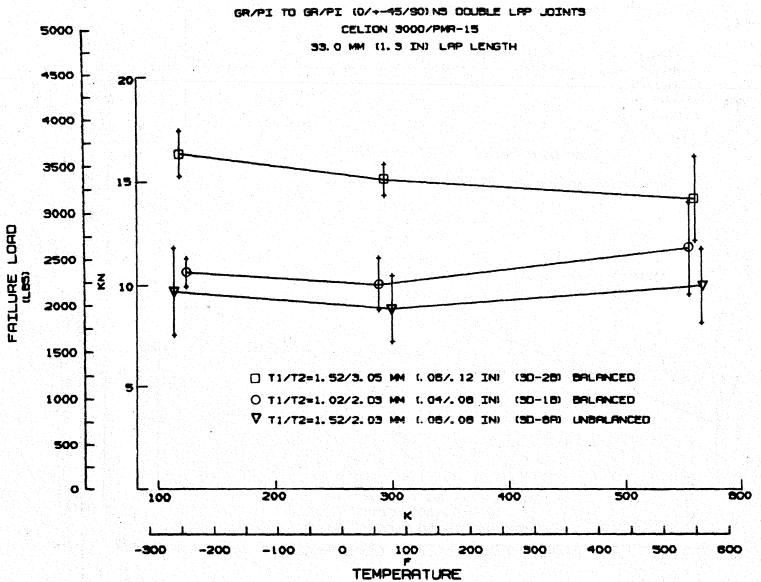


Figure 7-37: EFFECT OF ADHEREND STIFFNESS IMBALANCE

# EFFECT OF INCREASED AXIAL ADHEREND STIFFNESS

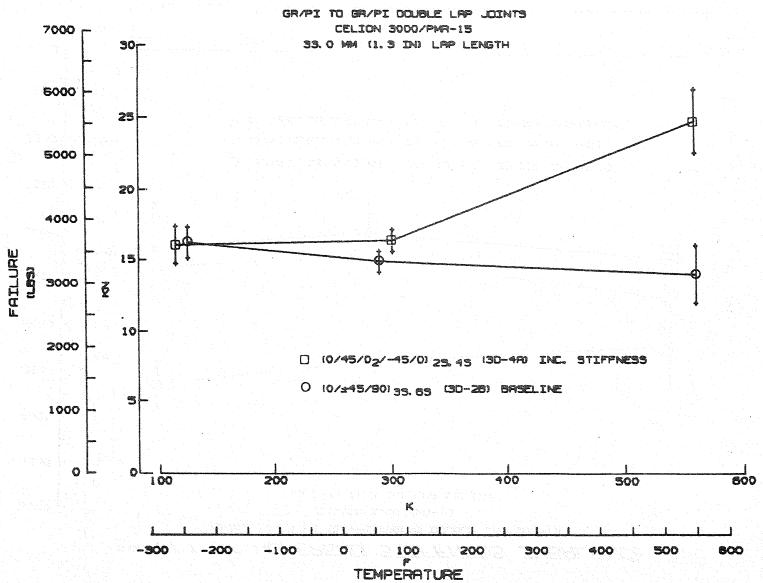
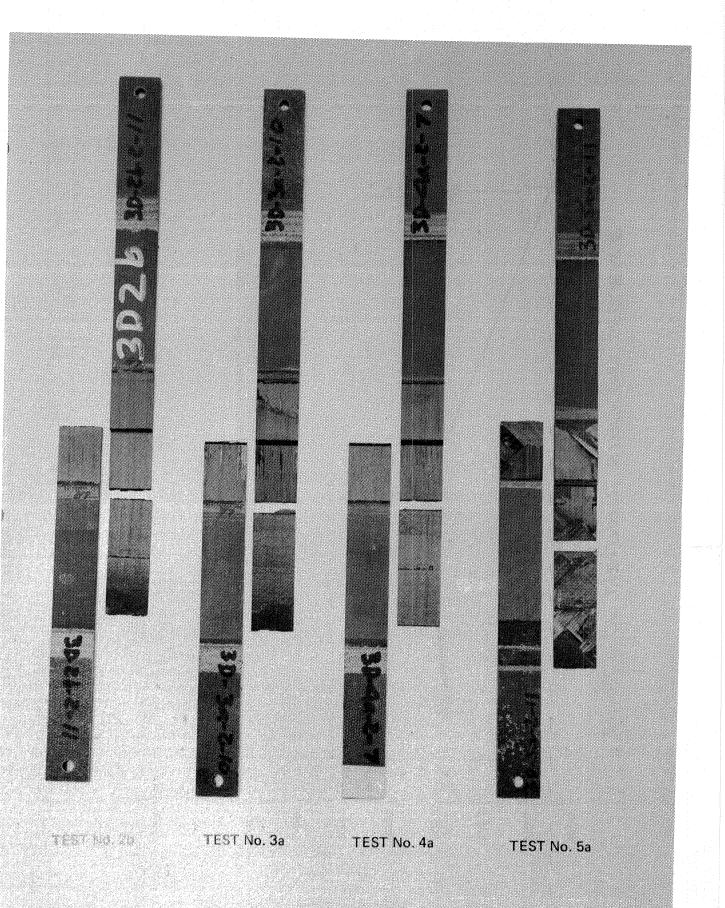


Figure 7-38: EFFECT OF INCREASED AXIAL ADHEREND STIFFNESS



MATRIX 3D Gr/Pi – Gr/Pi DOUBLE LAP

107

# EFFECT OF LAMINATE STACKING SEQUENCE

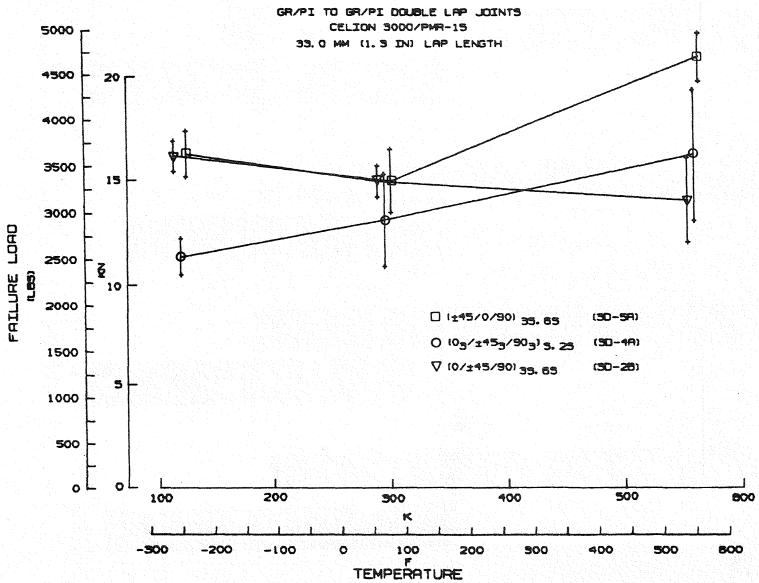


Figure 7-40: EFFECT OF LAMINATE STACKING SEQUENCE

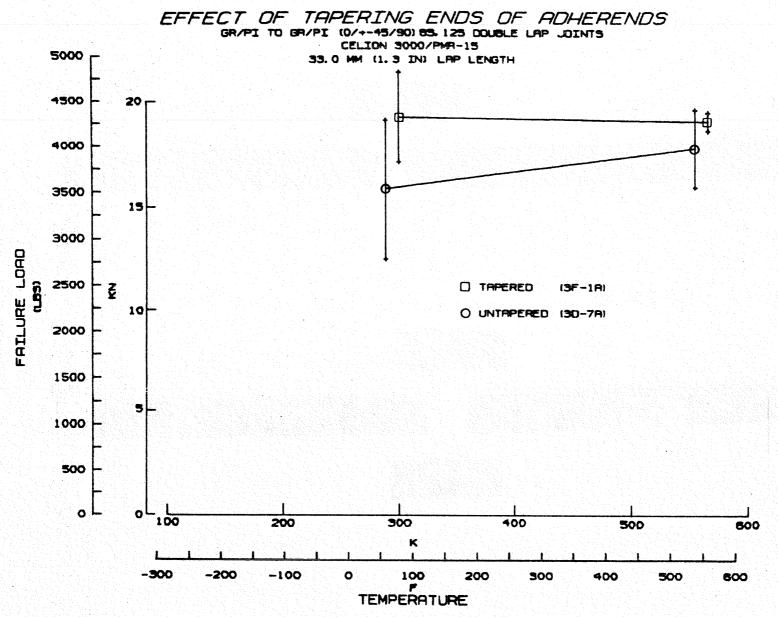
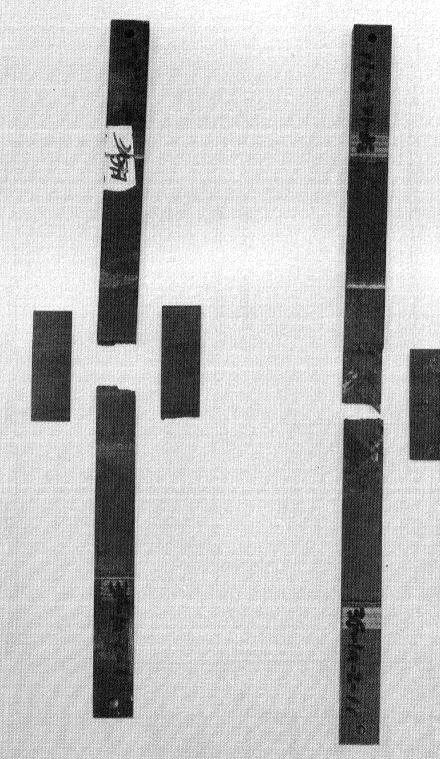


Figure 7-41: EFFECT OF TAPERING ENDS OF ADHERENDS



MATRIX 3F TEST NO. 1a DOUBLE LAP, TAPERED ADHERENDS GR/PLGR/PI

Figure 7-42: GR/PI DOUBLE LAP (TAPERED), TEST 3F-1A, 33.0 MM (1.3 1) LAP LENGTH - FAILED SPECIMENS

# EFFECT OF LAP LENGTH

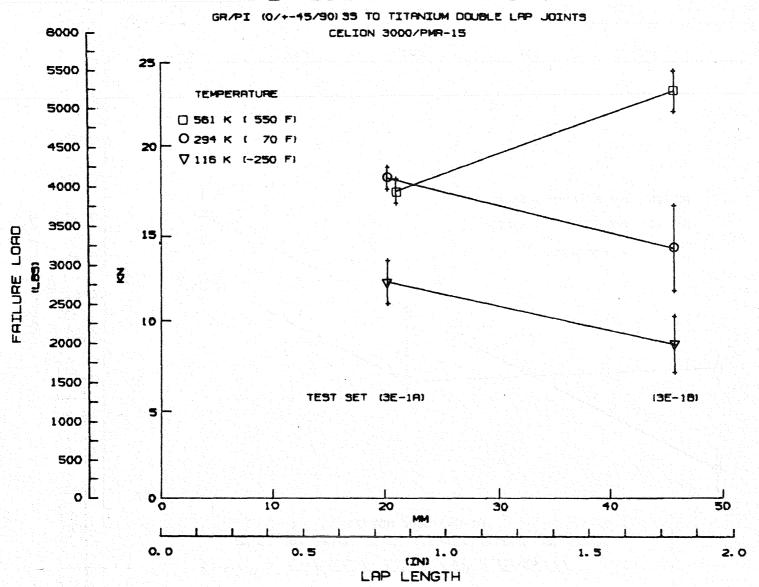


Figure 7-43: EFFECT OF LAP LENGTH

# EFFECT OF LAP LENGTH .

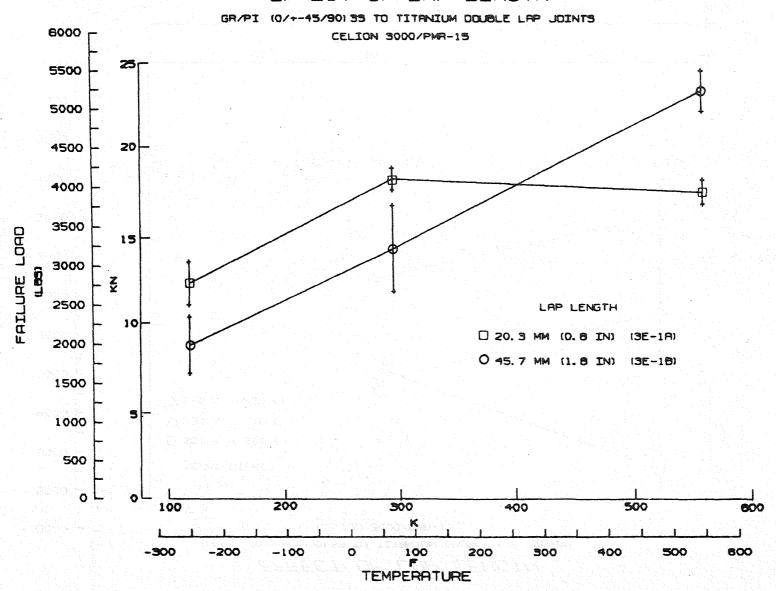


Figure 7-44: EFFECT OF LAP LENGTH

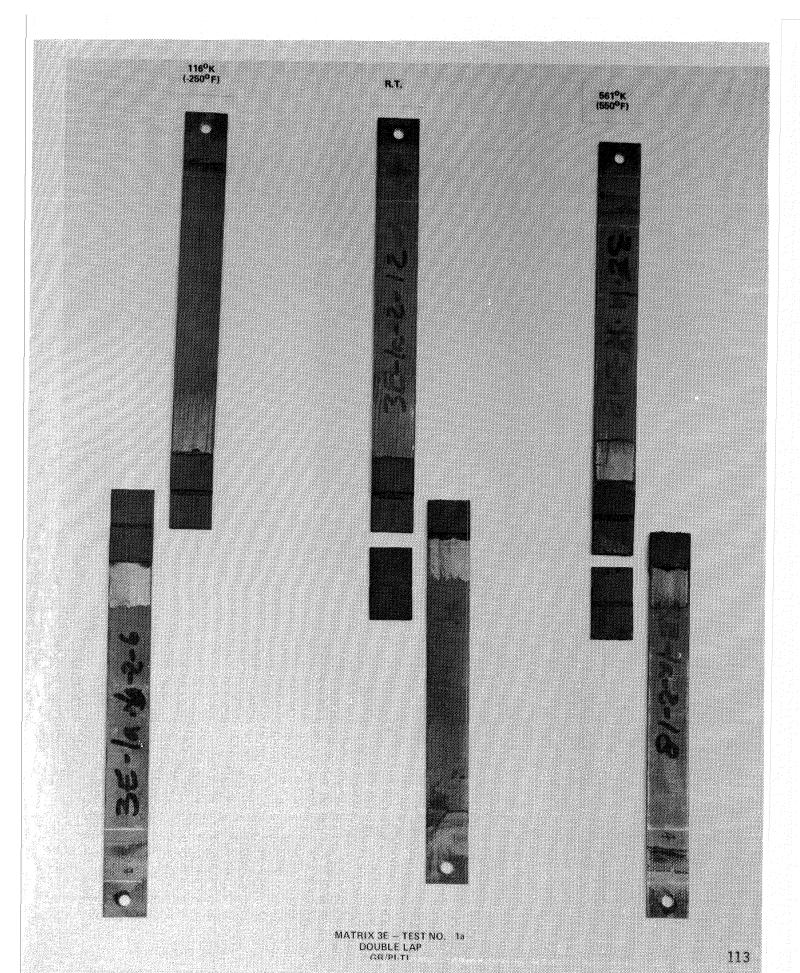
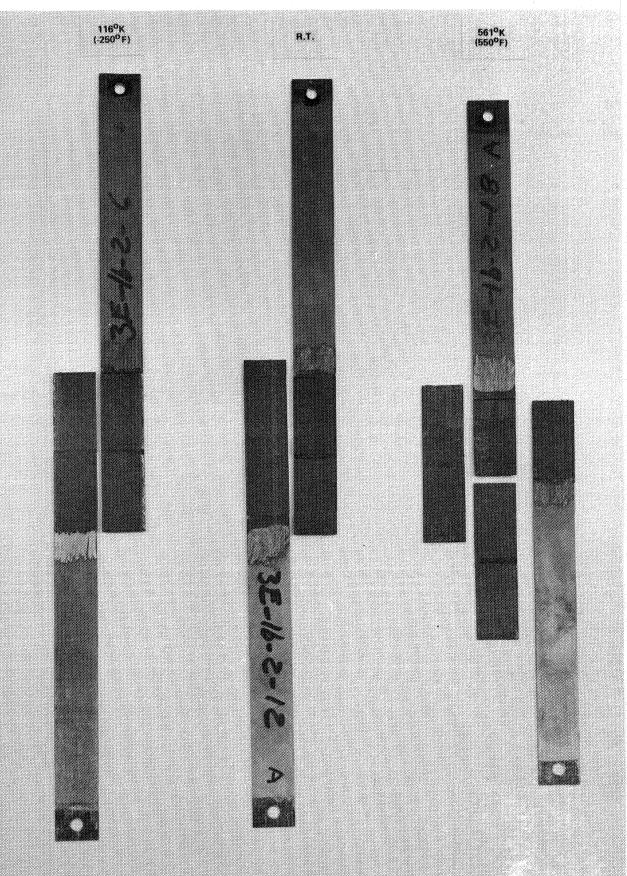


Figure 7-45: GR/PI-Ti DOUBLE LAP, TEST 3E-1A, 20.8 MM (.8 IN) LAP LENGTH - FAILED SPECIMENS



MATRIX 3E - TEST NO. 1b DOUBLE LAP

11

Figure 7-46: GR/PI-Ti DOUBLE LAP, TEST 3E-1B, 46.2 MM (1.8 IN) LAP LENGTH - FALLED SPECIME



MATRIX 3E - TEST NO. 26 DOUBLE LAP GR/PI-TI

115

gure 7-47: GR/PI-Ti DOUBLE LAP, TEST 3E-2A, 46.2 MM (1.8 IN) LAP LENGTH - FAILED SPECIMENS

# WEIGHT COEFFICIENT FOR INCREASING LAP LENGTH

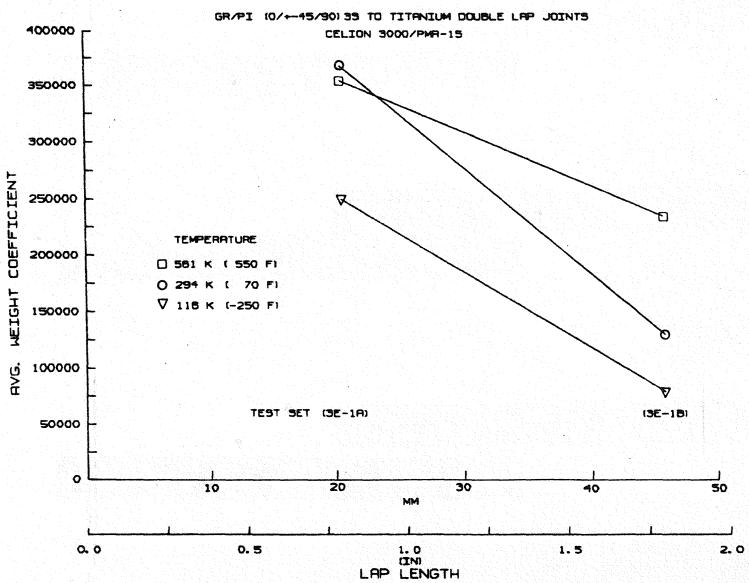


Figure 7-48: WEIGHT COEFFICIENT FOR INCREASING LAP LENGTH

# EFFECT OF LAMINATE STACKING SEQUENCE

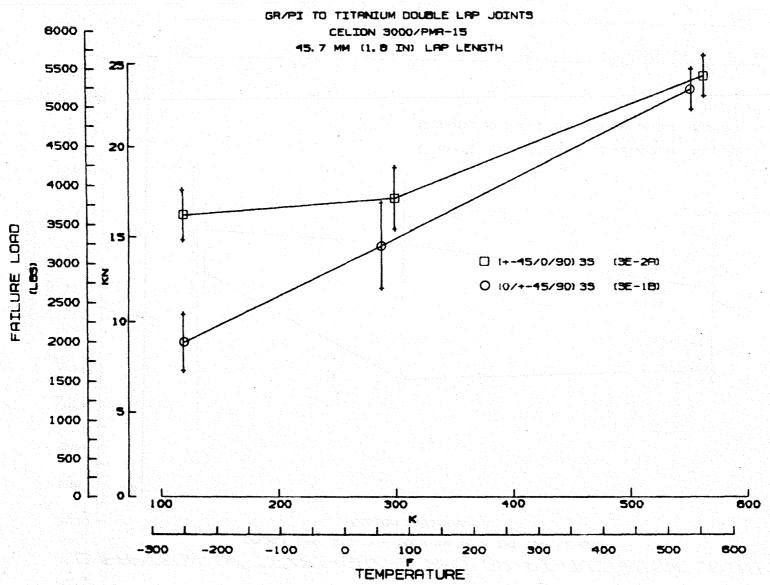


Figure 7-49: EFFECT OF LAMINATE STACKING SEQUENCE

# COMPARISON OF GR/PI-GR/PI AND GR/PI-TITANIUM JOINTS

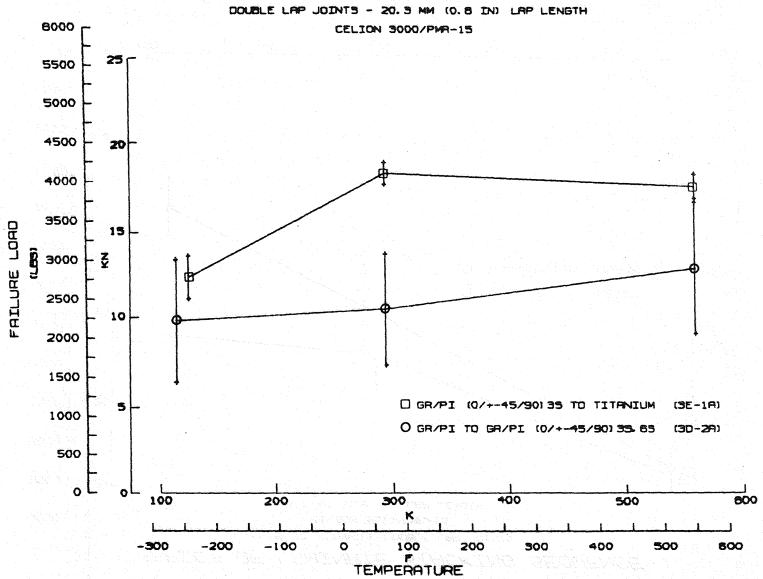


Figure 7-50: COMPARISON OF GR/PI-GR/PI AND GR/PI-TITANIUM JOINT

# COMPARISON OF GR/PI-GR/PI AND GR/PI-TITANIUM JOINTS

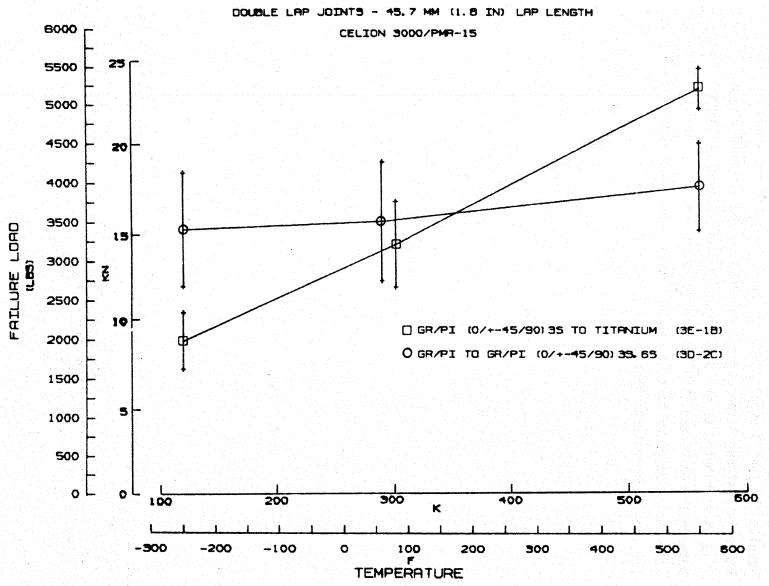


Figure 7-51: COMPARISON OF GR/PI-GR/PI AND GR/PI-TITANIUM JOINT

# 7.2.3 Step Lap Joints

Results for the "3-step" symmetric step-lap joint are shown in Figure 7-52. There is a strong temperature dependence in the strength of these joints. This is attributed to the difference in coefficients of thermal expansion between the Gr/PI and titanium and is as expected. Figure 7-53 shows the step-lap joint prior to test, while Figure 7-54 shows typical failed specimens for the 3 temperatures tested.

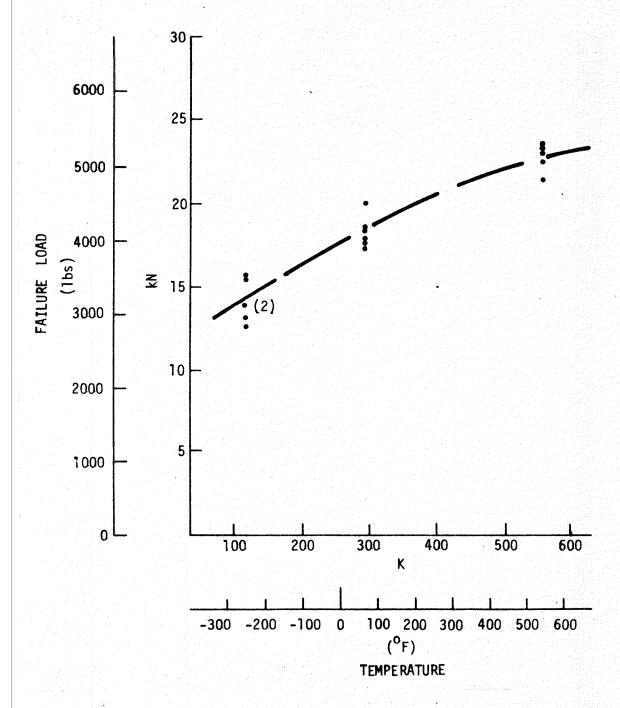


Figure 7-52: "3 STEP" SYMMETRIC STEP LAP JOINT, GR/PI TO TITANIUM

# 921

MATRIX 3G — TEST NO. 1a SYM. STEP LAP

Figure 7-54: GR/PI-Ti SYM. STEP LAP, TEST 3G-1A, 3-STEP - FAILED SPECIMENS

### 7.2.4 Trend Summaries

A summary of the changes in failure loads observed for single and double lap joints due to temperature changes is given in Tables 7-11 and 7-12 respectively. Areas that are crosshatched represent trends that are opposite of what was expected based on theoretical considerations. There are no apparent explanations for these cases other than processing or material variations. In general, failure loads increased with increasing temperature, with the change in loads from cryogenic to room temperature being less than the change in loads from room temperature to elevated temperature. The large data scatter precludes drawing conclusions about the effect of the various joint parameters on the temperature dependence of bonded joints, other than that a thermal expansion imbalance in the joint increases the temperature dependence. However, it appears that the beneficial effects of increased adherend stiffness, tapered adherends, etc. are much greater at 561K (550°F) than at room or cryogenic temperature.

Tables 7-13 and 7-14 summarize the observed trends for single and double lap joints versus the expected results for the various parameters tested: lap length, adherend stiffness, adherend thickness, ply stacking sequence, tapered adherend ends and adherend material. In most cases the observed and predicted trends agree. Exceptions are attributed to material and processing variations.

Table 7-11: EFFECT OF TEMPERATURE CHANGES - SINGLE LAP JOINTS (Based on Averages)

			PERCENT CHANGE IN FAILURE LOAD FROM 294K (70°F) (Read across only)			
TEST NO.	LAYUP	LAP LENGTH mm (in)	116 K (-250°F)	290 K (70°F)	561 K (550°F)	
3A-1a	(0/ <u>+</u> 45/90) <sub>3S</sub>	25.4 (1.0)	-36	REFERENCE	34	
1b	(0/ <u>+</u> 45/90) <sub>3S</sub>	50.8 (2.0)	-3		9	
1c	(0/ <u>+</u> 45/90) <sub>3S</sub>	76.2 (3.0)	-1		20	
2 <b>a</b>	(0/ <u>+</u> 45/0 <sub>3</sub> ) <sub>2S</sub>	76.2 (2.0)	8		85	
3 <b>a</b>	( <u>+</u> 45/0/90) <sub>3S</sub>	76.2 (2.0)				
4a	$(0_3/\pm 45_3/90_3)_S$	76.2 (2.0)				
5 <b>a</b>	(0/+45/90) <sub>2S</sub> / (0/+45/90) <sub>4S</sub>	76.2 (2.0)	-15		42	
6a	(0/+45/90) <sub>5S</sub>	76.2 (2.0)				
7a	(0/ <u>+</u> 45/90) <sub>3S</sub>	12.7 (0.5)	10		21	
3B-1a	(0/ <u>+</u> 45/90) <sub>3S</sub> - Titanium	12.7 (1.0)	-15		71	
1b	(0/ <u>+</u> 45/90) <sub>3S</sub> - Titanium	12.7 (2.0)	-30		44	
1c	(0/ <u>+</u> 45/90) <sub>3S</sub> - Titanium	12.7 (3.0)	-20		93	
3C-1a	(0/ <u>+</u> 45/90) <sub>5S</sub> - (Tapered Ends)	12.7 (2.0)		REFERENCE		

NOTE: Shading indicates results were not as expected.

Table 7-12: EFFECT OF TEMPERATURE CHANGES - DOUBLE LAP JOINTS (Based on Averages)

		PERCENT CHANGE IN FAILURE LOAD FROM 294K (70°F) (Read across only)			
TEST NO.	LAYUP	LAP LENGTH mm (in)	116 K (-250°F)	294 K (70°F)	561 K (550°F)
3D-1a	D-la (0/+45/90) <sub>25,45</sub>		24	REFERENCE	25
1b	(0/±45/90) <sub>25,45</sub>	33.0 (1.3)	6	1. 1. 1. 1. 1. 1. 1. 1. 1. 1. 1. 1. 1. 1	18
1c	$(0/\pm 45/90)_{25.45}$	45.7 (1.8)	2		11
2a	(0/ <del>+</del> 45/90) <sub>3S-6S</sub>	20.3 (0.8)	-6	·	22
2b	(0/ <del>+</del> 45/90) <sub>3S-6S</sub>	33.0 (1.3)	9		-6
2c	$(0/\pm 45/90)_{35.65}$	45.7 (1.8)	-3		13
3a	(0/45/0 <sub>2</sub> /-45/0) <sub>25.45</sub>	33.0 (1.3)	-2		51
4a	$(0_3/\pm 45_3/90_3)_{5.25}$	33.0 (1.3)	-13		24
5a	( <u>+45/0/90</u> ) <sub>3S 6S</sub>	33.0 (1.3)	8		40
6a	$(0/\pm 45/90)_{35.45}$	33.0 (1.3)	10		12
7a	(0/+45/90) <sub>65,125</sub>	33.0 (1.3)			13
3E-1a	(0/+45/90) <sub>35</sub> - Titanium	20.8 (0.8)	-32		-4
1b	$(0/\pm 45/90)_{3S}$ - Titanium	45.7 (1.8)	-38		62
2a	( <u>+45/0/90</u> ) <sub>3S</sub> - Titanium	45.7 (1.8)	-6		41
3F-1a	(0/+45/90) <sub>6S,12S</sub> - Tapered Ends				1
3G-1a	STEP Lap - 50% +45°	38.1 (1.5)	-23	REFERENCE	25

NOTE: Shading indicates results were not as expected.

Table 7-13: EXPECTED VS. OBSERVED TRENDS - SINGLE LAP JOINTS

EXPECTED RESULT	TEST RESULT			
Increasing the lap length increases the strength, increases structural joint efficiency and decreases the weight coefficient.	GR/PI — Agrees at all temperatures.  GR/PI-Titanium — Increase in strength from 25.4 mm  (1.0 in) to 50.8 mm (2.0 in)  Decrease in strength from 50.8 mm  (2.0 in) to 76.2 mm (3.0 in)			
Increasing flexural stiffness of adherends increases strength.	All layups except $(0/\pm45/90)_{3S}$ had same failure loads at 294K $(70^{\circ}F)$ - $(0/\pm45/90)_{3S}$ less than others.			
Increasing adherend thickness increases strength, reduces structural joint efficiency.	Agrees at 294K (70°F)			
A stiffness imbalance between adherends reduces strength.	Agrees at 116K (-250°F) 294K (70°F) No reduction at 561K (550°F)			
Tapering ends of adherends increases strength.	Agrees at 294K (70°F)			

Table 7-14: EXPECTED VS. OBSERVED TRENDS - DOUBLE LAP JOINTS

EXPECTED RESULT	TEST RESULT  GR/PI—Agrees at all temperatures (strength out for longer lap lengths).  GR/PI-Titanium—Agrees at 561K (550°F), does not agree at 116K (-250°F) 294K (70°F)			
Increasing the lap length increases strength, increases structural joint efficiency and decreases the weight coefficient.				
Increasing axial stiffness of adherends increases strength.	Agrees at all temperatures.			
Increasing adherend thickness increases strength, decreases structural joint efficiency and decreases the weight coefficient.	Agrees at all temperatures.			
A stiffness imbalance between adherends decreases strength.	Agrees at all temperatures.			
A "softer" ply group at joint interface (+45 vs 0° & 0°3) increases strength.	GR/PI—Agrees at all temperatures. GR/PI-Titanium—Agrees at all temperatures.			
Tapering ends of outer adherends increases strength.	Agrees at all temperatures.			

# 7.2.5 Comparison of Single and Double-Lap Joints

)

It was expected that double lap joints would have greater structural joint efficiencies than single lap joints. To be more structurally efficient, the double-lap joints with 3.0mm (.12 inch) inner adherends must be more than twice as strong as the single lap joints with 1.5mm (.06 inch) adherends. This is because the basic adherend is twice as thick and therefore twice as strong.

Failure loads versus lap length for single and double-lap joints of "Gr/PI-Gr/PI" and "Gr/PI-titanium" are shown in Figures 7-55 and 7-56 respectively. These shows that the "Gr/PI-Gr/PI" double-lap joints (3mm (.12 inch) adherend) are 3 to 4 times stronger than the corresponding single-lap joints (1.5mm (.06 inch) adherend). "Gr/PI-titanium" double-lap joints are 2 to 6 times stronger than the corresponding single-lap joints.

Structural joint efficiencies of "Gr/PI-Gr/PI" single-lap joints varied from .100 to .270 and for double-lap joints from .178 to .424. Efficiencies of "Gr/PI-titanium" single-lap joints varied from .135 to .382 and for double-lap joints from .238 to .619. The greater efficiency of the double-lap joints results from the elimination of the load eccentricity and corresponding moment inherent in unsupported single lap joints.

Failure loads versus weight increment for "Gr/PI-Gr/PI" and "Gr/PI-titanium" joints are shown in Figures 7-57 and 7-58. As was expected all of the curves approach an asymptote. Joint analyses show that a point is reached where adding more weight to a joint will not increase the strength. Note that these curves are only valid for the specific adherend thicknesses tested. Changing the adherend thicknesses will change the curves.

Figure 7-59 shows average weight coefficient versus lap length for single and double-lap joints. This curve shows that for the same lap length, single and double-lap joints are approximately equal in load carried per unit weight of joint.

GR/PI TO GR/PI JOINTS - AVERAGE FAILURE LOAD VS. LAP LENGTH

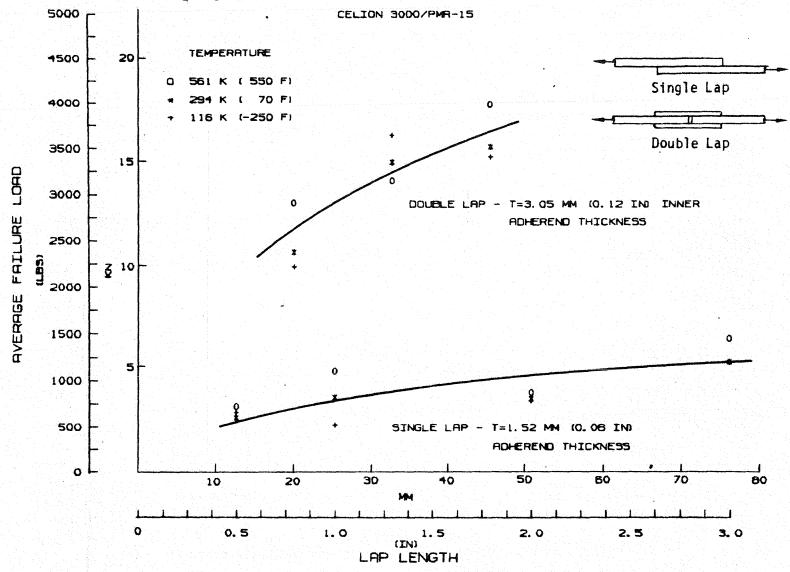


Figure 7-55: COMPARISON OF SINGLE AND DOUBLE LAP JOINTS

GR/PI TO TITANIUM JOINTS - AVG. FRILURE LOAD VS. LAP LENGTH 6000 CELION 3000/PMR-15 5500 TEMPERATURE 5000 Single Lap 70 FI 116 K (-250 F) 4500 Double Lap 4000 AVERAGE FAILURE LOAD 3500 15 3000 2500 T=3. 05 MM (0. 12 IN) ADHEREND THICKNESS 10 2000 1500 1000 SINGLE LAP -T=1.52 MM (0.06 IN) 500 ROHEREND THICKNESS o L 70 10 20 50 60 30 40 MM (IN) 1.5 0 0.5 2. 0 3. 0 1.0 2. 5 LAP LENGTH

Figure 7-56: COMPARISON OF SINGLE AND DOUBLE LAP JOINTS

GR/PI TO GR/PI JOINTS - RVG. FRILURE LOAD VS. HEIGHT INCREMENT

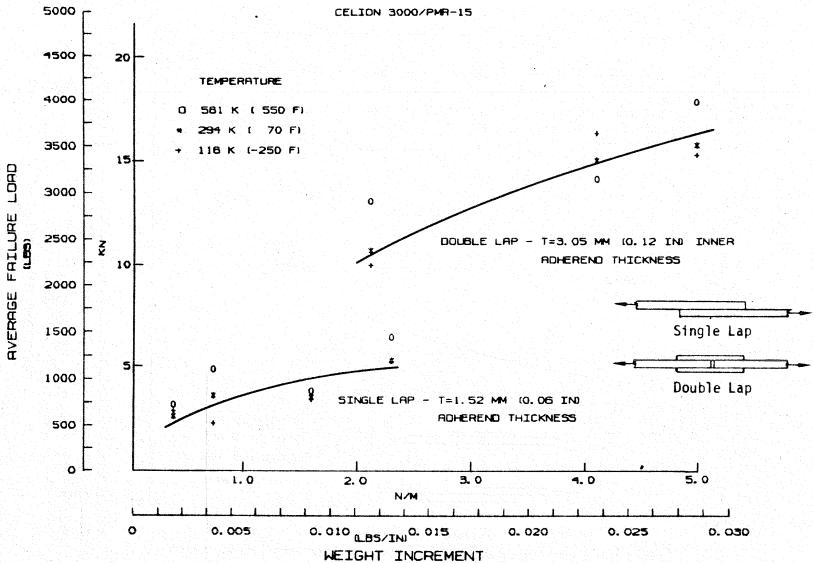


Figure 7-57: COMPARISON OF SINGLE AND DOUBLE LAP JOINTS

GR/PI TO TITANIUM JOINTS - AVG. FRILURE LOAD VS. WEIGHT INCREMENT 8000 CELION 3000/PMR-15 25 5500 TEMPERATURE Single Lap 5000 561 K ( 550 F) 294 K [ 70 F] 4500 116 K (-250 F) Double Lap 4000 AVERAGE FAILURE LOAD 3500 15 3000 T=3. 05 MM (Q. 12 IN) INNER 2500 ADHEREND THICKNESS 10 2000 0 1500 1000 SINGLE LAP - T=1.52 MM (0.06 IN) 500 ADHEREND THICKNESS 0 1 1.0 2. 0 3.0 4. 0 5.0 N/M

Figure 7-58: COMPARISON OF SINGLE AND DOUBLE LAP JOINTS

WEIGHT INCREMENT

0.020

0.025

0. 030

0.005

GR/PI TO GR/PI JOINTS - RVG. WEIGHT COEFFICIENT VS. LAP LENGTH 400000 CELION 3000/PMR-15 350000 TÉMPERATURE 561 K ( 550 F) 300000 294 K [ 70 F] 116 K (-250 F) COEFFICIENT 250000 200000 MEIGHT -DOUBLE LAP - T=3.05 MM (0.12 IN) INNER 150000 ADHEREND THICKNESS 100000 Single Lap SINGLE LAP - T=1.52 MM (0.06 IN) ADHEREND THICKNESS 50000 Double Lap 0 70 10 20 30 50 80 MM 0. 5 1. 5 1.0 2. 0 2.5 3. 0 LAP LENGTH

Figure 7-59: COMPARISON OF SINGLE AND DOUBLE LAP JOINTS

### 8.0 Advanced Bonded Joints

After completion of the standard bonded single and double lap joint testing, several advanced joint design concepts were selected which showed promise of improving the joint efficiency. Concepts selected were performed adherends, scalloped adherends and two hybrid systems. These specimens were fabricated from material lot 3W2187 which had quality control test results slightly lower than required (see Section 8.2). Because of this, standard single and double lap bonded joints were made from the same material lot and tested to provide a baseline for comparing the performance of the advanced joint concepts.

The preformed adherend concept consists of a single lap joint with the adherends angled at the lap ends (see Figure 8-1). Finite element analyses (Ref. 5) have shown that preforming the adherends reduces the stress concentrations in the joint, thus increasing the joint strength. The reduction in peak stresses results from reducing the angle between the line of action of the applied load and the bond line. This in turn reduces the applied bending moments in the adherends and the shear stresses in the joint.

Scalloping the ends of the adherends was expected to improve the joint strength by reducing the peel stress concentrations at the end of the lap.

The two hybrid systems consisted of 1) S-glass/PI fabric softening strips and 2) Gr/PI fabric layers placed between the adherends at the joint interface. These layers were intended to reduce the peak shear and peel stresses in the joint and thus allow a greater load transfer between the adherends.

### 8.1 Advanced Joint Test Matrices

)

The advanced joint test matrix is given in Table 8-1. Specimen configurations are given in Figures 8-1 through 8-7. Photographs of typical specimens before test are shown in Figures 8-8 and 8-9. All specimens were conditioned by soaking at 589K ( $600^{O}F$ ) in a one atmosphere environment (air) for 125 hr.

Tests were conducted at 116K, 294K and 561K ( $-250^{O}F$ ,  $70^{O}F$  and  $550^{O}F$ ). A total of 191 specimens were tested.

### 8.2 Specimen Fabrication

Advanced joint test specimens were fabricated using the procedures and processing described in Section 7.1. All specimens were fabricated from material lot 3W2187. Quality control test results for this material lot are shown in Table 8.2. As shown, the interlaminar shear test results were lower than the specification requirement. It was felt this was a critical parameter because of the interlaminar type failures on the standard bonded joints. Costs and schedule precluded ordering new material, therefore additional baseline tests of standard single and double lap joints were added to the test matrix. Specimens for these tests were made from the same material lot to provide a common baseline against which to measure any improvement in performance of the advanced joint concepts.

To fabricate the preformed adherend specimens, three aluminum tools with  $5^{\rm O}$ ,  $10^{\rm O}$ , and  $15^{\rm O}$  angles were machined from 38.1 mm (1.5 inch) thick 2024-T3 aluminum plate. The length at the angle surface was twice as long as the required lap length. The adherends were laid up as one laminate and then cut in half normal to the lap length to get the two required adherends. When they were bonded together, one bond surface was smooth as it was on the tool surface, and the other bond surface was rough as it was from the bag side. The effect of this on joint strength is not known.

The Celion 3000/PMR-15 prepreg was laid up on the tool per the test matrix, vacuum bagged and cured in one autoclave run using the cure cycle outlined in Reference 1. Ultrasonic C-scans of the panels indicated the the  $5^{\rm O}$  laminates were excellent, that the  $10^{\rm O}$  laminates had some porosities and that the  $15^{\rm O}$  laminates had numerous porosities and delaminations with some blisters on the outer surface.

Analysis of the cured parts indicated that the problem was caused by uneven heating of the parts and tools. The masses of the tools were different due to the amount of aluminum milled away to make the  $5^{\circ}$ ,  $10^{\circ}$  or  $15^{\circ}$  angles, with the  $5^{\circ}$  tool having the greatest mass. Since the autoclave was controlled from the  $5^{\circ}$  tool, the application of pressure for the  $10^{\circ}$  and  $15^{\circ}$  parts was too late for the material to flow properly.

The  $10^{\circ}$  and  $15^{\circ}$  preformed adherend panels were refabricated using a separate autoclave run for each tool. C-scans from all laminates were excellent.

Each preform panel was cut into two equal pieces and bonded with A7F adhesive film per the procedures in Reference 1. Soft aluminum tooling pins were used to maintain proper alignment and overlap distance. Pins were placed in areas (edges) which were trimmed away during specimen cutting.

The baseline and scalloped adherend single and double lap specimens were fabricated from Celion 3000/PMR-15 prepreg laid up per the test matrix, bagged and cured per the procedures in Reference 1. Scalloping of the adherends was done by rough cutting with a router and then hand filing to finished dimensions. The panels were trimmed and bonded with A7F adhesive film as before. During bonding the scalloped areas filled with adhesive. It is thought that this would effect the joint strength, although it is not known for sure.

)

The hybrid (fabric interface) specimens were fabricated from Celion 3000/PMR-15 tape prepreg, S-glass/PMR-15 fabric prepreg, and Celion 3000/PMR-15 fabric prepreg. Adherend laminates were laid up per the test matrix, bagged and cured per the procedures in Reference 1. The S-glass and Gr/PI fabric prepreg plies were co-cured simultaneous with bonding of the fabric to the panels using A7F adhesive.

After the bonded panels were conditioned per the test matrix, individual specimens were cut from the panels using a bandsaw equipped with a carbide blade. Edges of each specimen were sanded after cutting to assure uniformity.

The A7F adhesive film used to fabricate the advanced joint specimens was prepreged by U.S. Polymeric using A7F resin supplied by Boeing.

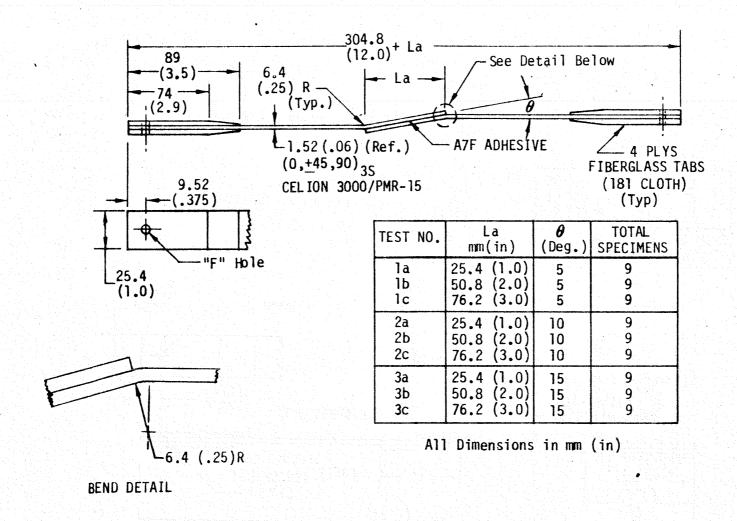
### 8.3 Test Procedures

Tests were conducted using the procedures described in Section 4.2. No special grip offset was provided for the preformed adherend specimens. A typical test set-up with a preformed adherend specimen is shown in Figure 8-10. Specimens were loaded using friction type zapel grips suspended on ball joints to permit automatic load alignment.

Table 8-1: TEST MATRIX 6 - ADVANCED JOINT CONCEPTS

SPEC.	TEST	LAP	NO. OF SPECIMENS AT:			TOTAL
CONFIG.	NO.	LENGTH	116K   294K		561K	SPEC
		mm (in)	(-250F)	(70F)	(550F)	
5 <sup>0</sup> Preformed	1a	25.4 (1.0)	3	3	3	9
	1b	50.8 (2.0)	3	3	3 3	9
See Fig. 8-1	1c	76.2 (3.0)	3	3	3	9
10 <sup>0</sup> Preformed	2a	25.4 (1.0)	3	3	3.100	9
	2b	50.8 (2.0)	3	3 3 0 0 0	3	9
See Fig. 8-1	2c	76.2 (3.0)	3 199	-44. <b>3</b>	3	9
15° Preformed	3a	25.4 (1.0)	3	3	3	9
15 Treformed	3b	50.8 (2.0)	3	3 3 3	3	9
See Fig. 8-1	3c	76.2 (3.0)	3	3	3	9
Scalloped	4a	25.4 (1.0)	:	3	3	6
Single-Lap	4b	50.8 (2.0)		4	4	8
See Fig. 8-2	4c	76.2 (3.0)		3	3	6
Scalloped	5a	20.3 (0.8)		3	3	6
Double-Lap	5b	33.0 (1.3)		3 3 3	3	6
See Fig. 8-3	5c	45.7 (1.8)		3	3	6
Coftoning Ctuin	6a	25.4 (1.0)		3	3	6
Softening Strip Single-Lap	6b	50.8 (2.0)		3 4	4	8
See Fig. 8-4	6c	76.2 (3.0)		3	3	6
Fabric Interfere	<b></b>	05 4 (7 0)		3	3	
Fabric Interface Single-Lap		25.4 (1.0) 50.8 (2.0)		3 4	3 4	6 8
See Fig. 8-5	7c	76.2 (3.0)		3	3	8 6
	0-			3	3	<u>e</u>
Baseline Single-Lap	8a 8b	25.4 (1.0) 50.8 (2.0)		3	3 4	6 8
See Fig. 8-6	8c	76.2 (3.0)		4 3	3	6
Baseline Double-Lap	9a 9b	20.3 (0.8)		3 3	3	6
See Fig. 8-7	טפ	33.0 (1.3)		3	3	
				l		201 7-4-1

191 Total



· Figure 8-1: Advanced Joints - Matrix 6 Preformed Adherends

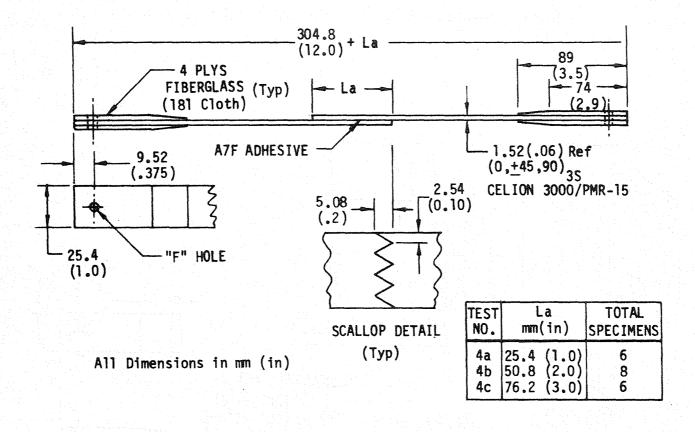


Figure 8-2: Advanced Joints - Matrix 6. Scalloped Single Lap

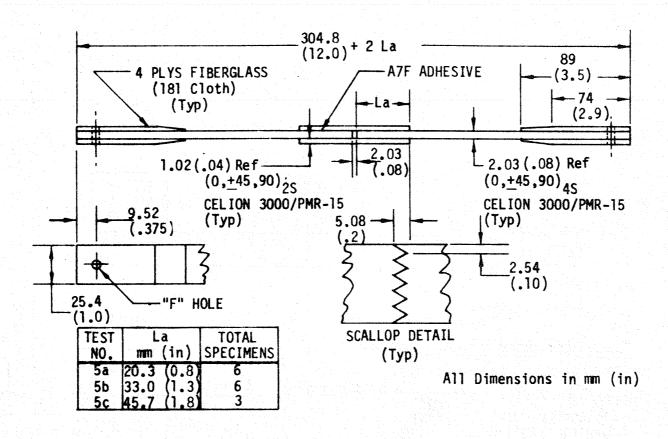


Figure 8-3: Advanced Joints - Matrix 6 Scalloped Double Lap

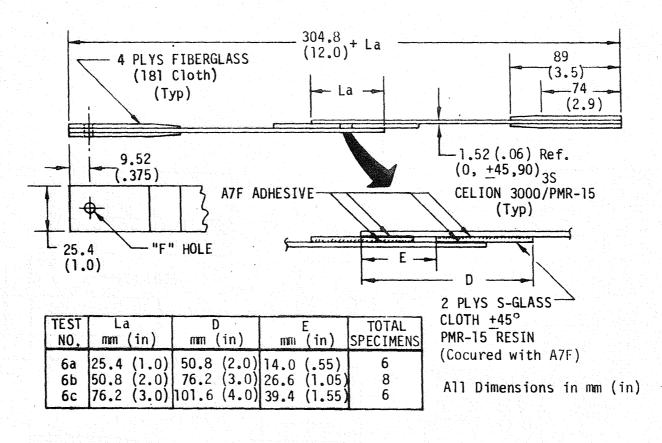


Figure 8-4: Advanced Joints - Matrix 6 Softening Strips - Single Lap

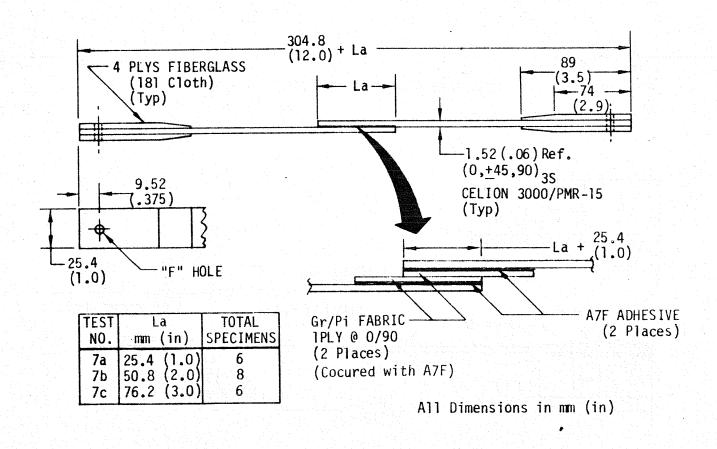
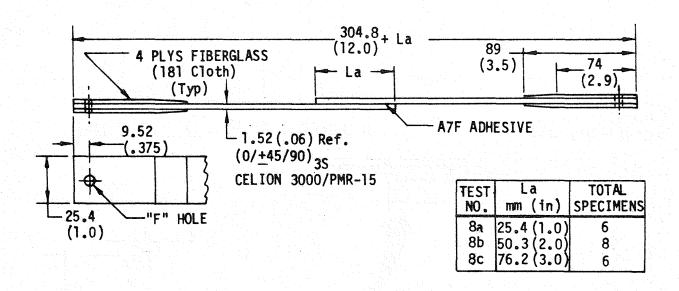


Figure 8-5: Advanced Joints - Matrix 6 Fabric Interface Single Lap



All Dimensions in mm (in)

Figure 8-6: Advanced Joints - Matrix 6 Baseline Single Lap

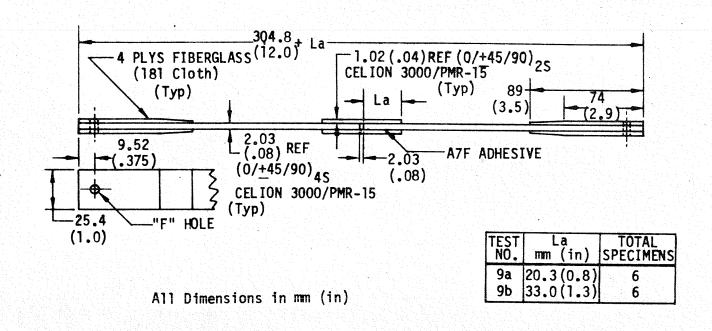
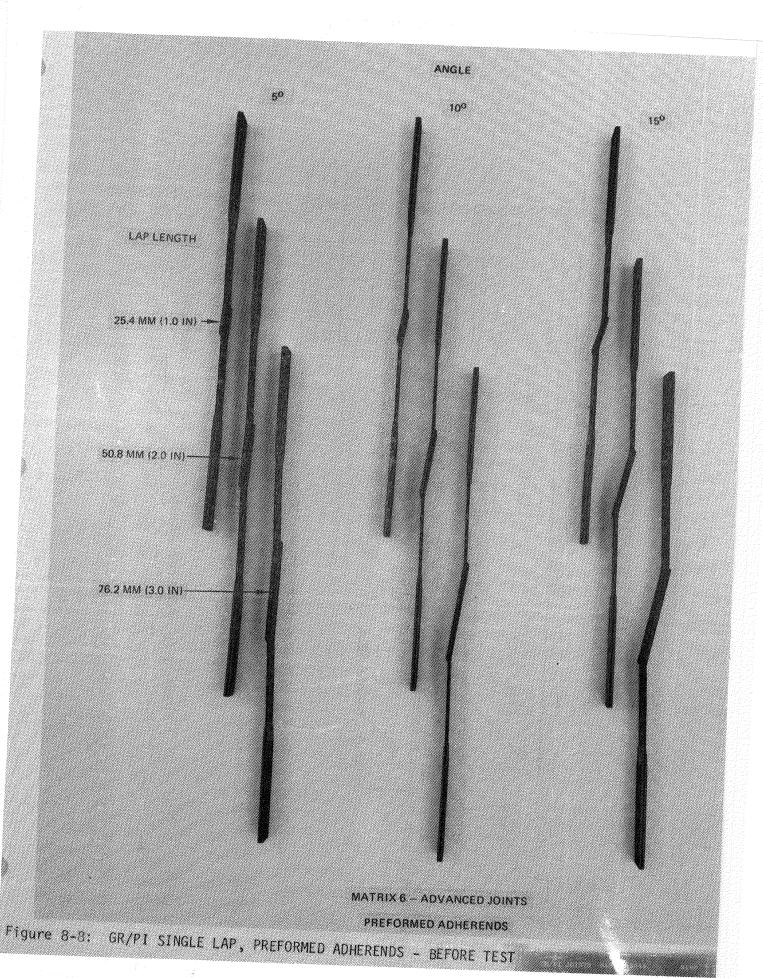


Figure 8-7: Advanced Joints - Matrix 6 Baseline Double Lap



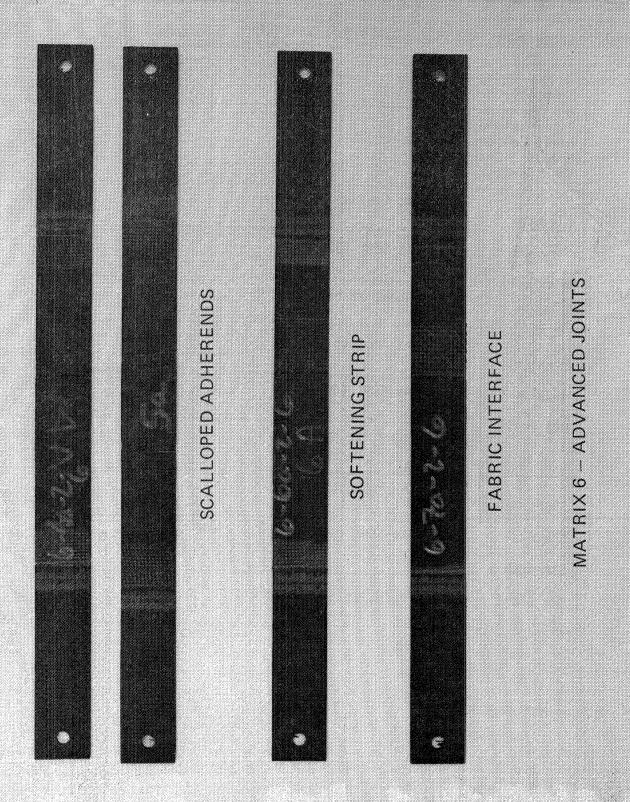
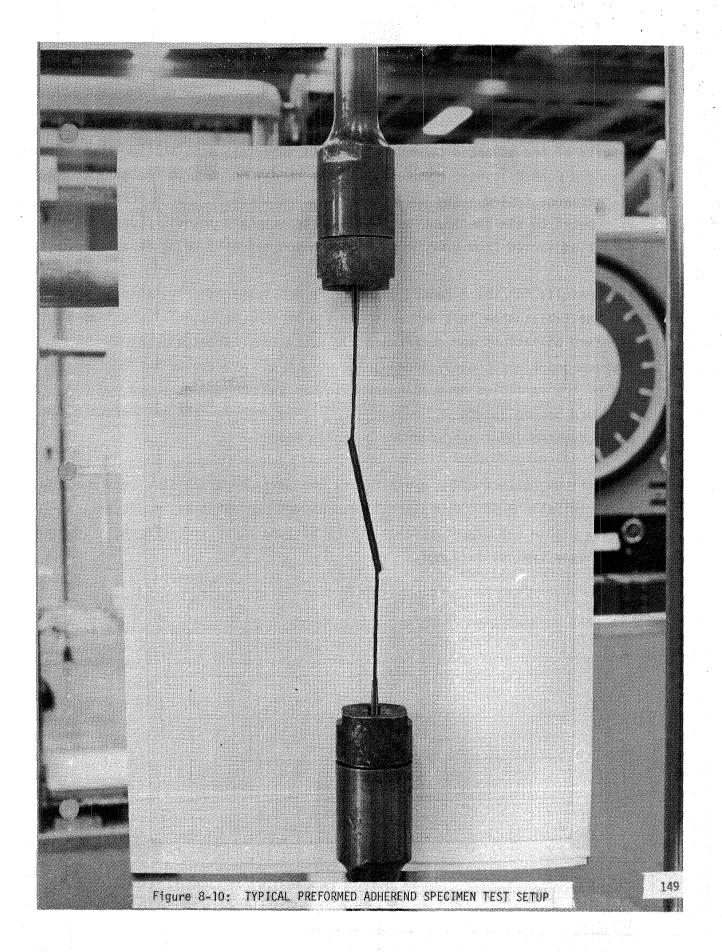


Figure 8-9: GR/PI SINGLE LAP, SCALLOPED ADHERENDS, FABRIC INTERFACES; DOUBLE LAP SCALLOPED ADHERENDS - BEFORE TEST

Table 8-2: ADVANCED JOINTS QUALITY CONTROL TEST PANEL PROPERTIES (Averaged) CELION 3000/PMR-15

Property		Requirement	58 35 1.56	
Fiber Volume, Resin Content, Specific Gravi Void Content,	% ty g/cc	58 +2 30 +3 1.54		
Flexural	At Ambient	1515 (220)	1424 (206.5)	
Strength	At 589K (600 <sup>0</sup> F)	757 (110)	809 (117.4) NA	
MPa (ksi)	Aged, at 589K (600 <sup>0</sup> F)	757 (110)		
Flexural	At Ambient	117 (17)	109 (15.8)	
Modulus	At 589K (600 <sup>o</sup> F)	103 (15)	103 (14.9)	
GPa (msi)	Aged, at 589K (600 <sup>0</sup> F)	103 (15)	NA	
Short Beam	At Ambient	96 (14)	75 (10.9)	
Shear Strength	At 589K (600 <sup>0</sup> F)	41 (6)	43 (6.3)	
MPa (ksi)	Aged, at 589K (600 <sup>0</sup> F)	41 (6)	NA	

N.A. - Not Available



### 8.4 Advanced Joint Test Results

Results of the advanced bonded joint tests show less data scatter than for the standard bonded joints; however, this may be due in part to the smaller number of specimens tested. The advanced joints had three or four specimens per set, as opposed to six specimens per set for the standard joints. Coefficients of variation varied from 0.022 to 0.246 with the majority being less than 0.100.

Test results for the advanced joint tests are summarized in Tables 8-3 and 8-4. The tables show test temperature, lap length, average failure load with standard deviations and coefficient of variations, average joint stress, average joint efficiency, added joint weight and average weight coefficient. All of the variables were calculated in the same manner as shown for the standard bonded joints in Section 7.2. Tables showing the test results for each advanced joint specimen are given in Appendix C.

The various failure modes exhibited by the advanced joint specimens are summarized in Table 8-5. Several test sets showed two different modes as indicated. Table 8-6 describes each of the failure modes and references figures which show typical failures.

TABLE 8-3 SUMMARY OF ADVANCED BONDED SINGLE LAP JOINT TEST RESULTS (PREFORMED ADHERENDS) - GR/PI TO GR/PI
(A) SI UNITS

TEST SET	PRE- FORMED ANGLE (DEG)	TEMPERATURE (K)	LAP LENGTH (MM)	AVERAGE FAILURE LOAD (KN)	STANDARD DEVIATION (KN)	COEFFICIENT OF VARIATION	AVERAGE JOINT STRESS (MPA)	AVERAGE JOINT EFFICIENCY	ADDED JOINT WEIGHT (N/M)	AVERAGE WEIGHT COEFFICIENT
6-1A 6-1A	5. 5. 5.	116. 294. 561.	25.32 25.57 25.48	8.10 8.37 7.38	0.61 0.29 0.95	.076 .035 .129	12.51 12.78 11.28	.351 .370 .271	0.692 0.706 0.696	4.61E5 4.67 4.17
6-18 6-18 6-18	<b>5.</b> 5.	116. 294. 561.	51.48 51.22 50.72	13.08 14.36 11.63	0.83 0.57 1.24	.063 .040 .106	9.93 10.98 9.00	.576 .630 .540	1.455 1.434 1.426	3.54 3.94 3.21
6-1C	5.	116.	76.62	16.41	0.47	.029	8.37	.684	2.073	3.12
6-1C	5.	294.	76.88	15.16	0.65	.043	7.76	.622	2.111	2.83
6-1C	5.	561.	76.96	13.09	0.45	.034	6.66	.540	2.113	2.44
6-2A	10.	116.	25.57	14.28	1.00	.070	21.71	.581	0.695	8.09
6-2A	10.	294.	25.91	12.00	0.96	.080	18.10	.562	0.705	6.71
6-2A	10.	561.	25.91	10.48	1.20	.114	15.81	.465	0.705	5.86
6-2B	10.	116.	51.31	15.18	3.74	.246	11.52	.477	1.423	4.20
6-2B	10.	294.	51.14	16.04	1.47	.092	12.27	.654	1.432	4.41
6-28	10.	561.	50.72	14.68	1.11	.076	11.36	.584	1.413	4.09
6-2C	-10.	116.	76.62	11.97	0.59	.049	6.09	.524	2.114	2.23
6-2C		294.	76.45	12.76	2.88	.226	6.54	.667	2.120	2.37
6-2C		561.	76.20	11.43	0.51	.045	5.86	.514	2.082	2.16
6-3A		116.	25.32	9.75	1.36	.139	15.06	.475	0.709	5.42
6-3A		294.	25.40	11.60	0.79	.068	17.79	.469	0.714	6.39
6-3A		561.	25.32	10.51	1.08	.102	16.21	.398	0.722	5.73
6-3B	15.	116.	50.80	13.49	0.94	.070	10.41	.515	1.436	3.70
6-3B	15.	294.	50.88	12.84	1.22	.095	9.89	.490	1.438	3.52
6-3B	15.	561.	50.80	10.29	0.77	.075	7.96	.422	1.429	2.84
6-3C	15.	116.	76.96	13.96	0.67	.048	7.09	.555	2.195	2.50
6-3C	15.	294.	76.96	15.37	0.45	.029	7.83	.609	2.195	2.76
6-3C	15.	561.	76.54	12.37	0.82	.066	6.34	.497	2.183	2.23

TABLE 8-3 CONCLUDED
(B) US CUSTOMARY UNITS

TES SET	PRE- FORMED ANGLE (DEG)	TEMPERATURE (F)	LAP LENGTH (IN)	AVERAGE FAILURE LOAD (LBS)	STANDARD DEVIATION (LBS)	COEFFICIENT OF VARIATION	AVERAGE JOINT STRESS (PSI)	AVERAGE JOINT EFFICIENCY	ADDED JOINT WEIGHT (LB/IN)	AVERAGE WEIGHT COEFFICIENT
6 - 1 :	5.	-250.	0.997	1822.	138.	.076	1814.	.351	3.95E-3	4.61E5
6 - 1 :		70.	1.007	1882.	65.	.035	1853.	.370	4.03	4.67
6 - 1 :		550.	1.003	1660.	214.	.129	1636.	.271	3.98	4.17
6 - 1	6.	-250.	2.027	2940.	186.	.063	1441.	.576	8.31	3.54
6 - 1		70.	2.017	3228.	128.	.040	1592.	.630	8.19	3.94
6 - 1		550.	1.997	2615.	278.	.106	1305.	.540	8.15	3.21
6-16	5.	-250.	3.017	3688.	105.	.029	1214.	.684	11.84	3.12
6-16		70.	3.027	3408.	145.	.043	1125.	.622	12.05	2.83
6-16		550.	3.030	2942.	101.	.034	967.	.540	12.07	2.44
6 - 2 i 6 - 2 i	10.	-250. 70. 550.	1.007 1.020 1.020	3210. 2698. 2355.	226. 216. 269.	.070 .080 .114	3148. 2624. 2293.	.581 .562 .465	3.97 4.02 4.02	8.09 6.71 5.86
6-21	10.	-250.	2.020	3413.	840.	. 246	1670.	.477	8.12	4.20
6-21		70.	2.013	3605.	332.	. 092	1779.	.654	8.17	4.41
6-21		550.	1.997	3300.	250.	. 076	1647.	.584	8.07	4.09
6-20 6-20 6-20	10. 10.	-250. 70. 550.	3.017 3.010 3.000	2692. 2868. 2570.	132. 647. 115.	.049 .226 .045	884. 948. 850.	.524 .667 .514	12.07 12.10 11.89	2.23 2.37 2.16
6-3/ 6-3/	15. 15.	-250. 70. 550.	0.997 1.000 0.997	2192. 2607. 2363.	305. 177. 242.	.139 .068 .102	2184. 2581. 2351.	.475 .469 .398	4.05 4.08 4.12	5.42 6.39 5.73
6-31 6-31 6-31	15. 15.	-250. 70. 550.	2.000 2.003 2.000	3032. 2887. 2313.	212. 274. 173.	.070 .095 .075	1510. 1435. 1155.	.515 .490 .422	8.20 8.21 8.16	3.70 3.52 2.84
6-30	15.	-250.	3.030	3138.	150.	.048	1028.	.555	12.54	2.50
6-30		70.	3.030	3455.	100.	.029	1135.	.609	12.54	2.76
6-30		550.	3.013	2780.	183.	.066	919.	.497	12.47	2.23

TEST SET	TEMPERATURE (K)	LAP LENGTH (MM)	AVERAGE FAILURE LOAD (KN)	STANDARD DEVIATION (KN)	COEFFICIENT OF VARIATION	AVERAGE JOINT STRESS (MPA)	AVERAGE JOINT EFFICIENCY	ADDED JOINT WEIGHT (N/M)	AVERAGE WEIGHT COEFFICIENT
6-4A 6-4A	294. 561.	25.40 25.40	2.61	0.11	.040 .055	4.05	.110	0.721	1.42E5 1.64
6-4B	294. 561.	50.80 50.80	5.32 5.58	0.21	.040 .169	4.12	.212	1.427	1.47
6-4C 6-4C	294. 561.	76.20 76.20	6.20 8.13	0.21 0.75	.033 .093	3.20 4.20	.259 .379	2.113	1.16
6-5A	294.	20.32	12.45	0.52	.042	24.13	. 409	3.077	1.59
6-5A	561.	20.32	12.34	0.27	.022	23.92	. 384		1.59
6-5B	294.	33.02	12.55	0.81	.065	14.97	. 422	4.965	1.00
6-5B	561.	33.02	14.79	1.46	.099	17.64	. 438		1.17
6-5C 6-5C	294. 561.	45.72 45.72	13.67 18.28	1.10	.080	11.76 15.75	.393	6.972	0.77
6-6A	294.	26.25	3.69	0.41	.112	5.54	.163	0.728	2.00
6-6A	561.	25.99	2.91	0.16	.056	4.41	.117	0.728	1.57
6-6B 6-6B	294. 561.	51.18 50.93	9.22 8.16	0.72	.078	7.09 6.31	.381 .379	1.422	2.55 2.26
6-6C	294. 561.	76.37 76.45	10.59 10.08	1.28 1.45	.121	5.45 5.19	. 428 . 356	2.117	1.97 1.86
6-7A	294.	25.58	5.34	0.26	.048	8.22	. 220	0.713	2.95
6-7A	561.	25.57	5.41	0.30		8.34	. 239	0.716	2.98
6-7B 6-7B	294. 561.	51.18 51.24	9.16 8.61	0.23 0.36	.025	7.05 6.62	.395 .350	1.448	2.49 2.36
6-7C	294.	76.62	10.94	1.03	.094	5.62	. 458	2.145	2.01
6-7C	561.	76.71	11.00		.033	5.65	. 442	2.168	2.00
6-8A	294.	25.99	3.31	0.21	.064	5.01	.139	0.731	1.78
6-8A	561.	25.57	3.15	0.14	.045	4.85	.127	0.719	1.72
6-8B 6-8B	294. 561.	51.05 50.99	5.25 5.18	0.15 0.64	.029 .123	4.04	. 225 . 206	1.414	1 . 46 1 . 45
6-8C	294.	76.54	6.65	0.27	.041	3.42	. 268	2.143	1.22
6-8C	561.	76.45	7.85	1.23	.157	4.04	. 277	2.099	1.48
6-9A	294.	20.32	10.27	0.62	.060	19.90	.302	3.055	1.32
6-9A	561.	20.32	10.53	0.62		20.38	.305	3.077	1.35
6-9B	294.	33.02	11.28	0.53	.047	13.43	.336	5.018	0.89
6-9B	561.	33.02	12.61	0.90	.071	15.03	.369	4.947	1.00

TABLE 8-4 CONCLUDED
(B) US CUSTOMARY UNITS

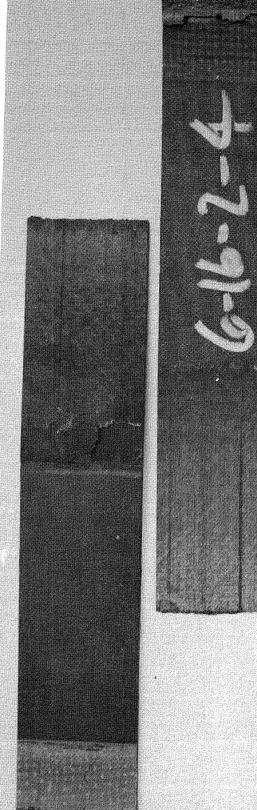
TEST SET	TEMPERATURE (F)	LAP LENGTH (IN)	AVERAGE FAILURE LOAD (LBS)	STANDARD DEVIATION (LBS)	COEFFICIENT OF VARIATION	AVERAGE JOINT STRESS (PSI)	AVERAGE JOINT EFFICIENCY	ADDED JOINT WEIGHT (LB/IN)	AVERAGE WEIGHT COEFFICIENT
6-4A 6-4A	70. 550.	1.000	587. 653.	24. 36.	.040	587. 654.	.110	4.12E-3 3.98	1.42E5 1.64
6-4B 6-4B	70. 550.	2.000	1196. 1254.	48. 211.	.040 .169	598. 627.	.212	8.15 7.92	1.47 1.58
6-4C 6-4C	70. 550.	3.000 3.000	1393. 1828.	46. 169.	.033	465. 609.	.259 .379	12.06 12.24	1.16 1.49
6-5A 6-5A	70. 550.	0.800	2798. 2775.	118. 61.	.042 .022	3499. 3469.	.409	17.57 17.45	1.59
6-5B 6-5B	70. 550.	1.300 1.300	2822. 3325.	183. 328.	.065 .099	2171. 2559.	.422	28.35 28.35	1.00 1.17
6-5C 6-5C	70. 550.	1.800 1.800	3073. 4110.	247. 193.	.080	1706. 2285.	.393	39.81 39.53	0.77
6-6A 6-6A	70. 550.	1.033 1.023	830. 654.	93. 37.	.112	804. 640.	.163	4.16	2.00 1.57
6-6B 6-6B	70. 550.	2.015 2.005	2074. 1835.	162. 222.	.078	1029. 915.	.381	8.12 8.11	2.55 2.26
6-6C 6-6C	70. 550.	3.007 3.010	2380. 2265.	287. 325.	.121	791. 752.	. 428 . 356	12.09 12.16	1.97 1.86
6-7A 6-7A	70. 550.	1.007 1.007	1200. 1217.	58. 66.	.048 .055	1192. 1210.	.220	4.07	2.95 2.98
6-7B	70. 550.	2.015 2.018	2060. 1936.	52. 81.	.025	1022. 960.	.395	8.27 8.19	2.49 2.36
6-7C 6-7C	70. 550.	3.017 3.020	2460. 2473.	231. 82.	.094 .033	815. 819.	.458	12.25	2.01 2.00
6-8A 6-8A	70. 550.	1.023 1.007	745. 708.	48. 32.	.064	727. 703.	.139	4.17	1.78 1.72
6-8B 6-8B	70. 550.	2.010 2.008	1180. 1165.	34. 143.	.029	587. 579.	. 225	8.07 8.06	1.46 1.45
6-8C 6-8C	70. 550.	3.013 3.010	1495. 1765.	61. 276.	.041	496. 586.	. 268 . 277	12.23	1.22 1.48
6-9A 6-9A	70. 550.	0.800 0.800	2308. 2367.	138. 140.	.060 .059	2886. 2956.	.302	17.45 17.57	1.32 1.35
6-9B 6-9B	70. 550.	1.300 1.300	2537. 2835.	119. 203.	.047 .071	1948. 2180.	.336	28.65 28.25	0.89 1.00

Table 8-5: ADVANCED JOINT FAILURE MODES

SPECIMEN CONFIGURATION	TEST NO.	LAP LENGTH		FAILURE MODE NUMBERS SEE TABLE 8-6				
		mm (in)	116K (-250°F)	294K (70°F)	561K (550°F)			
5° Preformed	la lb lc	25.4 (1.0) 50.8 (2.0) 76.2 (3.0)	] ] 2					
10° Preformed	2a 2b 2c	25.4 (1.0) 50.8 (2.0) 76.2 (3.0)	1 3 3	1 2 2, 3	1 2 3			
15° Preformed	3a 3b 3c	25.4 (1.0) 50.8 (2.0) 76.2 (3.0)	1, 2 3, 4 4	1 3 4	1 3 1, 4			
Scalloped Single-Lap	4a 4b 4c	25.4 (1.0) 50.8 (2.0) 76.2 (3.0)		5 5 5	5 5 5			
Scalloped Double-Lap	5a 5b 5c	20.3 (0.8) 33.0 (1.3) 45.7 (1.8)		6 6 6	6 6 6			
Softening Strip Single-Lap	<b>6a</b> 6b 6c	25.4 (1.0) 50.8 (2.0) 76.2 (3.0)		7 7A 7A	7 7,7A 7A			
Fabric Interface Single-Lap	7a 7b 7c	25.4 (1.0) 50.8 (2.0) 76.2 (3.0)		8 8 8A	8 8 8,8A			
Baseline Single-Lap	8a 8b 8c	25.4 (1.0) 50.8 (2.0) 76.2 (3.0)		9 9 9	9 9 9			
Baseline Double-Lap	9a 9b	20.3 (0.8) 33.0 (1.3)		10 10	10 10			

### Table 8-6 Advanced Joint Failure Modes

Failure Mode No.	<u>Failure Mode</u>	Typical Failure
1.	Intralamina failure in adherend first ply + adherend-adhesive interface failure	Figure 8-11
2.	Interlamina failure in adherend + some tensile failures of individual plies	Figure 8-12
3.	Interlamina failure through adherend + tensile failures of individual plies	Figure 8-13
4.	Tensile failure of adherend at preformed bend	Figure 8-14
5.	Adhesive failure at adherend-adhesive interface- single lap joint	Figure 8-15
6.	Adhesive failure at adherend-adhesive interface-double lap joint	Figure 8-16
7.	Interlamina failure between S-glass/PI plies	Figure 8-17
7A.	<pre>Interlamina failure between S-glass/PI plies + interlamina failure in adherend</pre>	Figure 8-18
8.	Interlamina failure between Gr/PI fabric plies	Figure 8-19
8A.	Interlamina failure between Gr/PI fabric plies + interlamina failure in adherend	Figure 8-20
9.	Intralamina failure in adherend	Figure 8-21
10.	Intralamina failure in adherend + adherend- adhesive interface failure	Figure 8-22



5° ANGLE 294K (70°F)

50.8 MM (2.0 IN) LAP LENGTH

Figure 8-11: GR/PI SINGLE LAP, PREFORMED ADHERENDS - FAILURE MODE #1





10° ANGLE 294K (70°F)

76.2 MM (3.0 IN) LAP LENGTH

Figure 8-12: GR/PI SINGLE LAP, PREFORMED ADHERENDS - FAILURE MODE #2

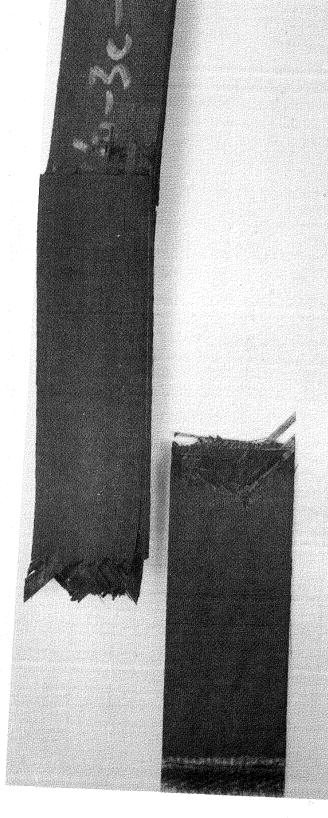




150 ANGLE 294K (700F)

50.8 MM (2.0 IN) LAP LENGTH

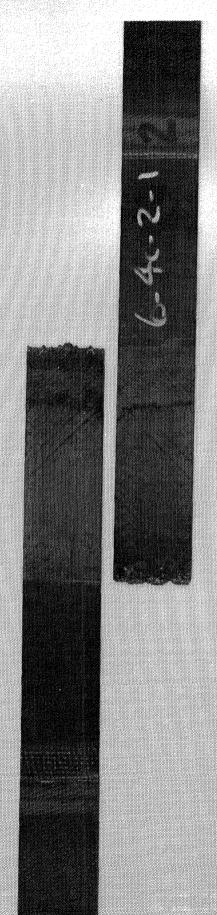
Figure 8-13: GR/PI SINGLE LAP, PREFORMED ADHERENDS - FAILURE MODE #3



15° ANGLE 294K (70°F)

# 76.2 MM (3.0 IN) LAP LENGTH

Figure 8-14: GR/PI SINGLE LAP, PREFORMED ADHERENDS - FAILURE MODE #4



SCALLOPED ADHERENDS

76.2 MM (3.0 IN) LAP LENGTH

294 K (70°F)

Figure 8-15: GR/PI SINGLE LAP, SCALLOPED ADHERENDS - FAILURE MODE #5

SCALLOPED ADTENDS

HONE OF CONTRACTOR

294 K (700F)

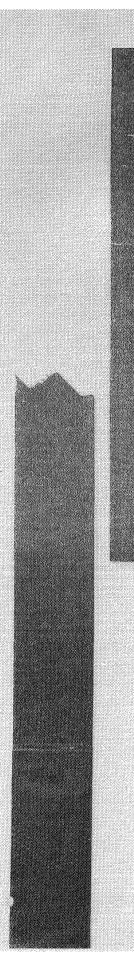
GR/PI DOUBLE LAP, SCALLOPED ADHERENDS - FAILURE MODE #6 Figure 8-16:

SOFTENING STRIP

25.4 MM (1.0 IN) LAP LENGTH

294 K (70°F)

Figure 8-17: GR/PI SINGLE LAP, S-GLASS/PI FABRIC INTERFACE - FAILURE MODE #7

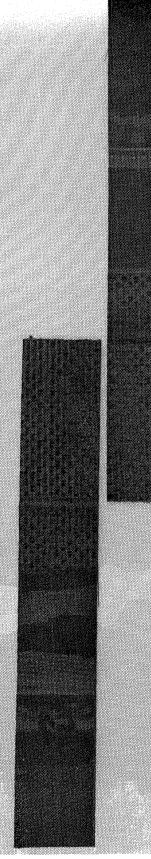


SOFTENING STRIP

50.8 MM (2.0 IN) LAP/LENGTH

294 K (700F)

Figure 8-18: GR/PI SINGLE LAP, S-GLASS/PI FABRIC INTERFACE - FAILURE MODE #7A

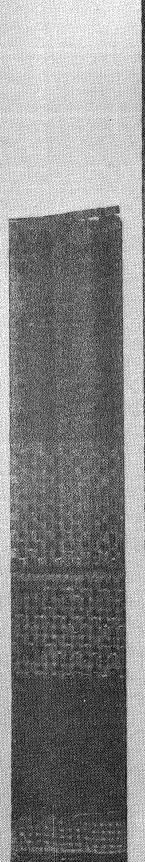


FABRIC INTERFACE

50.8 MM (2.0 IN) LAP LENGTH

294 K (700F)

Figure 8-19: GR/PI SINGLE LAP, GR/PI FABRIC INTERFACE - FAILURE MODE #8



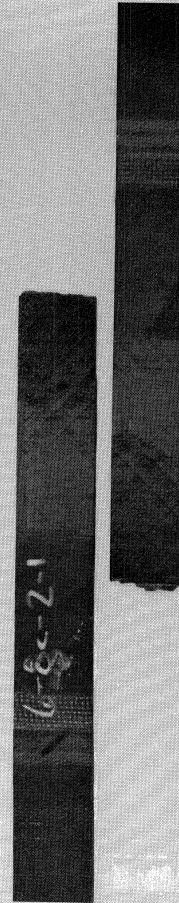


## FABRIC INTERFACE

76.2 MM (3.0 IN) LAP LENGTH

294 K (700F)

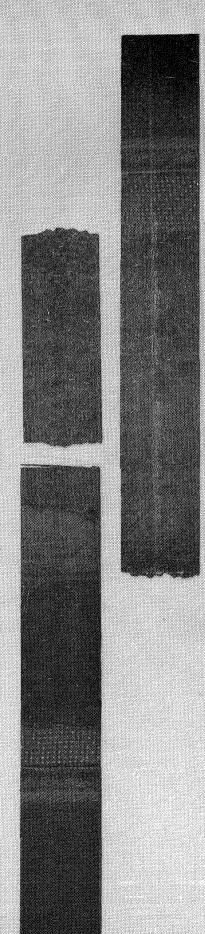
GR/PI SINGLE LAP, GR/PI FABRIC INTERFACE - FAILURE MODE #8A Figure 8-20:



76.2 MM (3.0 IN) LAP LENGTH

294 K (70°F)

Figure 8-21: GR/PI SINGLE LAP, BASELINE - FAILURE MODE #9



33.0 mm (1.3 in) LAP LENGTH

294 K (70<sup>o</sup>F)

Figure 8-22: GR/PI DOUBLE LAP, BASELINE - FAILURE MODE #10

### 8.4.1 Preformed Adherends

Results of the preformed adherend tests demonstrate that preforming the adherends of a single lap joint gives a significant increase in load carrying capability. Figures 8-23 and 8-24 show the effect of preforming for temperatures of 294K  $(70^{\circ}F)$  and 561K  $(550^{\circ}F)$ . The average failure load for each lap length is normalized by the average failure load for the baseline (straight adherends) configuration with the same lap length. In all cases, preforming the adherends increased the average failure load. Increases ranged from 92% to 262% at 294K  $(70^{\circ}F)$  and from 46% to 234% at 561K  $(550^{\circ}F)$ . No comparisons were made at 116K  $(-250^{\circ}K)$  because there was no baseline data at this temperature; however, results similar to the 294K  $(70^{\circ}F)$  tests would be expected.

Results of testing by Sawyer and Cooper (Ref. 5) of aluminum to aluminum preformed adherend single lap joints also indicated substantial improvement in performance over straight adherend single lap joints. Their results indicated that the longer the lap length, the greater the improvement in performance. The reverse trend is indicated in Figures 8-23 and 8-24 for the Gr/PI to Gr/PI joints. In this case the shortest lap length tested, 25.4mm (1.0 in), showed the greatest increase in performance.

The difference in performance trends exhibited by the aluminum to aluminum joints and the Gr/PI to Gr/PI joints can be explained by the different failure modes of the two joint types. The failures of the metal joints are characterized by shear and peel failures in the adhesive. Since preforming the adherends reduces the peak shear and peel stresses, and increasing the lap length reduces the average shear stress, it would be expected that there would be a greater increase in performance with longer lap lengths. However, failures of the composite joints are characterized by peel failures in the adherends. This is due to the low interlamina tension strength of the composite. Preforming the adherends reduces these peel stresses in the joint. This is indicated by the large improvement in performance for the 25.4mm (1.0 in) lap length joints. For the longer lap lengths the offset caused by the preformed angle is greater than that necessary to geometrically align the adherends.

This result in moments in the adherend causing the joint to deform as shown in Figure 8-25. This causes initial failures in the outer plies at the point indicated, resulting in a smaller percentage performance increase than for the shorter lap lengths. This failure trend is shown by failure modes 3 and 4 (see Figures 8-13 and 8-14). Mode 4 is the extreme case of complete adherend failure outside the joint.

Figures 8-26 through 8-28 show failure load versus preform angle for the three lap lengths tested. Data for 25.4mm and 50.8mm (1.0 and 2.0 inches) lap lengths show an increase in failure load going from  $5^{0}$  to  $10^{0}$  and a leveling off or dropping in load going from  $10^{0}$  to  $15^{0}$ . The  $15^{0}$  preform angle causes the maximum offset in the adherends and results in the largest moments in the area of the preformed angle (see Figure 8-10 and compare to Figure 8-25). This results in delaminations and peel failures of the laminate at these locations, as noted, and a corresponding reduction in joint strength. For the 76.2mm (3.0 inch) lap length the opposite performance trend is obtained. There is a drop in failure load going from  $5^{\circ}$  to  $10^{\circ}$  and then an increase going from  $10^{\circ}$  to  $15^{\circ}$ . The offset at  $10^{\circ}$  for the 76.2mm (3.0 inch) lap length is greater than or equal to the offset at  $15^{0}$  for the shorter lap lengths and may explain the similar drop in failure load. At 150 the specimens with 76.2mm (3.0 inch) lap lengths had a completely different failure mode. The adherends failed outside the joint area except for two specimens at 561K (550°F). There is no readily apparent explanation as to why there was not a interlaminar joint failure at a lower load similar to the  $10^{\circ}$ , 76.2mm (3.0 inch) specimens. It is possible that there was an early delamination of the adherend due to the large offset which weakened it and caused it to act as a hinge. This would result in a rapid alignment of load without introducing any peel stresses. The already weakened adherend would then fail in tension.

Typical failed specimens for the different angles, lap lengths and temperatures tested are shown in Figures 8-29 through 8-37.

### PREFORMED ADHEREND JOINTS VS. BASELINE JOINTS

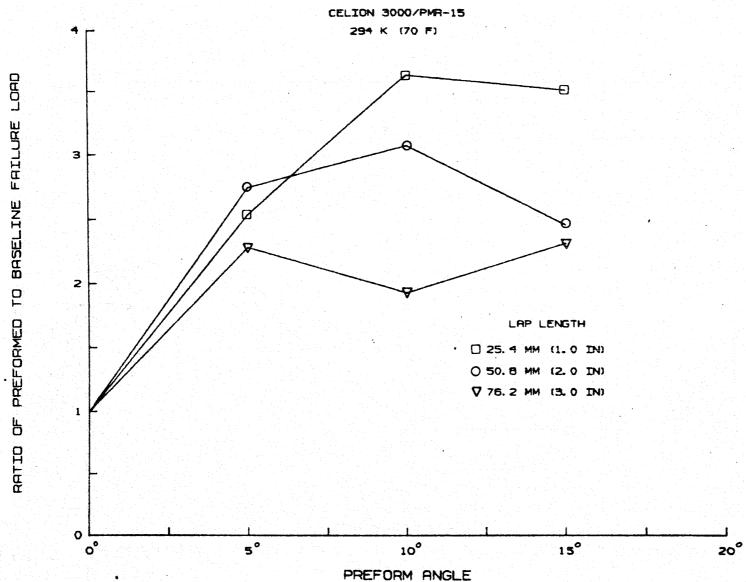


Figure 8-23: EFFECT OF PREFORMED ADHERENDS

### PREFORMED ADHEREND JOINTS VS. BASELINE JOINTS CELION 3000/PMR-15

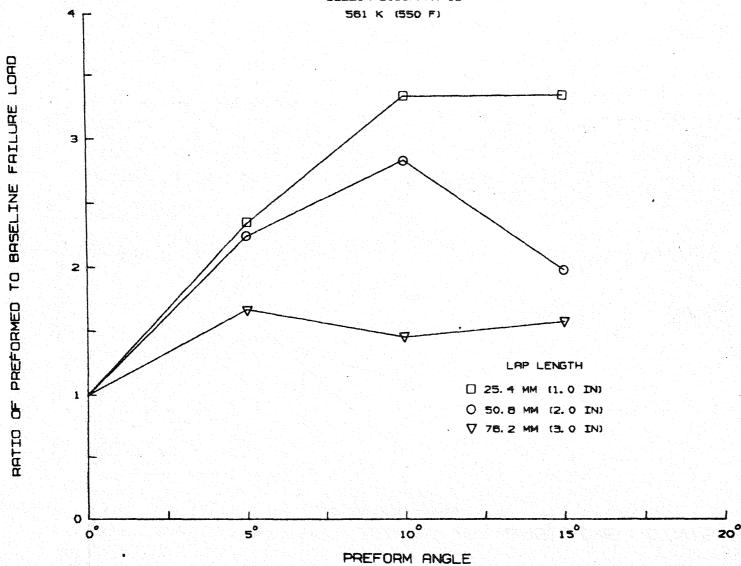
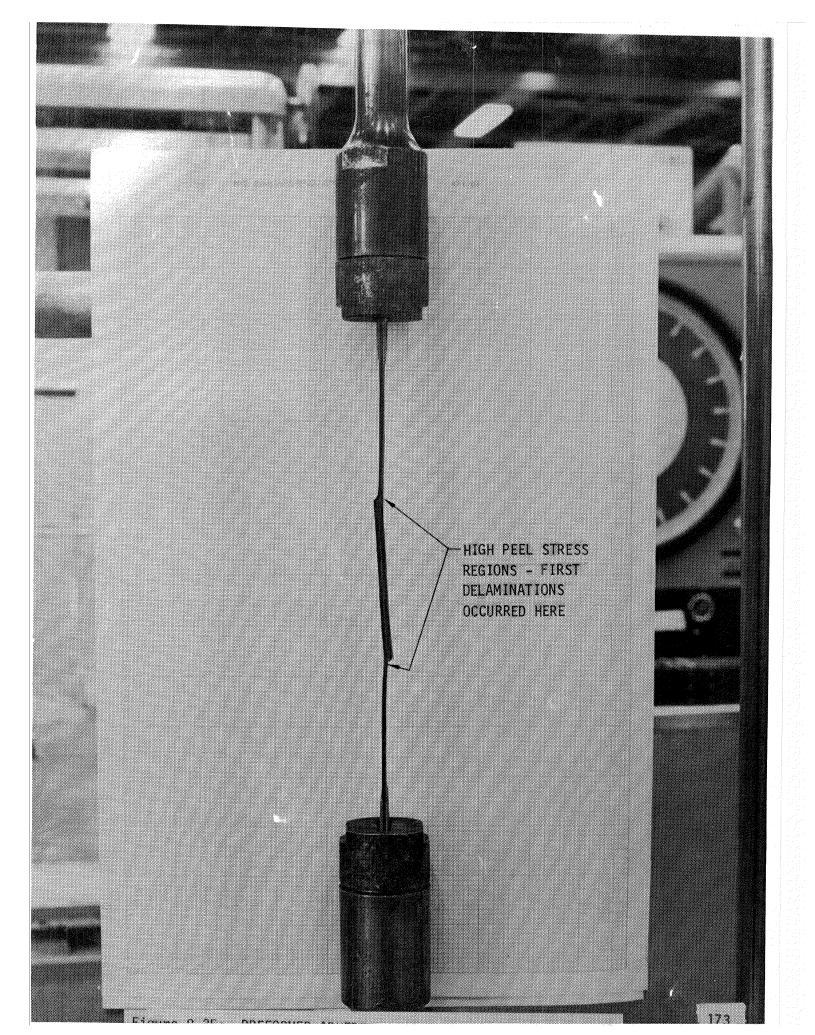


Figure 8-24: EFFECT OF PREFORMED ADHERENDS



### EFFECT OF ADHEREND PREFORM ANGLE

25.4 MM (1.0 DN) LAP LENGT

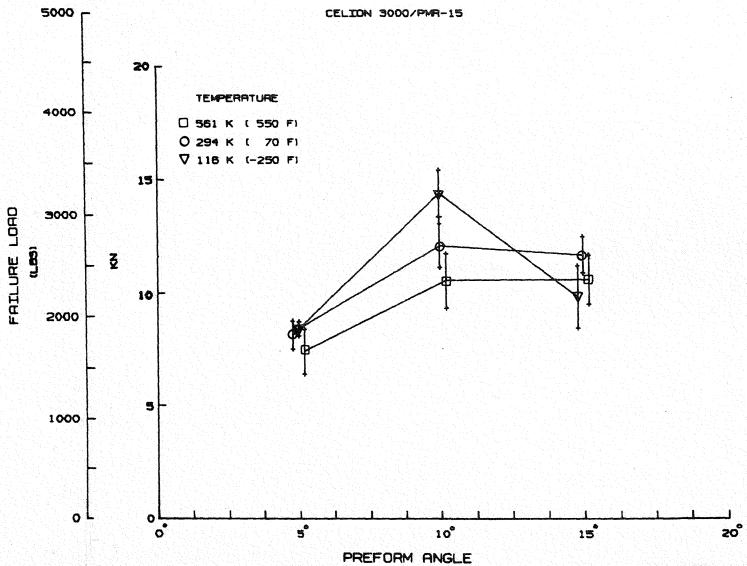


Figure 8-26: EFFECT OF ADHEREND PREFORM ANGLE

### EFFECT OF ADHEREND PREFORM ANGLE 50.8 MM (2.0 IN) LAP LENGTH 5000 CELION 3000/PMR-15 20 T 4000 15 FAILURE LOAD 3000 5 Z 10 2000 TEMPERATURE □ 561 K ( 550 F) O 294 K ( 70 F) V 118 K (-250 F) 1000 50 100 150

Figure 8-27: EFFECT OF ADHEREND PREFORM ANGLE

PREFORM ANGLE

# EFFECT OF ADHEREND PREFORM ANGLE

76. 2 MM (3. 0 IN) LAP LENGTH CELION 3000/PMR-15

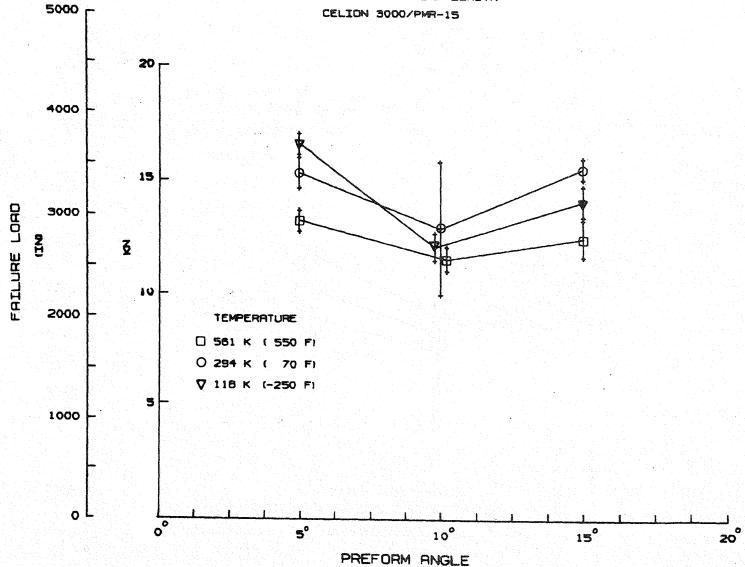
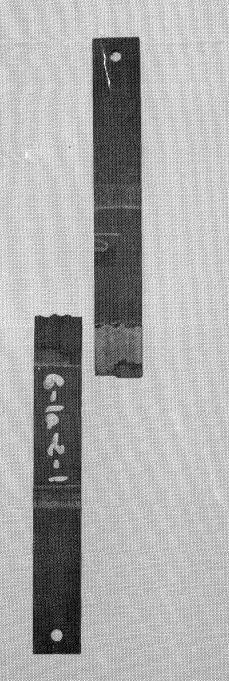
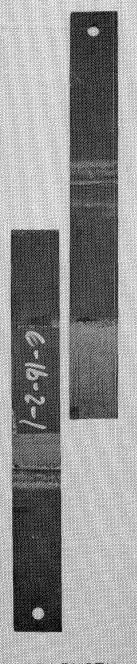
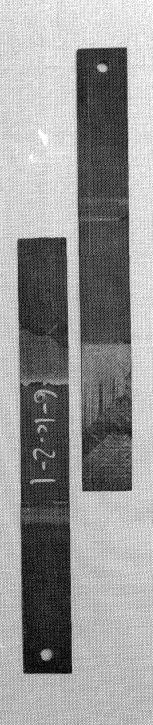


Figure 8-28: EFFECT OF ADHEREND PREFORM ANGLE







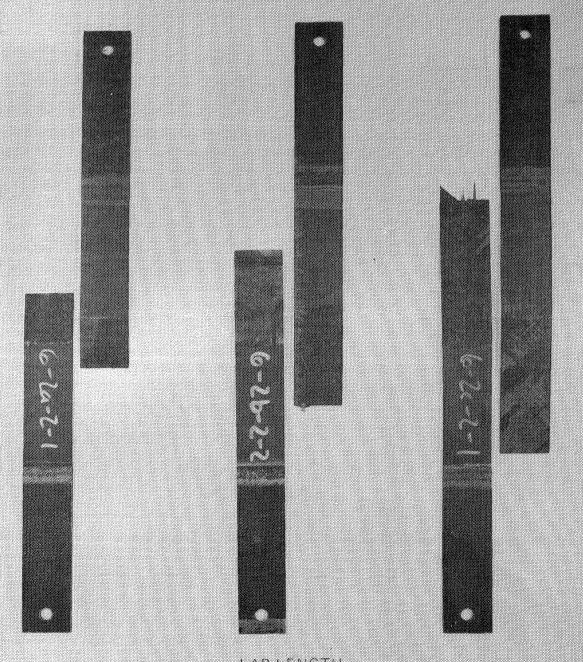
25.4 MM (1.0 IN)

LAP LENGTH 50.8 MM (2.0 IN)

76.2 MM (3.0 IN)

MATRIX 6 – ADVANCED JOINTS PREFORMED ADHERENDS

5° ANGLE 116K (-250°F)



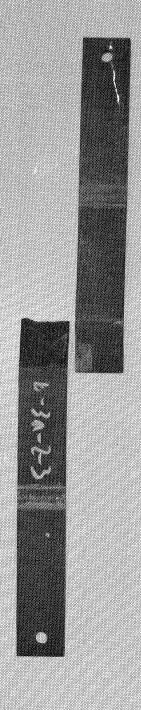
25.4 MM (1.0 IN)

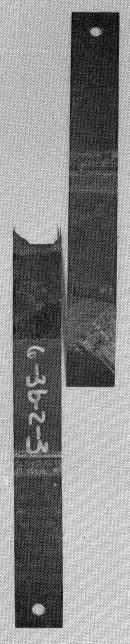
LAP LENGTH 50.8 MM (2.0 IN)

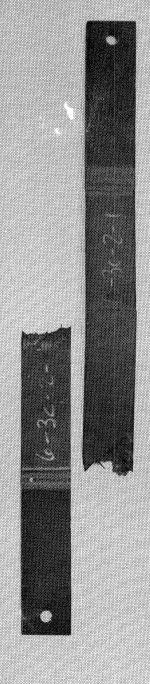
76.2 MM (3.0 IN)

MATRIX 6 – ADVANCED JOINTS PREFORMED ADHERENDS

10° ANGLE 116K (-250°F)





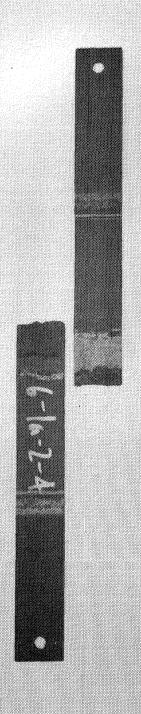


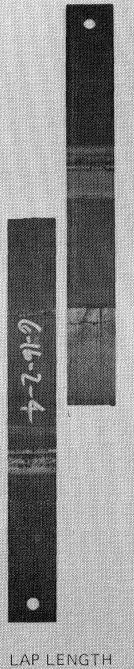
LAP LENGTH

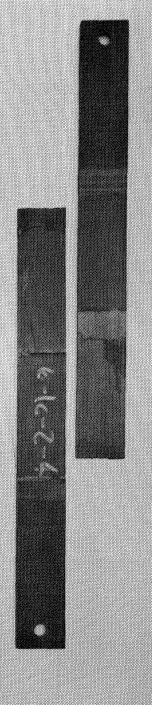
25.4 MM (1.0 IN) 50.8 MM (2.0 IN) 76.2 MM (3.0 IN)

MATRIX 6 - ADVANCED JOINTS PREFORMED ADHERENDS

15<sup>0</sup> ANGLE 116K (-250°F)



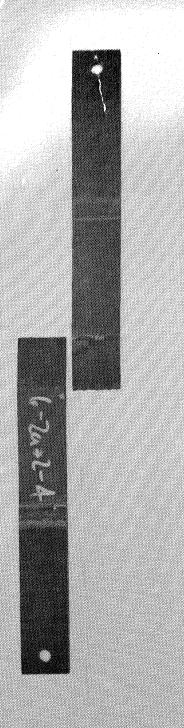




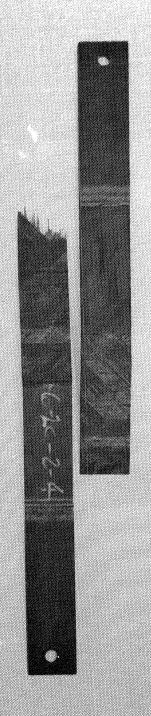
25.4 MM (1.0 IN) 50.8 MM (2.0 IN) 76.2 MM (3.0 IN)

MATRIX 6 - ADVANCED JOINTS PREFORMED ADHERENDS

50 ANGLE 294K (70°F)



LAP LENGTH



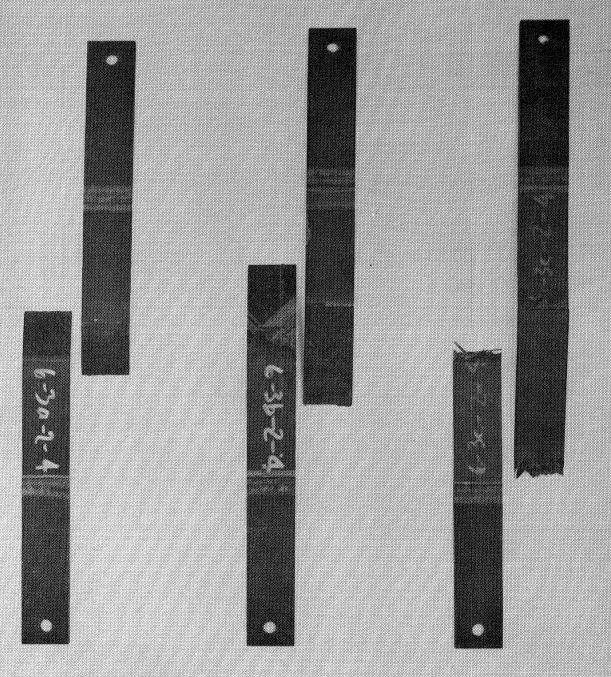
25.4 MM (1.0 IN) 50.8 MM (2.0 IN)

76.2 MM (3.0 IN)

MATRIX 6 - ADVANCED JOINTS PREFORMED ADHERENDS

100 ANGLE 294K (70°F)

Figure 8-33: GR/PI SINGLE LAP, 10° PREFORM, 294K (70°F) - FAILED SPECIMENS 181

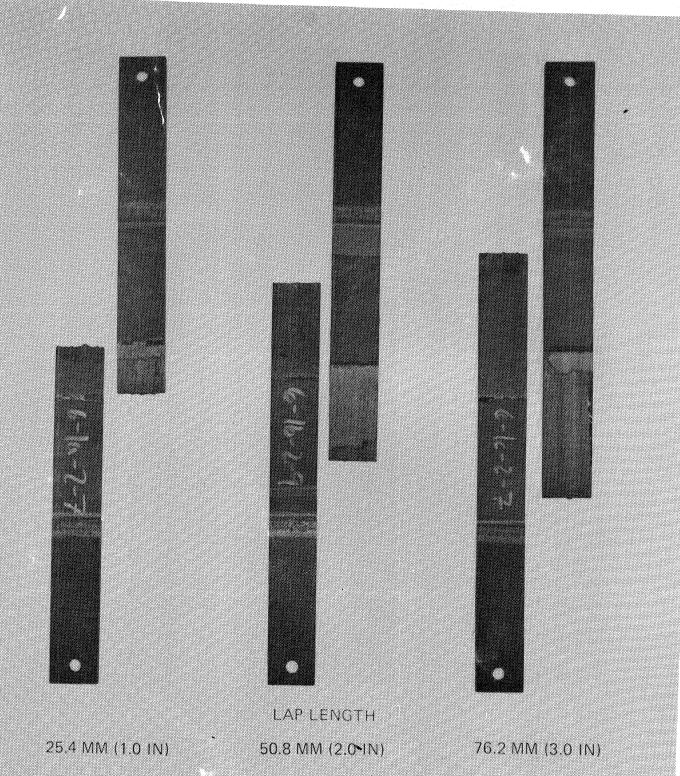


LAP LENGTH

25.4 MM (1.0 IN) 50.8 MM (2.0 IN) 76.2 MM (3.0 IN)

MATRIX 6 - ADVANCED JOINTS PREFORMED ADHERENDS

15° ANGLE **294K (70°F)** 



MATRIX 6 – ADVANCED JOINTS PREFORMED ADHERENDS

50 ANGLE 561 K (550°F)



25.4 MM (1.0 IN)

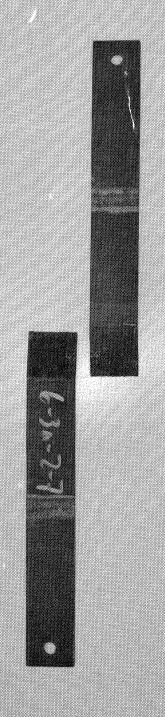
LAP LENGTH 50.8 MM (2.0 IN)

76.2 MM (3.0 IN)

MATRIX 6 - ADVANCED JOINTS PREFORMED ADHERENDS

10° ANGLE 561 K (550°F)

Figure 8-36: GR/PI SINGLE LAP, 10° PREFORM, 561K (550°F) - FAILED SPECIMENS 184







25.4 MM (1.0 IN) 50.8 MM (2.0 IN) 76.2 MM (3.0 IN)

MATRIX 6 - ADVANCED JOINTS PREFORMED ADHERENDS

15° ANGLE 561 K (550°F)

Figure 8-37: GR/PI SINGLE LAP, 15° PREFORM, 561K (550°F) - FAILED SPECIMENS

#### 8.4.2 Scalloped Adherends

Effects of scalloping the ends of the adherends in the single and double lap joints are shown in Figures 8-38 through 8-41. Average failure load versus lap length are shown for both the scalloped configurations and the baseline configurations at 294K  $(70^{\circ}F)$  and 561K  $(550^{\circ}F)$ . There was no change in strength for the single lap joints, while the scalloped double lap joints showed an average increase in strength of 17%. Figures 8-42 through 8-45 show typical failed specimens for the single and double lap joints.

The difference between these two cases can be attributed to the different failure mechanisms of a single versus double lap joint. The failure in a single lap joint is governed by both the moment introduced in the joint and by peel stresses. The failure in the double lap joints is governed primarily by the peel stresses in the inner adherend at the end of the lap. Since scalloping the ends of the adherends was designed to reduce the peel stresses at the end of the lap, it would be expected that the double lap joints would be more affected by scalloping than the single lap joints.

Figure 8-38: EFFECT OF SCALLOPED ADHERENDS - SINGLE LAP JOINTS

LAP LENGTH

#### EFFECT OF SCALLOPED ADHERENDS - SINGLE LAP JOINTS

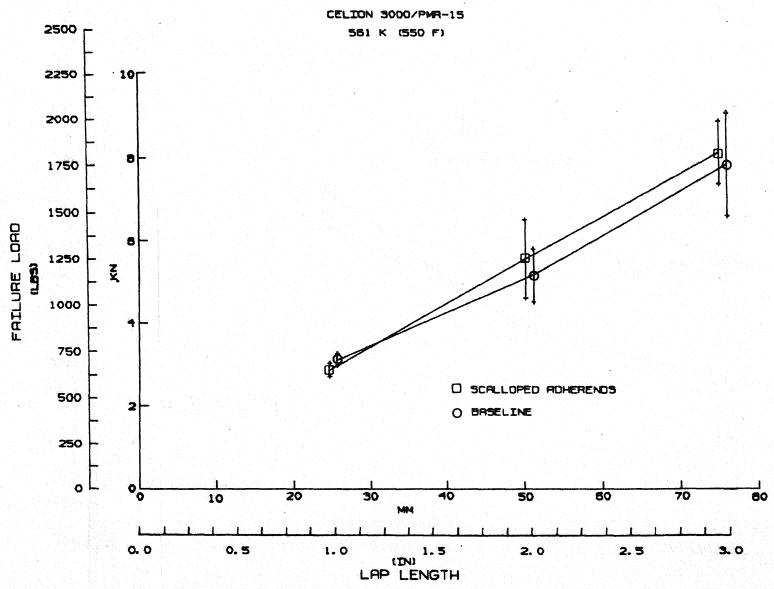


Figure 8-39: EFFECT OF SCALLOPED ADHERENDS - SINGLE LAP JOINTS

## EFFECT OF SCALLOPED ADHERENDS - DOUBLE LAP JOINTS

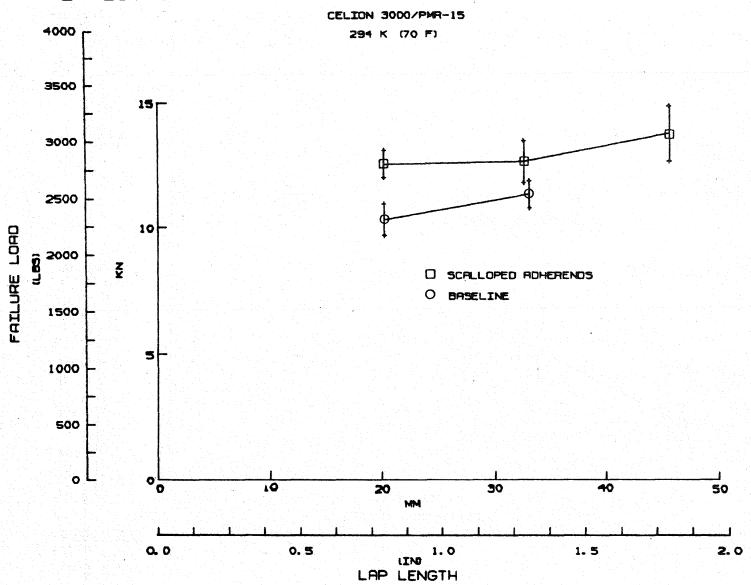


Figure 8-40: EFFECT OF SCALLOPED ADHERENDS - DOUBLE LAP JOINTS

## EFFECT OF SCALLOPED ADHERENDS - DOUBLE LAP JOINTS

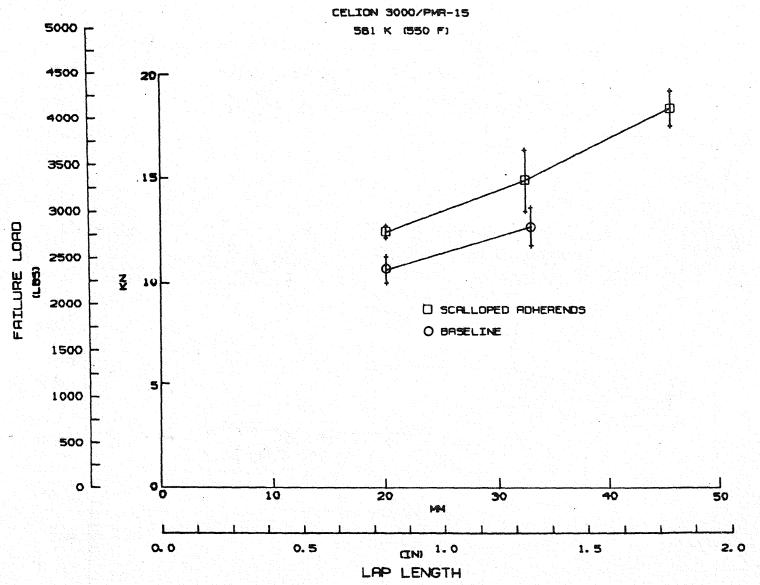
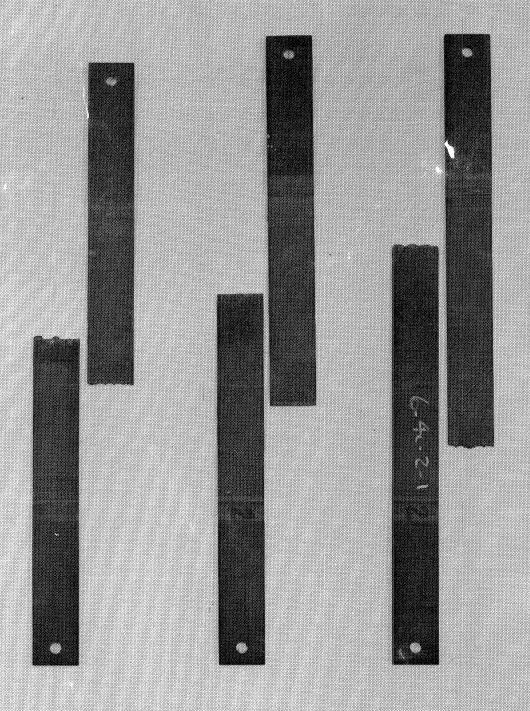


Figure 8-41: EFFECT OF SCALLOPED ADHERENDS - DOUBLE LAP JOINTS

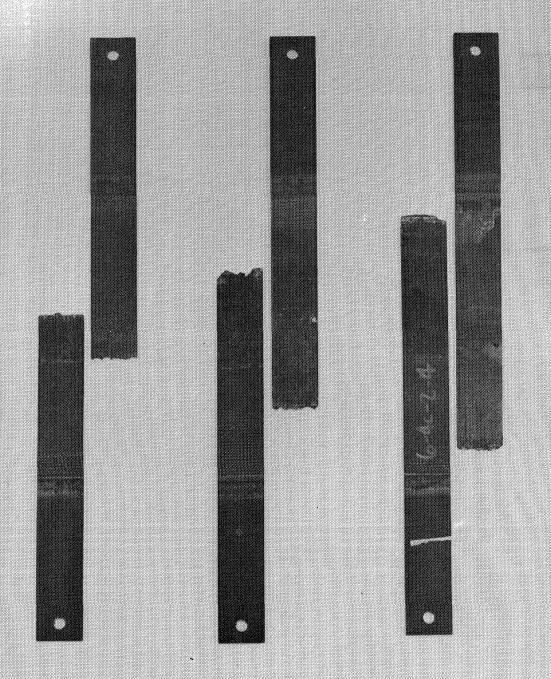


LAP LENGTH

25.4 MM (1.0 IN) 50.8 MM (2.0 IN) 76.2 MM (3.0 IN)

MATRIX 6 - ADVANCED JOINTS SCALLOPED ADHERENDS 294 K (70°F)

Figure 8-42: GR/PI SINGLE LAP, SCALLOPED ADHERENDS, 294K (70°F) - FAILED SPECIMENS



LAPLENGTH

25.4 MM (1.0 IN)

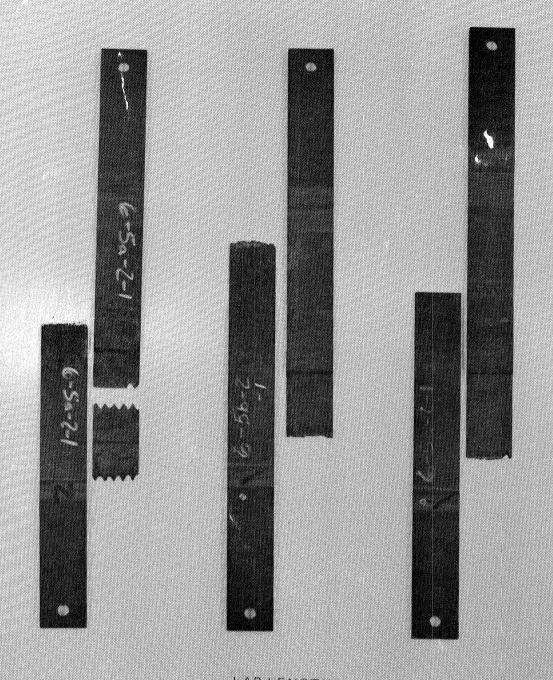
50.8 MM (2.0 IN) 76.2 MM (3.0 IN)

MATRIX 6 - ADVANCED JOINTS SCALLOPED ADHERENDS

561 K (550°F)

192

Figure 8-43: GR/PI SINGLE LAP, SCALLOPED ADHERENDS, 561K (550°F) - FAILED SPECIMENS



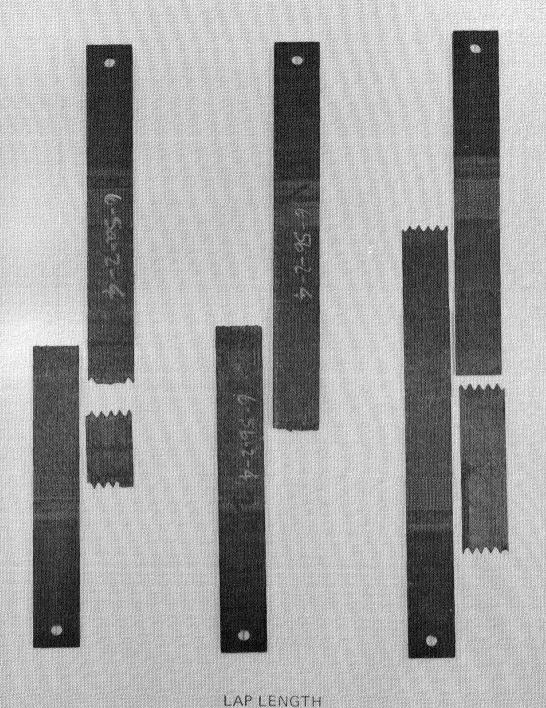
20.3 mm (0.8 in)

LAP LENGTH 33.0 mm (1.3 in) 45.7 mm (1.8 in)

MATRIX 6 - ADVANCED JOINTS SCALLOPED ADHERENDS 294 K (70°F)

Figure 8-44: GR/PI DOUBLE LAP, SCALLOPED ADHERENDS, 294K (70°F) - FAILED SPECIMENS

193



20.3 mm (0.8 in)

33.0 mm (1.3 in)

45.7 mm (1.8 in)

MATRIX 6 – ADVANCED JOINTS SCALLOPED ADHERENDS 561 K (550°F)

Figure 8-45: GR/PI DOUBLE LAP, SCALLOPED ADHERENDS, 561K (550°F) - FAILED SPECIMENS

194

#### 8.4.3 Fabric Interfaces

Figures 8-46 and 8-47 compare the strengths of single lap joints with a Gr/PI fabric interface and with a S-glass/PI fabric interface to the baseline data at 294K (70°F) and 561K (550°F). For all cases, except the 25.4mm (1.0 in) lap length S-glass/PI fabric specimens, there was a significant increase in joint strength. The increase in strength can be attributed to a reduction in peak shear and peel stresses due to the softer interface materials. Typical failed specimens for the S-glass/PI configuration are shown in Figures 8-48 and 8-49, while those for the Gr/PI fabric configuration are shown in Figures 8-50 and 8-51.

For both configurations there were two slightly different failure modes exhibited. The shorter lap lengths had delamination between the fabric layers over the total joint length (failure modes 7 and 8—see Figures 8-17 and 8-19). The longer lap lengths had delamination between the fabric layers on one-half of the joint length and delamination of the Gr/PI adherend between the first and second plies over the other one-half of the joint (failure modes on 7A and 8A—see Figures 8-18 and 8-20). It is believed that for the second case the failure between the fabric layers occurred first. If the Gr/PI tape had delaminated first, it seems its inherent low peel strength would have made it propagate along the entire joint length. It is not known what the effect would be of reducing the number of fabric layers from two to one in order to eliminate delaminations between the fabric layers.

#### EFFECT OF FABRIC INTERFACES - SINGLE LAP JOINTS

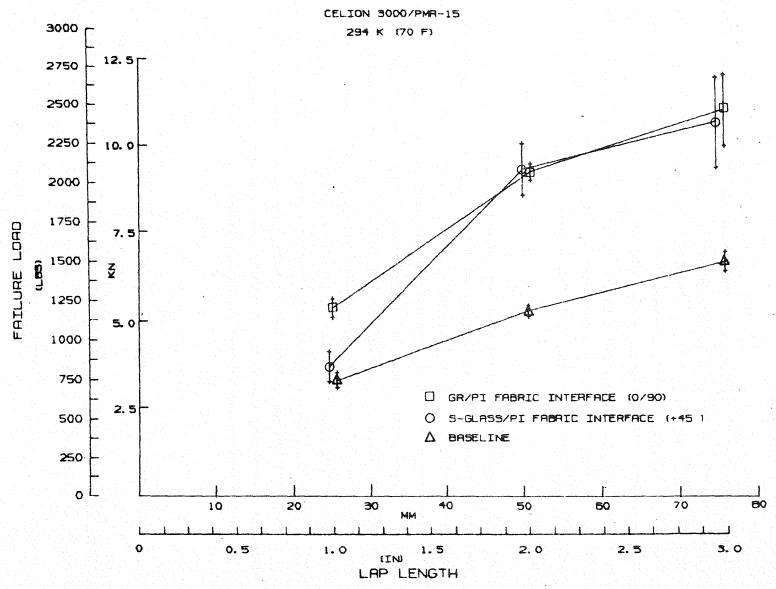


Figure 8-46: EFFECT OF FABRIC INTERFACES - SINGLE LAP JOINTS

#### EFFECT OF FABRIC INTERFACES - SINGLE LAP JOINTS

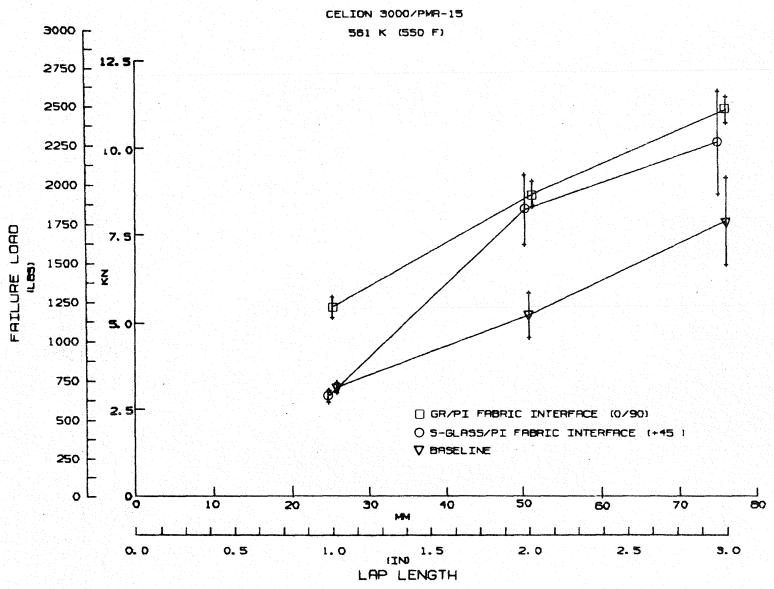
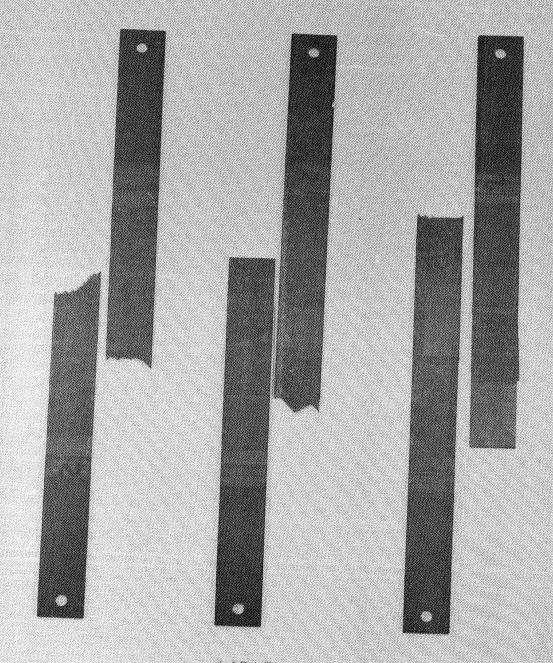


Figure 8-47: EFFECT OF FABRIC INTERFACES - SINGLE LAP JOINTS

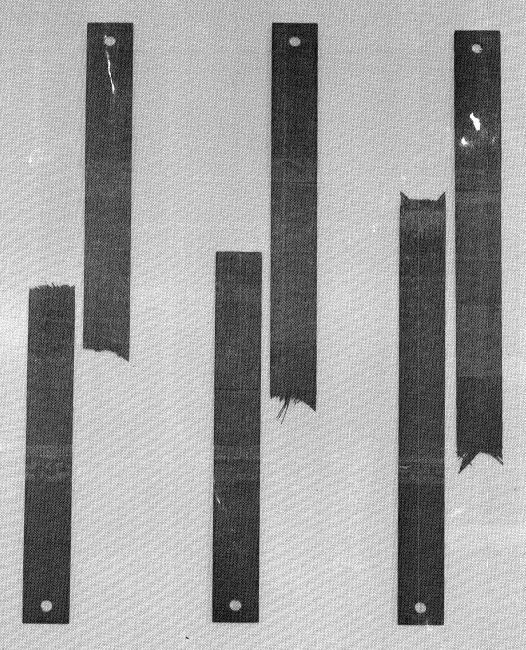


LAP LENGTH 25.4 MM (1.0 IN) 50.8 MM (2.0 IN) 76.2 MM (3.0 IN)

MATRIX 6 - ADVANCED JOINTS SOFTENING STRIP 294 K (709F)

Figure 8-48: GR/PI SINGLE LAP, S-GLASS/PI FABRIC INTERFACE, 294K (70°F) - FAILED SPECIMENS

198



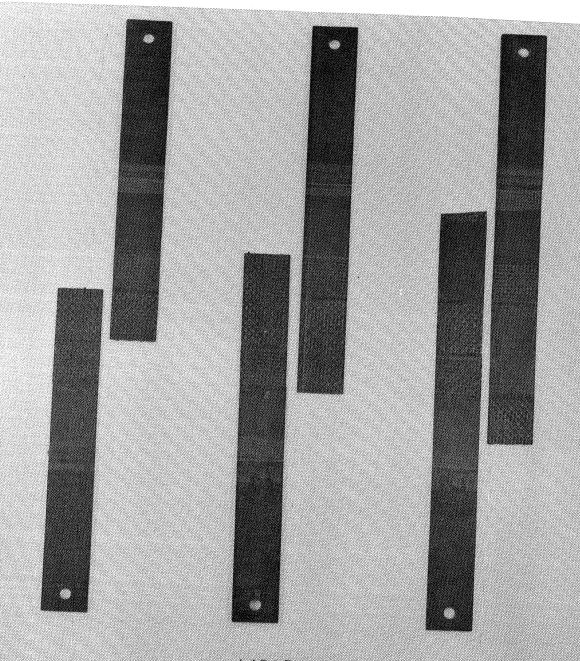
LAP LENGTH

25.4 MM (1.0 IN)

50.8 MM (2.0 IN) 76.2 MM (3.0 IN)

MATRIX 6 - ADVANCED JOINTS SOFTENING STRIP 561 K (550°F)

Figure 8-49: GR/PI SINGLE LAP, S-GLASS/PI FABRIC INTERFACE, 561K (550°F) -FAILED SPECIMENS



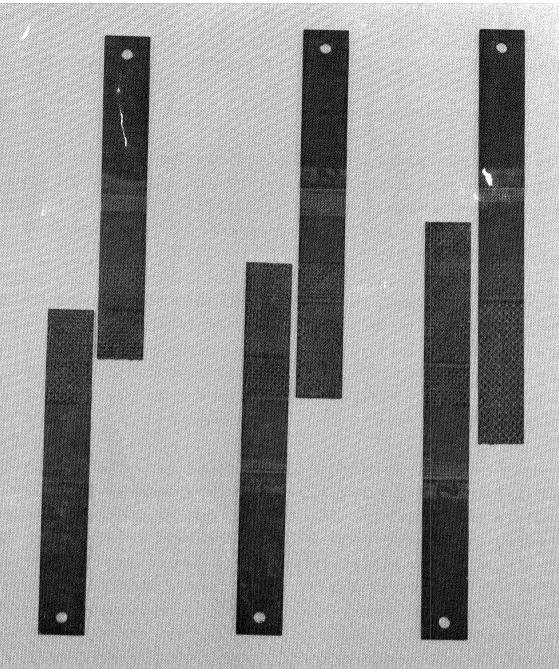
25.4 MM (1.0 IN)

LAP LENGTH 50.8 MM (2.0 IN) 76.2 MM (3.0 IN)

MATRIX 6 - ADVANCED JOINTS FABRIC INTERFACE 294 K (70°F)

Figure 8-50: GR/PI SINGLE LAP, GR/PI FABRIC INTERFACE, 294K (70°F) -FAILED SPECIMENS

200



LAP LENGTH 25.4 MM (1.0 IN) 50.8 MM (2.0 IN) 76.2 MM (3.0 IN)

MATRIX 6 - ADVANCED JOINTS FABRIC INTERFACE T 561 K (550<sup>0</sup>F)

Figure 8-51: GR/PI SINGLE LAP, GR/PI FABRIC INTERFACE, 561K (550°F) - FAILED SPECIMENS

201

#### 8.4.4 Quality Control Comparison

Since the advanced bonded joints were fabricated from a material lot which had quality control data slightly lower than required, standard single and double lap joints were included in Matrix 6 as a baseline. Comparisons of these baseline joints to the same joint configuration from Matrix 3 are made in Figures 8-52 through 8-55.

For single lap specimens, the Matrix 6 joints had a higher average failure load at 50.8mm (2.0 in) and 76.2mm (3.0 in) lap lengths, and a lower load for the 25.4mm (1.0 in) lap length. For double lap specimens the Matrix 6 joints were stronger at 294K ( $70^{\circ}$ F) and approximately equivalent at 561 ( $550^{\circ}$ F) to the Matrix 3 joints. Typical failed specimens for the single and double lap baseline joints are shown in Figures 8-56 through 8-59.

In general, Matrix 6 specimens, which were made from material considered poor quality, performed better than Matrix 3 specimens, which were made from acceptable quality material. This indicates that the quality control test parameters are not truly indicative of expected material performance. Better test standards should be developed to avoid discarding expensive material. Another possible explanation may be that the quality control panel was made from a portion of the prepreg roll that was bad. This would require that quality control panels be made from several locations within the prepreg roll to verify the entire lot of material. Normal processing would require a quality control panel be run in each autoclave run used to make laminates. This panel would be made from that portion of the prepreg roll currently being used. Test results from this panel would then verify the material as well as the autoclave run. This was not done on this program because of the additional cost and schedule implications. It is recommended that such a procedure be followed for any production type programs.

## MATRIX 6 VS. MATRIX 3 BASELINE SINGLE LAP JOINTS

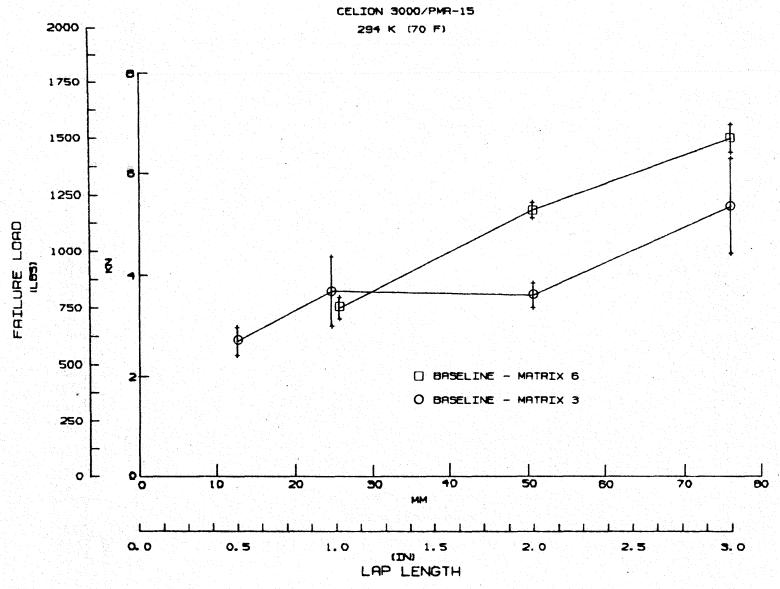


Figure 8-52: MATRIX 6 VS. MATRIX 3 BASELINE SINGLE LAP JOINTS

## MATRIX 6 VS. MATRIX 3 BASELINE SINGLE LAP JOINTS

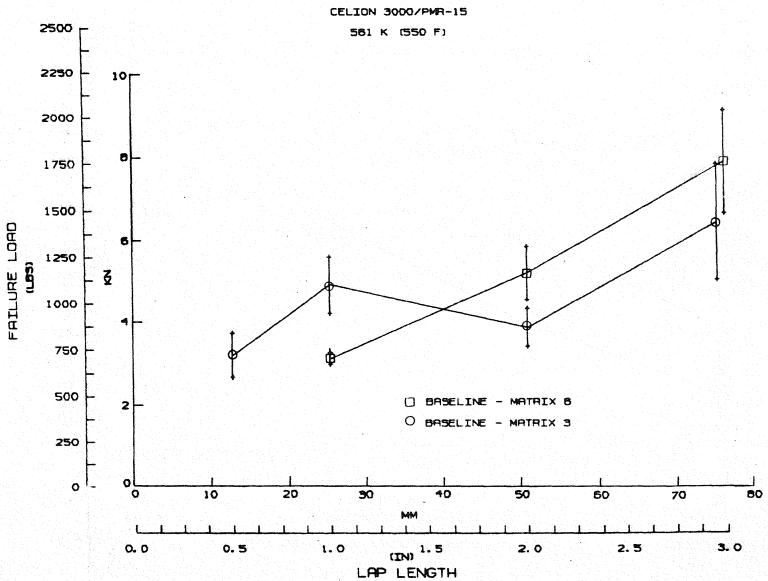


Figure 8-53: MATRIX 6 VS. MATRIX 3 BASELINE SINGLE LAP JOINTS

## MATRIX 6 VS. MATRIX 3 BASELINE DOUBLE LAP JOINTS

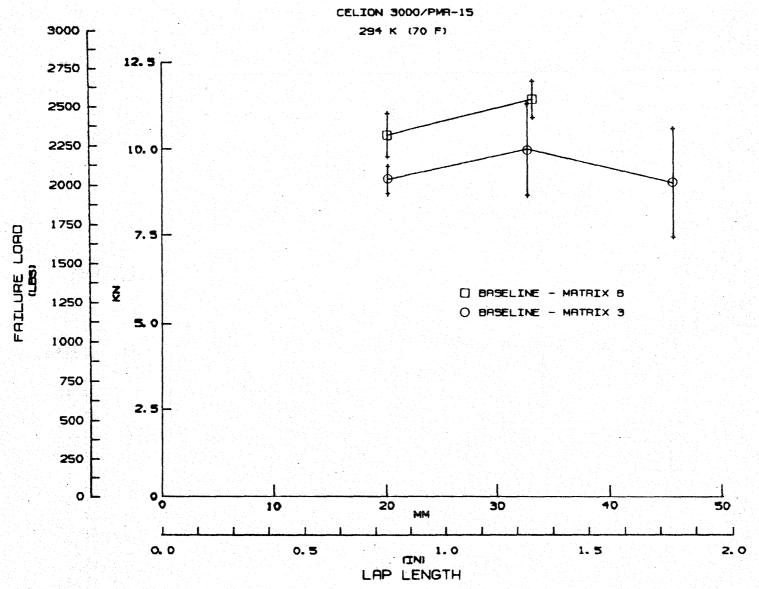


Figure 8-54: MATRIX 6 VS. MATRIX 3 BASELINE DOUBLE LAP JOINTS

## MATRIX 6 VS. MATRIX 3 BASELINE DOUBLE LAP JOINTS

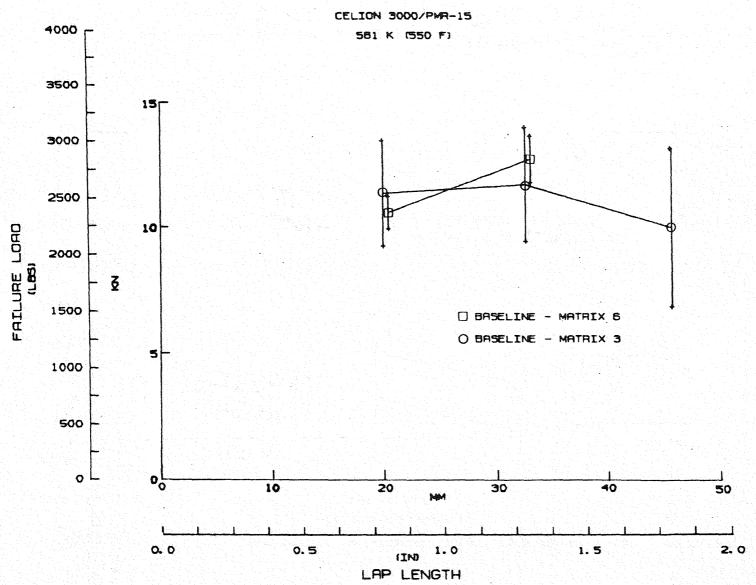


Figure 8-55: MATRIX 6 VS. MATRIX 3 BASELINE DOUBLE LAP JOINTS

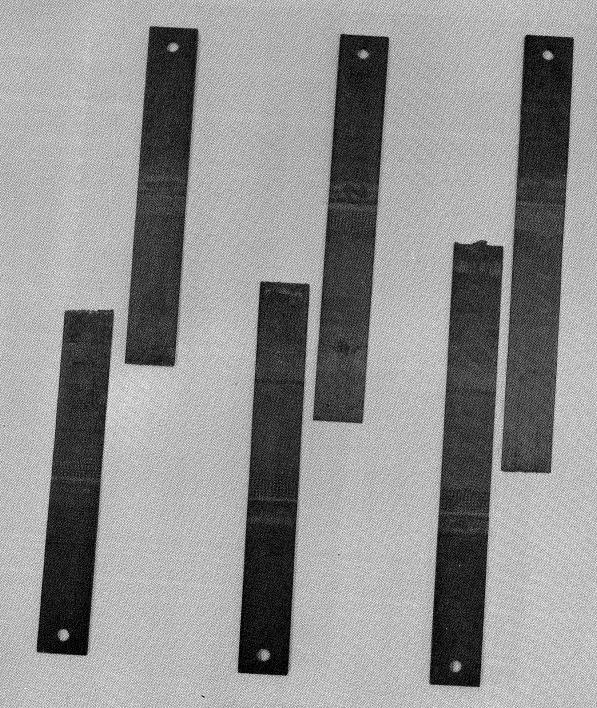


LAP LENGTH 25.4 MM (1.0 IN) 50.8 MM (2.0 IN) 76.2 MM (3.0 IN)

MATRIX 6 - ADVANCED JOINTS

294 K (70°F)

Figure 8-56: GR/PI SINGLE LAP, BASELINE, 294K (70°F) - FAILED SPECIMENS



LAP LENGTH

25.4 MM (1.0 IN)

50.8 MM (2.0 IN) 76.2 MM (3.0 IN)

# MATRIX 6 - ADVANCED JOINTS

561 K (550°F)

Figure 8-57: GR/PI SINGLE LAP, BASELINE, 561K (550°F) -FAILED SPECIMENS

208



LAP LENGTH

20.3 mm (0.8 in) 33.0 mm (1.3 in)

MATRIX 6 - ADVANCED JOINTS 294 K (70°F)

Figure 8-58: GR/PI DOUBLE LAP, BASELINE, 294K (70°F) - FAILED SPECIMENS



LAP LENGTH

20.3 mm (0.8 in) 33.0 mm (1.3 in)

MATRIX 6 - ADVANCED JOINTS 561 K (550<sup>O</sup>F)

Figure 8-59: GR/PI DOUBLE LAP, BASELINE, 561K (550°F) - FAILED SPECIMENS

#### 9.0 TEST/ANALYSIS CORRELATION

#### 9.1 Finite Element Analysis (Boeing IR&D)

Finite element analyses of single and double lap joints were performed using Boeing's BOPACE program. BOPACE allows detailed study of local stresses and deformations and has the following features and capabilities:

- o Material nonlinearity (adhesive plasticity, creep and viscosity)
- o Geometric nonlinearity (eccentricities, large rotations, large strains)
- o Temperature-dependent material properties
- o Material anisotropy
- o Automatic mesh generation
- o Graphics capability (undeformed & deformed pictures)
- o Accurate elements (appropriate high order, crack-tip & singular capability)

Simple analyses were performed on single lap joints with and without tapered adherends to demonstrate possible output formats and how visual display of results can be easily interpreted. Finite element models and deformations for the two joints analyzed are shown in Figures 9-1 through 9-4.

#### 9.1.1 Study of Finite Element Modeling Techniques—Double Lap Joints

Results of finite element analyses are strongly dependent on element size and modeling techniques. Ideally, smaller elements are required in areas of high stress concentrations; however, smaller elements also result in larger computer usage times and a corresponding increase in cost. Boeing IR&D funds were used to perform finite element modeling studies of bonded joints in an attempt to optimize element size and distributions and still obtain acceptable analysis results. Studies were performed to address the following areas and to assess their impact on analysis results.

- o Required element size near stress risers
- o Acceptability of rezoning to larger elements, away from stress risers

- o Effect of lamina property averaging when element size exceeds lamina thickness
- o Possible discretization requirements dictated by lamina and adhesive material interfaces.

The modeling studies were performed on a composite double lap bonded joint as shown in Figure 9-5. The ends of the outer adherends were cut at approximately a  $0.977 \, \text{rad.} \, (56^{\circ})$  angle to reduce the severity of the local stress/strain state. Previous calculations (see Figure 9-4) indicated that this provides improved joint performance. The joint was loaded in tension by displacing the ends  $0.254 \, \text{mm} \, (.01 \, \text{in})$ . An elastic, geometrically linear analysis was performed. Because of symmetry, only one quarter of the joint was actually modeled. The modeled area and boundary conditions and material properties used are shown in Figure 9-5.

Four models were studied, each using different mesh refinement and arrangements. Figures 9-6 through 9-15 show the finite element models used along with different stresses plotted along particular lines of elements. The stress plots given include:

- o  $\sigma_{\rm X}$ ,  $\sigma_{\rm Z}$ , and  $\tau_{\rm XZ}$  -vs- x in the 0<sup>0</sup> lamina adjacent to the adhesive layer. (Figures 9-6 through 9-9).
- o  $\tau_{xz}$  -vs- x along the adhesive centerline (Figures 9-10 through 9-13)
- o  $\tau_{xz}$  -vs- z (through the thickness) at the centerline of the joint. (Figures 9-10 through 9-13)
- o  $\sigma_x$  and  $\tau_{xz}$  -vs- z at x = 21.13 mm (0.832 in) (near the end of the overlap), to show stress dependence on lamina orientation angle and on element size relative to lamina thickness. (Figures 9-14 and 9-15)

The stress values plotted are at the geometric centers of the elements. Figures 9-16 and 9-17 show deformed models which illustrate the deformational behavior of the joints. Note that different plot scales have been used in some of the figures. All models were the same size and geometry except model #4 which had a particularly fine mesh in the regions of stress concentration

at the ends of the overlap zone. The 0.25 mm (0.01 in) half gap (see Fig. 9-9) between the principal adherends was made one element wide which is smaller in this model than in the previous three models which had 0.51 mm (0.02 in) half gaps (see Figures 9-6, 9-7, and 9-8). In fine mesh models such as this, economy dictated including zones of coarse elements in noncritical areas, particularly if nonlinear analysis is planned. Such rezoning was included in all of the three finer mesh models (Figures 9-7, 9-8, and 9-9) considered. In coarse models, or in models with local large element sizes, two lamina of material are often modeled by a single element. In these studies, the  $+45^{\circ}$  and  $-45^{\circ}$  and also the  $0^{\circ}$  and  $90^{\circ}$  lamina were sometimes combined. In these instances, the material properties were averaged for the appropriate elements.

In model #2 (Figures 9-7 and 9-11) each lamina near an area of stress concentration was represented by a single element in the z-direction. In model #1 (Figures 9-6 and 9-10) however, only specific lamina were represented by single elements in the z-direction and these were throughout the model. Models #3 and #4 (Figures 9-8 and 9-9) basically incorporated x-direction refinements of the #2 model, with model #4 (Figure 9-9) having a very fine grid near areas of stress concentration. Note also that in the plots for model #4 (Figure 9-13),  $\tau_{xz}$  is approaching zero near the free edge of the adhesive. This is due to the adhesive extension.

The plotted stresses and the deformed structure figures suggested the conclusions listed below which were incorporated into later models. Note that these conclusions were affected by several joint configuration details; namely, (1) the 0.977 rad  $(56^{\circ})$  tapering of the outer adherends, (2) the gap between the adherends at the joint centerline; and (3) the particular stacking arrangement used.

The peak stresses  $T_{xz}$ ,  $\sigma_x$ , and  $\sigma_z$  are not strongly dependent on mesh fineness, although for the coarsest model used some loss of accuracy is necessarily present. This assumes that the stresses are evaluated at some fixed point away from the end of the adherend.

- Lamina property averaging across large elements essentially results in predicted stresses which are an average of the values for the individual lamina (Figure 9-15). However it is seen in the deformed structure plots (Figures 9-16 and 9-17) that a deformation anomaly occurs at junctions between large and small elements where property averaging 0° and 90° plies have been done. This results from the load path eccentricity relative to the larger element size.
- The magnitude of the gap between the inner adherends has an important influence on stress levels\* ( $\tau_{xz}$  in Figure 9-13 as compared to Figures 9-10, 9-11, and 9-12).
- o Near stress concentrations, the value of the stress at the center of the element (or at other internal locations) may differ significantly from those at the edges of elements.

Results of the previous studies showed the critical areas to be  $\tau_{xz}$  in the adhesive and  $\sigma_z$  in the lamina adjacent to the adhesive in the inner adherend near the edge of the lap. Additional analyses were performed focusing on these two areas. The joint configuration, boundary conditions, loading and material properties used in this phase are shown in Figure 9-18. Analyses evaluated the effects of z-grid changes with the x-grid fixed and the effect of x-grid changes with the z-grid fixed. A summary of the models analyzed is given in Table 9-1.

Models 2A to 2E kept x-direction grid size unchanged while changing the lamina and adhesive representation. The coarsest model, 2A, used 1 element to represent the adhesive, 1 element to represent the  $0^{\circ}$  lamina, and 1 element to represent the  $(\pm 45,90_2,\pm 45)$  lamina. The finest model, 2E, used 3 elements through the thickness of the adhesive, represented the  $\pm 45$  and  $90_2^{\circ}$  laminae separately, and used 2 elements through the thickness of the  $0^{\circ}$  lamina nearest the adhesive.

\* The large  $\tau_{xz}$  (44.13 MN/m² (6.4 ksi)), Figure 9-13, for the finest mesh model resulted from a shortened gap between the inner adherends, rather than from the mesh fineness itself.

Changing from 1 element to 3 elements in the adhesive, Figure 9-19 and 9-20, changed the peak adhesive shear stress,  $\tau_{xz}$ , by less than 4%. (45.38 MPa (6568 psi) to 47.1 MPa (6830 psi)).

The normal stress,  $\sigma_z$ , in both the adhesive and the lamina adjacent to the adhesive increased as the adhesive representation was changed. Changing from 1 to 2 elements, Figures 9-21 and 9-22, changed  $\sigma_z$  in the adjacent adherend lamina by nearly 12% (8.3 MPa (1205 psi) to 9.3 MPa (1345 psi)). Changing from 2 to 3 elements, Figures 9-22 and 9-23, changed  $\sigma_z$  by an additional 2% (9.3 MPa (1345 psi) to 9.5 MPa (1370 psi)).

A summary of  $\tau_{XZ}$  and  $\sigma_{Z}$  stresses as a function of model changes is shown in Figure 9-24. Increasing the  $0^{0}$  lamina nearest the adhesive from 1 to 2 elements, Model 2D to 2E, (the number of adhesive elements remain constant at three) did not appreciably change  $\sigma_{z}$ .

Subsequently, models were analyzed which had 4 and 5 adhesive elements. The shear stress,  $\tau_{xz}$ , and normal stress,  $\sigma_z$ , for the adhesive and lamina adjacent to the adhesive for all of the adhesive models are summarized in Table 9-2.

An increase from 2 to 5 adhesive elements had no appreciable effect on the maximum shear stresses,  $\tau_{xz}$ ; however, the peak normal stress,  $\sigma_z$ , in the adhesive asymptotically approaches the value of  $\sigma_z$  in the splice plate lamina adjacent to the adhesive. Note, however, that the peak values of  $\sigma_z$  in the lamina adjacent to the adhesive do not appreciably change while going from 2 to 5 adhesive elements. Thus it was decided to use only 2 elements through the adhesive thickness for all subsequent finite element analyses.

Models 1A to 1D kept z-direction modeling constant and changed the x-direction grid size (see Table 9-1). All stresses in the areas of stress concentration increased with decreasing grid size, but again  $\tau_{\rm XZ}$  in the adhesive, and  $\sigma_{\rm Z}$  in the lamina adjacent to the adhesive near the edge of the lap are of greatest interest.

Between models 1C and 1D, Figures 9-25 and 9-26,  $\tau_{\rm XZ}$  increased and the peak of the curve moved closer to the edge of the lap. Plots of  $\tau_{\rm XZ}$  -vs-x show little divergence between the 2 models up to within 1-1/2 adhesive thicknesses .381 mm (.015 in) of the edge of the lap (see Figure 9-27).

Figures 9-28 and 9-29 show  $\sigma_{\rm Z}$  in the lamina adjacent to the adhesive increased significantly from Model 1C to Model 1D. Plots of  $\sigma_{\rm Z}$ -vs-x, (Figure 9-30) show that  $\sigma_{\rm Z}$  does not diverge appreciably from Model 1C to 1D until 1 adhesive thickness .254 mm (.01 in) from the edge of the lap. (At 1 adhesive thickness,  $\sigma_{\rm Z}$  differs by 4%, at 1-1/2 times the thickness,  $\sigma_{\rm Z}$  differs less than 2%.) A distance of 1 adhesive thickness in from the edge of the lap appears to be a good location for the comparison of  $\sigma_{\rm Z}$  from one layup to another (see Figure 9-31).

The effect of adding an adhesive fillet at the end of the splice plate was also studied. Models 1C and 1D were used as the reference models for this study. Analyses were conducted for two different minimum element sizes in the x-grid direction: 0.254 mm (0.01 in) minimum (Model 1C, Table 9-1) and 0.127 mm (0.005 in) minimum (Model 1D, Table 9-1). The fillet was assumed to be a 0.75 rad (45°) triangular shape. Analysis results are summarized in Table 9-3. Comparing adhesive stresses at a common reference point, 0.254 mm (0.01 in) inward (toward  $\mbox{\mbox{\bf 4}}$ ) from the edge of the splice plate, shows a reduction in  $\mbox{\mbox{\bf T}}_{\rm XZ}$  and a significant reduction in  $\mbox{\mbox{\bf O}}_{\rm Z}$  with the addition of a fillet; however, the  $\mbox{\mbox{\bf O}}_{\rm X}$  stress increases. At the same reference point, the  $\mbox{\mbox{\bf O}}_{\rm Z}$  stress in the adherend lamina adjacent to the adhesive is also significantly reduced with the addition of a fillet.

In a double lap joint the peak  $\sigma_z$  stress in the adherend lamina adjacent to the adhesive occurs near the end of the splice plate. Reducing the minimum element size, Model 1C to Model 1D, caused an increase in peak  $\sigma_z$  and also moved its location nearer the end of the splice plate. The peak occurs in the center of the last adhesive element. Adding a fillet to the coarse grid,

Model 1C, also increased the peak  $\sigma_{\rm Z}$  and, in addition, moved it so that it peaks directly under the fillet. Adding a fillet to the fine grid, Model 1D, did not increase the peak  $\sigma_{\rm Z}$  stress; however, the location did move so that it occurred directly under the fillet (see Figure 9-32).

The following conclusions can be drawn from the modeling studies:

- o Laminate property averaging across large elements gives valid results.
- o The magnitude of the gap between the inner adherends has an important influence on stress levels.
- o A highly refined mesh in the adhesive region is not required. Two elements through the adhesive thickness are sufficient.
- o When comparing results from two models it is important to keep the x-direction grid size constant.
- Adding an adhesive fillet would appear to have little effect on joint strength, as the fillet changes the location of the peak  $\sigma_z$  in the inner adherend but does not reduce it.

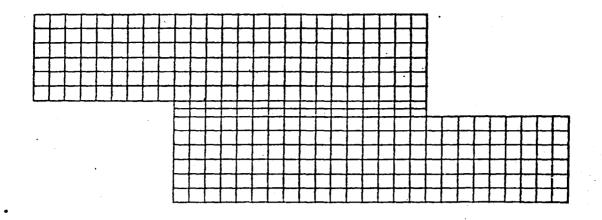


Figure 9-1: UNDEFORMED STRUCTURE - UNIFORM GRID MODEL

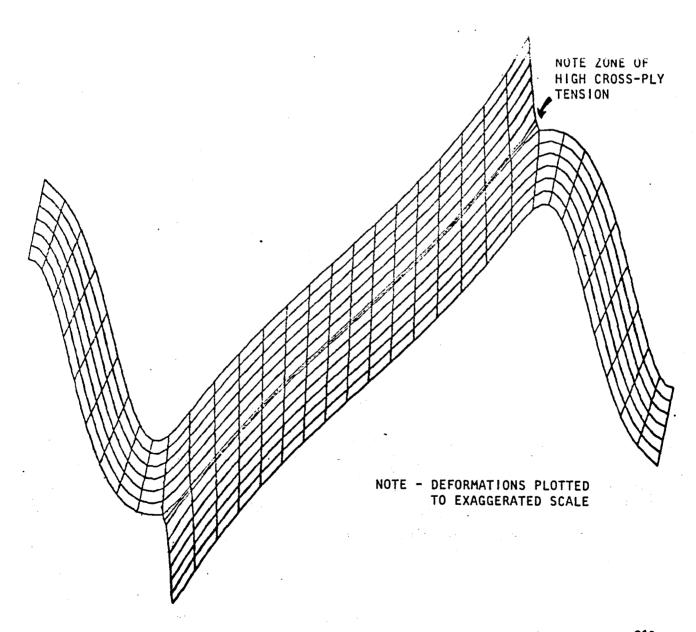


Figure 9-2: DEFORMED STRUCTURE - UNIFORM GRID MODEL

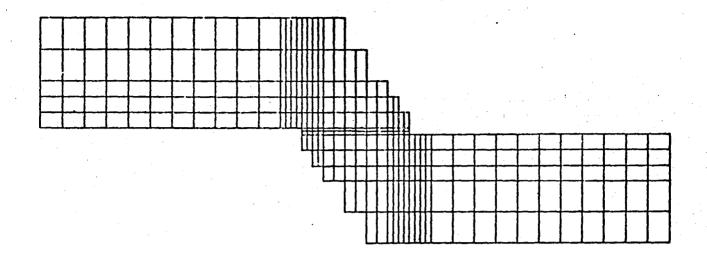


Figure 9-3: TAPERED SINGLE LAP UNDEFORMED STRUCTURE - VARIABLE GRID MODEL

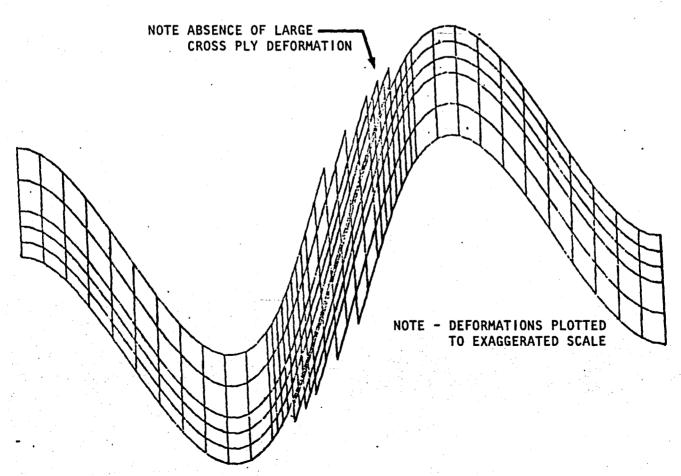


Figure 9-4: DEFORMED STRUCTURE - VARIABLE GRID MODEL

## BOUNDARY CONDITIONS ALONG MODEL EDGES

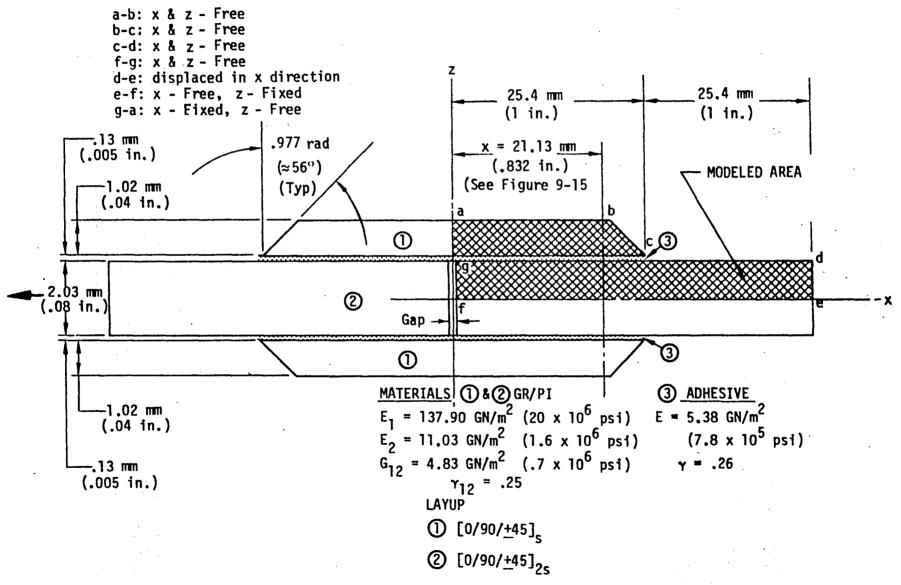


Figure 9-5: DOUBLE LAP BONDED JOINT USED FOR MODELING STILLIES

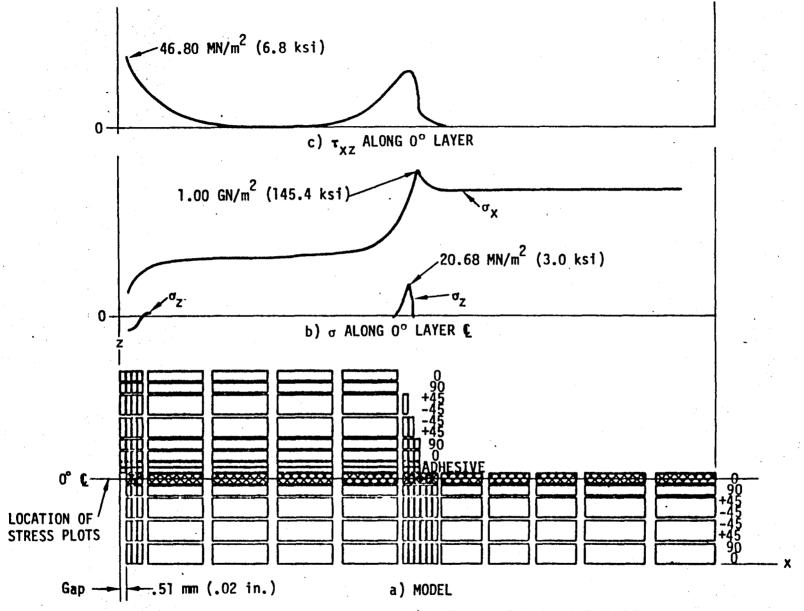


Figure 9-6: MODEL #1 - UNDEFORMED STRUCTURE

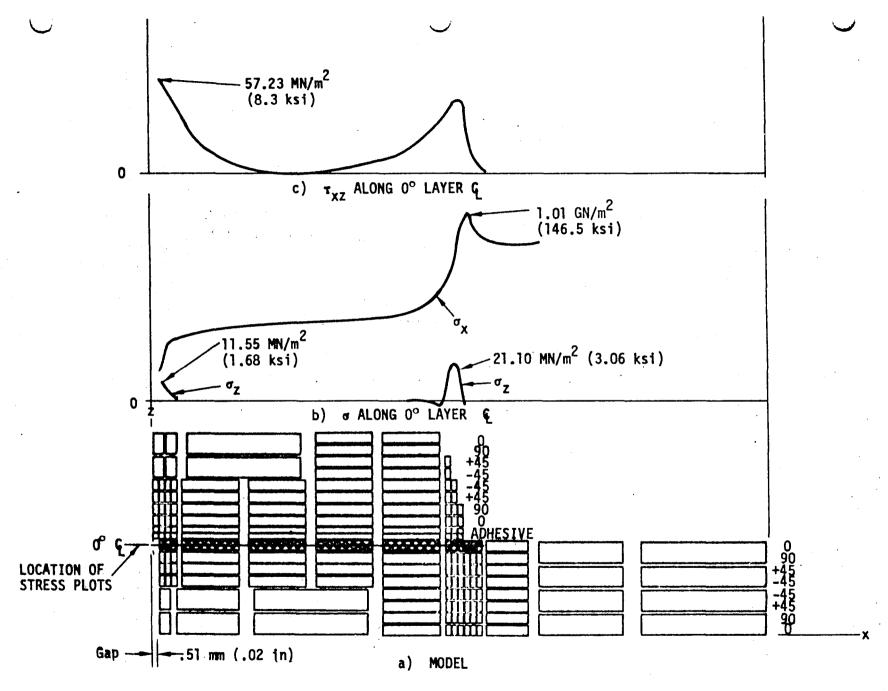


Figure 9-7: MODEL #2 - UNDEFORMED STRUCTURE (z-direction grid refinement of Model #1)

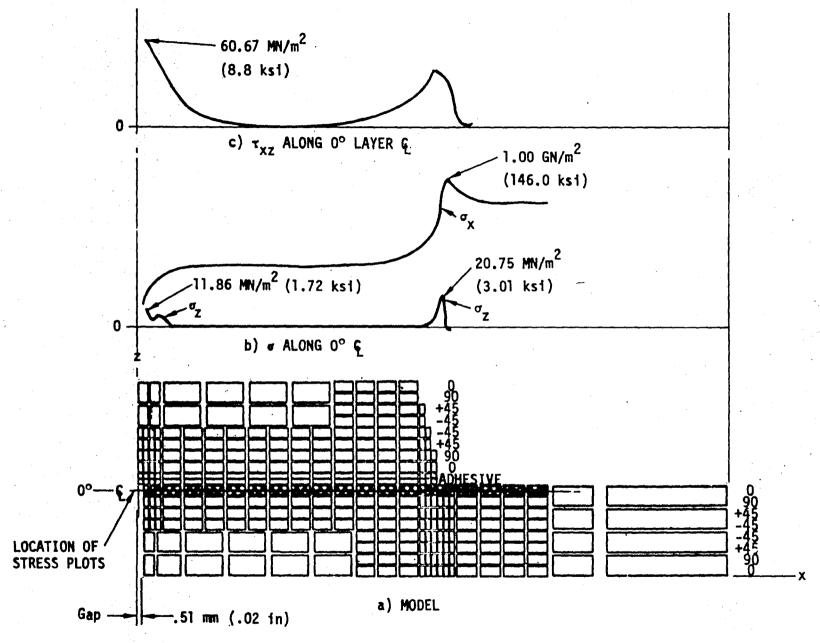


Figure 9-8: MODEL #3 - UNDEFORMED STRUCTURE (x-direction grid refinement of Model #2)

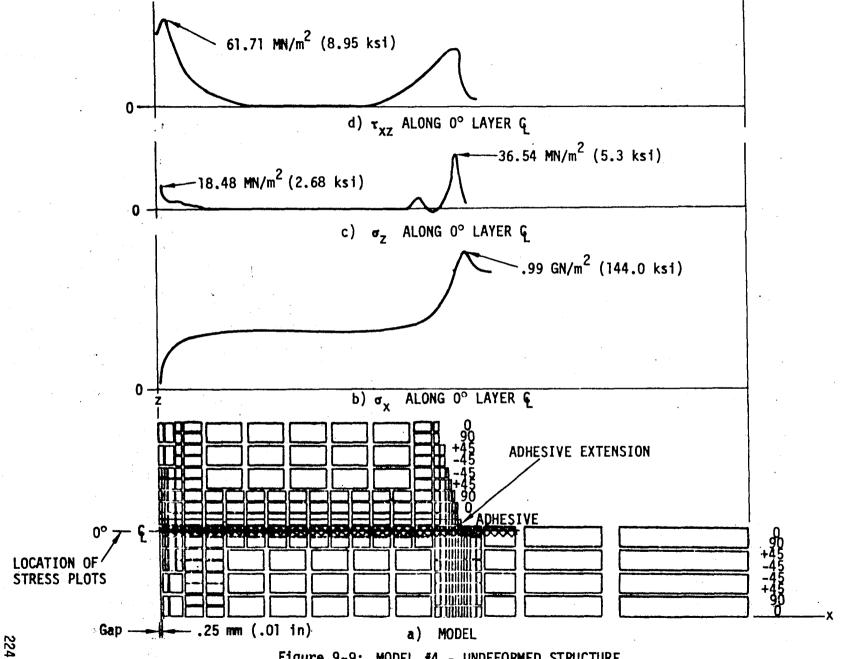


Figure 9-9: MODEL #4 - UNDEFORMED STRUCTURE (x-direction grid refinement of Model #2, very fine grid in stress concentration areas)

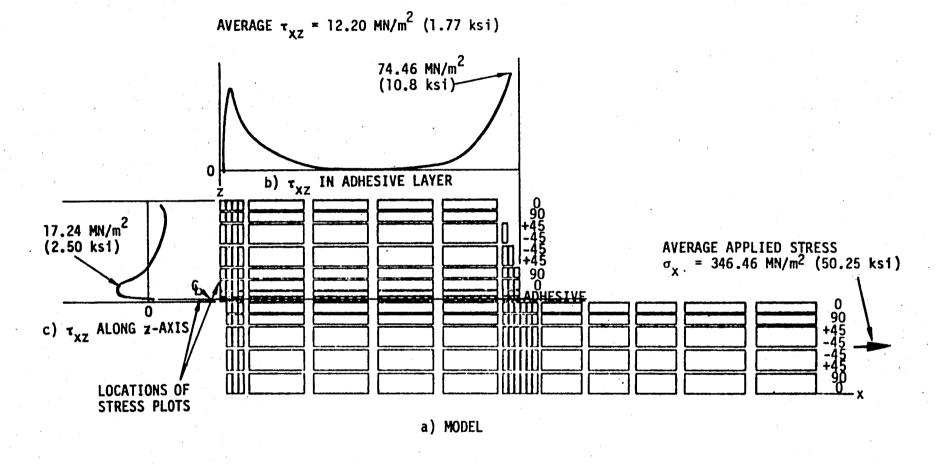


Figure 9-10: MODEL #1 -  $\tau_{xz}$  ADHESIVE AND SPLICE PLATE STRESSES

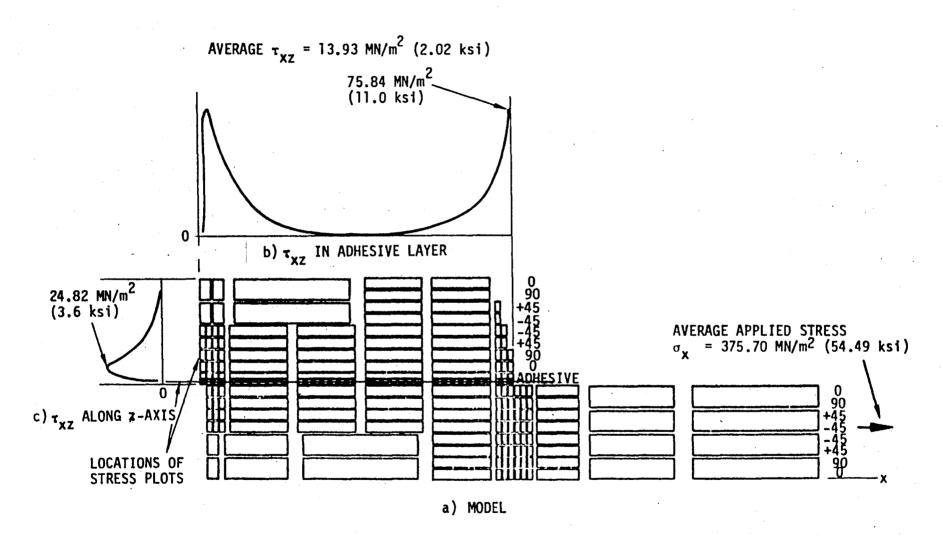


Figure 9-11: MODEL #2 -  $\tau_{\rm XZ}$  ADHESIVE AND SPLICE PLATE STRESSES

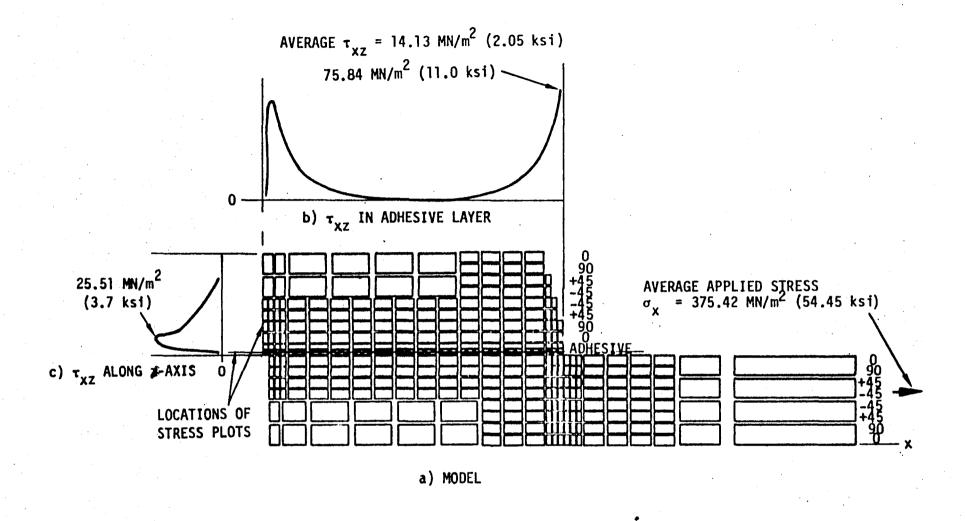
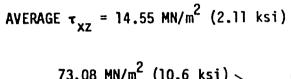


Figure 9-12: MODEL #3 -  $\tau_{xz}$  ADHESIVE AND SPLICE PLATE STRESSES



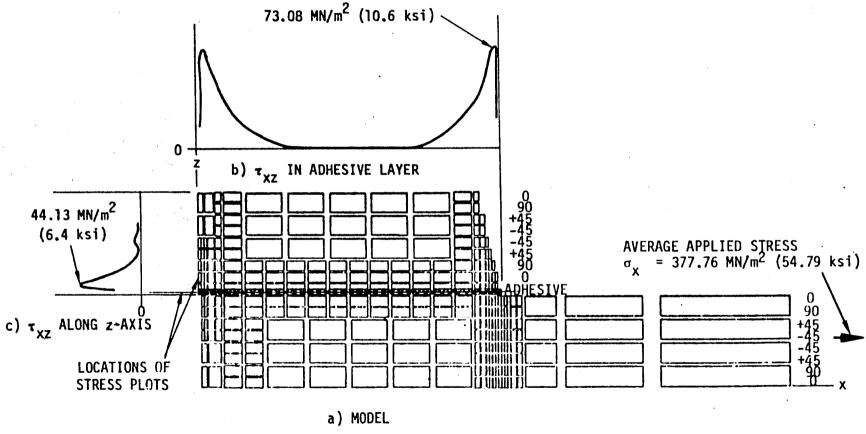


Figure 9-13: MODEL #4 -  $\tau_{XZ}$  ADHESIVE & SPLICE PLATE STRESSES

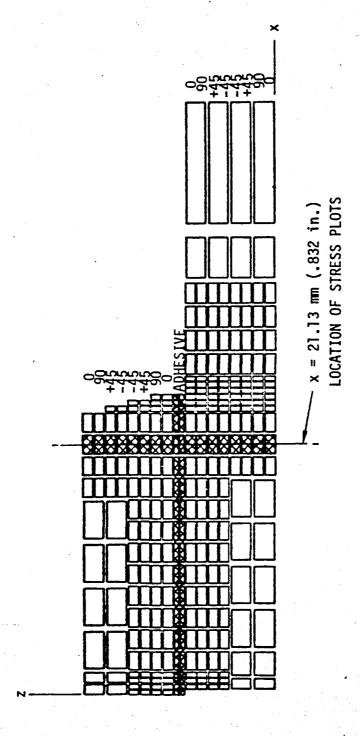


Figure 9-14: LOCATION OF STRESS PLOTS FOR (FIGURE 3.2.1-16)

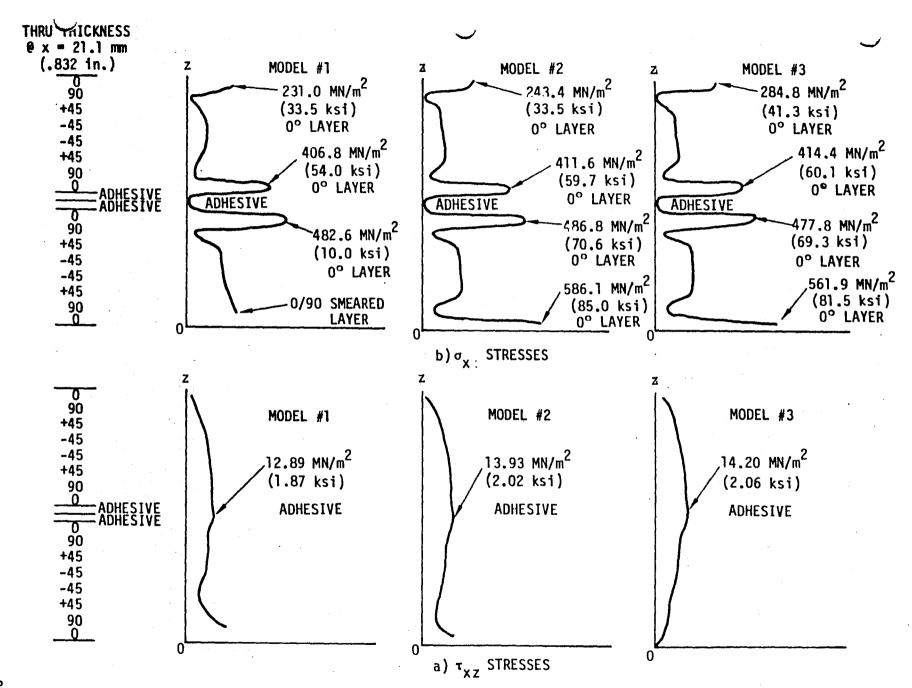


Figure 9-15: STRESSES IN MODELS #1, #2, and #3 AT LOCATION SPECIFIED IN FIGURE 9-14

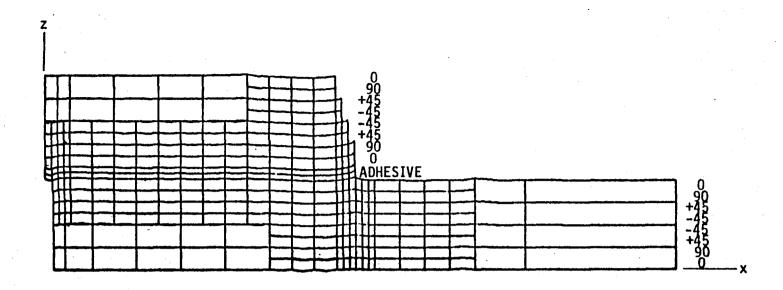


Figure 9-16: MODEL #3 - DEFORMED STRUCTURE

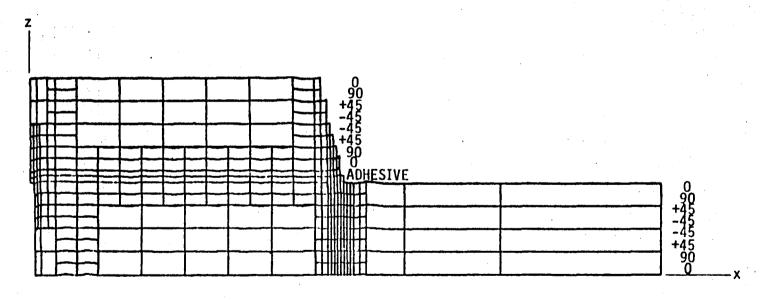
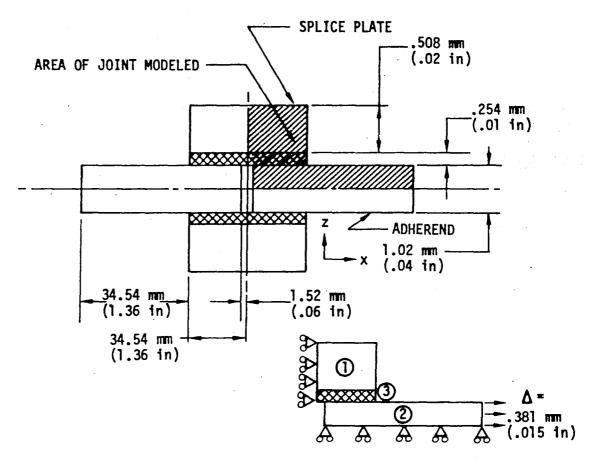


Figure 9-17: MODEL #4 - DEFORMED STRUCTURE



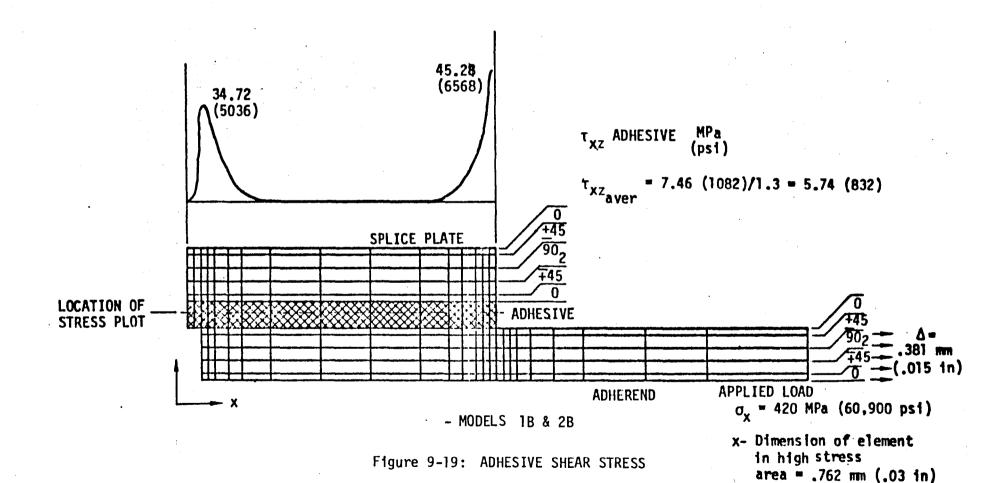
**BOUNDARY CONDITIONS** 

## MATERIAL PROPERTIES

Figure 9-18: STUDY MODEL CONFIGURATION

Table 9-1: SUMMARY OF MODELS USED IN STUDY OF MODELING TECHNIQUES OF A DOUBLE-LAP BONDED JOINT - (0,+45,90) LAMINATE

MODEL	X-DIRECTION GRID REPRESENTATION	Z-DIRECTION GRID REPRESENTATION			
NO.	DIM.OF SMALLEST ELEMENT IN AREAS OF HIGH STRESS	NO. OF ELEMENTS IN Z-DIRECTION			
		ADHESIVE	O° LAMINA	( <u>+</u> 45,90) <sub>s</sub>	
2A	0.762 mm (.03 in)	1	1	1	
2B	0.762 mm (.03 in)	1 ·	1.	3	
2C	0.762 mm (.03 in)	2	1	3	
2D	0.762 mm (.03 in)	3	. 1	3	
2E	0.762 mm (.03 in)	3	2	. 3	
1A	1.52 mm (.06 in)	1	. 1	3	
18	0.762 mm (.03 in)	1	1	3	
1C	0.254 mm (.01 in)	. 1	1	3	
1D	0.127 mm (.005 in)	1	1	3	



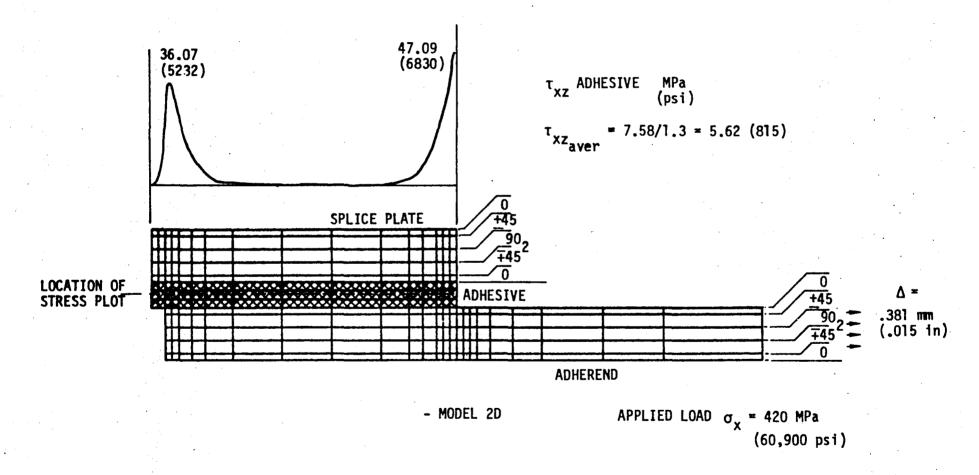
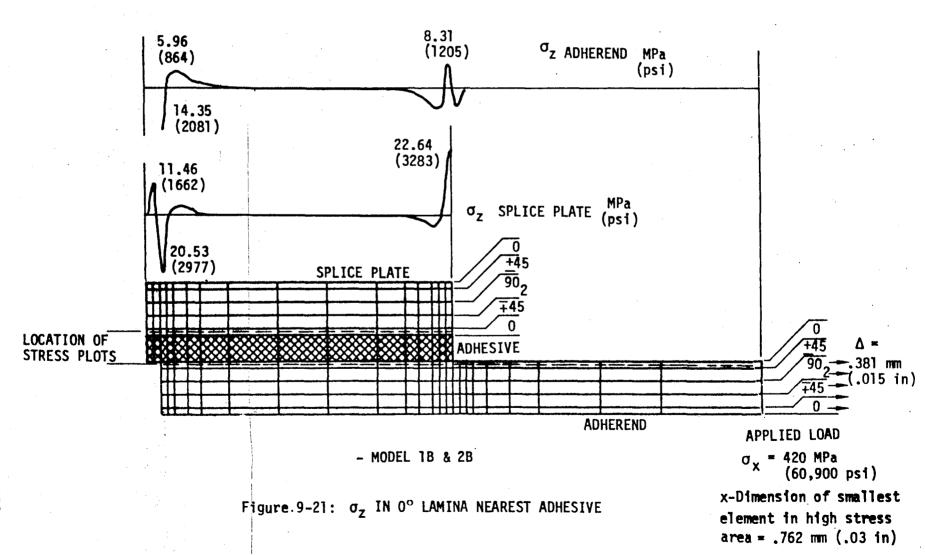


Figure 9-20: ADHESIVE SHEAR STRESS



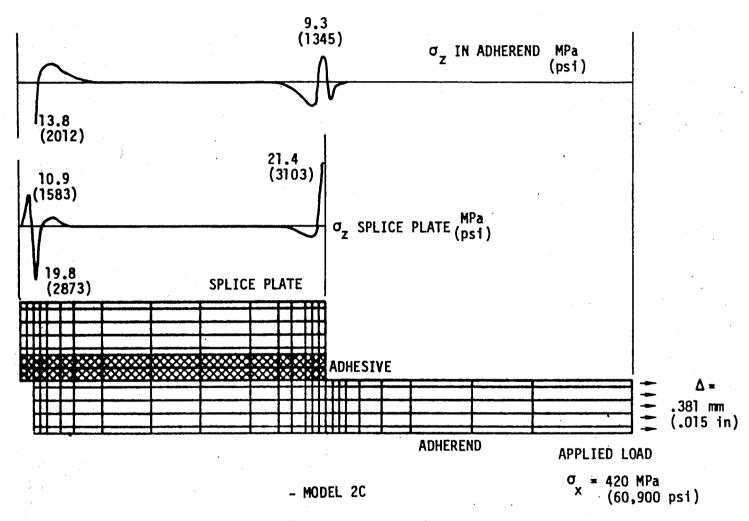


Figure 9-22:  $\sigma_z$  IN LAMINA NEAREST ADHESIVE

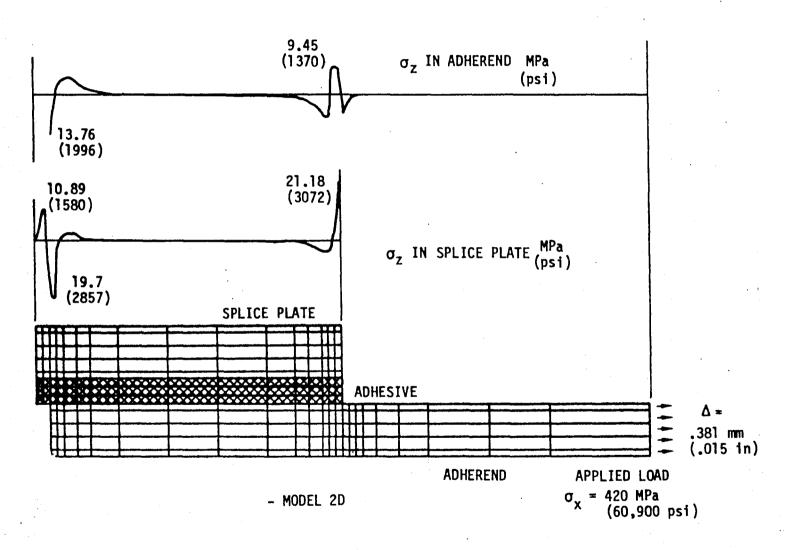


Figure 9-23:  $\sigma_z$  IN LAMINA NEAREST ADHESIVE

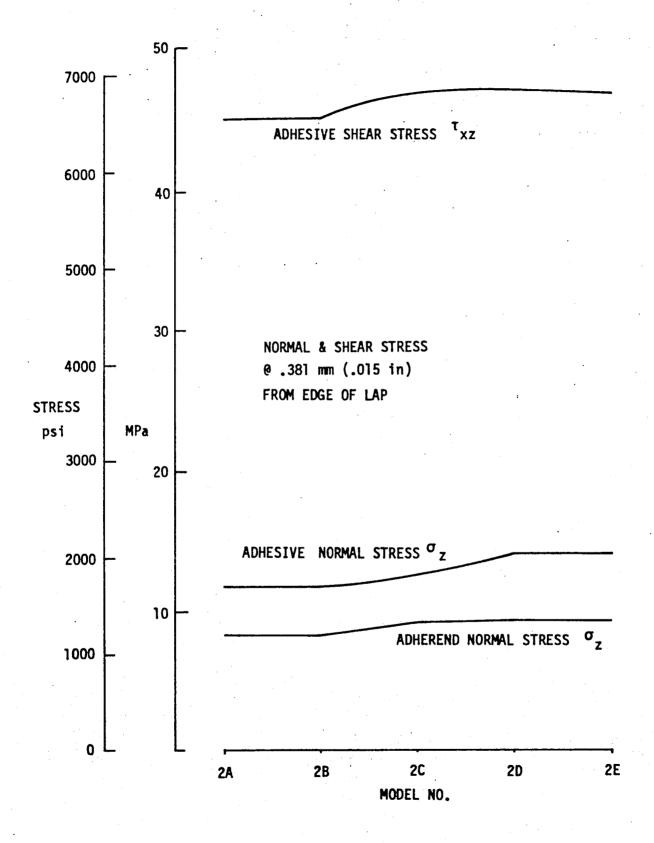


Figure 9-24: EFFECTS OF Z-GRID CHANGES ON STRESS LEVELS

Table 9-2: FINITE ELEMENT ANALYSIS - DOUBLE LAP JOINT VARYING NUMBER OF ADHESIVE ELEMENTS

STRESS	NUMBER OF ADHESIVE ELEMENTS					
31K233	1.	2	3	4	5	
PEAK T <sub>XZ</sub> ADHESIVE*	45.3	47.2	47.1	47.1	47.1	
MPa (psi)	(6570)	(6850)	(6830)	(6830)	(6830)	
T <sub>XZ</sub> ADHEREND <sup>*</sup>	30.1	31.6	31.9	32.0	32.1	
MPa (ps1)	(4370)	(4585)	(4625)	(4640)	(4650)	
τ <sub>XZ</sub> SPLICE PLATE <sup>*</sup>	35.3	33.3	33.2	33.0	33.0	
MPa (psi)	(5120)	(4830)	(4810)	(4790)	(4790)	
PEAK σ <sub>Z</sub> ADHESIVE <sup>*</sup>	11.7	18.4	19.5	20.0	20.3	
MPa (psi)	(1700)	(2665)	(2835)	(2905)	(2945)	
♂z ADHEREND <sup>*</sup>	8.3	9.3	9.4	9.5	9.5	
MPa (psi)	(1205)	(1345)	(1370)	(1380)	(1385)	
σ <sub>z</sub> SPLICE PLATE <sup>*</sup>	22.6	21.4	21.2	21.1	21.0	
MPa (psi)	(3285)	(3105)	(3070)	(3060)	(3050)	

<sup>\*</sup> Stresses shown are .381 mm (.015 in) from end of splice plate.

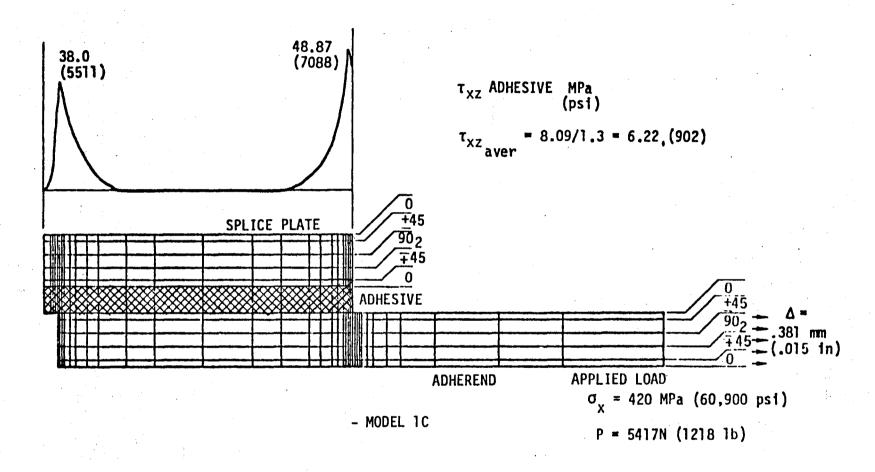
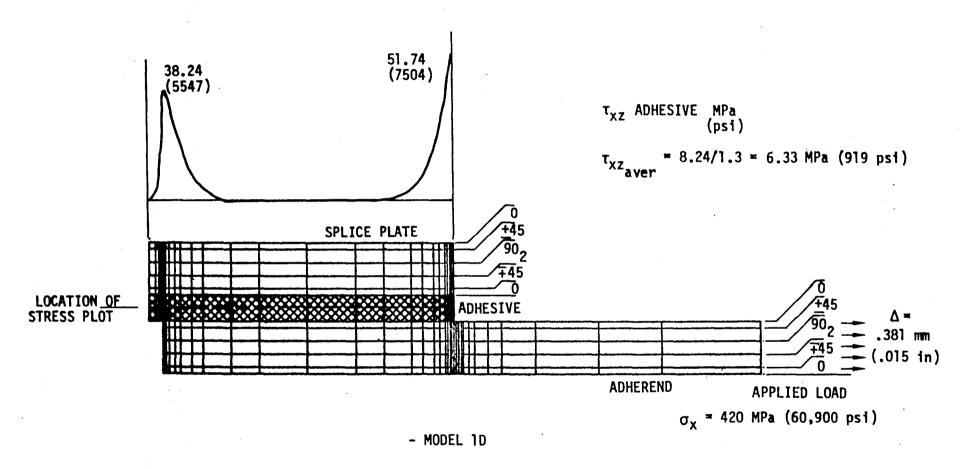


Figure 9-25: ADHESIVE SHEAR STRESS



x- Dimension of element in high stress area = .127 mm (.005 in)

Figure 9-26: ADHESIVE SHEAR STRESS

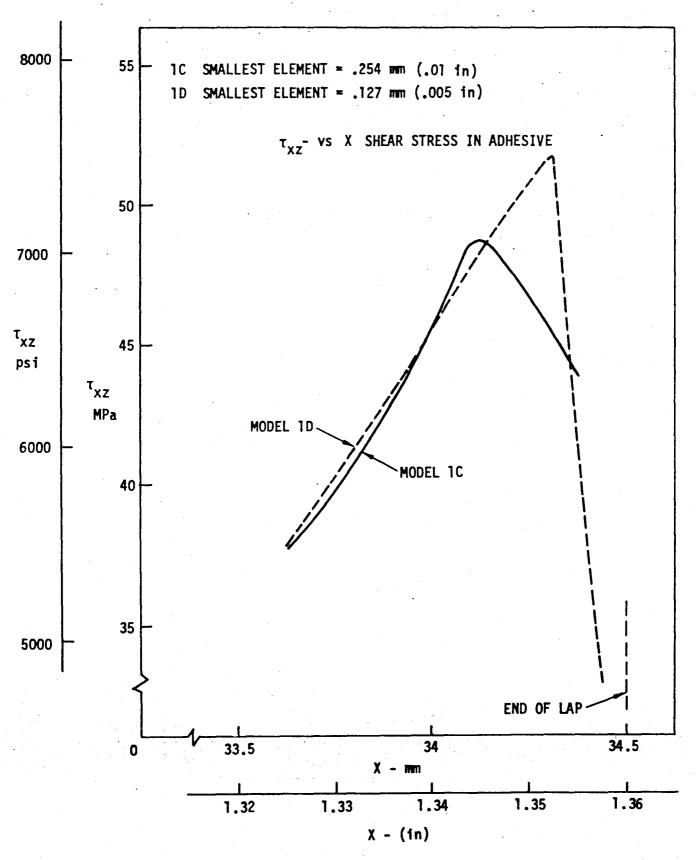


Figure 9-27: EFFECT OF X-GRID CHANGE ON  $\tau_{xz}$  ADHESIVE

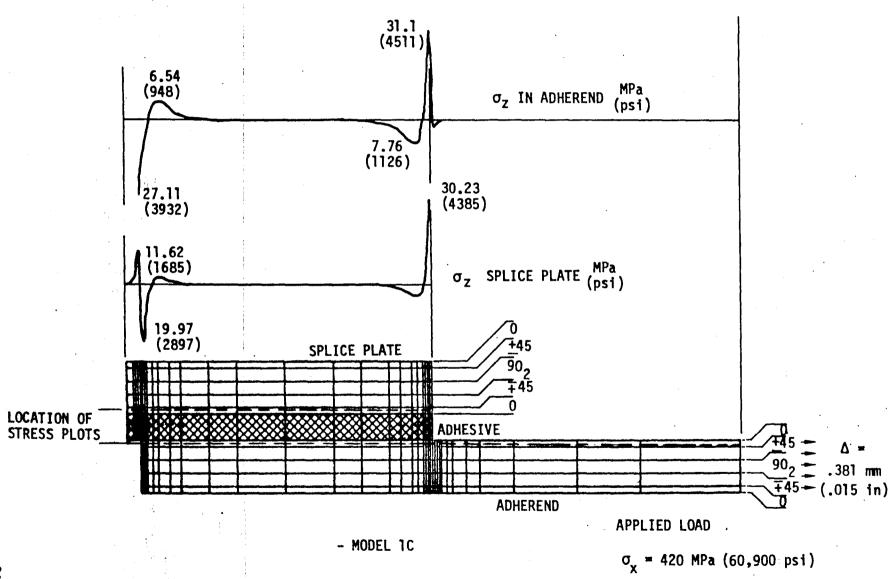
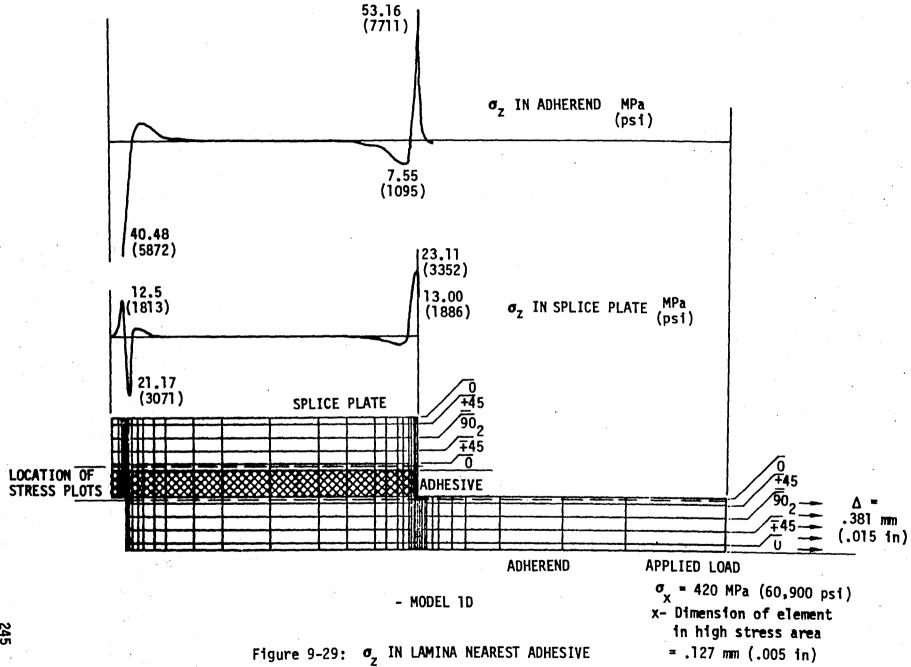


Figure 9-28:  $\sigma_{_{\!Z}}$  IN LAMINA NEAREST ADHESIVE



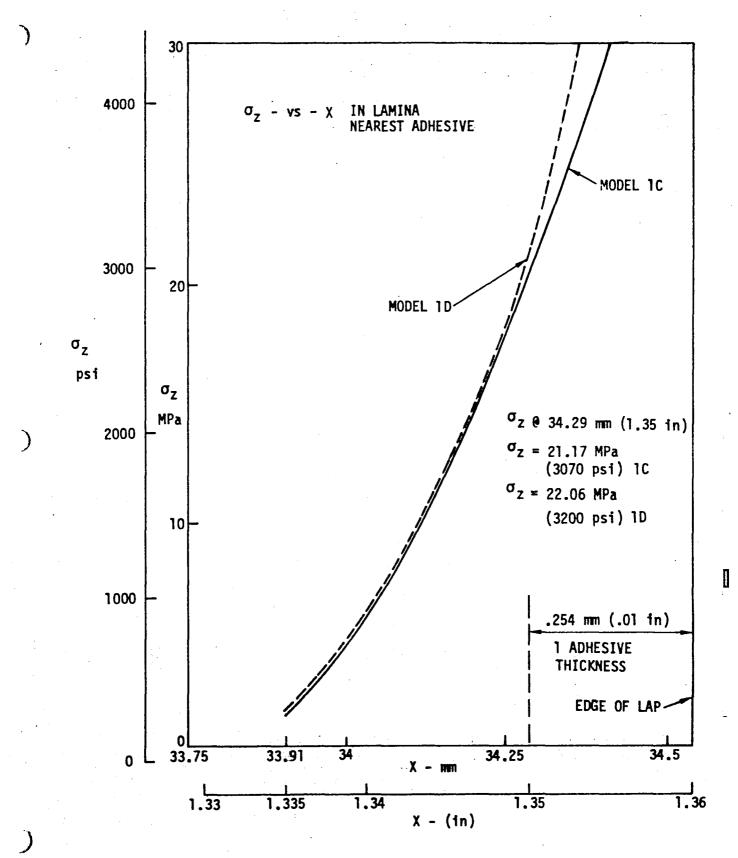


Figure 9-30: EFFECT OF X-GRID CHANGE ON  $\sigma_{\rm Z}$  IN LAMINATE

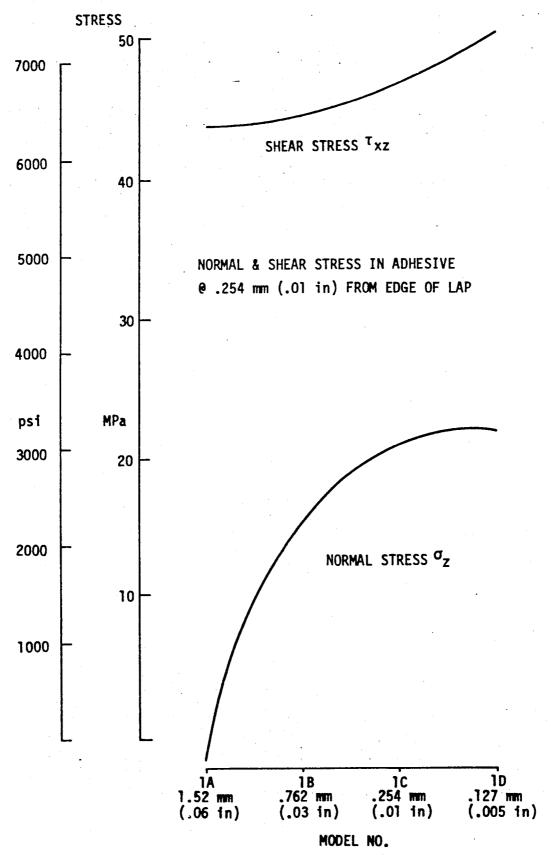
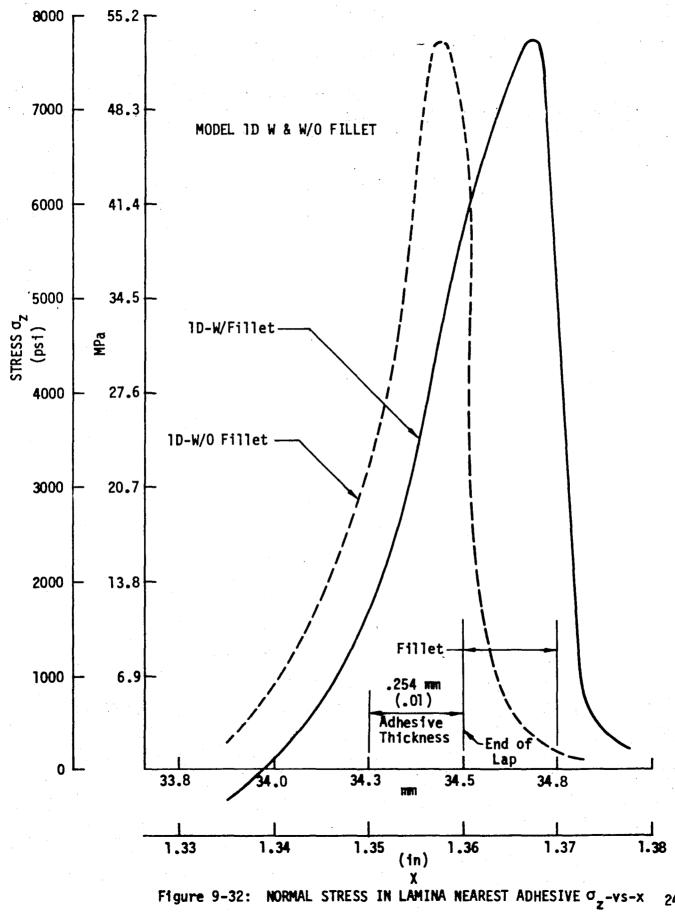


Figure 9-31: EFFECTS OF X-GRID CHANGES ON STRESS LEVELS IN ADHESIVE

Table 9-3: FINITE ELEMENT ANALYSIS - DOUBLE LAP JOINT EFFECT OF ADHESIVE FILLET

N.		MODEL 1C .245 mm (.01 in) Minimum Element		MODEL 1D .127 mm (.005 in) Minimum Element	
LOCATION	ITEM	WITHOUT FILLET MPa (psi)	WITH FILLET (MPa (psi)	WITHOUT FILLET MPa (psi)	WITH FILLET MPa (psi)
ADHESIVE .254 MM (.01 in) FROM END OF SPLICE PLATE	τ <sub>xz</sub>	46.9 (6800)	46.8 (6790)	50.7 (7360)	47.4 (6880)
	σ <sub>Z</sub>	23.4 (3400)	13.1 (1900)	23.8 (3450)	13.1 (1900)
	σ <sub>χ</sub>	23.6 (3420)	34.1 (4950)	27.9 (4050)	34.1 (4950)
ADHEREND LAMINA ADJACENT TO ADHESIVE	$\sigma_{_{ m Z}}$ Lamina $igtriangleright$	22.0 (3190)	12.5 (1820)	22.2 (3220)	11.7 (1700)
	Peak <sup>O</sup> Z Lamina	31.2 (4520)	52.3 (7580)	53.3 (7730)	53.4 (7750)

▶ .254 mm (.01 in) From End of Splice Plate



## 9.1.2 Double Lap Joints

Finite element analyses were conducted on 3 double lap bonded joint configurations chosen from standard joint test matrix 3D, (See Section 4-1, Fig. 4-6). Configurations chosen were test set 3D-4a- $(0_3, \pm 45_3, 90_3)_{2s}$ , 3D-2b  $(0, \pm 45, 90)_{6s}$ , 3D-5a- $(\pm 45, 0, 90)_{6s}$ . The first had a very stiff zone, three  $0^0$  lamina adjacent to the adhesive, the second, one  $0^0$  lamina adjacent to the adhesive and the third a very soft zone,  $\pm 45^0$  lamina nearest the adhesive. Figure 9-33 shows the general characteristics of the three models. Figure 9-34 gives the modulus matrix used for the analysis.

These analyses were used to predict trends or to compare stress levels in one joint with another. No predictions of failure load or joint strength were made at the time the analyses were conducted.

The modeling studies showed it is important to keep x-direction grid size constant when making comparisons between models. Z-direction grid size is somewhat less important. The representation of the adhesive by two elements in the z-direction was kept constant for each joint, but the z-direction grid for the laminates was dictated by individual lamina groups.

Model 3D-4a had 408 quadrilateral plate elements and both 3D-2b and 3D-5a had 512 elements. The x-direction grid remained unchanged from model to model. The width of the smallest element in areas of stress concentration was .254 mm (.01 in). The thickest element in model 3D-2b was .381 mm (.015 in) in height which represented  $(\pm 45^{\circ}, 90_{2}, \pm 45^{\circ})$  lamina. The  $0^{\circ}$  lamina were represented individually. The thickest element in 3D-4a was also .381 mm (.015 in) and represented both  $\pm 45_{3}$  and  $90_{6}$  lamina. Again, the  $0^{\circ}$  lamina were represented individually. The thickest element in 3D-5a was .254 mm (.01 in) and represented the  $(0^{\circ}, 90^{\circ}_{2}, 0^{\circ})$  lamina. Both of the  $0^{\circ}$  lamina nearest the adhesive were represented individually.

The analysis assumed a geometrically linear and elastic material and a plain strain condition. Boundary conditions are as shown in Figure 9-18. The joint

was loaded by displacing the free end by .254 mm (.01 in) in the "positive" x-direction, ( $\sigma_{\rm X}$  = 267 MPa (38.7 ksi)). This loading overstresses the adhesive, but as these analyses are elastic, the displacements and stresses may be ratioed as necessary.

A comparison of the three joints show that all have the same extensional stiffness, but the flexural stiffness is quite different; however, flexural stiffness is a much less important parameter for double lap joints than for single lap.

Each of the joints studied was designed to fail in the joint rather than the adherend outside the joint. Thus, the adherend laminate is lightly loaded and the critical stresses are the adhesive shear stress,  $\tau_{xz}$ , and the inner adherend peel stress,  $\sigma_z$ , in the lamina adjacent to the adhesive near the edge of the lap. The latter becomes increasingly important as the adherend becomes thicker.

Approximately a 4% drop (53.12 MPa (7705 psi) to 51.0 MPa (7397 psi)) in peak shear stress in the adhesive was achieved by changing the three  $0^{\circ}$  lamina nearest the adhesive to one  $0^{\circ}$  lamina. Another 4.5% reduction (51.0 MPa (7397 psi) to 48.88 MPa (7090 psi)) in the peak adhesive shear stress was achieved by placing the  $\pm 45^{\circ}$  lamina next to the adhesive (see Figures 9-35 through 9-38).

A very stiff zone, such as the three  $0^{0}$  lamina next to the adhesive, together with the condition of equal strain,  $\epsilon_{\chi}$ , in the adherend and the splice plate requires extremely rapid transfer of load between the stiff three  $0^{0}$  lamina resulting in a very high peak shear stress in the adhesive. A soft buffer next to the adhesive, i.e., the  $\pm 45^{0}$  lamina, transfers load more slowly with lower shear stress in the adhesive. This is accomplished by allowing additional shear strain across this soft zone, weakening the condition of equal strain,  $\epsilon_{\chi}$ , in the adherends and in the splice plates.

The  $\sigma_z$  stress in the lamina nearest the adhesive is also an important parameter. Changing from a stiff zone, three  $0^{0}$  lamina, to a soft zone, the  $\pm 45^{0}$  lamina, increased  $\sigma_z$  by approximately 6% (50.08 MPa (7264 psi) to 53.07 MPa (7697 psi)) as shown in Figures 9-39 through 9-42.

In conclusion, these analyses indicate that it would be advantageous to have a soft zone (i.e.,  $\pm 45^{\circ}$ ) adjacent to the adhesive in a double lap joint. This would produce a decrease in adhesive shear stress, leading to an increase in joint strength provided the  $\sigma_{7}$  strength of the laminate is not exceeded.

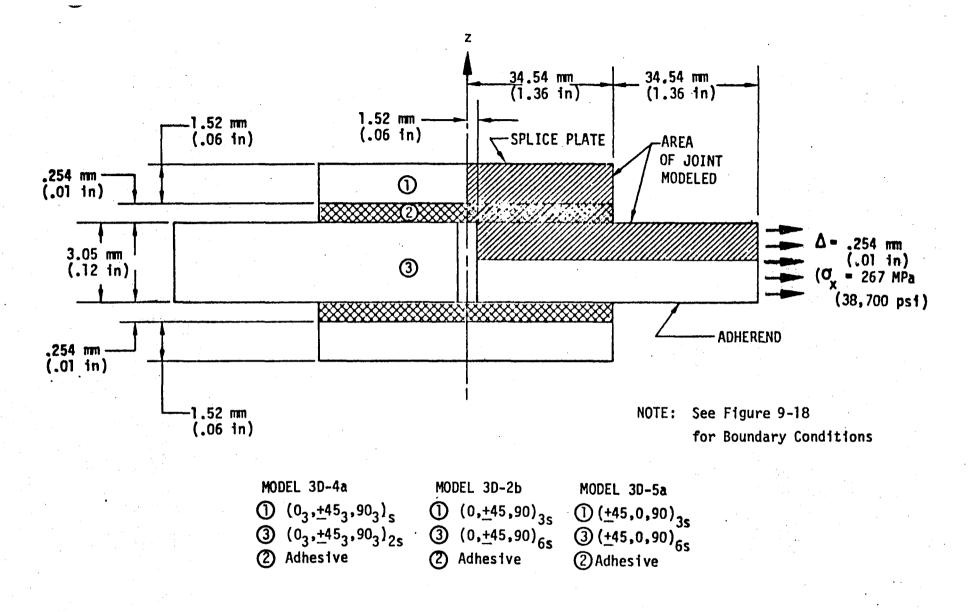


Figure 9-33: DOUBLE LAP BONDED JOINT CONFIGURATION

$$[Q] = \begin{bmatrix} 139.9 & 3.997 & 3.997 & 0 & 0 & 0 \\ 12.24 & 3.75 & 0 & 0 & 0 \\ & & 12.24 & 0 & 0 & 0 \\ & & & 4.8 & 0 & 0 \\ & & & & 4.8 & 0 \\ & & & & 4.8 \end{bmatrix} GPa$$

$$= \begin{bmatrix} 20.29 & .5797 & .5797 & 0 & 0 & 0 \\ 1.775 & .544 & 0 & 0 & 0 \\ & & 1.775 & 0 & 0 & 0 \\ & & & .70 & 0 & 0 \\ & & & .70 & 0 & 0 \\ & & & .70 & 0 & 0 \\ & & & .70 & 0 \end{bmatrix} Msi$$

Figure 9-34: ON-AXIS MATERIAL PROPERTIES (MODULUS) USED IN FINITE ELEMENT ANALYSIS

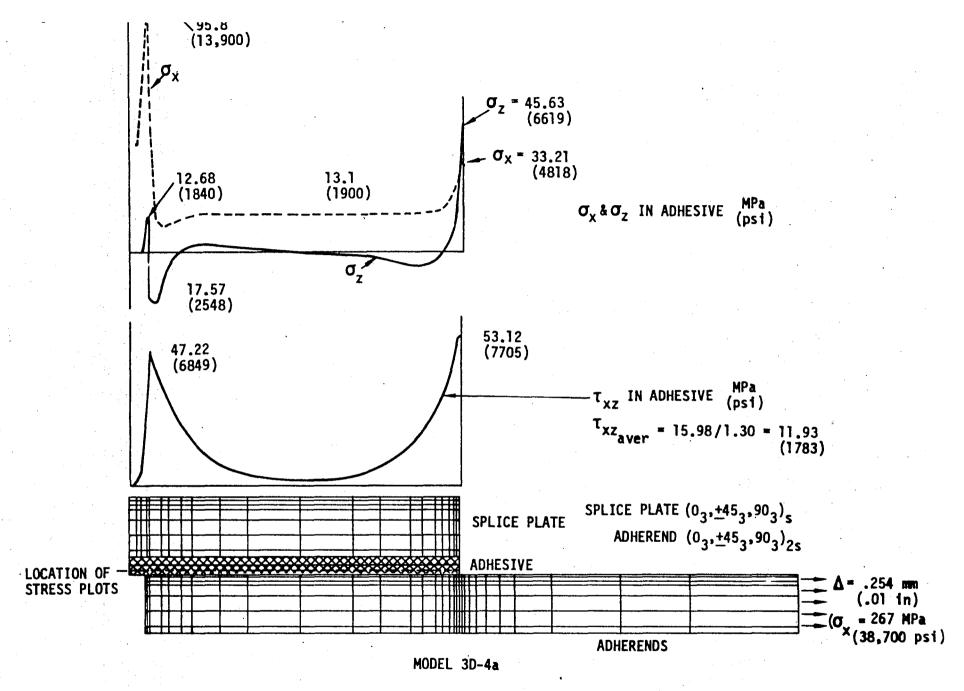
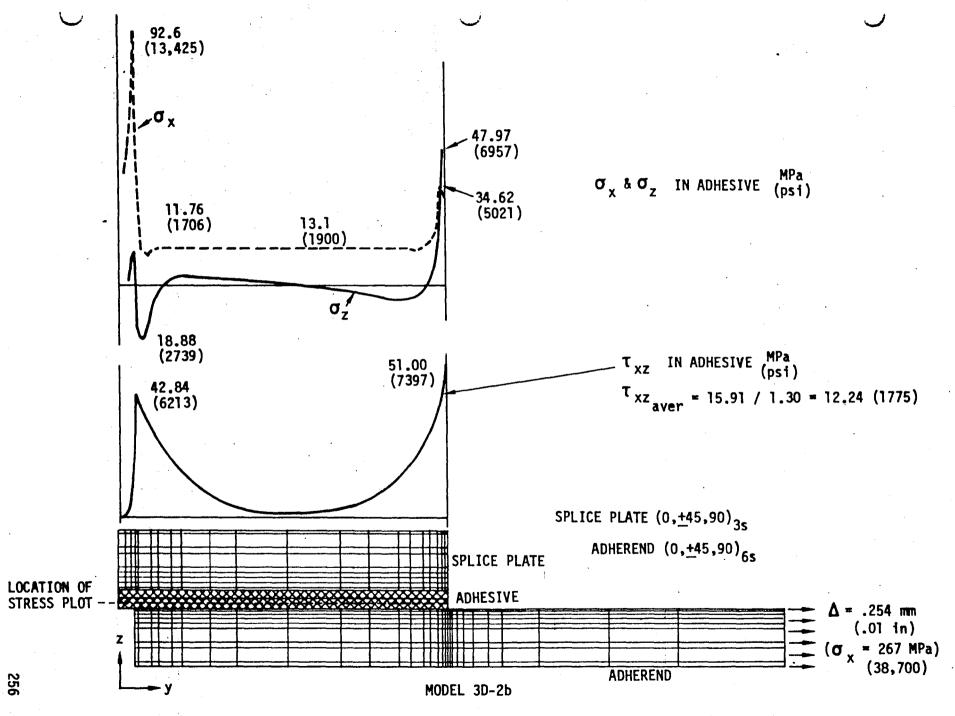


Figure 9-35: ADHESIVE SHEAR,  $\sigma_{x}$  &  $\sigma_{z}$  STRESS



TI ..... O TE: ADDECTIVE CUEAD A LA CTOFCC

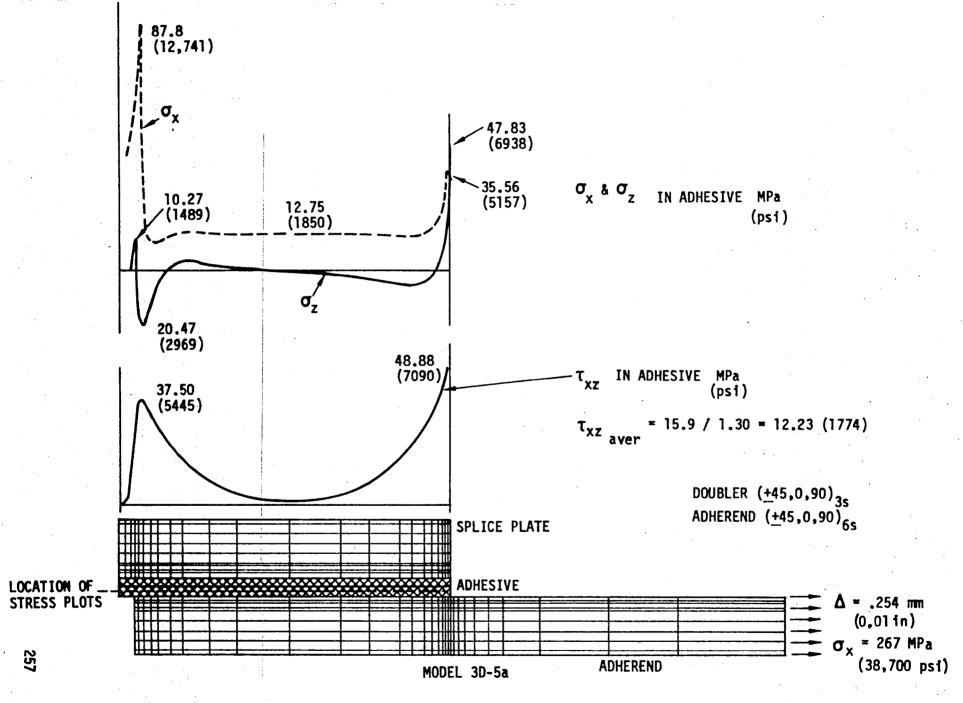


Figure 9-37: ADHESIVE SHEAR,  $\sigma_{_{X}}$  &  $\sigma_{_{Z}}$  STRESS

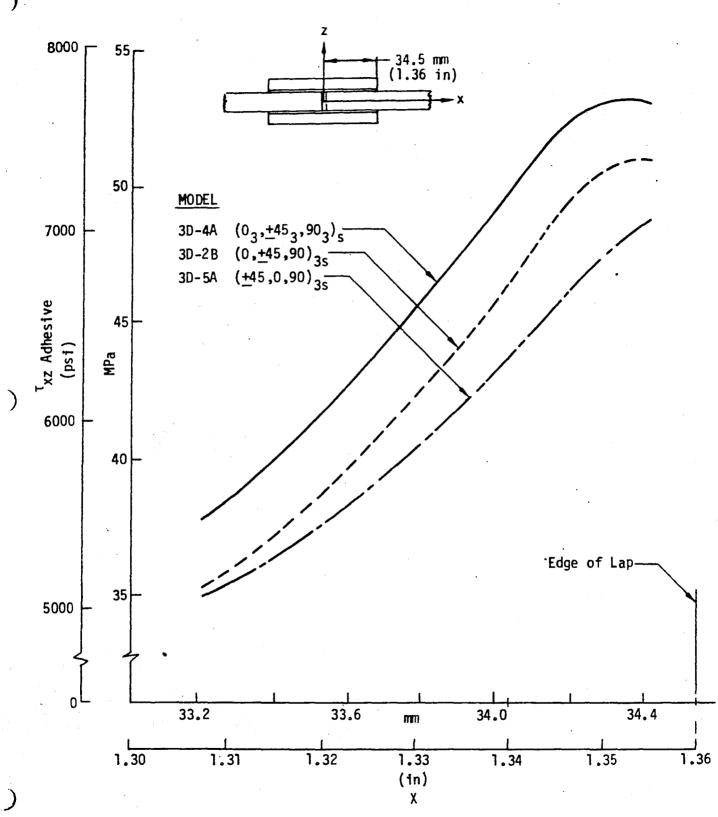


Figure 9-38: SHEAR STRESS IN ADHESIVE -  $\tau_{xz}$  vs x

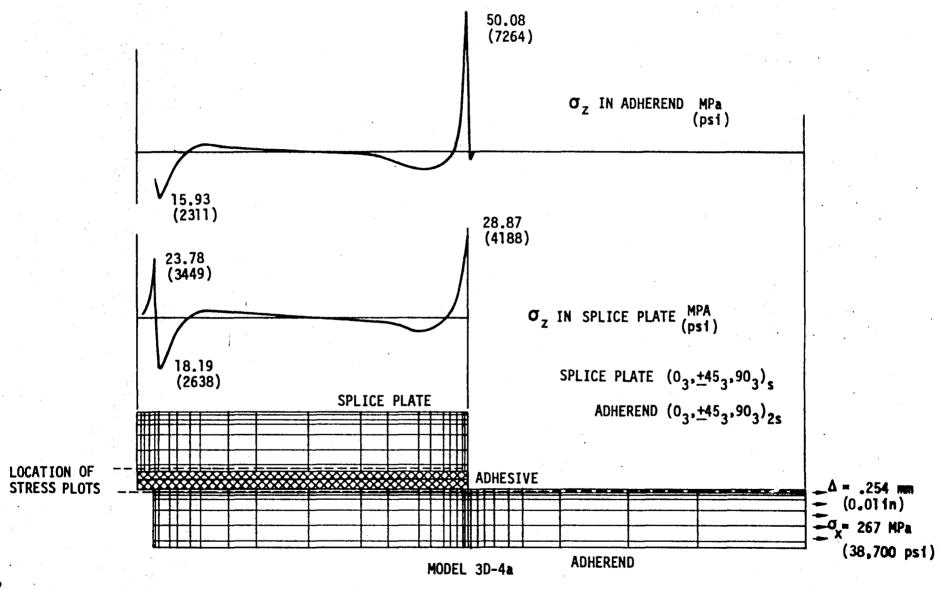


Figure 9-39:  $\sigma_z$  IN 0° LAMINA

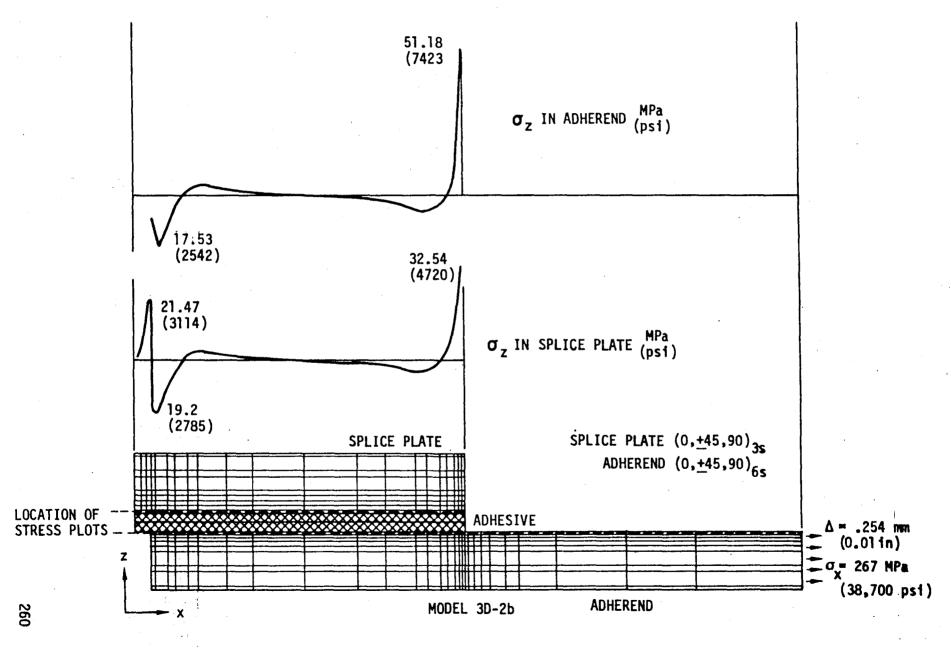


Figure 9-40. O. IN 0º LAMINA

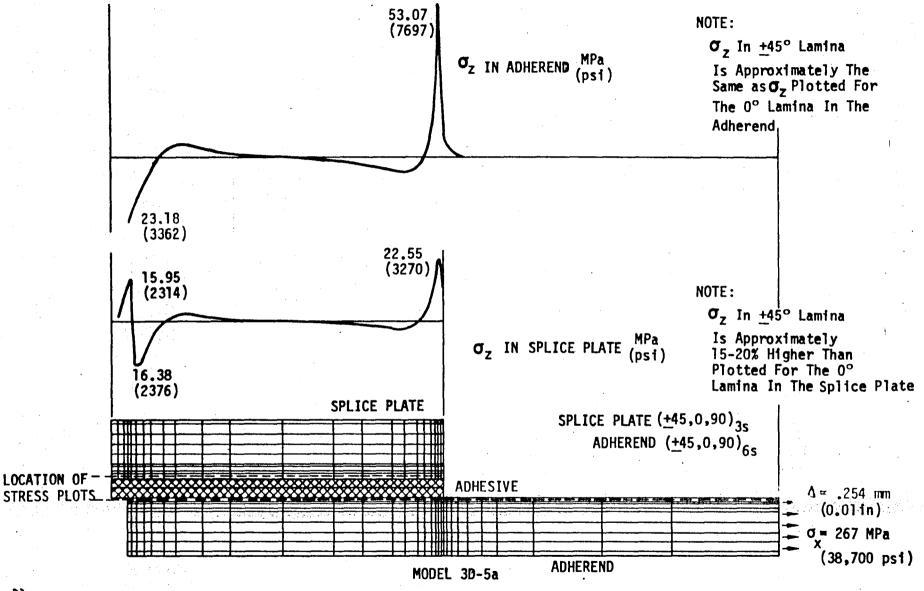


Figure 9-41:  $\sigma_z$  IN 0° LAMINA NEAREST ADHESIVE

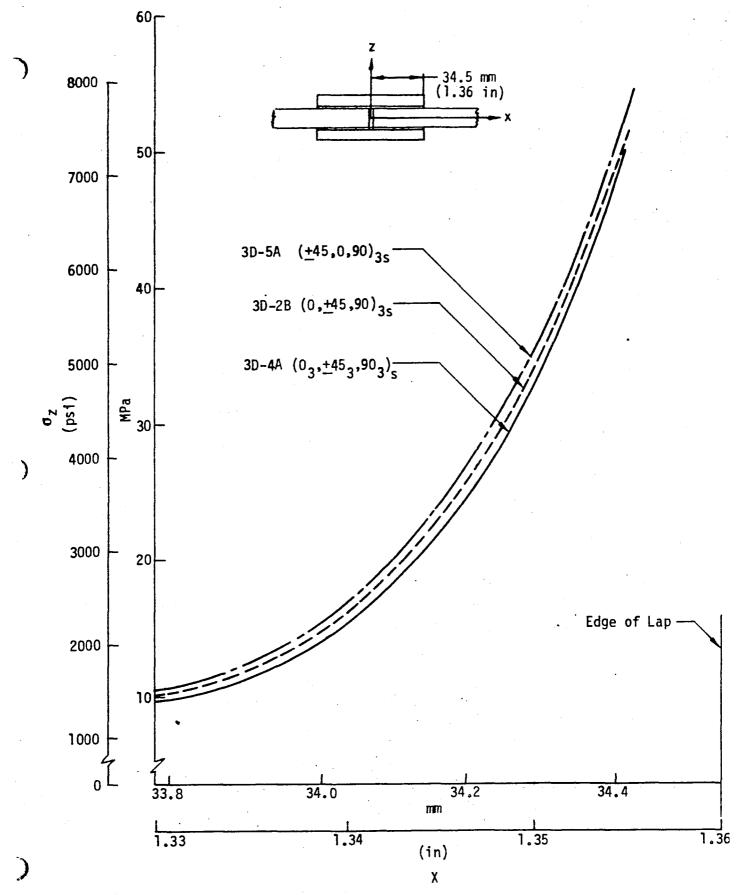


Figure 9-42: PEEL STRESS IN LAMINA NEAREST ADHESIVE -  $\sigma_{_{Z}}$  vs x

#### 9.1.3 Single Lap Joints

L. J. Hart-Smith suggests three distinct failure modes in a single lap bonded composite joint: 1) failure of the adherend outside the bonded region because of additional bending stresses, 2) failure of the adhesive in shear, and 3) failure of the composite at the interface near the end of the joint because of "peel" stresses in the adhesive or lamina (Ref. 6).

Examination of the failed single lap joints tested for this program suggests the 3rd type of failure governed in nearly all cases. Therefore, any change that can reduce the peel stess,  $\sigma_z$ , in the adhesive and in the lamina adjacent to the adhesive should increase the efficiency of the single lap joint.

An elastic, geometrically nonlinear finite element analysis was performed on a graphite/polyimide to graphite/polyimide single lap bonded joint. The joint was loaded in tension in three steps;  $P_1$  = 43.18 N/cm (25 lb/in),  $P_2$  = 87.5 N/cm (50 lb/in),  $P_3$  = 175 N/cm (100 lb/in). Based on symmetry, one-half the joint was modeled. Joint model, boundary conditions and material proportion used are shown in Figure 9-43.

The finite element analyses considered two layups for comparison: the 1st  $(0_3/\pm45_3/90_3)_S$  (model #4) and the 2nd  $(\pm45_3/0_3/90_3)_S$  (model #5). The extensional stiffness of the two layups is the same, but the flexural stiffness of the 1st is 66% greater than the 2nd.

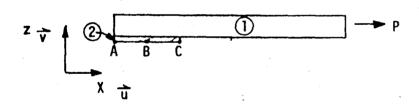
Stress distributions through the thickness of the joint are shown in Figures 9-44 through 9-46 for the two models. A comparison between them shows greater peel stresses in the adhesive for the 2nd layup (model 5). Peak peel stresses near the edge of the joint are approximately 30% greater. Shear stresses in the adhesive do not change significantly. Analysis results indicate that if the peel stresses are governing the joint failure, it is advantageous to increase the adherend bending stiffness.

31.8 mm (1.25 in)

6.35 mm (.25 in)

254 mm (.06 in)

P



### **BOUNDARY CONDITIONS**

A & C 
$$\overrightarrow{u}_A = -\overrightarrow{u}_C$$
B  $\overrightarrow{u} = \overrightarrow{v} = 0$ 

# MATERIAL DATA

- ① GR/PI  $E_1 = 137 \text{ GPa} (20x10^6 \text{ psi})$   $E_2 = 11 \text{ GPa} (1.6x10^6 \text{ psi})$  u = .25 $G_{12} = 5.8 \text{ GPa} (.85x10^6 \text{ psi})$
- (Assumed Homogeneous & Isotropic)

Figure 9-43: GR/PI BONDED SINGLE-LAP JOINT

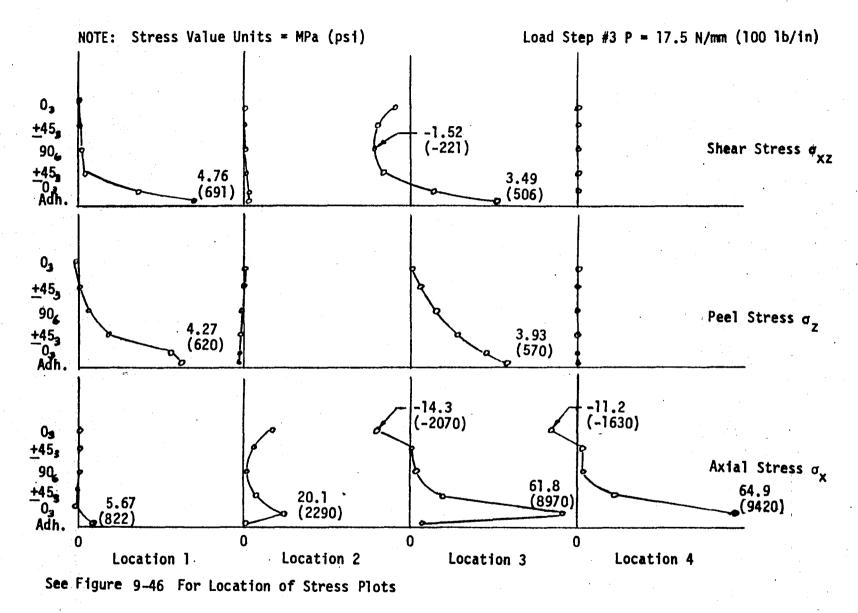
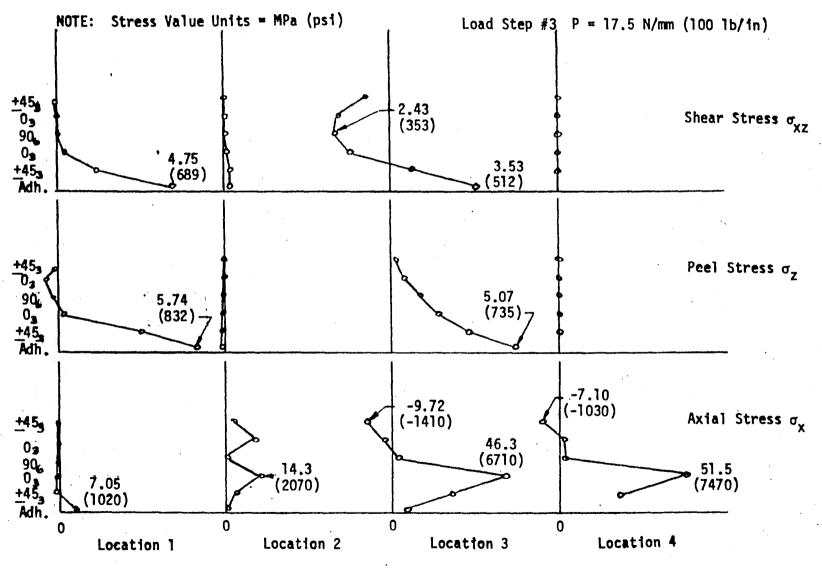
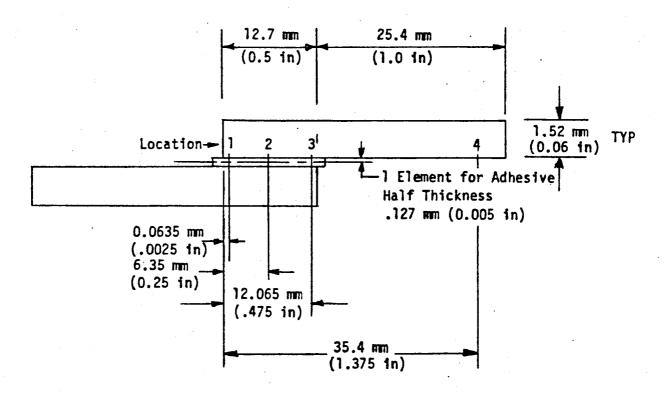


Figure 9-44: STRESS THROUGH THICKNESS MODEL #4



See Figure 9-46 for Location of Stress Plots

Figure 9-45: STRESS THROUGH THICKNESS MODEL #5



Model 4 Adherend Lay-Up  $(0_3/\pm 45_3/90_3)_S$ 

Model 5 Adherend Lay-Up  $(\pm 45_3/0_3/90_3)_S$ 

Figure 9-46: LOCATION OF STRESS PLOTS

### 9.2 Standard Joint Test/Analysis Correlation

This section presents the various analysis methods used to correlate the standard joint test data. While several methods appear to give reasonable results, it is felt that these should be viewed only as "rough" prediction techniques.

All bonded joints tested in this program had interlaminar peel or shear failures, with only a few exceptions of partial adhesive failure as noted in the previous sections. Analyses in the literature deal primarily with defining stress distributions in the adhesive. The Hart-Smith analyses do, however, address the peel and bending stresses in the adherends also. The types of failure modes in these tests present several problems in analyzing the bonded joint. The analysis must address the composite adherend stress state since this is where the failure occurred. The first problem is in determining the entire stress tensor—all six stress components—for the points in the adherends where the failure is believed to initiate. Only those stresses in the x-z plane  $(\sigma_x, \sigma_z & \tau_{xz})$  (see Figure 9-44) were obtainable by the finite element analyses. This meant that the other three stress components  $(\sigma_{v}, \tau_{vv})$  $au_{vz}$ ) have to be neglected. It is not obvious that this is a good assumption when analyzing joints which do not fail in the adhesive. Another difficulty in analyzing these joints was the inability to determine the initial failure mode - peel, interlaminar shear or bending - in the composite adherends. All of the specimens failed in the composite adherend, usually in the ply nearest to the adherend-adhesive interface. Since the primary failure mode, or combination of modes was not known, the predominate stress component(s) could not be determined.

Discussions of analysis/correlation attempts for single-lap and double-lap joints are presented separately in the following sections. Nomenclature used for these analyses are given in Table 9-4.

Table 9-4 Test/Analysis Correlation Nomenclature

```
Average stress in adherend
\sigma_{av}
                Eccentricity parameter = 2M_0/Pt (1+\frac{\eta}{t})
K
                Adhesive thickness
η
t
                Adherend thickness
                Young's Modulus (longitudinal) for adherend
E_1
                Poisson's ratio for adherend
ν
                D/(E_1 t^3/12(1-v^2)) = bending shiftness parameter
Kh
                Flexural rigidity of adherents
D
\sigma_{c_{\text{max}}}
                Maximum peel strength of adhesive or adherend
E'c
                Effective adhesive transverse tensile modulus
G
                Adhesive shear modulus
Ρ
                Applied load on joint
                Half length of overlap = L/2
С
                Overlap length
L
                Curvature in longitudinal direction in adherend
k_1
                Strain in longitudinal direction in adherend
\epsilon_1
d_{11}
                Flexural compliance
E_{X}
                Young's modulus of a lamina in fiber direction
```

### 9.2.1 Single Lap Joints.

The A4EA single lap joint analysis code developed by L. J. Hart-Smith (Ref. 6) was chosen to be used to predict joint strengths. This code was selected because it addresses the adherend peel and bending stresses. First the program was modified to calculate the bending stress on the outer fiber of the composite adherend in the following manner. The bending moment in the adherend at the end of the overlap is given by:

$$M_0 \simeq KP_2^{t}$$

Calculating the strain on the outer fiber in the adherend.

$$k_1 = d_{11}M_0$$

$$\epsilon_1 = \frac{P}{E_1 t} + \frac{1}{2} t d_{11} M_0$$

The ratio of the stress in the outer fiber to the average stress in the adherend is given by,

$$\sigma_{\text{max}} = E_{x} \varepsilon_{1} = E_{x} \left[ \frac{1}{E_{1}} \left( \frac{P}{t} \right) + \frac{1}{4} d_{11} K \left( \frac{P}{t} \right) t^{3} \right]$$

$$\frac{\sigma_{\text{max}}}{\sigma_{\text{av}}} = E_{x} \left[ \frac{1}{E_{1}} + \frac{1}{4} d_{11} t^{3} K \right]$$

These modifications were used to calculate the outer fiber stress as a function of load. Joint failure was predicted when the outer fiber exceeded its ultimate strength. The failure load for this assumed failure mode was then compared to that for assumed peel and adhesive shear failures. It was found that the peel strength was the critical strength, as opposed to the bending

and shear strengths of the joint. This was as expected based on the test results. The peel strength is given by the equation (Ref. 6):

$$\sigma_{av} = \frac{1}{K(1 + \frac{\eta}{t})} \left[ \frac{2K_b E_1 \eta}{3(1 - v^2)} \right]^{\frac{1}{2}} \left[ \frac{\sigma_{c_{max}}^2}{E_c^1} \right]^{\frac{1}{2}}$$

Since the parameters  $\sigma_{c_{max}}$  and  $E_c^{'}$  were not known with any degree of certainty, the ratio of these parameters,  $\sigma_{c_{max}}^2$  /  $E_c^{'}$  was varied in an attempt to find a correlation with the test data. This was unsuccessful. After further investigation of the A4EA code it was decided that changes should be made in the calculation of the moment in the adherends at the end of the overlap. Two different moment equations were substituted for the original equation in the code.

The first involved the solution as derived by Hart-Smith (Ref. 6). The moment equation derived in that paper is:

$$\mathsf{M}_{0} = \left(\frac{\mathsf{t} + \mathsf{\eta}}{2}\right) \frac{\left[1 + \frac{\xi^{2} \lambda^{2}}{32(\lambda')^{4}} \left(1 + \frac{(2\lambda'c)^{2}}{3} - \frac{2\lambda'c}{\mathsf{tanh}(2\lambda'c)}\right)\right]}{1 + \xi^{2}c^{2} + \frac{\xi^{2}c^{2}}{6} - \left(\frac{\mathsf{t} + \mathsf{\eta}}{2\mathsf{t}}\right) \left[\frac{6\lambda^{2}\xi^{2}}{32\,\mathsf{K}_{b}(\lambda')^{4}}\right] \left[1 + \frac{(2\lambda'c)^{2}}{3} - \frac{2\lambda'c}{\mathsf{tanh}(2\lambda'c)}\right]}$$

where

$$\xi = \frac{P}{D}$$

$$\lambda^2 = \frac{2G}{E \ln}$$

$$(\lambda')^2 = \left[\frac{1 + 3(1 - v^2)/K_b}{4}\right] \lambda^2$$

However, Hart-Smith simplified this equation down to:

$$M_0 = P(\frac{t+\eta}{2}) \frac{1}{1+\xi_c + \xi^2 c^2/6}$$

Taking the limit as  $c \leftarrow \infty$  in the above two moment equations, it is found that the simplified moment equation approaches zero, while the full equation approaches a finite number, namely:

limit 
$$_{c \to \infty} M_0 = P(\frac{t + \eta}{2}) \left[ \frac{K_b}{K_b - 3(v^2 + \frac{\eta}{t})} \right]$$

Thus, it appears that the simplifications made by Hart-Smith give different results, and the full moment equation was tried in the analysis. This moment equation was substituted into the A4EA code and produced a significantly better correlation with the test data.

The second moment equation to be substituted into the A4EA code resulted from the analysis of Goland and Reissner (Ref. 7). They derived the following equation for the moment at the end of the overlap:

$$M_0 = P\left(\frac{t + \eta}{2}\right) \left(\frac{\cosh(u_2c)}{\cosh(u_2c) + 2\sqrt{2}\sinh(u_2c)}\right)$$

where

$$u_2 = \sqrt{\frac{P}{80}}$$

This equation also produced a good correlation with the test data, and appeared to be slightly better than the full Hart-Smith moment equation discussed above.

Figures 9-47 and 9-48 compare test results with predicted joint strengths for assumed bending and peel failure modes. Predictions are based on the A4EA code with the three different equations for the moment. Bending strengths

were based on the outer fiber stress as discussed previously. Predicted joint strengths based on bending (Figure 9-47) are significantly higher than measured and do not provide a reasonable correlation. Predicted strengths based on an assumed peel failure (Figure 9-48) provided significantly better correlation with test results. The best correlation is for the predictions using the modified moment equations.

Figures 9-49 and 9-50 show the predicted strength curves and corresponding test data versus the lap length over thickness ratio (1/t) for 294K (70°F) and 561K (550°F). No analysis was done for the -250°F cases as there was no material property data available for that temperature. Peel failures were assumed to occur when the assumed value of  $(\sigma_{c_{\max}}^2/\epsilon_c^*)$  was exceeded. Possible values of  $(\sigma_{c_{\max}}^2/\epsilon_c^*)$  were estimated from known material properties. These values were then varied to establish the best correlation with test results. Values of  $(\sigma_{c_{\max}}^2/\epsilon_c^*)$  used for the best correlation are given in each figure. Note that slightly different values were used depending on which set of moment equations were being evaluated. In addition, the values were adjusted to reflect effects of temperature. Material property testing indicates that E'c would probably drop faster with increased temperature than  $\sigma_{c_{\max}}$ , resulting in a net increase in  $\sigma_{c_{\max}}^2/\epsilon_c^*$ .

Actual thicknesses of the single-lap adherends varied significantly as discussed previously. This had an effect on the flexural stiffness as summarized in Table 7-5. To determine the sensitivity of the joint strength to the flexural stiffness, predictions were made using the correlation discussed above. Predicted strengths for a range of flexural stiffness are shown in Figure 9-51. Increasing the flexural stiffness from 11.3 N-m (100 in-lbs) to 113 N-m (1000 in-lbs) resulted in an increase in predicted strength from 10% to 41% depending on the lap length to thickness ratio. Most of the parameters evaluated on single lap joints were tested using lap length to thickness ratio of 33. At this ratio the analysis indicates only a ±10% change in joint strength for an order of magnitude change in flexural stiffness. The significance of this is that variations in measured thicknesses discussed previously should not have an adverse effect on the test results. Possible variations

are well within the range of data scatter. On the other hand, possible changes in joint performance expected based on planned increases in flexural stiffness may not be discernible because of the large data scatter.

No predictions were made for the unbalanced adherends and graphite-titanium configurations as the program was unable to handle these cases.

The program still has several deficiencies. There is no provision for distinguishing between adherends with different ply orientations at the joint interface, and the effect of combined bending and peel stresses is not accounted for.

An empirical correlation approach was also investigated. It was postulated that failure occurs when the maximum principal stress at the critical point in the adherend reaches a certain value. The stresses at the critical point (directly under the end of the adherend) were calculated by:

$$\sigma_{x} = \frac{1}{E_{1}} \left( \frac{P}{E_{x}t} + \frac{1}{2} t d_{11} M_{0} \right)$$

$$\sigma_{z} = P/t$$

$$\tau_{xx} = 5P/c$$

Where  $M_{\Omega}$  is given by the following equation from Reference 8:

$$M_{O} = P\left(\frac{t+\eta}{2}\right) \cos \Phi \frac{u_{2} \cosh\left(u_{2}c\right) \sinh\left(u_{1}k\right)}{u_{2} \sinh\left(u_{1}k\right) \cosh\left(u_{2}c\right) + u_{1} \cosh\left(u_{1}k\right) \sinh\left(u_{2}c\right)}$$

where

$$\cos \varphi = \frac{\ell + c}{\sqrt{(\ell + c)^2 + \left(\frac{t + \eta}{2}\right)^2}}, \quad u_1 = \sqrt{\frac{P \cos \varphi}{D}}, \quad u_2 = \sqrt{\frac{P \cos \varphi}{8D}}$$

Critical Points The relations for  $\sigma_z$  and  $\tau_{xz}$  were the performance trends as determined from the analysis results presented in Reference 8. These relations were picked as typical of the range of values. The limiting maximum principal stress was found by using the measured failure load for test set (3A-7A). This maximum principal stress was then used to predict the failure loads for the other test sets. Figure 9-52 shows the empirically predicted and actual failure loads vs lap length for test sets (3A-7A), (3A-1A), (3A-1B) and (3A-1C).

A summary of all the predictions is given in Figures 9-53 and 9-54. Actual strengths as compared with A4EA analysis program predictions and empirical predictions for eight single lap joint configurations at 294K ( $70^{\circ}$ F) and five at 561K ( $550^{\circ}$ F). The plus/minus one standard deviation range is shown for the actual strengths.

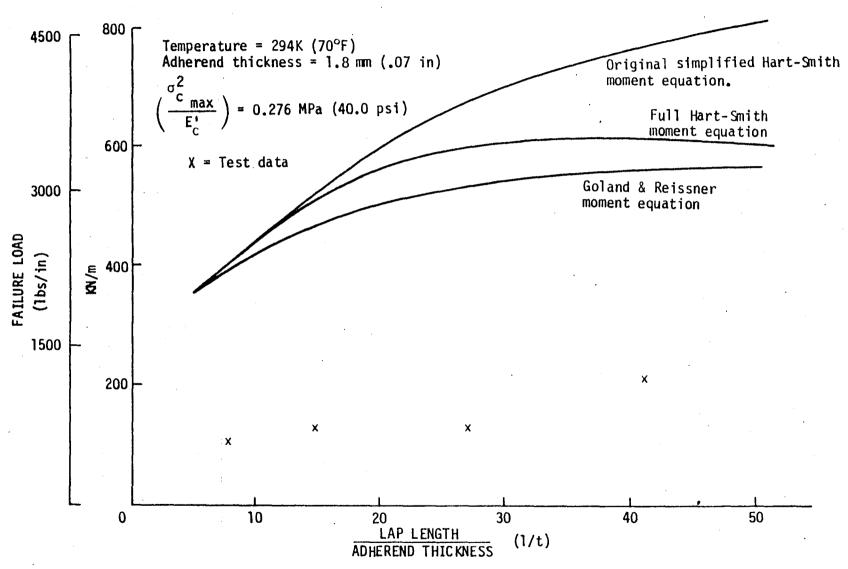


Figure 9-47: PREDICTED STRENGTH OF SINGLE LAP JOINTS - BENDING FAILURES

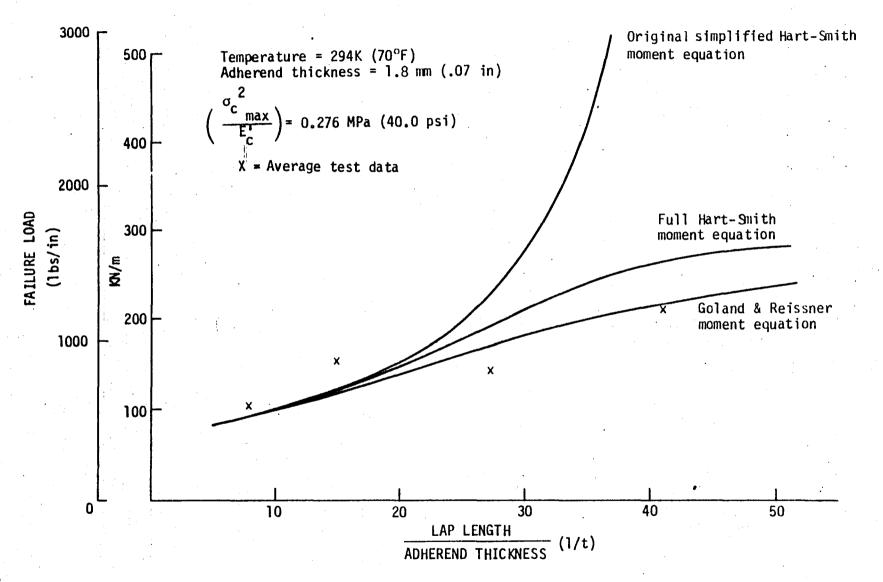


Figure 9-48: PREDICTED STRENGTH OF SINGLE LAP JOINTS - PEEL FAILURES

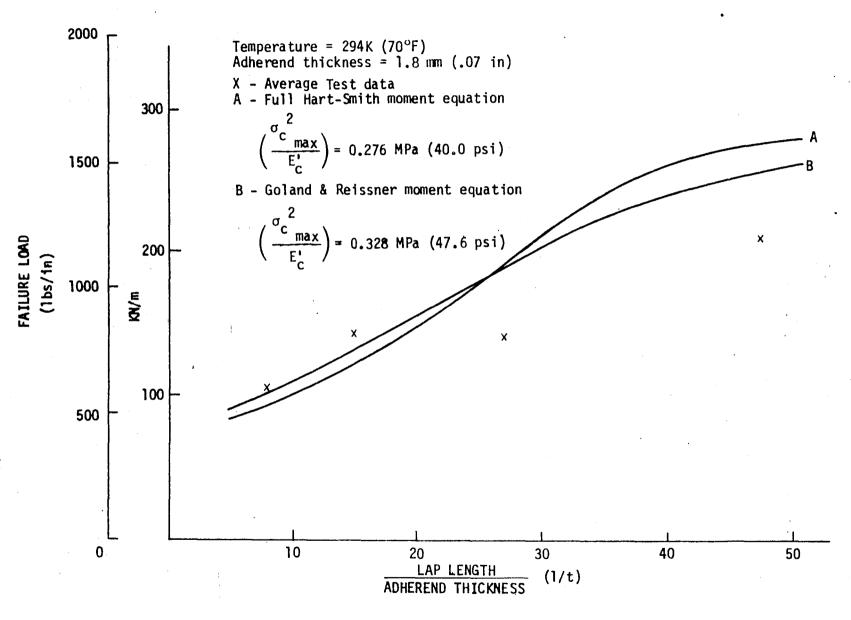


Figure 9-49: A4EA PEEL STRENGTH PREDICTIONS - SINGLE LAP JOINTS

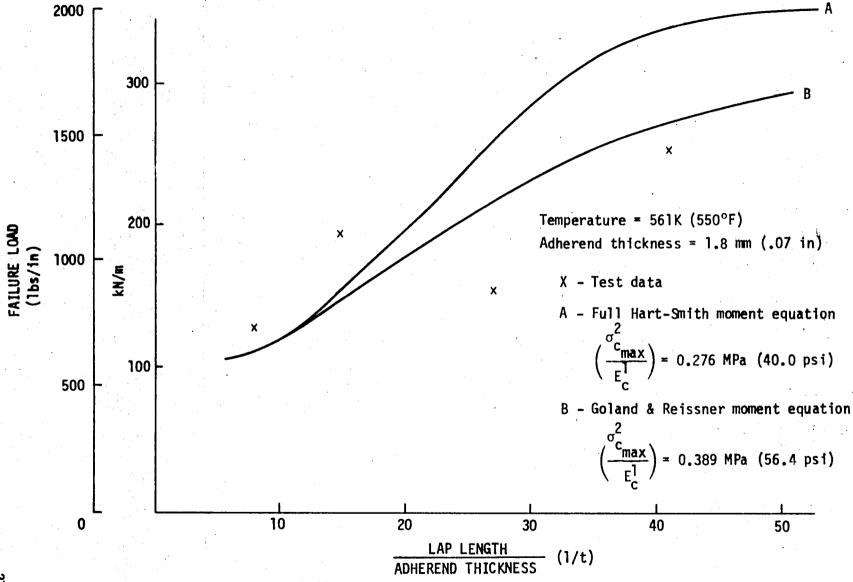


Figure 9-50: A4EA PEEL STRENGTH PREDICTIONS - SINGLE LAP JOINTS

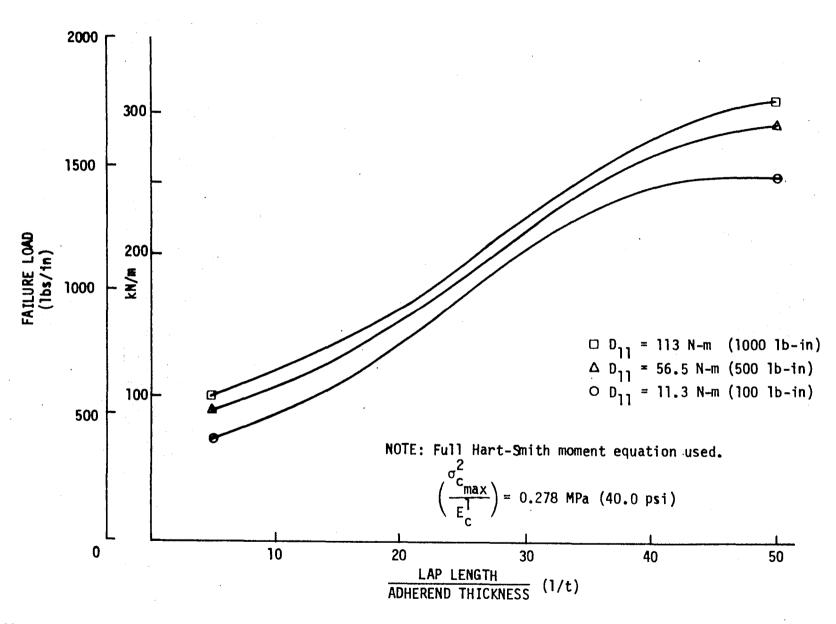


Figure 9-51: EFFECT OF ADHEREND FLEXURAL STIFFNESS (D11) ON PEEL STRENGTH OF SINGLE LAP JOINTS

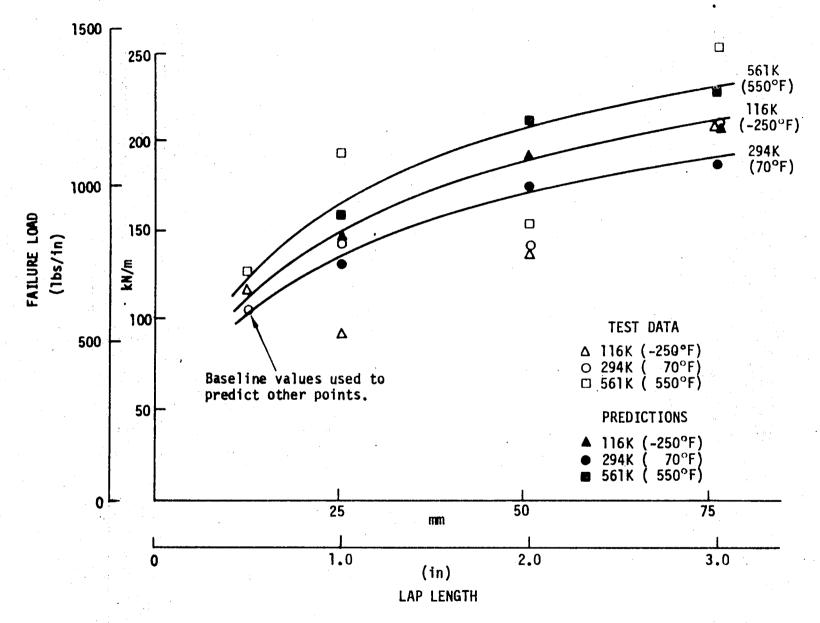


Figure 9-52: EMPIRICAL CORRELATION - SINGLE LAP JOINTS

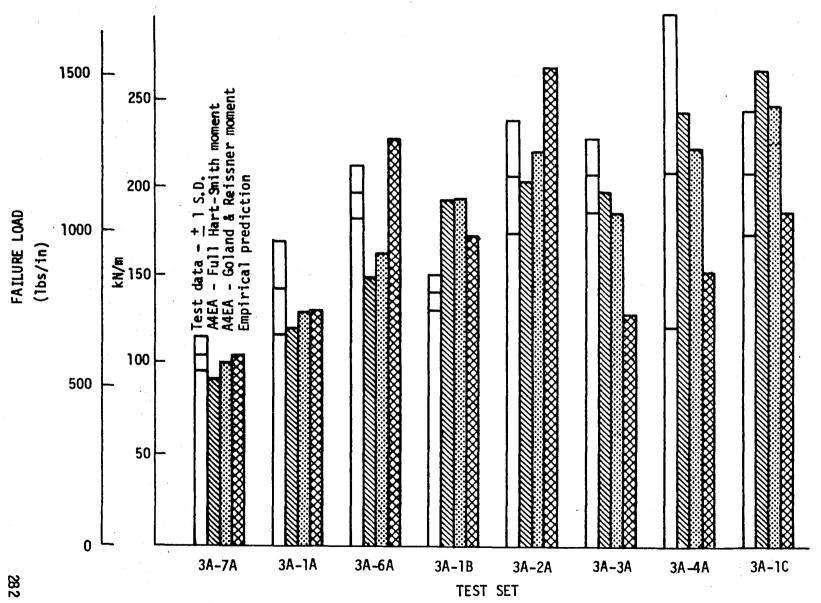


Figure 9-53: PREDICTED STRENGTHS VS TEST RESULTS - 294K (70°F) SINGLE LAP JOINTS

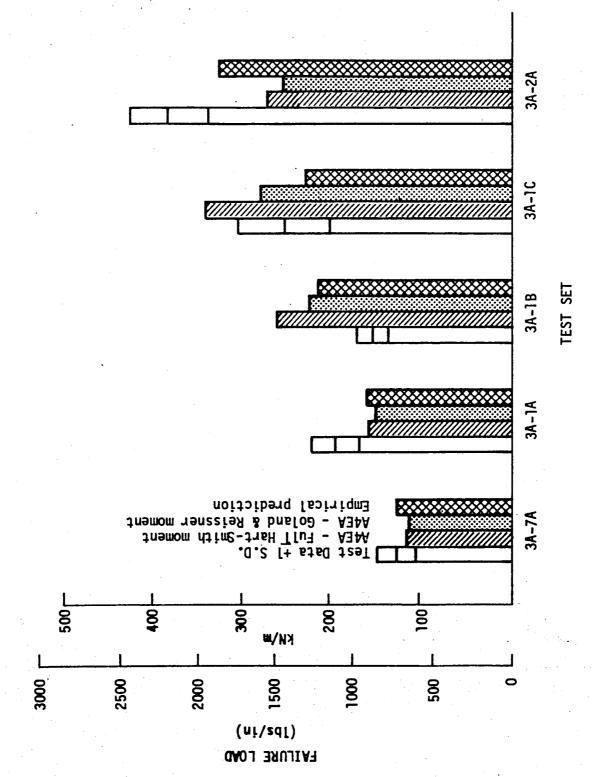


Figure 9-54: PREDICTED STRENGTHS VS TEST RESULTS - 561K (550°F) SINGLE LAP JOINTS

#### 9.2.2 Double Lap Joints.

The A4EB double lap joint analysis program developed by L. J. Hart-Smith (Ref. 9) was not used to correlate the test data. This program assumes a shear failure in the adhesive and does not allow for peel failures in the adherends other than in the limiting sense. It defines the outer adherend thickness beyond which peel is critical. Also, there is no way to input the stacking sequence of the composite adherends.

An empirical method similar to the approach used for the single lap joints was investigated to predict the strength of double lap joints. The maximum principal stress was again used as the failure criteria. The stresses at the failure point, the point in the inner adherend directly below the end of the outer adherend, were given by:

$$\sigma_{x} = \frac{E_{1}P}{E_{x}t}$$

$$\sigma_{z} = P/5t$$

$$\tau_{xz} = 2.1P/L$$

These relations were determined from the finite element analyses of test set configurations 3D-2B, 4A & 5A (see Section 9.1.2).

As for the single-lap case, the limiting maximum principal stress was determined by using the actual failure load for one test set, in this case, test set 3D-1A. This maximum principal stress was then used to predict the failure load for other test sets.

Figures 9-55 to 9-57 show comparisons of the actual and predicted stengths for ten joint configurations at 116K (-250°F), 294K (70°F) and 561K (550°F). Also shown are standard deviations for the measured test results.

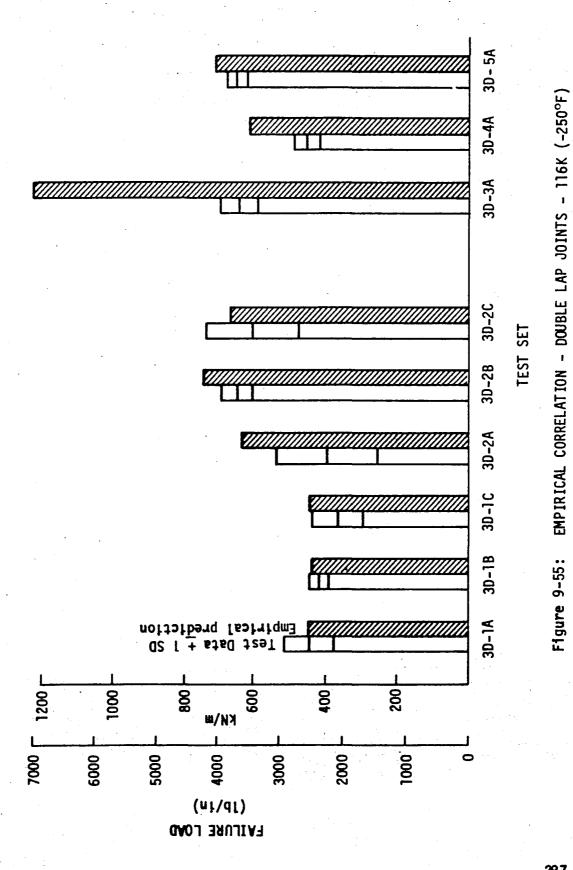
Tsai-Hill and Tsai-Wu failure criteria were applied to the stress ratios found from finite element analyses (see Section 9.1.2). The finite element analyses used were the three joint configurations shown in Figure 9-33. The stress

ratios for  $\sigma_{\rm X}$ ,  $\sigma_{\rm Z}$ ,  $\tau_{\rm XZ}$  for the critical element as indicated by the analysis were inserted into the failure criteria and the predicted ultimate stress determined. The ply strengths used were obtained from the design allowables data (Ref. 4). Neither of the criteria gave reasonable correlations to the actual test data. Also, there was no way to extend this analysis to other specimen types as finite element analyses for those configurations were not available and are needed to define the stress state.

The Design Handbook for Adhesive Bonding resulting from the Primary Adhesively Bonded Structure (PABST) program (Ref. 10) presents a simplified design method for double-lap joints. This method gives the optimum overlap length for the joint. Figure 9-58 shows the joint configuration and pertinent equations. Calculated optimum overlap lengths for the joint configurations tested are given in Table 9-5. Curves of joint strength versus lap length for double-lap joints (see Figures 7-28 and 7-29) are not sufficiently definitive to allow selection of an optimum lap length. In a qualitative sense, the curves for test sets 3D-1A, 1B and 1C indicate an optimum length in the neighborhood of 25 mm to 38.8 mm (1.0 inch to 1.5 inch). For test sets 3D-2A, 2B and 2C and optimum length of 33 mm to 46 mm (1.3 inch to 1.8 inch) is indicated. These lengths are in the range of values predicted. The values used for  $T_p$  and G are those for the high modulus, brittle adhesive HT424 (Ref. 11) and not the values obtained by testing the A7F adhesive. It was indicated by the supplier of the A7F adhesive that the A7F was also a high modulus, brittle adhesive. If the test values for  $\,\tau_{p}\,$  and G are used, the optimum overlap lengths increase by a factor of about 2.5.

The percent changes in joint strength predicted by L. J. Hart-Smith (Ref. 9) for various joint parameter changes were compared to the actual percent changes resulting from the test program. Only the predictions for the strength reduction due to unbalanced adherends showed a correlation. Reasons for this limited success is due to the assumption of shear failures in the Hart-Smith analysis. The analysis also does not include the effect of the stacking sequence of the plies in the composite adherends.

The unbalanced adherend strength reduction figures from Hart-Smith are shown in Figure 9-59. Joints can be compared with either common inner adherends or common outer adherends. Figure 9-60 shows the predicted vs. actual strength reductions for both comparison types. In both cases the predictions are fairly good; however, this is probably more coincidental than factual since Hart-Smith equations are based on adhesive shear failures and not laminate peel failures as was actually experienced.



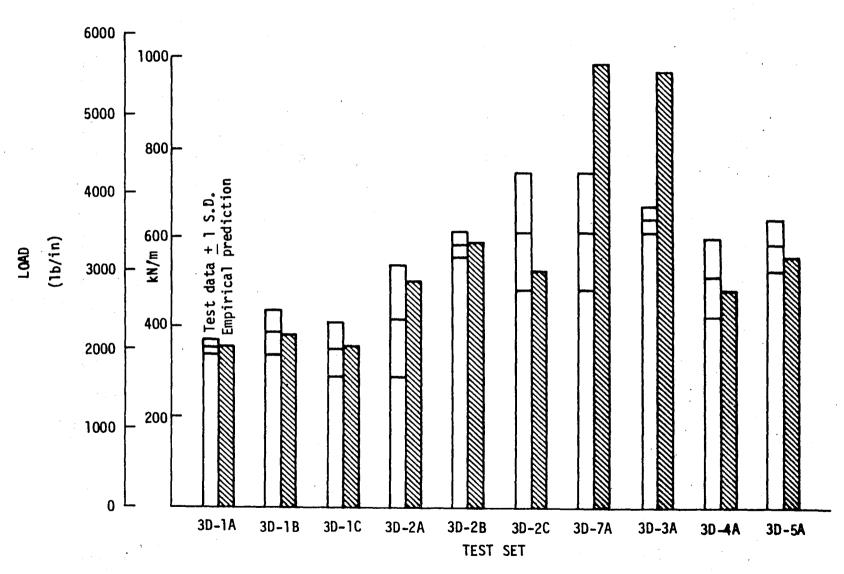


Figure 9-56: EMPIRICAL CORRELATION - DOUBLE LAP JOINTS - 294K (70°F)

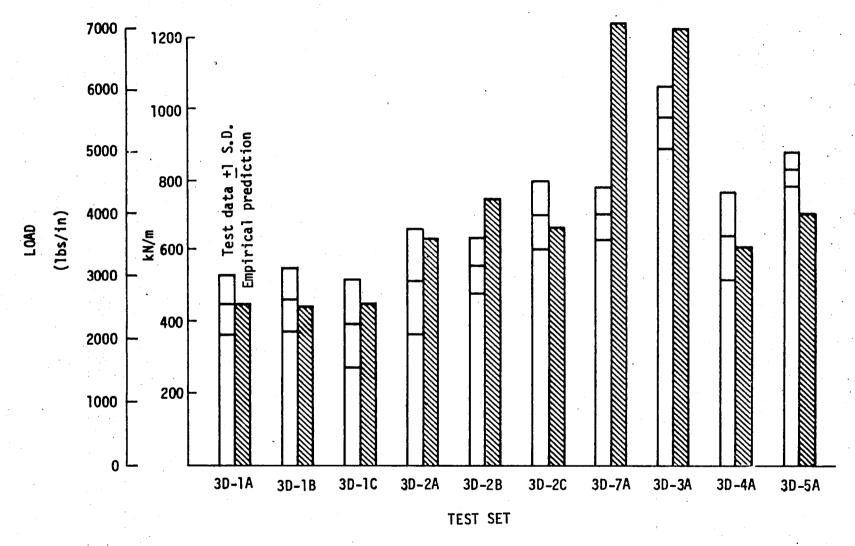
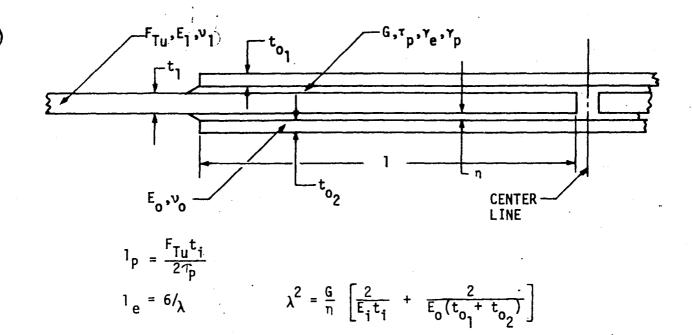


Figure 9-57: EMPIRICAL CORRELATION - DOUBLE LAP JOINTS - 561K (550°F)



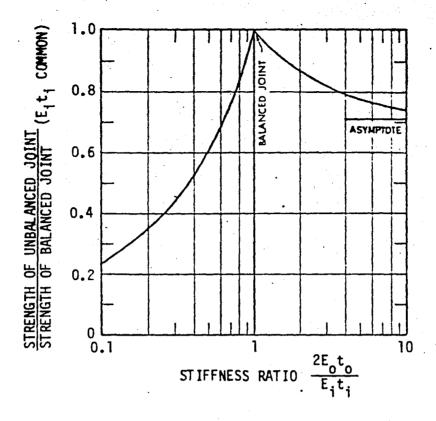
OPTIMUM OVERLAP =  $1_p + 1_e$ 

Figure 9-58: CALCULATION OF OPTIMUM OVERLAP LENGTH

Table 9-5: OPTIMUM OVERLAP LENGTHS FOR VARIOUS JOINT CONFIGURATIONS

TEST SETS	t <sub>i</sub> mm (in)	t o mm (in)	E <sub>i</sub> GPa (Msi)	E <sub>o</sub> GPa (Msi)	F <sub>Tu</sub> (MPa (ksi)	OPTIMUM OVERLAP mm (in)
3D-1A, 1B, 1C		i i		1		30.7 (1.21)
3D-2A, 2B, 2C, 4A, 5A	3.0 (.12)	.15 (.06)	53 (7.7)	53 (7.7)	524 ( 76)	43.4 (1.71)
3D-3A	3.0 (.12)	.15 (.06)	103 (15.0)	103 (15.0)	972 (141)	75.2 (2.96)
3D-6A	2.0 (.08)	.15 (.06)	53 (7.7)	53 (7.7)	524 ( 76)	31.8 (1.25)
3D-7A, 3F-1A	.61 (.24)	.30 (.12)	53 (7.7)	53 (7.7)	524 ( 76)	80.0 (3.15)
3E-1A, 1B, 1C	.15 (.06)	.15 (.06)	110 (16.0)	53 (7.7)	924 (134)	39.9 (1.57)

 $\tau_p$  = 25.3 MPa (3670 psi) G = 2.07 GPa (300 ksi)  $\eta$  = 0.203 mm (.008 in) HT424 Adhesive Properties



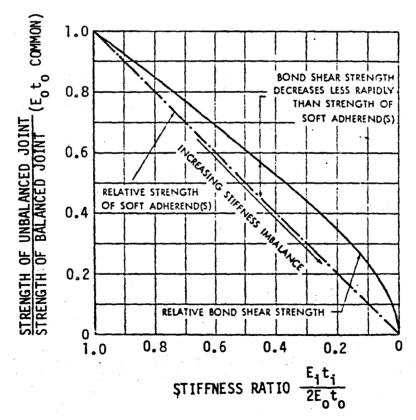


Figure 9-59: STRENGTH REDUCTION FACTOR IN DOUBLE-LAP BONDED JOINTS, DUE TO ADHEREND STIFFNESS IMBALANCE (Ref. 9)

COMMON OUTER ADHERENDS (compare test set 3D-2B to 3D-6A)

$$\frac{E_1 t_1}{2E_0 t_0} = \frac{t_1}{2t_0} = \frac{.091}{2 \cdot .068} = .67$$

strength-unbalanced
strength-balanced = .67

TEMPE	ERATURE O <sub>E</sub>		FAILURE kN/m (1			MEASURED REDUCTION RATIO	PREDICTED REDUCTION RATIO
K	°F	31	D-2B	31	D-6A	3D-6A/3D-2B	
116 294 561	(-250) (70) (550)	636 586 552	(3629) (3347) (3150)	377 344 287	(2153) (1963) (2208)	.59 .59 .70	.67 .67 .67

COMMON INNER ADHERENDS (compare test set 3D-1B to 3D-6A)

$$\frac{2E_0t_0}{E_1t_1} = \frac{2t_0}{t_1} = \frac{2 \cdot .068}{.091} = 1.5$$

strength-unbalanced = .90

ļ	ERATURE			LOAD 16/1n)			PREDICTED REDUCTION RADIO
K	°F	3D-1	В	3D-		3D-6A/3D-1B	
116 294 561	(-250) (70) (550)	389 (2	2356) 2219) 2613)	377 344 387	(2153) (1963) (2208)	.91 .88 .84	.90 .90 .90

Figure 9-60: PREDICTED VS. ACTUAL STRENGTH REDUCTIONS FOR UNBALANCED DOUBLE LAP JOINTS

#### 9.2.3 Step-Lap Joints

Joint strength predictions for the "3-step" symmetric step-lap joint were calculated using the computer program A4EGX developed by Hart-Smith (Ref. 12). A failure prediction was obtained only for the 561K ( $550^{\circ}F$ ) case. Results were not obtained for the 116K ( $-250^{\circ}F$ ) and 294K ( $70^{\circ}F$ ) cases because code problems were encountered when a large temperature differential was input. The predicted failure load for the 561K ( $550^{\circ}F$ ) case was 898 kN/m (5126 1b/in) compared to an average failure load of 901 kN/m (5147 1b/in). The program however predicted an adhesive failure, whereas the actual joints appeared to have interlaminar composite failures.

The actual joints were co-cured onto the titanium using only an adhesive primer. They were not precured laminates bonded on with a separate adhesive. The analysis code requires adhesive thickness and properties as an input. The co-cured joints were simulated for analysis purposes by inputting adhesive properties and a thickness of .005 in. The adhesive properties were those from the thick adherend tests conducted at the University of Delaware (see section 3.1.3)

Predictions were also made using assumed adhesive properties of HT424 (Ref. 11) since it was felt the adhesive was significantly more brittle than indicated by test. This also resulted in predicting an adhesive failure but at a significantly lower load. Predictions along with actual failure load are shown in Table 9-6 for the two sets of adhesive properties.

Table 9-6: "3-STEP" STEP LAP JOINT STRENGTH A4EGX CODE PREDITIONS (ΔT = 00)

			PR	EDICTED	STRE	NGTH			]	
	ADHESIVE THICKNESS = ADHESIVE THICKNESS = .25 mm (.01 in) .13 mm (.005 in)									
ANALYSIS TYPE	ADH	[424 ESIVE (lb/in)	ADH	A7F ESIVE (lb/in)	ADH	7424 ESIVE (1b/in)	ADH		ACTU STREI kN/n	NGTH
ELASTIC	229	(1309)	606	(3458)	162	(926)	468	(2674)	901	(5147)
ELASTIC PLASTIC	767	(4379)	1102	(6290)	544	(3108)	897	(5126)	901	(5147)

HT424 ADHESIVE 
$$\begin{cases} T & \text{(shear strength)} = 25.3 \text{ MPa } (3670 \text{ psi}) \\ G & \text{(shear modulus)} = 2.07 \text{ GPa } (300000 \text{ psi}) \\ \gamma_p & \text{(shear strain to failure} = .075 \end{cases}$$
 A7F ADHESIVE 
$$\begin{cases} T = 16.1 \text{ MPa } (2333 \text{ psi}) \\ G = 80.0 \text{ MPa } (11600 \text{ psi}) \\ \gamma_p = .526 \end{cases}$$

#### 10.0 CONCLUSIONS/RECOMMENDATIONS

The following conclusions have resulted from this program:

- o Bonded "Gr/PI-Gr/PI" and "Gr/PI-titanium" joints can be designed and fabricated to carry loads of the magnitude expected for advanced aerospace vehicles over the 116K (-250°F) to 561K (550°F) temperature range.
- o Joint strength for these material combinations increases with:
  - increased lap length
  - increased temperature
  - increased adherend stiffness
  - increased adherend thickness
  - adherend tapering
  - +450 plies at the joint surface
- o Hybrid systems (fabric interfaces) provide a simple and effective way to increase joint strength.
- o Preformed adherends significantly increase single-lap joint strength.

  Large deflections under load cause joints with preformed adherends to act as scarf joints.
- o A7F has a shear strength greater than 8.3 MPa (1200 psi) in the 116K (-250°F) and to 589K (550°F) temperature range.
- o Finite element analyses of composite bonded joints can successfully predict joint performance trends.
- o Composite bonded joint strength prediction techniques are at this time limited to simple joint configurations and result in "rough" predictions only.

a omore

- Based on the results and conclusions derived from this program, the following areas for further work on bonded composite joints are recommended:
- o The combined effect of the following joint parameters and configurations investigated in this program should be explored in order to further increase joint strengths:
  - hybrid systems (fabric interfaces)
  - adherend tapering
  - increased stiffness
  - ±450 plies at joint interfaces
- o Hybrid systems for double lap joints should be investigated.
- o Further work in predicting bonded joint strengths needs to be undertaken in order to improve confidence in using bonded composite joints for designs. The complex failure modes of composite adherends are not well understood. Since the interlamina strengths of composite laminates are low, composite bonded joints are susceptible to peel and/or interlamina shear failures, as opposed to an adhesive failure.
- o Preformed joints should be considered for use in two areas: 1) an internal structural attachment or in external joints which can be covered by fairings and 2) as a possible replacement for the ASTM D-1002 lap shear specimens so that the results approach the true adhesive shear strength (because of the reduced peel stresses).

APPENDIX A

ADHESIVE TEST RESULTS TABLES

Table A-1: MATRIX 2 TEST 3 THIN ADHEREND SINGLE LAP SHEAR TESTS OF A7F ADHESIVE

					ULTIMATE	FAILURE	
CONDITION CODE	SPECIMEN NUMBER	TEMPERATURE K (OF)	LAP LENGTH mm (in)	WIDTH mm (in)	LOAD N (1bs)	SHEAR STRESS MPa ksi	NOTES
	3-2-1 3-2-2 3-2-3 3-2-4 3-2-5 3-2-6 3-2-7 3-2-8 3-2-9	116 (-250) 116 (-250) 116 (-250) 294 (70) 294 (70) 294 (70) 561 (550) 561 (550)	13 (.50) 13 (.51) 13 (.50) 12 (.49) 13 (.50) 13 (.50) 13 (.50) 12 (.49) 12 (.49)	25 (1.00) 25 (1.00) 25 (1.00) 26 (1.01) 25 (1.00) 25 (1.00) 25 (1.00) 25 (1.00) 25 (.99)	7224 (1624) 7082 (1592) 5894 (1325) 6539 (1470) 6183 (1390) 6183 (1390) 4582 (1030) 3781 (850) 4493 (1010)	22.4 (3.25) 21.5 (3.12) 18.3 (2.65) 20.5 (2.97) 19.2 (2.78) 19.2 (2.78) 14.2 (2.06) 12.0 (1.73) 14.4 (2.08)	
2 2 2 2 2 2 2 2 2 2 2 2 2 2 2 2 2 2 2	3-2-11 3-2-12 3-2-13 3-2-14 3-2-15 3-2-16 3-2-17 3-2-18 3-2-19	116 (-250) 116 (-250) 116 (-250) 294 (70) 294 (70) 294 (70) 561 (550) 561 (550)	13 (.50) 13 (.50) 13 (.51) 13 (.50) 13 (.51) 13 (.50) 13 (.50) 13 (.50)	25 (1.00) 26 (1.01) 25 (1.00) 25 (1.00) 25 (1.00) 25 (1.00) 25 (1.00) 25 (1.00) 25 (1.00)	5614 (1262) 4404 (990) 4582 (1030) 4270 (960) 4448 (1000) 5026 (1130) 5026 (1130) 4804 (1080) 4048 (910)	17.4 (2.52) 13.5 (1.96) 13.9 (2.02) 13.2 (1.92) 13.5 (1.96) 15.6 (2.26) 15.6 (2.26) 14.9 (2.16) 12.5 (1.82)	•
3 3 3 3 3 3 3 3 3	2-3-21 2-3-22 2-3-23 2-3-24 2-3-25 2-3-26 2-3-27 2-3-28 2-3-29	116 (-250) 116 (-250) 116 (-250) 294 (70) 294 (70) 294 (70) 561 (550) 561 (550)	13 (.50) 13 (.50) 13 (.50) 13 (.50) 13 (.50) 13 (.50) 13 (.50) 13 (.50)	25 (1.00) 26 (1.01) 26 (1.01) 26 (1.01) 25 (1.00) 25 (1.00) 26 (1.01) 26 (1.01)	3870 (870) 3559 (800) 3763 (846) 3443 (774) 3772 (848) 4617 (1038) 4991 (1122) 4813 (1082) 4760 (1070)	12.0 (1.74) 10.9 (1.58) 11.6 (1.68) 10.6 (1.53) 11.7 (1.70) 14.3 (2.08) 15.3 (2.22) 14.9 (2.16) 14.6 (2.12)	

Table A-2: MATRIX 2 TEST 4 THICK ADHEREND SHEAR TESTS OF A7F ADHESIVE

a) SI Units

					ULTII	MATE FAI	LURE	SHEAR	MODULUS	SHEAR	
CONDITION CODE	SPECIMEN NUMBER	TEMPERATURE K	ADHESIVE THICKNESS mm	WIDTH mm 2	LAP LENGTH mm	LOAD kn	SHEAR STRESS MPa	SHEAR STRAIN	INITIAL MPa	SECONDARY MPa.	PROPORTIONAL LIMIT MPa
1	20	116	.328	23.95	25.53	$\Delta$			61.83		
1	23	116	.345	24,32	25.42						
]	24	. 116	.279	24.79	25.36	15.79	25.11	.7085			
] ]	21	116	.333	24.89	25.59	12.75	20.02	'			
1	13	294	.340	24.85	25.45	10.59	16.75	.3904	71.51		10.64
1	14	294	.376	24.43	25.43	10.24	16.48	.3758	69.13		8.52
1	15	294	.366	23.79	25.57	10.40	17.09	.4337	70.47		6.21
1	17	561	.269	24.37	25.39	6.846	11.07	.4375	45.48		3.88
1 -	18	561	.348	25.00	25.42	5.293	8.33	.4311			
1	19	561	.391	24.75	25.54	4.413	6.98	.4144	46.15		2.25
2	2-20	116	.318	24.44	25.50	13.43	21,55	,6645	45,08	**	
2	2-23	116	.272	24.47	24.76	13.16	21.73	.6429	35.31		
2	2-24	116	.351	24.42	25.59	12.61	20.18	.5842	41.78	**	<b>***</b>
2	2-13	294	.353	24.19	25.45	11.47	18.63	,5320	137.5	70,02	3,58
2	2-14	294	.262	24.01	25,36	7.993	13.13	.4975	49.21	46.11	4.03
2	2-15	294	.282	24.43	24.27	9.808	16.54	.5495	53.10	44.46	5.71
2	2-16	561	.279	24.12	25.54	7.896	12.82	,4377	42.54		4.30
2 2	2-17	561	.381	24.44	25.51	8.140	13.05	.3729	67.62		3.30
2	2-18	561	.300	24.94	25.45	8.963	14.12	.5271	47,93	~~	4,94

Average of eight measurements

Average of two measurements

Grip slipped

Table A-2: CONCLUDED

b) U.S. Customary Units

		FORMEN TOWNSDATING ADMESTIVE				ULTII	MATE FAI	LURE	SHEAR	MODULUS	SHEAR
CONDITION	SPECIMEN NUMBER	TEMPERATURE OF	ADHESIVE THICKNESS in.	WIDTH in.	LAP LENGTH in.	LOAD 1bs	SHEAR STRESS ps1	SHEAR STRAIN	INITIAL psi	SECONDARY pst	PROPORTIONAL LIMIT psi
1	20	-250	.0129	.9429	1.0051				8968		
].	23	-250	.0136	.9574	1.0009	3					
1 1	24	-250	.0110	.9760	.9983	3549	3642	.7085			
	21	-250	.0131	.9798	1.0073	2866	2904				
1	13	70	.0134	.9782	1.0020	2381	2429	.3904	10371		1543
1	14	70	.0148	.9619	1.0013	2302	2390	.3758	10027	~~	1236
1	15	70	.0144	.9368	1.0065	2337	2479	.4337	10221		900
1	17	550	.0106	.9593	.9995	1539	1605	.4375	6597		563
] 3	18	550	.0137	.9841	1.0009	1190	1208	.4311			
1	19	550	.0154	.9744	1.0057	992	1012	.4144	6693	~~	326
2	2-20	-250	.0125	.9623	1.0039	3020	3126	.6645	6539	***	~~
2 2	2-23	-250	.0107	.9632	.9749	2959	3151	,6429	5121		
2	2-24	-250	.0138	.9616	1.0073	2835	2927	.5842	6059		2,5
2	2-13	70	.0139	.9525	1.0018	2579	2703	.5320	19938	10156	518.7
2 2	2-14	70	.0103	.9453	.9986	1797	1904	.4975	7138	6688	583.9
2	2-15	70	.0111	.9618	.9555	2205	2399	.5495	7701	6448	827.6
2	2-16	550	.0110	.9495	1.0056	1775	1859	.4377	6170	~~	623
2	2-17	550	.0150	.9622	1.0045	1830	1893	.3729	9808		479
2 2	2-18	550	.0118	.9819	1.0021	2015	2048	.5271	6951		717

Average of eight measurements

Average of two measurements

Grtp slipped

Table A-3: MATRIX 2 TEST 5 FLATWISE TENSION TESTS OF A7F ADHESIVE

CONDITION	SPECIMEN NUMBER	TEMPI K			ETER in.	<del></del>	ULTIMATE DAD Kip	FAILUI STRE MPa		NOTES
1	2-5-1-5 2-5-1-6 2-5-1-10	116 116 116	(-250) (-250) (-250)	31.50 31.47 31.70	(1.240) (1.239) (1.248)	42.3	(10.84) (9.51) (9.02)	61.9 54.4 50.8	(8.98) (7.89) (7.37)	
] ] ]	2-5-1-1 2-5-1-2 2-5-1-3	294 294 294		31.57 31.67 31.70	(1.243) (1.247) (1.248)	13.8	(2.08) (3.11) (6.87)	11.8 17.6 38.7	(1.71) (2.55) (5.62)	
] ] ]	2-5-1-7 2-5-1-8 2-5-1-9	561 561 561	(550) (550) (550)		(1.248) (1.248) (1.248)	7.16		13.8 9.07 12.2	(2.00) (1.32) (1.77)	
2 2 2 2	2-5-2-1 2-5-2-2 2-5-2-4 2-5-2-9	116 116 116 116		31.65 31.67 31.65 31.67	(1.246) (1.247) (1.246) (1.247)	35.3 45.1	(8.86) (7.93) (10.14) (5.30)	50.1 44.8 57.3 29.9	(7.27) (6.49) (8.32) (4.34)	
2 2 2	2-5-2-5 2-5-2-6 2-5-2-7	294 294 294	(70)	31.67 31.67 31.67	(1.247) (1.247) (1.247)	29.3	(4.60) (6.58) (3.44)	26.0 37.1 19.4	(3,77) (5.39) (2,82)	$\Delta \Delta \Delta$
2 2 2	2-5-2-8 2-5-2-10 2-5-2-3	561 561 561	(550)	31.67 31.67 31.67	(1.247) (1.247) (1.247)	15.3	(4.83) (3.43) (3.54)	27,3 19.4 20,0	(3.95) (2.81) (2.90)	ΔΔΔ

Cohesive failure

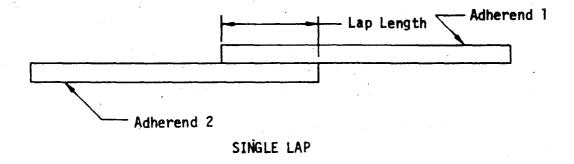
1/2 outer edge had adhesive failure, remainder cohesive failure

40% adhesive failure, 60% cohesive failure

Bolt sheared simultaneously at failure

APPENDIX B

STANDARD BONDED JOINT
TEST RESULT TABLES



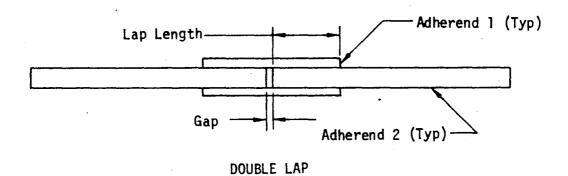


Figure B-1: STANDARD JOINT NOMENCLATURE

TABLE 8-1 SINGLE LAP JOINT TEST RESULTS

SPECIMEN NUMBER	TEMPERATURE (K)	LAP LENGTH (MM)	LAP WIDTH (MM)	CONFIG		THIC	HEREND KNESSES (MM) 2	FAILURE LOAD (KN)	AVERAGE JOINT STRESS (MPA)	UTT (APM)	JOINT EFFICIENCY
3A-7A-2-1C 3A-7A-2-2C 3A-7A-2-3C 3A-7A-2-4C 3A-7A-2-5C 3A-7A-2-6C	116. 116. 116. 116. 116. 116.	13.46 13.72 13.46 13.21 13.46 13.21	25.74 25.29 25.40 25.38 25.34 25.45	s s s s s s s	A A A A A A A A A	1.70 1.70 1.70	02 1.702 02 1.702 02 1.702 02 1.702	2.233 3.559 2.753 3.109	8.665 6.439 10.408 8.212 9.113 8.866	524. 524. 524. 524. 524. 524.	0.131 0.039 0.157 0.122 0.138 0.131
3A-7A-2-7A 3A-7A-2-8A 3A-7A-2-10A 3A-7A-2-11A 3A-7A-2-12A 3A-7A-2-13A	294. 294.	13.46 13.21 13.21 13.21 13.72 13.46	25.28 25.31 25.24 25.38 25.37 25.39	S S S S S S S	A A A A A A A A A	1.70 1.70 1.70	02 1.702 02 1.702 02 1.702 02 1.702	2.558 2.451 2.905 2.420	7.555 7.650 7.351 8.665 6.955 9.046	524. 524. 524. 524. 524.	0.114 0.113 0.109 0.128 0.107 0.137
3A-7A-2-14H 3A-7A-2-15H 3A-7A-2-16H 3A-7A-2-17H 3A-7A-2-18H 3A-7A-2-19H	561. 561. 561. 561.	13.46 13.21 13.46 13.21 13.21	25.38 25.40 25.35 25.35 25.41 25.42	s s s s s	A A A A A A A A A A A A A A A A A A A	1.70 1.70 1.70	02 1.702 02 1.702 02 1.702 02 1.702	3.123 2.544 3.501 3.630	7.823 9.307 7.455 10.454 10.814 11.459	524. 524. 524. 524. 524. 524.	0.118 0.138 0.113 0.155 0.160 0.170
3A-1A-2-1C 3A-1A-2-2C 3A-1A-2-3C 3A-1A-2-4C 3A-1A-2-5C 3A-1A-2-6C	116. 116. 116. 116. 116.	25.65 25.65 25.65 25.91 25.65 25.65	25.45 25.48 25.43 25.43 25.48 25.37	\$ \$ \$ \$ \$ \$ \$ \$	A A A A A A A A A A A A A A A A A A A	1.75 1.75 1.75	53 1.753 53 1.753 53 1.753 53 1.753	2.171 2.064 2.295 2.331	4.769 3.321 3.164 3.484 3.566 3.082	524. 524. 524. 524. 524.	0.133 0.093 0.088 0.098 0.100 0.086
3A-1A-2-7A 3A-1A-2-8A 3A-1A-2-9A 3A-1A-2-10A 3A-1A-2-11A 3A-1A-2-12A	294.	26.16 26.16 25.65 26.16 25.91 25.65	25.43 25.45 25.45 25.48 25.37 25.37	\$ \$ \$ \$ \$ \$ \$ \$ \$ \$	A A A A A A A A A A A A	1.75 1.75 1.75	33 1.753 33 1.753 33 1.753 33 1.753	3.158 3.541 4.804 2.847	5.818 4.743 5.423 7.208 4.330 5.654	524. 524. 524. 524. 524.	0.166 0.135 0.151 0.205 0.122 0.158
3A-1A-2-14H 3A-1A-2-15H 3A-1A-2-16H 3A-1A-2-17H 3A-1A-2-18H 3A-1A-2-19H	561. 561. 561. 561.	25.65 25.91 25.91 20.16 25.65 25.91	25.45 25.45 25.43 25.48 25.40 25.48	888888	A A A A A A A A	1.75 1.75 1.75	53 1.753 53 1.753 53 1.753 53 1.753	5.089 5.093 5.765 3.745	7.058 7.718 7.732 8.649 5.743 7.777	524. 524. 524. 524. 524.	0.197 0.218 0.218 0.246 0.101 0.219

TABLE B-1 CONTINUED

SPECIMEN TEMPERATURE NUMBER (K)	LAP LAP LENGTH WIDTH (MM) (MM)	CONFIG LAYUP CODE* CODE+ 1 2	ADHEREND THICKNESSES (MM) 1 2	FAILUNE LOAD (KN)	AVENAGE JOINT STRESS FTU (MPA) (MPA)	JOINT EFFICIENCY
3A-1B-2-1C 116.	51.82 25.83	S A A S A A S A A S A A S	1.930 1.930	3.603	2.692 524.	0.138
3A-1B-2-2C 116.	52.07 25.83		1.930 1.930	3.185	2.368 524.	0.122
3A-1B-2-3C 116.	52.32 25.81		1.930 1.930	3.541	2.622 524.	0.136
3A-1B-2-4C 116.	52.32 25.07		1.930 1.930	3.692	2.814 524.	0.146
3A-1B-2-5C 116.	52.07 25.86		1.930 1.930	3.434	2.551 524.	0.131
3A-1B-2-5C 116.	52.32 25.81		1.930 1.930	3.372	2.497 524.	0.129
3A-1B-2-7A 294.	52.32 25.86	S A A A S A A S A A S A A S	1.930 1.930	3.470	2.564 524.	0.133
3A-1B-2-8A 294.	52.32 25.01		1.930 1.930	3.327	2.543 524.	0.132
3A-1B-2-9A 294.	52.32 25.81		1.930 1.930	3.959	2.932 524.	0.152
3A-1B-2-10A 294.	52.32 25.86		1.930 1.930	3.532	2.611 524.	0.135
3A-1B-2-11A 294.	52.07 25.83		1.930 1.930	3.407	2.533 524.	0.130
3A-1B-2-12A 294.	52.07 25.83		1.930 1.930	3.781	2.811 524.	0.145
3A-1B-2-13H 561.	52.32 25.15	S A A A S A A S A A S A A	1.930 1.930	3.923	2.982 524.	0.154
3A-1B-2-14H 561.	52.32 25.81		1.930 1.930	3.292	2.438 524.	0.126
3A-1B-2-15H 561.	52.32 25.78		1.930 1.930	4.644	3.443 524.	0.178
3A-1B-2-16H 561.	52.32 25.81		1.930 1.930	3.986	2.952 524.	0.153
3A-1B-2-17H 561.	52.32 25.81		1.930 1.930	3.923	2.906 524.	0.150
3A-1B-2-18H 561.	52.32 25.83		1.930 1.930	3.559	2.633 524.	0.136
3A-1C-2-1C 116.	77.47 25.91	S A A A S A A S A A S A A	1.880 1.880	4.955	2.469 524.	0.194
3A-1C-2-2C 116.	77.72 25.91		1.890 1.880	4.724	2.346 524.	0.185
3A-1C-2-3C 116.	77.47 25.91		1.880 1.880	5.240	2.611 524.	0.205
3A-1C-2-4C 116.	77.47 25.91		1.880 1.880	5.316	2.648 524.	0.208
3A-1C-2-5C 116.	77.22 25.91		1.880 1.880	6.299	3.149 524.	0.247
3A-1C-2-6C 116.	77.98 25.91		1.880 1.880	5.276	2.611 524.	0.207
3A-1C-2-7A 294. 3A-1C-2-8A 294. 3A-1C-2-9A 294. 3A-1C-2-1OA 294. 3A-1C-2-11A 294. 3A-1C-2-12A 294.	77.47 25.91 77.47 25.91 77.72 25.91 77.72 25.91 77.72 25.91 77.72 25.91 77.22 25.91	S A A S A A S A A S A A S A A S	1.880 1.880 1.880 1.880 1.880 1.880 1.880 1.880 1.830 1.880 1.880 1.880	5.987 5.729 3.550 5.987 5.596 5.151	2.983 524. 2.855 524. 1.763 524. 2.993 524. 2.779 524. 2.575 524.	0.235 0.225 0.139 0.235 0.219 0.202
3A-1C-2-13H 561.	77.22 25.91	S A A S A A S A A S A A S A A	1.830 1.880	7.891	3.945 524.	0.309
3A-1C-2-14H 561.	77.72 25.91		1.880 1.880	6.699	3.327 524.	0.203
3A-1C-2-15H 561.	76.96 25.91		1.880 1.880	4.181	2.097 524.	0.164
3A-1C-2-16H 561.	77.47 25.15		1.880 1.830	6.850	3.516 524.	0.277
3A-1C-2-17H 561.	77.22 25.91		1.880 1.880	5.436	2.717 524.	0.213
3A-1C-2-18H 561.	77.22 25.15		1.880 1.880	7.420	3.821 524.	0.300

TABLE B-1 CONTINUED

NUMBER	TEMPERATURE (K)	LAP LENGTH (MM)	LAP WIDTH (MM)	CONFIG CODE*	CODE		ADHEREND THICKNESSES (MM) 1 2	FAILURE LOAD (KN)	AVERAGE JOINT STRESS (MPA)	FTU (MPA)	JOINT EFFICIENCY
3A-2A-2-1C 3A-2A-2-2C 3A-2A-2-3C 3A-2A-2-4C 3A-2A-2-5C 3A-2A-2-6C	116. 116. 116. 116. 116. 116.	51.31 51.18 50.80 51.31 51.44 50.93	25.48 25.36 25.44 25.44 25.51 25.39	\$ \$ \$ \$ \$	B B B	0 B B B B B	1.753 1.753 1.753 1.753 1.753 1.753 1.753 1.753 1.753 1.753 1.753 1.753	6.272 5.249 5.182 6.650	4.662 4.832 4.062 3.970 5.067 3.526	972. 972. 972. 972. 972. 972.	0.140 0.145 0.121 0.120 0.153 0.105
3A-2A-2-7A 3A-2A-2-8A 3A-2A-2-9A 3A-2A-2-10A 3A-2A-2-11A 3A-2A-2-12A	294.	50.93 51.44 50.80 50.80 51.05 51.31	25.37 25.40 25.27 25.38 25.41 25.48	s s s s s	B   B   B	B B B B B	1.753 1.753 1.753 1.753 1.753 1.753 1.753 1.753 1.753 1.753 1.753 1.753	5.004 3 4.760 3 5.115 3 4.582	4.114 3.830 3.708 3.968 3.531 5.189	972. 972. 972. 972. 972. 972.	0.123 0.116 0.111 0.118 0.106 0.156
3A-2A-2-13H 3A-2A-2-14H 3A-2A-2-15H 3A-2A-2-16H 3A-2A-2-17H 3A-2A-2-18H 3A-2A-2-19H	561. 561. 561. 561. 561.	51.05 51.18 51.31 51.18 51.56 51.18 51.56	25.47 25.45 25.51 25.59 25.46 25.48 25.58	****	B B B	2 8 8 8 8 8	1.753 1.753 1.753 1.753 1.753 1.753 1.753 1.753 1.753 1.753 1.753 1.753	8.977 3 9.844 3 10.444 3 9.942 3 9.866	5.976 6.891 7.522 7.974 7.574 - 7.565 8.459	972. 972. 972. 972. 972. 972.	0.179 0.207 0.227 0.240 0.229 0.227 0.256
3A-3A-2-1A 3A-3A-2-2A 3A-3A-2-3A 3A-3A-2-4A 3A-3A-2-6A 3A-3A-2-6A 3A-3A-2-7A 3A-3A-2-8A	294. 294. 294. 294. 294. 294.	51.31 50.80 51.05 51.31 50.80 51.05 51.05	25.50 25.52 25.53 25.48 25.55 25.48 25.48	******	00000	00000000	1.600 1.600 1.600 1.600 1.600 1.600 1.600 1.600 1.600 1.600 1.600 1.600	5.685 5.498 5.436 4.315 5.529 6.036	4.046 4.386 4.219 4.157 3.324 4.251 4.646	524. 524. 524. 524. 524. 524.	0.248 0.266 0.257 0.254 0.201 0.259 0.283
3A-4A-2-1A 3A-4A-2-2A 3A-4A-2-3A 3A-4A-2-4A 3A-4A-2-5A 3A-4A-2-6A	294. 294. 294. 294. 294. 294.	51.05 51.05 52.07 51.56 51.82 51.82	25.53 25.76 25.83 25.93 25.77 25.83 25.89	* ******	D   D   D   D   D   D   D   D   D   D	C D D D D D	1.600 1.600 1.499 1.499 1.499 1.499 1.499 1.499 1.499 1.499 1.499 1.499	6.201 5.889 7.802 6.512 1.601	3.533 4.715 4.466 5.778 4.901 1.197 3.051	524. 524. 524. 524. 524. 524.	0.214 0.307 0.290 0.383 0.322 0.079 0.201
3A-5A-2-1C 3A-5A-2-2C 3A-5A-2-3C 3A-5A-2-4C 3A-5A-2-5C	116. 116. 116. 116.	51.56 51.56 51.56 51.82 51.31	25.65 25.65 25.40 25.65 25.65	S S S S S	E	G G G G	1.143 2.21 1.143 2.31 1.143 2.31 1.143 2.31 1.143 2.31	2.589 2.375 2.286	2.011 1.957 1.814 1.720 1.859	524. 524. 521. 524. 524.	0.173 0.168 0.156 0.149 0.159

TABLE B-1 CONTINUED

SPECIMEN NUMBER	TEMPERATURE (K)	LAP LENGTH (MM)	LAP WIDTH (MM)	CONFIG CODE#	CODE		ADHEF THICKNE (M) 1	ESSES	FAILURE LOAD (KN)	AVERAGE JOINT STRESS (MPA)	FTU (MPA)	JOINT EFFICIENCY
3A-5A-2-6A 3A-5A-2-7A 3A-5A-2-8A 3A-5A-2-9A 3A-5A-2-10A 3A-5A-2-11A		51.56 51.31 51.56 50.80 51.56 51.56	25.65 25.65 25.65 25.91 25.65 25.65	\$ 5 5 5 5 5 5 5 5 5 5 5 5 5 5 5 5 5 5 5	E	G G G G G	1.143 1.143 1.143 1.143 1.143 1.143	2.311 2.311 2.311 2.311 2.311 2.311	2.874 2.295 2.420 3.892 2.180 3.754	2.172 1.744 1.829 2.957 1.648 2.838	524. 524. 524. 524. 524. 524.	0.187 0.149 0.157 0.251 0.142 0.244
3A-5A-2-12H 3A-5A-2-13H 3A-5A-2-14H 3A-5A-2-15H 3A-5A-2-16H	561. 561. 561.	51.31 51.56 51.56 51.56 51.56	25.65 25.65 25.40 25.65 25.65	\$ \$ \$ \$	E	G G G	1.143 1.143 1.143 1.143 1.143	2.311 2.311 2.311 2.311 2.311	3.594 3.754 4.849 6.156 2.340	2.731 2.838 3.702 4.654 1.769	524. 524. 524. 524. 524.	0.234 0.244 0.319 0.401 0.152
3A-6A-2-1A 3A-6A-2-2A 3A-6A-2-3A 3A-6A-2-4A 3A-6A-2-5A 3A-6A-2-6A	294. 294. 294. 294. 294. 294.	51.82 51.56 51.31 51.05 51.56 51.56	25.91 25.91 25.91 25.91 25.91 25.91	\$ 5 5 5 5 5 5 5 5	H H H	H H H H H	2.946 2.946 2.946 2.946 2.946 2.946	2.946 2.946 2.946 2.946 2.946 2.946	4.688 5.391 4.422 5.293 5.071 5.293	3.492 4.036 3.328 4.002 3.796 3.963	524. 524. 524. 524. 524. 524.	0.117 0.135 0.111 0.132 0.127 0.132
3B-1A-2-1C 3B-1A-2-2C 3B-1A-2-3C 3B-1A-2-4C 3B-1A-2-5C 3B-1A-2-6C	116. 116. 116. 116. 116.	25.40 25.40 25.65 25.91 25.40 25.91	25.15 25.15 24.89 25.15 25.15 25.15	555555	A A A	T T T T	1.778 1.778 1.778 1.778 1.778	0.787 0.787 0.787 0.787 0.787 0.787	2.740 2.607 2.847 2.108 2.464 2.068	4.290 4.081 4.458 3.236 3.858 3.175	924. 924. 924. 924. 924.	0.150 0.142 0.157 0.115 0.135 0.113
3B-1A-2-7A 3B-1A-2-8A 3B-1A-2-9A 3B-1A-2-10A 3B-1A-2-11A 3B-1A-2-11A	294.	25.40 25.91 26.16 25.65 25.65 25.65	25.15 25.15 25.15 24.89 25.15 25.15	s s s s s s s	A A A A	T T T T	1.778 1.778 1.778 1.778 1.778	0.787 0.787 0.787 0.787 0.787	3.327 2.660 3.363 2.571 3.087 2.375	5.209 4.083 5.112 4.026 4.785 3.682	924. 924. 924. 924. 924.	0.182 0.145 0.184 0.142 0.169 0.130
3B-1A-2-13H 3B-1A-2-14H 3B-1A-2-15H 3B-1A-2-16H 3B-1A-2-17H 3B-1A-2-18H	561. 561. 561. 561.	25.40 25.65 25.65 25.91 25.91 25.91	25.15 25.15 25.15 25.15 25.15 25.15	\$ \$ \$ \$ \$ \$ \$ \$ \$ \$	A A A	T T T T T	1.778 1.778 1.778 1.778 1.778 1.778	0.787 0.787 0.787 0.787 0.787 0.787	6.112 2.518 5.160 3.932 5.872 6.156	9.569 3.903 7.999 6.036 9.013 9.450	924. 924. 924. 924. 924.	0.334 0.138 0.282 0.215 0.321 0.337

TABLE B-1 CONTINUED

SPECIMEN Number	TEMPERATURE (K)	LAP LENGTH (MM)	LAP WIDTH (MM)	CONFIG	CODE		THICKN	REND ESSES M) 2	FAILURE LOAD (KN)	AVERAGE JOINT STRESS (MPA)	FTU (MPA)	JOINT EFFICIENCY
3B-1B-2-1C 3B-1B-2-2C 3B-1B-2-3C 3B-1B-2-4C 3B-1B-2-5C 3B-1B-2-6C	116. 116. 116. 116. 116. 116.	51.56 50.80 51.05 50.80 51.31 51.05	25.15 25.15 25.15 25.15 25.15 25.15	\$ \$ \$ \$ \$	A A A	T T T T	1.778 1.778 1.778 1.778 1.778 1.778	0.787 0.787 0.787 0.787 0.787 0.787	2.945 3.559 3.888 3.737 2.687 3.621	2.271 2.786 3.028 2.925 2.082 2.820	924. 924. 924. 924. 924. 924.	0.161 0.195 0.213 0.204 0.147 0.198
3B-1B-2-7A 3B-1B-2-8A 3B-1B-2-9A 3B-1B-2-10A 3B-1B-2-11A 3B-1B-2-12A	294.	51.05 51.05 50.80 51.56 51.31 51.05	25.15 24.89 24.89 25.15 24.89 25.15	s s s s s	A A A	T T T T	1.778 1.778 1.778 1.778 1.778 1.778	0.787 0.787 0.787 0.787 0.787 0.787	5.694 4.982 5.089 4.075 4.680 4.546	4.435 3.920 4.024 3.143 3.664 3.541	924. 924. 924. 924. 924. 924.	0.311 0.275 0.281 0.223 0.258 0.249
3B-1B-2-13H 3B-1B-2-14H 3B-1B-2-16H 3B-1B-2-16H 3B-1B-2-17H 3B-1B-2-18H	561. 561. 561. 561.	51.31 51.05 51.05 51.31 51.05 50.80	25.15 25.15 25.15 25.15 25.15 25.15	\$ \$ \$ \$ \$ \$	A A A	T T T T	1.778 1.778 1.778 1.778 1.778 1.778	0.787 0.787 0.787 0.787 0.787 0.787	6.868 6.832 7.357 7.437 6.761 6.646	5.323 5.322 5.731 5.765 5.267 5.202	924. 924. 924. 924. 924. 924.	0.375 0.373 0.402 0.407 0.370 0.363
3B-1C-2-1C 3B-1C-2-2C 3B-1C-2-3C 3B-1C-2-4C 3B-1C-2-5C 3B-1C-2-6C	116. 116. 116. 116. 116. 116.	77.22 76.45 76.20 77.22 76.96 77.22	25.15 25.15 25.15 25.15 24.89 25.15	\$ \$ \$ \$ \$ \$ \$ \$	A A A	T T T T	1.778 1.778 1.778 1.778 1.778 1.778	0.787 0.787 0.787 0.787 0.787 0.787	2.669 2.544 3.105 2.856 2.802 2.509	1.375 1.323 1.620 1.471 1.463 1.292	924. 924. 924. 924. 924. 924.	O.146 O.139 O.170 O.156 O.155 O.137
3B-1C-2-7A 3B-1C-2-8A 3B-1C-2-9A 3B-1C-2-10A 3B-1C-2-11A 3B-1C-2-12A	294.	76.45 76.71 76.45 77.47 76.45 77.47	25.15 25.15 25.15 25.15 25.15 25.15	S S S S S S	A :	T T T T T	1.778 1.778 1.778 1.778 1.778 1.778	0.787 0.787 0.787 0.787 0.787 0.787	2.713 3.941 4.181 4.066 3.336 2.393	1.411 2.043 2.175 2.087 1.735 1.228	924. 924. 924. 924. 924. 924.	0.148 0.215 0.229 0.222 0.182 0.131
3B-1C-2-13H 3B-1C-2-14H 3B-1C-2-15H 3B-1C-2-16H JB-1C-2-17H 3B-1C-2-18H	561. 561. 561. 561.	76.45 76.71 77.47 77.47 76.20 76.45	25.15 24.64 25.15 25.15 24.39 25.15	\$ \$ \$ \$ \$	A	T T T T	1.778 1.778 1.778 1.778 1.778 1.778	0.787 0.787 0.787 0.787 0.787 0.787	6.228 5.916 7.402 6.779 5.605 7.909	3.239 3.130 3.800 3.480 2.955 4.114	924. 924. 924. 924. 924. 924.	0.340 0.330 0.405 0.371 0.310 0.432

TABLE 8-1 CONTINUED

SPECIMEN	TEMPERATURE	LAP LENGTH	LAP WIDTH	CONFIG CODE#			THICKN	REND IESSES IM)	FAILURE LOAD	AVERAGE JOINT STRESS	FTU	JOINT EFFICIENCY
NUMBER	(K)	(MM)	(MM)		1	2	1	2	(KN)	(MPA)	(MPA)	
3C-1A-2-1A	294.	51.31	25.91	T	Н	Н	2.946	2.946	6.539	4.919	524.	0.163
3C-1A-2-2A	294.	51.31	25.91	T	Н	Н	2.946	2.946	5.276	3.969	524.	0.132
3C-1A-2-4A	294.	50.80	25.91	Τ '	H	H	2.946	2.946	5.783	4.394	524.	0.145
3C-1A-2-5A	294.	51.05	25.91	Ť	Ĥ	Н	2.946	2.946	7.660	5.791	524.	0.191
3C-1A-2-6A	294.	51.56	25.91	Ť	H	Ĥ	2.946	2.946	6.201	4.642	524.	0.155
3C-1A-2-7A	294.	51.56	25.65	Ť	H	H	2.946	2.946	5.854	4.425	524.	0.148

#### \* CONFIGURATION CODE

S = STANDARD T = TAPERED ADHEREND

#### + LAYUP CODE

A = [0,+/-45,90]3S	G = [0,+/-45,90]4S	$M = \{0(3), +/-45(3), 90(3), +/-45(3),$	3)125
B = [0, +/-45, 0(3)]2S	H = [0, +/-45, 90]5	N = [+/-45, 0, 90]6S	
C = [+/-45,0,90]35	J = [0, +/-45, 90]65	P = [0,+/-45,90]12S	
D = [0(3), +/-45(3), 0(3)]S	K = [0, +45, 0(2), -45, 0]2S	T = TITANIUM	
E = [0.+/-45.9012S]	L = [0.+45.0(2)45.0145]		

TABLE B-1 CONTINUED
(B) US CUSTOMARY UNITS

SPECIMEN NUMBER	TEMPERATURE (F)	LAP LENGTH (IN)	LAP WIDTH (IN)	CONFIG CODE*	LAYUP CODE+ 1 2		FAILURE LOAD (LBS)	AVERAGE JOINT STRESS (PSI)	FTU (K\$1)	JOINT EFFICIENCY
3A-7A-2-1C 3A-7A-2-2C 3A-7A-2-3C 3A-7A-2-4C 3A-7A-2-5C 3A-7A-2-6C	-250. -250. -250. -250. -250. -250.	0.530 0.540 0.530 0.520 0.530 0.520	1.013 0.996 1.000 0.999 0.998 1.002	\$ 5 5 5 5 5 5 5	A A A A A A A A A	0.067 0.067 0.067 0.067 0.067 0.067 0.067 0.067	675. 502. 800. 619. 699.	1257. 934. 1510. 1191. 1322. 1286.	76. 76. 76. 76. 76.	0.131 0.099 0.157 0.122 0.138
3A-7A-2-7A 3A-7A-2-8A 3A-7A-2-10/ 3A-7A-2-11/ 3A-7A-2-12/ 3A-7A-2-13/	A 70. A 70.	0.530 0.520 0.520 0.520 0.540 0.530	0.995 0.997 0.994 0.999 0.999	S S S S S S S S	A A A A A A A A	0.067 0.067 0.067 0.067 0.067 0.067 0.067 0.067 0.067 0.067	578. 575. 551. 653. 544.	1096. 1110. 1066. 1257. 1009.	76. 76. 76. 76. 76.	0.114 0.113 0.109 0.128 0.107 0.137
3A-7A-2-14I 3A-7A-2-15I 3A-7A-2-16I 3A-7A-2-17I 3A-7A-2-18I 3A-7A-2-19I	f 550. f 550. f 550. f 550.	0.530 0.520 0.530 0.520 0.520 0.520	0.999 1.000 0.998 0.998 1.000	s s s s s s	A A A A A A A A A	0.067 0.067 0.067 0.067 0.067 0.067 0.067 0.067	601. 702. 572. 787. 816. 865.	1135. 1350. 1081. 1516. 1568.	76. 76. 76. 76. 76.	0.118 0.138 0.113 0.155 0.160 0.170
3A-1A-2-1C 3A-1A-2-2C 3A-1A-2-3C 3A-1A-2-4C 3A-1A-2-5C 3A-1A-2-6C	-250. -250. -250. -250. -250. -250.	1.010 1.010 1.010 1.020 1.010	1.002 1.003 1.001 1.001 1.003 0.999	s s s s s s	A A A A A A A A A	0.069 0.069 0.069 0.069 0.069 0.069 0.069 0.069	700. 488. 464. 516. 524. 451.	692. 482. 459. 505. 517. 447.	76. 76. 76. 76. 76.	0.133 0.093 0.088 0.098 0.100 0.086
3A-1A-2-7A 3A-1A-2-8A 3A-1A-2-9A 3A-1A-2-10/ 3A-1A-2-11/ 3A-1A-2-12/	70.	1.030 1.030 1.010 1.030 1.020 1.010	1.001 1.002 1.002 1.003 0.999 1.001	\$ \$ \$ \$ \$ \$ \$ \$	A A A A A A A A	0.069 0.069 0.069 0.069 0.069 0.069 0.069 0.069	870. 710. 796. 1080. 640. 829.	844. 688. 787. 1045. 628. 820.	76. 76. 76. 76. 76.	0.166 0.135 0.151 0.205 0.122 0.158
3A-1A-2-14 3A-1A-2-15 3A-1A-2-16 3A-1A-2-17 3A-1A-2-18 3A-1A-2-19	550. 550. 550. 550.	1.010 1.020 1.020 1.030 1.010 1.020	1.002 1.002 1.001 1.003 1.000	5 5 5 5 5 5	A A A A A A A A A A A	0.069 0.069 0.069 0.069 0.069 0.069 0.069 0.069	1036. 1144. 1145. 1298. 842. 1154.	1024. 1119. 1121. 1254. 834. 1128.	76. 76. 76. 76. 76.	0.197 0.218 0.213 0.246 0.161 0.219

TABLE B-1 CONTINUED
(B) US CUSTOMARY UNITS

SPECIMEN 1	TEMPERATURE (F)	LAP LENGTH (IN)	LAP WIDTH (IN)	CONFIG CODE*		(IN)	FAILURE LOAD (LBS)	AVERAGE JOINT STRESS (PSI)	FTU (KSI)	THIOL YOKAIOI 473
3A-1B-2-1C 3A-1B-2-2C 3A-1B-2-3C 3A-1B-2-4C 3A-1B-2-5C 3A-1B-2-6C	-250. -250. -250. -250. -250. -250.	2.040 2.050 2.060 2.060 2.050 2.060	1.017 1.017 1.016 0.987 1.018 1.016	s s s s s	A A A A A A A A	0.076 0.076 0.076 0.076 0.076 0.076 0.076 0.076	810. 716. 796. 830. 772. 758.	390. 343. 380. 408. 370. 362.	76. 76. 76. 76. 76.	0.138 0.122 0.136 0.146 0.131 0.129
3A-1B-2-7A 3A-1B-2-8A 3A-1B-2-9A 3A-1B-2-1OA 3A-1B-2-11A 3A-1B-2-12A	70. 70. 70. 70. 70. 70.	2.060 2.060 2.060 2.060 2.050 2.050	1.018 0.984 1.016 1.018 1.017	s s s s s s s	A A A A A A A A	0.076 0.076 0.076 0.076 0.076 0.076 0.076 0.076	780. 748. 890. 794. 766.	372. 369. 425. 379. 367. 408.	76. 76. 76. 76. 76.	0.133 0.132 0.152 0.135 0.130 0.145
3A-1B-2-13H 3A-1B-2-14H 3A-1B-2-15H 3A-1B-2-16H 3A-1B-2-17H 3A-1B-2-18H	550. 550. 550. 550. 550.	2.060 2.060 2.060 2.060 2.060 2.060	0.990 1.016 1.015 1.016 1.016	\$ \$ \$ \$ \$ \$ \$	A A A A A A A A	0.076 0.076 0.076 0.076 0.076 0.076 0.076 0.076	882. 740. 1044. 896. 882. 800.	432. 354. 499. 428. 421. 382.	76. 76. 76. 76. 76.	0.154 0.126 0.178 0.153 0.150 0.156
3A-1C-2-1C 3A-1C-2-2C 3A-1C-2-3C 3A-1C-2-4C 3A-1C-2-5C 3A-1C-2-6C	-250. -250. -250. -250. -250. -250.	3.050 3.060 3.050 3.050 3.040 3.070	1.020 1.020 1.020 1.020 1.020 1.020	s s s s s	A A A A A A A A	0.074 0.074 0.074 0.074 0.074 0.074 0.074 0.074	1114. 1062. 1178. 1195. 1416. 1186.	358. 340. 379. 384. 457. 379.	76. 76. 76. 76. 76.	0.194 0.185 0.205 0.208 0.247 0.207
3A-1C-2-7A 3A-1C-2-8A 3A-1C-2-9A 3A-1C-2-1OA 3A-1C-2-11A 3A-1C-2-12A	70. 70. 70. 70. 70.	3.050 3.050 3.060 3.040 3.060 3.040	1.020 1.020 1.020 1.020 1.020 1.020	S	A A A A A A A A A	0.074 0.074 0.074 0.074 0.074 0.074 0.074 0.074	1346. 1288. 798. 1346. 1258.	433. 414. 256. 434. 403. 373.	78. 76. 76. 76. 76.	0.235 0.225 0.139 0.235 0.219 0.202
3A-1C-2-13H 3A-1C-2-14H 3A-1C-2-15H 3A-1C-2-16H 3A-1C-2-17H 3A-1C-2-18H	550. 550. 550. 550. 550.	3.040 3.060 3.030 3.050 3.040 3.040	1.020 1.020 1.020 0.990 1.020 0.990	\$ \$ \$ \$ \$ \$	A A A A A A A	0.074 0.074 0.074 0.074 0.074 0.074 0.074 0.074	1774. 1506. 940. 1540. 1222. 1668.	572. 463. 304. 510. 394. 554.	76. 76. 76. 76. 76. 76.	0.309 0.263 0.164 0.277 0.213 0.300

TABLE B-1 CONTINUED (B) US CUSTOMARY UNITS

				(R) (	s cus	i Oi	MARY UN	ITS				
NUMBER	TEMPERATURE (F)	LAP LENGTH (IN)	LAP WIDTH (IN)	CONF I G	CODE		ADHE THICKN (I	ESSES	FAILURE LOAD (LBS)	AVERAGE JOINT STRESS (PSI)	FTU (KSI)	JOINT EFFICIENCY
3A-2A-2-1C 3A-2A-2-2C 3A-2A-2-3C 3A-2A-2-4C 3A-2A-2-5C 3A-2A-2-6C	-250. -250. -250. -250. -250. -250.	2.020 2.015 2.000 2.020 2.025 2.005	1.003 0.998 1.002 1.002 1.005	s s s s s	B   B   B   B   B   B   B   B   B   B	B B B B B	0.069 0.069 0.069 0.069 0.069	0.069 0.069 0.069 0.069 0.069	1370. 1410. 1180. 1165. 1495. 1025.	676. 701. 589. 576. 735. 511.	141. 141. 141. 141. 141.	0.140 0.145 0.121 0.120 0.153 0.105
3A-2A-2-7A 3A-2A-2-8A 3A-2A-2-9A 3A-2A-2-10A 3A-2A-2-11A 3A-2A-2-12A	70.	2.005 2.025 2.000 2.000 2.010 2.020	0.999 1.000 0.995 0.999 1.000 1.003	5 5 5 5 5 5	B   B   B   B   B   B   B   B   B   B	B B B B	0.069 0.069 0.069 0.069 0.069	0.069 0.069 0.069 0.069 0.069	1195. 1125. 1070. 1150. 1030. 1525.	597. 556. 538. 575. 512. 753.	141. 141. 141. 141. 141.	0.123 0.110 0.111 0.118 0.106 0.156
3A-2A-2-13H 3A-2A-2-14H 3A-2A-2-15H 3A-2A-2-16H 3A-2A-2-17H 3A-2A-2-18H 3A-2A-2-19H	550. 550. 550. 550.	2.010 2.015 2.020 2.015 2.030 2.015 2.030	1.003 1.002 1.904 1.008 1.002 1.003	****	8 8 8 8	B B B B B B	0.069 0.069 0.069 0.069 0.069 0.069	0.069 0.069 0.069 0.069 0.069 0.069	1747. 2018. 2213. 2348. 2235. 2218. 2508.	867. 999. 1091. 1157. 1098. 1097.	141. 141. 141. 141. 141. 141.	0.179 0.207 0.227 0.240 0.229 0.227 0.256
3A-3A-2-1A 3A-3A-2-2A 3A-3A-2-3A 3A-3A-2-5A 3A-3A-2-6A 3A-3A-2-7A 3A-3A-2-8A	70. 70. 70. 70. 70. 70. 70.	2.020 2.000 2.010 2.020 2.000 2.010 2.010 2.000	1.004 1.005 1.005 1.003 1.006 1.003	5555555	00000	00000000	0.063 0.063 0.063 0.063 0.063 0.063 0.063	0.063 0.063 0.063 0.063 0.063 0.063 0.063	1190. 1278. 1236. 1222. 970. 1243.	587. 636. 612. 603. 482. 617.	76. 76. 76. 76. 76. 76.	0.248 0.266 0.257 0.254 0.201 0.259 0.283
3A-4A-2-1A 3A-4A-2-2A 3A-4A-2-3A 3A-4A-2-4A 3A-4A-2-5A 3A-4A-2-6A	70. 70. 70. 70. 70. 70.	2.010 2.010 2.050 2.030 2.040	1.014 1.017 1.021 1.015 1.017	5 555555	D	000000000000000000000000000000000000000	0.059 0.059 0.059 0.059 0.059 0.059	0.059 0.059 0.059 0.059 0.059 0.059	1030. 1394. 1324. 1754. 1464. 360. 920.	512. 684. 648. 838. 711. 174. 443.	76. 76. 76. 76. 76. 76.	0.214 0.307 0.290 0.383 0.322 0.079 0.201
3A-5A-2-1C 3A-5A-2-2C 3A-5A-2-3C 3A-5A-2-4C 3A-5A-2-5C	-250. -250. -250. -250. -250.	2.030 2.030 2.030 2.040 2.020	1.010 1.010 1.000 1.010 1.010	\$ \$ \$ \$	E	G G G	0.045 0.045 0.045 0.045 0.045	0.091 0.091 0.091 0.091 0.091	598. 582. 534. 514. 550.	292. 284. 263. 249. 270.	76. 76. 76. 76.	0.173 0.168 0.156 0.149 0.159

TABLE B-1 CONTINUED

## (B) US CUSTOMARY UNITS .

SPECIMEN NUMBER	TEMPERATURE (F)	LAP LENGTH (IN)	LAP WIDTH (IN)	CONFIG CODE*		THICK	EREND NESSES IN) 2	FAILURE LOAD (LBS)	AVERAGE JOINT STRESS (PSI)	FTU (KSI)	JOINT EFFICIENCY	
3A-5A-2-6A 3A-5A-2-7A 3A-5A-2-8A 3A-5A-2-9A 3A-5A-2-10A 3A-5A-2-11A		2.030 2.020 2.030 2.000 2.030 2.030	1.010 1.010 1.010 1.020 1.010 1.010	55555	E E E E	0.045 0.045 0.045	0.091 0.091 0.091 0.091 0.091	646. 516. 544. 875. 490. 844.	315. 253. 265. 429. 239. 412.	76. 76. 76. 76. 76.	0.187 0.149 0.157 0.251 0.142 0.244	
3A-5A-2-12H 3A-5A-2-13H 3A-5A-2-14H 3A-5A-2-15H 3A-5A-2-16H	550. 550. 550.	2.020 2.030 2.030 2.030 2.030	1.010 1.010 1.000 1.010 1.010	\$ \$ \$ \$ \$		0.045 0.045 0.045	0.091 0.091 0.091 0.091 0.091	808. 844. 1090. 1384. 526.	398. 412. 537. 675. 257.	76. 76. 76. 76.	0.234 0.244 0.319 0.401 0.152	
3A-6A-2-1A 3A-6A-2-2A 3A-6A-2-3A 3A-6A-2-4A 3A-6A-2-5A 3A-6A-2-6A	70. 70. 70. 70. 70. 70.	2.040 2.030 2.020 2.010 2.030 2.030	1.020 1.020 1.020 1.020 1.020	S S S S S S S	H I H I H I	0.116	0.116 0.116 0.116 0.116 0.116 0.116	1054. 1212. 994. 1190. 1140. 1190.	507. 585. 482. 580. 551.	76. 76. 76. 76. 76.	0.117 0.135 0.111 0.132 0.127 0.132	
3B-1A-2-1C 3B-1A-2-2C 3B-1A-2-3C 3B-1A-2-4C 3B-1A-2-5C 3B-1A-2-6C	-250. -250. -250. -250. -250. -250.	1.000 1.000 1.010 1.020 1.000 1.020	0.990 0.990 0.980 0.990 0.990	s s s s s	Ä '	0.070 0.070 0.070	0.031 0.031 0.031 0.031 0.031 0.031	616. 586. 640. 474. 554. 465.	G22. 592. 647. 469. 500. 460.	134. 134. 134. 134. 134.	0.150 0.142 0.157 0.115 0.135 0.113	1
3B-1A-2-7A 3B-1A-2-8A 3B-1A-2-9A 3B-1A-2-10A 3B-1A-2-11A 3B-1A-2-11A	70.	1.000 1.020 1.030 1.010 1.010	0.990 0.990 0.990 0.980 0.990	S S S S S S S	A	0.070 0.070 0.070 0.070	0.031 0.031 0.031 0.031 0.031	748. 598. 756. 578. 694. 534.	756. 592. 741. 584. 694.	134. 134. 134. 134. 134.	0.182 0.145 0.184 0.182 0.169 0.130	
3B-1A-2-13H 3B-1A-2-14H 3B-1A-2-15H 3B-1A-2-16H 3B-1A-2-17H 3B-1A-2-18H	550. 550. 550. 550.	1.000 1.010 1.010 1.020 1.020 1.020	0.990 0.990 0.990 0.990 0.990	s s s s s s s	A A A A A A A A A A A A A A A A A A A	0.070 0.070 0.070 0.070	0.031 0.031 0.031 0.031 0.031	1374. 566. 1160. 884. 1320. 1384.	1388. 566. 1160. 875. 1307.	134. 134. 134. 134. 134.	0 334 0.138 0.282 0.213 0.321 0.337	•

TABLE B-1 CONTINUED
(B) US CUSTOMARY UNITS

SPECIMEN NUMBER	TEMPERATURE (F)	LAP LENGTH (IN)	LAP WIDTH (IN)	CONFIG CODE*			ADHE THICKN (1		FAILURE LOAD (LBS)	AVERAGE JOINT STRESS	FTU	JOINT EFFICIENCY
					•		-	2		(PSI)	(KSI)	
3B-1B-2-1C 3B-1B-2-2C	-250. -250.	2.030	0.990		Ą	Ţ	0.070	0.031	662.	329.	134.	0.161
3B-1B-2-3C	-250.	2.010	0.990	S S	Ą	Ţ	0.070	0.031	800.	404.	134.	0.195
3B-1B-2-4C	-250.	2.000	0.990	3 S	A A	T	0.070	0.031	874. 840.	439. 424.	134.	0.213
3B-1B-2-5C	-250.	2.020	0.990	Š	Â	τ̈́	0.070	0.031	604.	302.	134. 134.	0.204 0.147
3B-1B-2-6C	-250.	2.010	0.990	Š	Ä	Ť	0.070	0.031	814.	409.	134.	0.198
3B-1B-2-7A	70.	2.010	0.990	S	A	T	0.070	0.031	1280.	643.	134.	0.311
3B-1B-2-8A	70.	2.010	0.980	\$	A	Ť	0.070	0.031	1120.	569.	134.	0.275
3B-1B-2-9A	70.	2.000	0.980	S	A	T	0.070	0.031	1144.	584.	134.	0.281
3B-1B-2-10/ 3B-1B-2-11/		2.030	0.990	Ş	Ă	Ţ	0.070	0.031	916.	456.	134.	0.223
3B-1B-2-12		2.020	0.980	Ş	À	Ţ	0.070	0.031	1052.	531.	134.	0.258
		2.010	0.990	S	A	T	0.070	0.031	1022.	514.	134.	0.249
3B-1B-2-13		2.020	0.990	S	A	T	0.070	0.031	1544.	772.	134.	0.375
3B-1B-2-141		2.010	0.990	Ş	Ą	T	0.070	0.031	1536.	772.	134.	0.373
3B-1B-2-151 3B-1B-2-161		2.010	0.990	S	A	T	0.070	0.031	1654.	831.	134.	0.402
3B-1B-2-17	H 550.	2.020	0.990	S	Ă	Ţ	0.070	0.031	1672.	836.	134.	0.407
3B-1B-2-18	H 550. H 550.	2.010	0.990	S S	Ą	Ţ	0.070	0.031	1520.	764.	134.	0.370
	ii 330.	2.000	0.990	3	A	T	0.070	0.031	1494.	755.	134.	0.363
3B-1C-2-1C	-250.	3.040	0.990	S	A	T	0.070	0.031	600.	199.	134.	0.146
3B-1C-2-2C	-250.	3.010	0.990	S	Α	T	0.070	0.031	572.	192.	134.	0.139
3B-1C-2-3C	-250.	3.000	0.990	S	A	T	0.070	0.031	698.	235.	134.	0.170
3B-1C-2-4C 3B-1C-2-5C	-250.	3.040	0.990	Ş	A	T	0.070	0.031	642.	213.	134.	0.156
3B-1C-2-6C	-250.	3.030	0.980	S	A	Ţ	0.070	0.031	630.	212.	134.	0.155
	-250.	3.040	0.990	S	Λ	T	0.070	0.031	564.	187.	134.	0.137
3B-1C-2-7A	70.	3.010	0.990	S	A	T	0.070	0.031	610.	205.	134.	0.148
3B-1C-2-8A	70.	3.020	0.990	S	A	Ť	0.070	0.031	886.	296.	134.	0.215
3B-1C-2-9A	70.	3.010	0.990	· \$	A	T	0.070	0.031	940.	315.	134.	0.229
3B-1C-2-10/		3.050	0.990	Ş	Ą	T	0.070	0.031	914.	303.	134.	0.222
3B-1C-2-11/ 3B-1C-2-12/	A 70.	3.010	0.990	S	À	Ţ	0.070	0.031	750.	252.	134.	0.182
• •		3.050	0.990	S	A	T	0.070	0.031	538.	178.	134.	0.131
3B-1C-2-131 3B-1C-2-141		3.010	0.990	S	A	Ţ	0.070	0.031	1400.	470.	134.	0.340
3B-1C-2-15	H 550. H 550.	3.020	0.970	S	Ā	Ţ	0.070	0.031	1330.	454.	134.	0.330
3B-1C-2-16	1 550.	3.050 3.050	0.990	Ş	Ą	Ţ	0.070	0.031	1664.	551.	134.	0.405
3B-1C-2-17		3.000	0.930	\$ \$	A A	T	0.070	0.031	1524. 1260.	505.	134.	0.371
3B-1C-2-18		3.010	0.990	Š	Â	Ť	0.070	0.031	1778	429. 597	134.	0.310 0.432

TABLE B-1 CONCLUDED

### (B) US CUSTOMARY UNITS

SPECIMEN	TEMPENATURE	LAP LENGTH	LAP WIDTH	CONFIG CODE*			THICKN	REND ESSES N)	FAILURE LOAD	AVERAGE JOINT STRESS	FTU	JOIN1 EFFICIENCY
NUMBER	(F)	(10)	(IN)		1	2	1	2	(LBS)	(PSI)	(KSI)	
3C-1A-2-1A	70.	2.020	1.020	T	Н	Н	0.116	0.116	1470.	713.	76.	0.163
3C-1A-2-2A	70.	2.020	1.020	T	Н	Н	0.116	0.116	1186.	576.	76.	0.132
3C-1A-2-4A	70.	2.000	1.020	T	н	Н	0.116	0.116	1300.	637.	76.	0.145
3C-1A-2-5A	70.	2.010	1.020	T	Н	H	0.116	0.116	1722.	840.	76.	0.191
3C-1A-2-6A	70.	2.030	1.020	T	H	H	0.116	0.116	1394.	673.	76.	0.155
3C-1A-2-7A	70.	2.030	1.010	T	Н	Н	0.116	0.116	1316.	642.	76.	0.148

#### \* CONFIGURATION CODE

S = STANDARD T = TAPERED ADHEREND

### + LAYUP CODE

A = [0, +/-45, 90]3S	G = [0,+/-45,90]4S	M = [0(3), +/-45(3), 90(3)]25
B = [0, +/-45, 0(3)]2S	H = [0, +/-45, 90]5S	N = [+/-45, 0, 90]6S
C = [+/-45,0,90]35	J = [0, +/-45, 90]6S	P = [0, +/-45, 90]12S
D = [0(3), +/-45(3), 0(3)]S	K = [0, +45, 0(2), -45, 0]28	T = TITANIUM
$E = \{0, +/-45, 90125\}$	$L = \{0.+45.0(2)45.0(4)\}$	

TABLE B-2 DOUBLE LAP JOINT TEST RESULTS

SPECIMEN Number	TEMPERATURE (K)	LAP LENGTHS (MM) 1 2	LAP GAP WIDTH LENGTH (MM) (MM)	CONFIG CODE*	LAYUP CODE+ 1 2	ADHEREND THICKHESSES (MM) 1 2	FAILURE LOAD (KN)	AVERAGE JOINT STRESS (MPA)	FTU (MPA)	JOINT EFFICIENCY
3D-1A-2-1C 3D-1A-2-2C 3D-1A-2-3C 3D-1A-2-4C 3D-1A-2-5C 3D-1A-2-6C	116. 116. 116. 116.	20.6 21.3 20.8 20.8 20.6 21.1 21.1 20.8 22.1 19.6 19.8 22.1	25.52 1.27 25.44 1.27 25.48 1.27 25.51 1.27 25.36 1.27 25.54 1.27	\$ \$ \$ \$ \$ \$ \$ \$	E G G G G G	1.168 2.337 1.168 2.337 1.168 2.337 1.168 2.337 1.168 2.337 1.168 2.337	13.167 12.077 9.853 11.743 8.207 12.099	12.310 11.395 9.282 10.983 7.768 11.301	524. 524. 524. 524. 524.	0.421 0.388 0.316 0.376 0.264 0.387
3D-1A-2-7A 3D-1A-2-8A 3D-1A-2-9A 3D-1A-2-10A 3D-1A-2-11A 3D-1A-2-12A	294. 294. 294. 294.	22.4 19.3 20.3 20.8 19.3 21.8 20.8 20.3 20.6 21.3 20.6 20.8	25.54 1.27 25.48 1.27 25.45 1.27 25.44 1.27 25.43 1.27 25.48 1.27	S S S S S S		1.168 2.337 1.168 2.337 1.168 2.337 1.168 2.337 1.168 2.337 1.168 2.337	9.163 8.541 8.941 8.710 9.626 9.065	8.613 8.146 8.538 8.322 9.031 8.595	524. 524. 524. 524. 524. 524.	0.293 0.274 0.287 0.280 0.309 0.291
3D-1A-2-13H 3D-1A-2-14H 3D-1A-2-15H 3D-1A-2-16H 3D-1A-2-17H 3D-1A-2-18H	561. 561. 561. 561.	20.6 21.1 22.4 19.3 19.8 22.4 22.1 19.0 20.8 21.3 22.4 19.6	25.52 1.27 25.47 1.27 25.45 1.27 25.53 1.27 25.47 1.27 25.53 1.27	s s s s s s		1.168 2.337 1.168 2.337 1.168 2.337 1.168 2.337 1.168 2.337 1.168 2.337	11.210 10.053 8.674 14.368 10.453 12.900	10.544 9.477 8.082 13.679 9.733 12.058	524. 524. 524. 524. 524. 524.	0.359 0.322 0.278 0.460 0.335 0.413
3D-1B-2-1C 3D-1B-2-2C 3D-1B-2-3C 3D-1B-2-4C 3D-1B-2-5C 3D-1B-2-6C	116. 116. 116. 116.	32.8 33.0 33.3 33.0 32.5 33.3 33.0 32.8 32.5 34.0 32.5 33.8	25.41 1.27 25.28 1.27 25.37 1.27 25.48 1.27 25.42 1.27 25.46 1.27	S S S S S S		1.143 2.286 1.143 2.286 1.143 2.286 1.143 2.286 1.143 2.286 1.143 2.286	11.121 10.053 11.276 10.008 9.653 10.765	6.654 6.000 6.755 5.972 5.705 6.378	524. 524. 524. 524. 524.	0.365 0.332 0.371 0.328 0.317 0.353
3D-1B-2-7A 3D-1B-2-8A 3D-1B-2-9A 3D-1B-2-10A 3D-1B-2-11A 3D-1B-2-12A	294. 294. 294. 294.	32.5 33.8 32.5 33.8 33.0 33.0 32.0 33.8 33.3 33.0 33.0 33.0	25.52 1.52 25.36 1.27 25.48 1.27 25.50 1.27 25.37 1.27 25.36 1.02	S S S S S S		1.143 2.286 1.143 2.286 1.143 2.286 1.143 2.286 1.143 2.286 1.143 2.286	8.247 10.262 9.946 11.966 9.920 8.874	4.912 6.105 5.912 7.132 5.898 5.298	524. 524. 524. 524. 524.	0.270 0.338 0.326 0.392 0.326 0.292
3D-1B-2-13H 3D-1B-2-14H 3D-1B-2-15H 3D-1B-2-16H 3D-1B-2-17H 3D-1B-2-18H	561. 561. 561. 561.	33.0 33.3 34.3 32.5 32.0 34.3 32.3 34.0 34.3 32.5 32.3 34.3	25.39 1.27 25.46 1.27 25.51 1.27 25.39 1.27 25.53 1.02 25.50 1.27	S S S S S S		1.143 2.286 1.143 2.286 1.143 2.286 1.143 2.286 1.143 2.286 1.143 2.286	10.409 13.967 8.585 14.457 11.121	6.183 8.213 5.076 8.589 6.521 6.606	524. 524. 524. 524. 524. 524.	0.342 0.458 0.281 0.475 0.364 0.367

TABLE B-2 CONTINUED

SPECIMEN NUMBER	TEMPERATURE (K)	LAP LENGTHS (MM) 1 2	LAP GAP WIDTH LENGTH (MM) (MM)	CONFIG CODE:	LAYUP CODE+ 1 2	ADHEREND THICKNESSES (MM) 1 2	FAILURE LOAD (KN)		FTU MPA)	JOINT EFFICIENCY
3D-1C-2-1C 3D-1C-2-2C 3D-1C-2-3C 3D-1C-2-4C 3D-1C-2-5C 3D-1C-2-6C	116. 4 116. 4 116. 4	16.0 45.5 15.5 45.7 15.5 46.0 15.5 46.0 15.5 46.0	25.50 1.27 25.44 1.27 25.42 1.27 25.28 1.27 25.41 1.27 25.32 1.27	s s s s s s s		1.156 2.311 1.156 2.311 1.156 2.311 1.156 2.311 1.156 2.311 1.156 2.311	9.541 9.208 7.317 7.851 12.366 8.496	4.092 3.969 3.148 3.406 5.323 3.670	524. 524. 524. 524. 524. 524.	0.309 0.299 0.238 0.256 0.402 0.277
3D-1C-2-7A 3D-1C-2-8A 3D-1C-2-9A 3D-1C-2-10A 3D-1C-2-11A 3D-1C-2-12A	294. 4 294. 4 294. 4	45.5 46.0 45.5 46.0 45.5 46.0 45.7 46.0 45.5 46.0 45.2 46.0	25.47 1.27 25.48 1.27 25.35 1.27 25.37 1.27 25.37 1.27 25.54 1.27	s s s s		1.156 2.311 1.156 2.311 1.156 2.311 1.156 2.311 1.156 2.311 1.156 2.311	11.521 7.406 9.452 9.275 8.474 7.473	4.947 3.179 4.078 3.968 3.653 3.209	524. 524. 524. 524. 524.	0.373 0.240 0.308 0.300 0.276 0.242
3D-1C-2-13H 3D-1C-2-14H 3D-1C-2-15H 3D-1C-2-16H 3D-1C-2-17H 3D-1C-2-18H	1 561. 4 1 561. 4 1 561. 4 1 561.	45.2 46.0 45.5 46.0 45.5 45.7 45.7 45.7 46.0 45.2 45.5 46.0	25.33 1.27 25.48 1.27 25.42 1.27 25.49 1.27 25.38 1.27 25.38 1.27	S S S S S S		1.156 2.311 1.156 2.311 1.156 2.311 1.156 2.311 1.156 2.311 1.156 2.311	7.562 10.342 15.813 9.897 7.540 8.585	3.274 4.439 6.823 4.247 3.257 3.699	524. 524. 524. 524. 524. 524.	0.246 0.335 0.514 0.321 0.245 0.279
3D-2A-2-1C 3D-2A-2-2C 3D-2A-2-3C 3D-2A-2-4C 3D-2A-2-5C 3D-2A-2-6C	116. 2 116. 2 116. 2	21.6 20.3 20.8 20.3 20.8 20.1 20.1 21.1 21.3 20.1 20.1 20.8	25.70 1.27 25.66 1.27 25.60 1.27 25.62 1.27 25.73 1.27 25.60 1.27	S S S S S S	A J A J A J A J A J	1.664 3.327 1.664 3.327 1.664 3.327 1.664 3.327 1.664 3.327 1.664 3.327	8.340 8.229 16.970 9.163 8.741 7.807	7.743 7.793 16.211 8.691 8.204 7.458	524. 524. 524. 524. 524. 524.	0.186 0.184 0.380 0.205 0.195 0.175
3D-2A-2-7A 3D-2A-2-8A 3D-2A-2-9A 3D-2A-2-10A 3D-2A-2-11A 3D-2A-2-12A	294. 2 294. 2 294. 2 4 294. 2	20.1 21.3 20.3 20.1 21.1 20.1 20.1 20.6 20.3 20.1 20.1 20.8	25.61 1.27 25.39 1.27 25.65 1.27 25.65 1.27 25.67 1.27 25.65 1.27	\$ \$ \$ \$ \$	A J A J A J A J A J	1.664 3.327 1.664 3.327 1.664 3.327 1.664 3.327 1.664 3.327 1.664 3.327	8.563 8.007 12.655 8.674 9.364 16.080	8.076 7.807 12.018 8.321 9.033 15.332	524. 524. 524. 524. 524.	0.192 0.181 0.284 0.194 0.209 0.360
3D-2A-2-13H 3D-2A-2-14H 3D-2A-2-16H 3D-2A-2-17H 3D-2A-2-18H	561. 2 561. 2 561. 2	20.3 20.1 20.3 19.8 20.3 21.1 20.1 20.8 20.1 20.8	25.52 1.27 25.46 1.27 25.53 1.27 25.54 1.27 25.62 1.27	s s s s s s	A J A J A J A J	1.664 3.327 1.664 3.327 1.664 3.327 1.664 3.327 1.664 3.327	10.974 10.253 13.474 19.194 10.653	10.647 10.033 12.749 18.378 10.167	524. 524. 524. 524. 524.	0.247 0.231 0.303 0.431 0.238

TABLE B-2 CONTINUED

SPECIMEN NUMBER			LAP GAP WIDTH LENGT! (MM) (MM)	CONFIG CODE*	LAYUP CODE+ 1 2	ADHEREND THICKNESSES (MM) 1 2	FAILURE LOAD (KH)	AVERAGE JOINT STRESS (MPA)	FTU (MPA)	JOINT EFFICIENCY
3D-2B-2-1C 3D-2B-2-2C 3D-2B-2-3C 3D-2B-2-4C 3D-2B-2-5C 3D-2B-2-5C	116. 34. 116. 34. 116. 34. 116. 33. 116. 34. 116. 33.	0. 33.8 0 33.8 5 34.3 0 33.5	25.51 0.76 25.50 0.76 25.52 0.76 25.43 0.51 25.48 0.76 25.53 0.76	\$ \$ \$ \$ \$ \$	A J A J A J A J A J	1.943 3.886 1.943 3.886 1.943 3.886 1.943 3.886 1.943 3.886	16.547 16.903 14.056 16.325 16.970	9.565 9.776 8.123 9.468 9.858 9.428	524. 524. 524. 524. 524. 524.	0.319 0.326 0.271 0.315 0.327 0.314
3D-2B-2-7A 3D-2B-2-8A 3D-2B-2-9A 3D-2B-2-10A 3D-2B-2-11A 3D-2B-2-12A	294. 34.	3 33.8 5 34.3 0 33.5 0 34.0	25.59 0.76 25.45 0.76 25.54 0.76 25.50 0.76 25.54 0.76 25.36 0.76	\$ \$ \$ \$ \$ \$ \$	A J A J A J A J A J	1.943 3.886 1.943 3.886 1.943 3.886 1.943 3.886 1.943 3.886 1.943 3.886	14.768 13.745 15.524 15.769 15.035 14.479	8.511 7.934 8.961 9.153 8.648 8.420	524. 524. 524. 524. 524. 524.	0.203 0.265 0.298 0.304 0.289 0.280
3D-2B-2-13H 3D-2B-2-14H 3D-2B-2-15H 3D-2B-2-16H 3D-2B-2-17H 3D-2B-2-18H	561. 34. 561. 34. 561. 34. 561. 33.	0 33.8 3 33.8 0 33.5 8 34.0	25.57	\$ \$ \$ \$ \$ \$	A J A J A J A J A J	1.943 3.886 1.943 3.886 1.943 3.886 1.943 3.886 1.943 3.886	11.165 16.725 13.789 14.590 12.366 15.435	6.391 9.679 7.951 8.503 7.200 8.923	524. 524. 524. 524. 524. 524.	0.214 0.322 0.266 0.282 0.240 0.297
3D-2C-2-1C 3D-2C-2-2C 3D-2C-2-3C 3D-2C-2-4C 3D-2C-2-5C 3D-2C-2-6C	116. 46. 116. 46. 116. 46. 116. 46. 116. 46. 116. 46.	0 45.7 0 46.5 2 45.7 2 46.0	25.50 2.29 25.45 2.54 25.40 2.54 25.45 2.29 25.48 2.54 25.35 2.54	s s s s s	A J A J A J A J A J	1.727 3.454 1.727 3.454 1.727 3.454 1.727 3.454 1.727 3.454 1.727 3.454	16.280 12.544 10.142 15.524 18.727 17.659	6.943 5.375 4.319 6.634 7.972 7.577	524. 524. 524. 524. 524.	0.353 0.272 0.221 0.337 0.406 0.385
3D-2C-2-7A 3D-2C-2-8A 3D-2C-2-9A 3D-2C-2-10A 3D-2C-2-11A 3D-2C-2-12A	294. 46.	2 46.0 2 46.0 0 46.0 0 46.2	25.45 2.54 25.45 2.54 25.43 2.54 25.43 2.54 25.37 2.54 25.43 2.54	5 5 5 5 5	A J A J A J A J	1.727 3.454 1.727 3.454 1.727 3.454 1.727 3.454 1.727 3.454 1.727 3.454	17.748 19.439 13.434 13.345 18.594 11.254	7.563 8.284 5.730 5.708 7.947 4.827	524. 524. 524. 524. 524. 524.	0.385 0.422 0.292 0.290 0.405 0.245
3D-2C-2-13H 3D-2C-2-14H 3D-2C-2-15H 3D-2C-2-16H 3D-2C-2-17H 3D-2C-2-18H	561. 46. 561. 46. 561. 46. 561. 46.	2 46.0 2 45.7 0 46.0 2 45.7	25.43 2.54 25.50 2.54 25.45 2.54 25.40 2.54 25.43 2.54 25.43 2.54	s s s s s s s	A J A J A J A J A J	1.727 3.454 1.727 3.454 1.727 3.454 1.727 3.454 1.727 3.454 1.727 3.454	18.238 13.434 20.195 16.725 19.795 17.615	7.700 5.713 8.630 7.161 8.467 7.507	524. 524. 524. 524. 524. 521.	0.396 0.291 0.438 0.364 0.430 0.382

TABLE B-2 CONTINUED

SPECIMEN NUMBER	TEMPERATURE (K)	LAP LENGTHS (MM) 1 2	LAP G/ WIDTH LEI (MM) (R		LAYUP CODE+ 1 2	ADHEREND THICKNESSES (MM) 1 2	FAILURE LOAD (KN)	AVERAGE JOINT STRESS (MPA)	FTU (MPA)	JOINT EFFICIENCY	
3D-3A-2-1C 3D-3A-2-2C 3D-3A-2-3C 3D-3A-2-4C 3D-3A-2-5C 3D-3A-2-6C	116. 116. 116. 116.	33.3 33.8 33.3 33.3 33.5 33.8 34.0 33.3 34.0 33.3	25.43 2 25.50 2 25.41 2 25.46 2	03 S 29 S 03 S 03 S 03 S	K L L K L L K L	1.676 3.353 1.676 3.353 1.676 3.353 1.676 3.353 1.676 3.353 1.676 3.353	16.303 16.258 17.170 14.679 14.234 17.393	9.549 9.606 10.005 8.582 8.306 10.124	972. 972. 972. 972. 972. 972.	0.196 0.196 0.207 0.177 0.172 0.209	-
3D-3A-2-7A 3D-3A-2-8A 3D-3A-2-9A 3D-3A-2-10A 3D-3A-2-11A 3D-3A-2-12A	294. 294. 294. 294.	34.0 33.3 34.0 33.3 34.0 33.3 34.0 33.3 34.0 33.3 34.0 33.3	25.36 2 25.33 2 25.47 2 25.53 2	.03 S .03 S .03 S .03 S .03 S	K L K L K L K L	1.676 3.353 1.676 3.353 1.676 3.353 1.676 3.353 1.676 3.353 1.676 3.353	17.615 16.280 15.346 15.902 16.280 16.592	10.288 9.537 9.000 9.275 9.473 9.709	972. 972. 972. 972. 972. 972.	0.212 0.197 0.186 0.192 0.196 0.200	
3D-3A-2-13H 3D-3A-2-14H 3D-3A-2-15H 3D-3A-2-17H 3D-3A-2-18H 3D-3A-2-19H	561. 561. 561. 561.	33.5 33.5 34.0 33.3 34.0 33.3 33.8 33.3 34.0 33.3	25.52 2 25.25 2 25.51 2 25.48 2	29 S 03 S 03 S 29 S 03 S	K L L K L L K L	1.676 3.353 1.676 3.353 1.676 3.353 1.676 3.353 1.676 3.353 1.676 3.353	24.243 23.175 28.380 22.819 23.042 26.200	14.164 13.491 16.700 13.338 13.437 15.277	972. 972. 972. 972. 972. 972.	0.291 0.279 0.345 0.274 0.277 0.315	
3D-4A-2-1C 3D-4A-2-2C 3D-4A-2-3C 3D-4A-2-4C 3D-4A-2-5C 3D-4A-2-6C	116. 116. 116.	33.5 33.3 34.0 33.3 33.0 34.0 33.8 33.0 33.5 33.3 33.5 33.5	25.46 2. 25.52 2. 25.45 2. 25.56 2.	.79 S .03 S .29 S .29 S .54 S .29 S	D M D M D M D M	1.587 3.175 1.587 3.175 1.587 3.175 1.587 3.175 1.587 3.175 1.587 3.175	12.811 10.409 10.720 10.765 11.321 11.632	7.506 6.074 6.265 6.332 6.631 6.823	524. 524. 524. 524. 524. 524.	0.301 0.246 0.252 0.254 0.266 0.275	
3D-4A-2-7A 3D-4A-2-8A 3D-4A-2-9A 3D-4A-2-10A 3D-4A-2-11A 3D-4A-2-12A	294. 294. 294. 294.	33.5 34.0 32.8 34.3 34.3 33.0 33.5 33.5 33.8 33.0 33.8 33.5	25.55 2 25.26 2 25.50 2 25.55 2	29 S 03 S 29 S 29 S 29 S	D M D M D M D M D M	1.587 3.175 1.587 3.175 1.587 3.175 1.587 3.175 1.587 3.175 1.587 3.175	12.455 16.169 13.523 12.499 13.967 9.497	7.214 9.439 7.953 7.310 8.183 5.570	524. 524. 524. 524. 524.	0.293 0.380 0.322 0.205 0.329 0.225	
3D-4A-2-13H 3D-4A-2-14H 3D-4A-2-15H 3D-4A-2-16H 3D-4A-2-17H 3D-4A-2-18H	561. 561. 561. 561.	33.5 33.5 33.5 33.8 32.8 34.0 33.0 33.5 33.5 33.8 33.3 33.5	25.21 2. 25.47 2. 25.50 2. 25.34 2.	29 S 29 S 29 S 03 S 29 S 54 S	D M D M D M D M D M D M	1.587 3.175 1.587 3.175 1.587 3.175 1.587 3.175 1.587 3.175 1.587 3.175	14.145 15.524 13.656 22.241 15.836 15.524	8.272 9.148 8.027 13.106 9.286 9.117	524. 524. 524. 524. 524.	0.333 0.370 0.322 0.524 0.376 0.366	

TABLE B-2 CONTINUED

SPECIMEN NUMBER	TEMPERATURE (K)	LAP LENGTHS (MM) 1 2		P CONFIG GTH CODE*		ADHEREND THICKNESSES (MM) 1 2	FAILURE LOAD (KN)	AVERAGE JOINT STRESS (MPA)	FTU (MPA)	JOINT EFFICIENCY
3D-5A-2-1C 3D-5A-2-2C 3D-5A-2-3C 3D-5A-2-4C 3D-5A-2-5C 3D-5A-2-6C	116. 32 116. 32 116. 33 116. 32 116. 32 116. 33	.3 33.5 .0 32.5 .5 34.0 .5 33.5	25.57 3. 25.30 3. 25.34 3. 25.55 3.	30 S 30 S 30 S 68 S 30 S	C N C N C N C N C N	1.841 3.683 1.841 3.683 1.841 3.683 1.841 3.683 1.841 3.683 1.841 3.683	15.346 15.391 17.170 15.969 16.681 16.014	9.112 9.151 10.357 9.471 9.885 9.430	524. 524. 524. 524. 524.	0.312 0.312 0.352 0.327 0.328 0.325
3D-5A-2-7A 3D-5A-2-8A 3D-5A-2-9A 3D-5A-2-10A 3D-5A-2-11A 3D-5A-2-12A	294. 33	.0 32.8 .5 33.8 .8 33.5 .8 32.5	25.44 3. 25.53 3. 25.50 3. 25.60 3.	68 S 30 S 30 S 30 S 68 S 68 S	C N C N C N C N C N	1.841 3.683 1.841 3.683 1.841 3.683 1.841 3.683 1.841 3.683 1.841 3.683	13.567 13.612 15.213 17.615 14.902 14.412	8.030 8.134 8.988 10.420 8.779 8.547	524. 524. 524. 524. 524. 524.	0.275 0.277 0.309 0.358 0.302 0.292
3D-5A-2-13H 3D-5A-2-14H 3D-5A-2-15H 3D-5A-2-16H 3D-5A-2-17H 3D-5A-2-16H	561. 32 561. 32 561. 32 561. 33	.8 33.0 .8 33.3 .8 33.5 .5 32.5	25.53 3. 25.56 3. 25.54 3. 25.52 3.	30 S 30 S 30 S 68 S 30 S 68 S	C N C N C N C N C N C	1.841 3.683 1.841 3.683 1.841 3.683 1.841 3.683 1.841 3.683 1.841 3.683	21.574 22.241 20.239 21.663 20.818 18.949	12.756 13.243 11.990 12.793 12.351 11.224	524. 524. 524. 524. 524. 524.	0.436 0.451 0.410 0.439 0.423 0.384
3D-6A-2-1C 3D-6A-2-2C 3D-6A-2-3C 3D-6A-2-4C 3D-6A-2-5C 3D-6A-2-7C	116. 33 116. 33 116. 33 116. 33 116. 33	.5 33.5 .3 33.3 .5 33.3 .3 33.8	25.47 2. 25.57 2. 25.56 2. 25.54 2.	31 S 31 S 31 S 31 S 31 S	A G A G A G A G A G	1.727 2.311 1.727 2.311 1.727 2.311 1.727 2.311 1.727 2.311 1.727 2.311	11.632 7.340 7.784 10.453 12.121 8.118	6.787 4.297 4.575 6.122 7.078 4.755	524. 524. 524. 524. 524.	0.377 0.238 0.251 0.338 0.392 0.263
3D-6A-2-8A 3D-6A-2-9A 3D-6A-2-10A 3D-6A-2-11A 3D-6A-2-12A 3D-6A-2-13A	294. 33 294. 34	.8 33.3 .8 33.5 .3 33.8 .0 33.0	25.51 2 25.41 2 25.48 2 25.52 2	31 S 31 S 31 S 29 S 29 S	A G A G A G A G	1.727 2.311 1.727 2.311 1.727 2.311 1.727 2.311 1.727 2.311 1.727 2.311	7.406 8.741 7.295 7.718 11.054 10.186	4.326 5.109 4.266 4.517 6.458 5.960	524. 524. 524. 524. 524. 524.	0.240 0.293 0.237 0.250 0.358 0.330
3D-6A-14H 3D-6A-15H 3D-6A-16H 3D-6A-17H 3D-6A-18H 3D-6A-19H	561. 33 561. 33 561. 33 561. 33 561. 33	.5 33.5 .5 33.8 .5 33.3 .3 33.5	25.55 2. 25.32 2. 25.42 2. 25.37 2.	31 S 31 S 31 S 31 S 31 S 03 S	A G A G A G A G A G	1.727 2.311 1.727 2.311 1.727 2.311 1.727 2.311 1.727 2.311 1.727 2.311	12.055 8.674 8.674 11.476 10.498 7.562	7.035 5.062 5.090 6.758 6.193 4.440	524. 524. 524. 524. 524. 524.	0.300 0.280 0.203 0.373 0.342 0.246

TABLE B-2 CONTINUED

SPECIMEN NUMBER	TEMPERATURE (K)	LAP LENGTHS (MM) 1 2	LAP GAP WIDTH LENGTH (MM) (MM)	CONFIG CODE*	LAYUP CODE+ 1 2	ADHEREND THICKNESSES (MM) 1 2	FAILURE LOAD (KN)	AVERAGE JOINT STRESS (MPA)	FTU (MPA)	JOINT EFFICIENCY
3D-7A-2-1A 3D-7A-2-2A 3D-7A-2-3A 3D-7A-2-4A 3D-7A-2-5A 3D-7A-2-6A	294. 34 294. 35 294. 35 294. 35	4.0 33.3 4.0 33.8 3.3 34.0 3.3 34.0 3.3 34.0 4.0 33.5	25.40 5.33 25.38 5.33 25.46 5.33 25.47 5.59 25.48 5.33 25.49 5.33	\$ 5 5 5 5 5 5 5 5 5 5 5 5 5 5 5 5 5 5 5	J P J P J P J P	3.302 6.629 3.302 6.629 3.302 6.629 3.302 6.629 3.302 6.629 3.302 6.629	18.972 16.414 16.325 9.341 17.659 15.480	11.097 9.536 9.527 5.449 10.298 8.987	524. 524. 524. 524. 524.	0.215 0.186 0.185 0.106 0.200 0.175
3D-7A-2-7H 3D-7A-2-8H 3D-7A-2-9H 3D-7A-2-10I 3D-7A-2-11E 3D-7A-2-12E	561. 3: 561. 3: H 561. 3: H 561. 3:	3.5 33.8 3.8 33.5 3.3 34.0 3.5 34.0 3.5 33.8 3.8 34.0	25.48 5.33 25.51 5.59 25.53 5.33 25.53 5.33 25.46 5.33 25.54 5.08	S S S S S S	J P J P J P J P	3.302 6.629 3.302 6.629 3.302 6.629 3.302 6.629 3.302 6.629 3.302 6.629	18.282 14.368 19.661 17.526 17.259 19.261	10.661 8.368 11.443 10.162 10.070 11.121	524. 524. 524. 524. 524.	0.207 0.162 0.222 0.198 0.195 0.217
3F-1A-2-1A 3F-1A-2-2A 3F-1A-2-3A 3F-1A-2-4A 3F-1A-2-5A 3F-1A-2-6A	294. 3: 294. 3: 294. 3: 294. 3:	4.0 33.5 5.3 32.8 3.0 35.3 4.0 32.8 5.1 33.0 5.1 32.8	25.41 4.57 25.50 4.06 25.41 4.06 25.47 4.83 25.45 4.32 25.53 4.06	T T T T	J P J P J P J P	3.327 6.655 3.327 6.655 3.327 6.655 3.327 6.655 3.327 6.655 3.327 6.655	17.793 19.038 21.574 21.974 18.594 16.280	10.365 10.966 12.427 12.913 10.733 9.403	524. 524. 524. 524. 524. 524.	0.201 0.214 0.243 0.247 0.210 0.183
3F-1A-2-7H 3F-1A-2-8H 3F-1A-2-9H 3F-1A-2-10H 3F-1A-2-11H 3F-1A-2-12H	561. 34 561. 34 1 561. 34 1 561. 35	5.1 34.0 4.5 33.0 4.8 33.5 4.5 33.3 5.1 33.0 3.0 35.1	25.51 4.06 25.48 4.06 25.46 4.06 25.51 4.32 25.49 4.06 25.47 4.57	T T T T	J P J P J P P J P	3.327 6.655 3.327 6.655 3.327 6.655 3.327 6.655 3.327 6.655 3.327 6.655	19.261 18.949 18.238 19.216 18.905 19.528	10.928 11.007 10.484 11.106 10.897 11.261	\$24. 524. 524. 524. 524.	0.217 0.213 0.205 0.216 0.213 0.220
3E-1A-2-1C 3E-1A-2-2C 3E-1A-2-3C 3E-1A-2-4C 3E-1A-2-5C 3E-1A-2-6C	116. 20 116. 20 116. 20 116. 20	0.1 20.3 0.3 19.0 0.3 19.6 0.3 20.8 0.3 20.3 0.3 20.3	25.15 3.30 25.15 4.32 25.40 3.81 24.38 2.29 25.15 2.79 25.15 2.54	\$ \$ \$ \$ \$ \$ \$ \$	A T A T A T A T	1.524 1.600 1.524 1.600 1.524 1.600 1.524 1.600 1.524 1.600 1.524 1.600	14.056 13.300 12.811 11.032 11.121 11.877	13.841 13.435 12.648 10.995 10.882 11.622	924. 924. 924. 924. 924.	0.378 0.358 0.341 0.306 0.299 0.319
3E-1A-2-7A 3E-1A-2-8A 3E-1A-2-9A 3E-1A-2-10/ 3E-1A-2-11/ 3E-1A-2-12/	294. 20 294. 20 294. 20 4 294. 20	0.3 19.6 0.3 20.1 0.1 20.1 0.1 20.1 0.3 20.3 0.3 20.1	25.15 3.56 25.40 3.05 25.40 3.56 25.40 3.81 25.15 3.81 25.40 3.81	s s s s	A T A T A T A T A T	1.524 1.600 1.524 1.600 1.524 1.600 1.524 1.600 1.524 1.600 1.524 1.600	18.949 18.594 18.149 17.526 18.683 17.526	18.897 18.126 17.804 17.193 18.282 17.085	924. 924. 924. 924. 924.	0.510 0.495 0.483 0.467 0.503 0.467

TABLE B-2 CONTINUED

SPECIMEN NUMBER	TEMPERATURE (K)	LAP LENGTHS (MM) 1 2	LAP GAP WIDTH LENGTH (MM) (MM)	CONFIG CODE*	LAYUP CODE+ 1 2	ADHEREND THICKNESSES (MM) 1 2	FAILURE LOAD (KN)	AVERAGE JOINT STRESS (MPA)	FTU (AIPA)	JOINT EFFICIENCY
3E-1A-2-13H 3E-1A-2-14H 3E-1A-2-15H 3E-1A-2-16H 3E-1A-2-17H 3E-1A-2-18H	561. 561. 561. 561.	20.1 20.1 20.6 20.3 20.1 19.8 19.8 20.6 20.6 20.1 20.3 20.3	25.15 3.81 25.15 2.79 25.40 3.81 24.89 2.79 25.15 3.81 24.89 3.05	S S S S S S	A T A T A T A T A T	1.524 1.600 1.524 1.600 1.524 1.600 1.524 1.600 1.524 1.600 1.524 1.600	18.104 17.926 18.282 16.770 17.215 16.814	17.940 17.433 18.049 16.682 16.845 16.621	924. 924. 924. 924. 924.	0.487 0.482 0.487 0.456 0.463 0.457
3E-2A-2-1C 3E-2A-2-2C 3E-2A-2-3C 3E-2A-2-4C 3E-2A-2-5C 3E-2A-2-6C	116. 116. 116. 116.	45.7 45.5 45.5 45.5 45.5 45.5 45.7 45.7 45.7 45.7 45.7 45.7	25.15 3.05 25.40 3.56 24.89 2.79 25.65 2.79 25.65 2.54 25.15 3.05	S S S S S S S S	C T C T C T C T C T C T	1.524 1.600 1.524 1.600 1.524 1.600 1.524 1.600 1.524 1.600 1.524 1.600	14.501 17.348 16.103 14.234 17.437 16.859	6.324 7.511 7.114 6.068 7.433 7.352	924. 924. 924. 924. 924. 924.	0.390 0.462 0.438 0.375 0.460 0.453
3E-2A-2-7A 3E-2A-2-8A 3E-2A-2-9A 3E-2A-2-10A 3E-2A-2-11A 3E-2A-2-12A	294. 294. 294. 294.	45.7 45.5 45.5 45.5 45.2 45.5 45.7 45.5 46.0 45.5 45.2 45.7	25.40 3.05 25.40 3.56 25.40 2.79 25.15 3.05 25.40 3.30 25.15 2.79	\$ \$ \$ \$ \$ \$ \$ \$ \$ \$	C T C T C T C T C T C T	1.524 1.600 1.524 1.600 1.524 1.600 1.524 1.600 1.524 1.600 1.524 1.600	16.814 15.391 18.460 16.636 19.661 15.257	7.260 6.664 8.015 7.255 8.465 6.673	924. 924. 924. 924. 924. 924.	0.448 0.410 0.492 0.447 0.524
3E-2A-2-13H 3E-2A-2-14H 3E-2A-2-15H 3E-2A-2-16H 3E-2A-2-17H 3E-2A-2-18H	561. 561. 561. 561.	46.0 45.7 45.7 45.2 45.7 45.2 45.5 45.7 45.7 45.5 45.5 45.5	25.15 2.29 25.65 3.05 25.40 2.79 25.65 2.79 25.40 2.54 25.40 3.05	s s s s s s s	C T C T C T C T C T	1.524 1.600 1.524 1.600 1.524 1.600 1.524 1.600 1.524 1.600 1.524 1.600	24.688 25.844 23.398 22.997 23.398 7.429	10.707 11.079 10.130 9.831 10.102 3.216	924. 924. 924. 924. 924.	0.664 0.681 0.623 0.606 0.623 0.198
3E-1B-2-1C 3E-1B-2-2C 3E-1B-2-3C 3E-1B-2-4C 3E-1B-2-5C 3E-1B-2-6C	116. 4 116. 4 116. 4	45.5 45.5 45.2 45.5 45.5 45.5 45.7 45.2 45.5 45.7 46.0 45.2	24.89 2.79 25.15 3.30 25.15 2.79 25.40 2.54 25.15 3.05 25.15 2.54	555555	A T A T A T A T A T	1.524 1.600 1.524 1.600 1.524 1.600 1.524 1.600 1.524 1.600 1.524 1.600	9.074 11.699 7.651 7.206 9.203 8.274	4.009 5.131 3.346 3.120 4.016 3.608	924. 924. 924. 924. 924.	0.247 0.315 0.206 0.192 0.248 0.223
3E-1B-2-7A 3E-1B-2-8A 3E-1B-2-9A 3E-1B-2-1OA 3E-1B-2-11A 3E-1B-2-12A	294. 4 294. 4 294. 4	45.0 45.7 45.5 45.0 46.0 45.7 45.0 45.5 45.5 45.5 45.7 45.2	25.40 3.05 25.15 3.05 24.89 1.78 25.65 3.05 25.40 2.79 25.65 2.79	\$ \$ \$ \$ \$ \$ \$ \$ \$	Α Τ Α Τ Α Τ Α Τ Λ Τ	1.524 1.600 1.524 1.600 1.524 1.600 1.524 1.600 1.524 1.600 1.524 1.600	18.594 13.389 12.989 14.457 15.124 11.521	8.073 5.888 5.691 6.232 6.548 4.939	924. 924. 924. 924. 924. 924.	0.495 0.360 0.353 0.381 0.403 0.304

TABLE B-2 CONTINUED

SPECIMEN	TEMPERATURE	LAP Lengths (MM)	LAP WIDTH	GAP . LENGTH	CONFIG CODE*		YUP DE+	THICKN	REND ESSES M)	FAILURE LOAD	AVERAGE JOINT STRESS	FTU	JOINT EFFICIENCY
NUMBER	-(K)	1 2	(MM)	(MA)		1	2	1	2	(KN)	(APA)	(MPA)	
3E-1B-2-13H	561.	45.5 45.7	25.65	2.54	s	A	T	1.524	1.600	23.576	10.078	924.	0.622
3E-1B-2-14H	4 561.	45.2 45.2	25,40	3.05	S	Α	T	1.524	1.600	23.665	10.303	924.	0.630
3E-1B-2-15H	561.	45.0 46.0	25.40	2.79	S	Α	T	1.524	1.600	22.375	9.687	924.	0.596
3E-1B-2-16H	561.	45.7 45.5	25.65	2.79	S	A	Т	1.524	1.600	23.620	10.097	924.	0.623
3E-1B-2-17H	561.	45.2 45.2	25.15	3.05	Š	Ā	Ť	1.524	1.600	21.440	9.429	924.	0.577
3E-1B-2-18H	561.	45.7 45.0	25.15	2.54	Š	A	Ť	1.524	1.600	24.821	10.886	924.	0.668

### \* CONFIGURATION CODE

S = STANDARD T = TAPERED ADHEREND

### + LAYUP CODE

A = [0, +/-45, 90]3S	G = [0,+/-45,90]4S	M = [0(3), +/-45(3), 90(3)]2S
B = [0, +/-45, 0(3)]2S	H = [0, +/-45, 90]5S	N = [+/-45,0,90]6S
C = [+/-45, 0, 90]3S	J = [0,+/-45,90]6S	P = [0, +/-45, 90]125
D = [0(3), +/-45(3), 0(3)]S	K = [0, +45, 0(2), -45, 0]25	T = TITANIUM
E = [0, +/-45, 90]25	L = [0, +45, 0(2), -45, 0]48	

TABLE B-2 CONTINUED

(B) US CUSTOMARY UNITS

SPECIMEN NUMBER	TEMPERATURE (F)	LAP LENGTHS (IN) 1 2	LAP WIDTH (IN)	GAP LENGTH (IN)	CONFIG CODE*		ADHEREND THICKNESSES (IN) 1 2	FAILURE LOAD (LBS)	AVERAGE JOINT STRESS (PSI)	FTU (K31)	JOINT EFFICIENCY
3D-1A-2-1C 3D-1A-2-2C 3D-1A-2-3C 3D-1A-2-4C 3D-1A-2-5C 3D-1A-2-6C	-250. 0 -250. 0 -250. 0	0.81 0.84 0.82 0.82 0.81 0.83 0.83 0.82 0.87 0.77 0.78 0.87	1.005 1.002 1.003 1.004 0.998 1.006	0.05 0.05 0.05 0.05 0.05	s s s s s s s	E G G G G G	0.046 0.092 0.046 0.092 0.046 0.092 0.046 0.092 0.046 0.092 0.046 0.092	2960. 2715. 2215. 2640. 1845. 2720.	1785. 1653. 1346. 1593. 1127. 1639.	76. 76. 76. 76. 76.	0.421 0.388 0.316 0.376 0.264 0.387
3D-1A-2-7A 3D-1A-2-8A 3D-1A-2-9A 3D-1A-2-10A 3D-1A-2-11A 3D-1A-2-12A	70. 0 70. 0 70. 0	0.88 0.76 0.80 0.82 0.76 0.86 0.82 0.80 0.81 0.84 0.81 0.82	1.005 1.003 1.002 1.001 1.001	0.05 0.05 0.05 0.05 0.05 0.05	5 5 5 5 5 5	E G G G G G G G	0.046 0.092 0.046 0.092 0.046 0.092 0.046 0.092 0.046 0.092 0.046 0.092	2060. 1920. 2010. 1958. 2164. 2038.	1249. 1182. 1238. 1207. 1310. 1247.	76. 76. 76. 76. 76.	
3D-1A-2-13H 3D-1A-2-14H 3D-1A-2-15H 3D-1A-2-16H 3D-1A-2-17H 3D-1A-2-18H	550. 0 550. 0 550. 0	0.81 0.83 0.88 0.76 0.78 0.88 0.87 0.75 0.82 0.84 0.88 0.77	1.005 1.003 1.002 1.005 1.003	0.05 0.05 0.05 0.05 0.05 0.05	s s s s s s	E G G G G G G G	0.046 0.092 0.046 0.092 0.046 0.092 0.046 0.092 0.046 0.092 0.046 0.092	2520. 2260. 1950. 3230. 2350. 2900.	1529. 1374. 1172. 1984. 1412. 1749.	76. 76. 76. 76. 76.	0.359 0.322 0.278 0.460 0.335 0.413
3D-1B-2-1C 3D-1B-2-2C 3D-1B-2-3C 3D-1B-2-4C 3D-1B-2-5C 3D-1B-2-6C	-250. 1 -250. 1 -250. 1	1.29 1.30 1.31 1.30 1.28 1.31 1.30 1.29 1.28 1.34 1.28 1.33	1.000 0.995 0.999 1.003 1.001	0.05 0.05 0.05 0.05 0.05	\$ \$ \$ \$ \$ \$ \$ \$ \$	E G G G G G G G	0.045 0.090 0.045 0.090 0.045 0.090 0.045 0.090 0.045 0.090 0.045 0.090	2260. 2535. 2250. 2170.	965. 870. 980. 866. 827. 925.	76. 76. 76. 76. 76.	0.365 0.332 0.371 0.328 0.317 0.353
3D-1B-2-7A 3D-1B-2-8A 3D-1B-2-9A 3D-1B-2-1OA 3D-1B-2-11A 3D-1B-2-12A	70. 1 70. 1 70. 1	1.28 1.31 1.28 1.33 1.30 1.30 1.26 1.33 1.31 1.30 1.30 1.30	1.005 0.998 1.003 1.004 0.999 0.999	0.06 0.05 0.05 0.05 0.05 0.05	55555	E G G G G G G G	0.045 0.090 0.045 0.090 0.045 0.090 0.045 0.090 0.045 0.090	2307. 2236. 2690. 2230.	712. 885. 857. 1034. 855. 768.	76. 76. 76. 76. 76.	0.270 0.338 0.326 0.392 0.326 0.292
3D-1B-2-13H 3D-1B-2-14H 3D-1B-2-15H 3D-1B-2-16H 3D-1B-2-17H 3D-1B-2-18H	550. 1 550. 1 550. 1 550. 1	1.30 1.31 1.35 1.28 1.26 1.35 1.27 1.34 1.35 1.28 1.27 1.35	1.000 1.002 1.005 1.000 1.005	0.05 0.05 0.05 0.05 0.04 0.05	s s s s s s	E G G G G G G	0.045 0.090 0.045 0.090 0.045 0.090 0.045 0.090 0.045 0.090 0.045 0.090	3140. 1930. 3250. 2500.	897. 1191. 736. 1246. 946. 958.	76. 76. 76. 76. 76.	0.342 0.458 0.281 0.475 0.364 0.367

TABLE B-2 CONTINUED
(B) US CUSTOMARY UNITS

SPECIMEN Number	TEMPERATURE (F)	LAP LENGTHS (IN) 1 2	LAP GAP WIDTH LENGTH (IN) (IN)	CONFIG CODE*		ADHEREND THICKNESSES (IN) 1 2	FAILURE LOAD (LBS)	AVERAGE JOINT STRESS (PSI)	FTU (KSI)	JOINT EFFICIENCY	
3D-1C-2-1C 3D-1C-2-2C 3D-1C-2-3C 3D-1C-2-4C 3D-1C-2-5C 3D-1C-2-6C	-250. -250. -250. -250.	1.81 1.79 1.79 1.80 1.79 1.81 1.79 1.80 1.79 1.81 1.79 1.81	1.004 0.05 1.002 0.05 1.001 0.05 0.995 0.05 1.000 0.05 0.997 0.05	\$ \$ \$ \$ \$	E G G G G	0.045 0.091 0.045 0.091 0.045 0.091 0.045 0.091 0.045 0.091 0.045 0.091	2145. 2070. 1645. 1765. 2780. 1910.	594. 576. 457. 494. 772. 532.	76. 76. 76. 76. 76.	0.309 0.299 0.238 0.256 0.402 0.277	
3D-1C-2-7A 3D-1C-2-8A 3D-1C-2-9A 3D-1C-2-10A 3D-1C-2-11A 3D-1C-2-12A	70. 70. 70. 70.	1.79 1.81 1.79 1.81 1.79 1.81 1.80 1.81 1.79 1.81 1.78 1.81	1.003 0.05 1.003 0.05 0.998 0.05 1.004 0.05 0.999 0.05 1.006 0.05	5 5 5 5 5 5 5 5 5 5 5 5 5 5 5 5 5 5 5		0.045 0.091 0.045 0.091 0.045 0.091 0.045 0.091 0.045 0.091 0.045 0.091	2590. 1665. 2125. 2085. 1905. 1680.	718. 461. 591. 575. 530. 465.	76. 76. 76. 76. 76.	0.373 0.240 0.308 0.300 0.276 0.242	
3D-1C-2-13H 3D-1C-2-14H 3D-1C-2-15H 3D-1C-2-16H 3D-1C-2-17H 3D-1C-2-18H	550. 550. 550. 550.	1.78 1.81 1.79 1.81 1.79 1.80 1.80 1.80 1.81 1.78 1.79 1.81	0.997 0.05 1.003 0.05 1.001 0.05 1.003 0.05 0.999 0.05 0.999 0.05	55555	E G G G G	0.045 0.091 0.045 0.091 0.045 0.091 0.045 0.091 0.045 0.091 0.045 0.091	1700. 2325. 3555. 2225. 1695. 1930.	475. 644. 990. 616. 472. 536.	76. 76. 76. 76. 76.	0.246 0.335 0.514 0.321 0.245 0.279	
3D-2A-2-1C 3D-2A-2-2C 3D-2A-2-3C 3D-2A-2-4C 3D-2A-2-5C 3D-2A-2-6C	-250. -250. -250. -250.	0.85 0.80 0.82 0.80 0.82 0.79 0.79 0.83 0.84 0.79 0.79 0.82	1.012 0.05 1.010 0.05 1.008 0.05 1.009 0.05 1.013 0.05 1.008 0.05	55555	A J A J A J A J A J	0.065 0.131 0.065 0.131 0.065 0.131 0.065 0.131 0.065 0.131 0.065 0.131	1875. 1850. 3815. 2060. 1965. 1755.	1123. 1130. 2351. 1261. 1190. 1082.	76. 76. 76. 76. 76.	0.186 0.184 0.380 0.205 0.195 0.175	
3D-2A-2-7A 3D-2A-2-8A 3D-2A-2-9A 3D-2A-2-10A 3D-2A-2-11A 3D-2A-2-12A	70. 70. 70. 70.	0.79 0.84 0.80 0.79 0.83 0.79 0.79 0.81 0.80 0.79 0.79 0.82	1.008 0.05 1.000 0.05 1.008 0.05 1.010 0.05 1.010 0.05 1.010 0.05	55555	A J A J A J A J	0.065 0.131 0.065 0.131 0.065 0.131 0.065 0.131 0.065 0.131 0.065 0.131	1925. 1800. 2845. 1950. 2105. 3615.	1171. 1132. 1743. 1207. 1310. 2224.	76. 76. 76. 76. 76.	0.192 0.181 0.284 0.194 0.209 0.360	
3D-2A-2-13H 3D-2A-2-14H 3D-2A-2-16H 3D-2A-2-17H 3D-2A-2-18H	550. 550. 550.	0.80 0.79 0.80 0.78 0.80 0.83 0.79 0.82 0.79 0.82	1.005 0.05 1.003 0.05 1.005 0.05 1.005 0.05 1.009 0.05	S S S S S S	A J A J A J A J	0.065 0.131 0.065 0.131 0.065 0.131 0.065 0.131 0.065 0.131	2467. 2305. 3029. 4315. 2395.	1544. 1455. 1849. 2665. 1475.	76. 76. 76. 76.	0.247 0.231 0.303 0.431 0.238	

TABLE 8-2 CONTINUED
(B) US CUSTOMARY UNITS

SPECIMEN NUMBER	TEMPERATURE	LAP LENGTHS (IN) 1 2	LAP WIDTH (IN)	GAP LENGTH (1N)	CONFIG CODE*	LAYUP CODE+ 1 2	ADHER THICKNE (IM	SSES	FAILURE LOAD (LBS)	AVERAGE JOINT STRESS (PSI)	FTU (KS1)	JOINT EFFICIENCY
3D-2B-2-1C 3D-2B-2-2C 3D-2B-2-3C 3D-2B-2-4C 3D-2B-2-5C 3D-2B-2-5C	-250. -250. -250. -250.	1.34 1.33 1.34 1.33 1.34 1.33 1.32 1.35 1.34 1.32 1.33 1.34	1.004 1.004 1.005 1.001 1.003 1.005	0.03 0.03 0.03 0.02 0.03 0.03	S S S S S S	A J A J A J A J A J	0.076 0.076 0.076 0.076	0.153 0.153 0.153 0.153 0.153 0.153	3720. 3800. 3160. 3670. 3815. 3670.	1387. 1418. 1178. 1373. 1430. 1367.	76. 76. 76. 76. 76.	0.319 0.326 0.271 0.315 0.327 0.314
3D-2B-2-7A 3D-2B-2-8A 3D-2B-2-9A 3D-2B-2-10A 3D-2B-2-11A 3D-2B-2-12A	70. 70. 70.	1.34 1.33 1.35 1.33 1.32 1.35 1.34 1.32 1.34 1.34 1.33 1.34	1.007 1.002 1.006 1.004 1.005 0.998	0.03 0.03 0.03 0.03 0.03	S S S S S S S	A J A J A J A J	0.076 0.076 0.076 0.076	0.153 0.153 0.153 0.153 0.153	3320. 3090. 3490. 3545. 3380.	1234. 1151. 1300. 1328. 1254.	76. 76. 76. 76. 76.	0.283 0.265 0.298 0.304 0.289
3D-2B-2-13H 3D-2B-2-14H 3D-2B-2-15H 3D-2B-2-16H 3D-2B-2-17H 3D-2B-2-18H	550. 550. 550.	1.36 1.33 1.34 1.33 1.35 1.33 1.34 1.32 1.33 1.34 1.34 1.33	1.007 1.003 1.003 1.000 0.997 1.004	0.02 0.02 0.03 0.03 0.03	s s s s s s	A J A J A J A J	0.076 0.076 0.076 0.076	0.153 0.153 0.153 0.153 0.153 0.153	2510. 3760. 3100. 3280. 2780. 3470.	927. 1404. 1153. 1233. 1044. 1294.	76. 76. 76. 76. 76.	0.214 0.322 0.266 0.282 0.240 0.297
3D-2C-2-1C 3D-2C-2-2C 3D-2C-2-3C 3D-2C-2-4C 3D-2C-2-5C 3D-2C-2-6C	-250. -250. -250. -250.	1.81 1.81 1.81 1.80 1.81 1.83 1.82 1.80 1.82 1.81 1.81 1.81	1.004 1.002 1.000 1.002 1.003 0.998	0.09 0.10 0.10 0.09 0.10 0.10	s s s s s s	A J A J A J A J A J A	0.068 0.068 0.068 0.068	0.136 0.136 0.136 0.136 0.136	3660. 2820. 2280. 3490. 4210. 3970.	1007. 780. 626. 962. 1156. 1099.	76. 76. 76. 76. 76.	0.353 0.272 0.221 0.337 0.406 0.385
3D-2C-2-7A 3D-2C-2-8A 3D-2C-2-9A 3D-2C-2-10A 3D-2C-2-11A 3D-2C-2-12A	70. 70. 70. 70.	1.82 1.81 1.82 1.81 1.82 1.81 1.81 1.81 1.81 1.82 1.80 1.81	1.002 1.002 1.001 1.001 0.999 1.001	0.10 0.10 0.10 0.10 0.10 0.10	s s s s s	A J A J A J A J A J	0.068 0.068 0.068 0.068	0.136 0.136 0.136 0.136 0.136 0.136	3990. 4370. 3020. 3000. 4180. 2530.	1097. 1201. 831. 828. 1153. 700.	76. 76. 76. 76. 76.	0.385 0.422 0.292 0.290 0.405 0.245
3D-2C-2-13H 3D-2C-2-14H 3D-2C-2-15H 3D-2C-2-16H 3D-2C-2-17H 3D-2C-2-18H	550. 1 550. 1 550. 1	1.81 1.82 1.82 1.81 1.82 1.80 1.81 1.81 1.82 1.80 1.82 1.80	1.001 1.004 1.002 1.000 1.001	0.10 0.10 0.10 0.10 0.10 0.10	s s s s	A J A J A J A J A J	0.068 0.068 0.068 0.068	0.136 0.136 0.136 0.136 0.136	4100. 3020. 4540. 3760. 4450. 3960.	1128. 829. 1252. 1039. 1228. 1089.	76. 76. 76. 76. 76.	0.396 0.201 0.433 0.364 0.400 0.352

TABLE B-2 CONTINUED

SPECIMEN NUMBER	TEMPERATURE (F)	LAP LENGTHS (IN) 1 2	LAP GAP WIDTH LENGTH (IN) (IN)	CONFIG CODE*	LAYUP CODE+ 1 2	ADHEREND THICKNESSES (IN) 1 2	FAILURE LOAD (LBS)	AVERAGE JOINT STRESS (PSI)	FTU (KSI)	JOINT EFFICIENCY
3D-3A-2-1C 3D-3A-2-2C 3D-3A-2-3C 3D-3A-2-4C 3D-3A-2-5C 3D-3A-2-6C	-250. 1 -250. 1 -250. 1 -250. 1	.31 1.33 .31 1.31 .32 1.33 .34 1.31 .34 1.31	1.002 0.08 1.001 0.09 1.004 0.08 1.000 0.08 1.002 0.08 1.005 0.08	S S S S S S S	K L K L K L K L	0.066 0.132 0.066 0.132 0.066 0.132 0.066 0.132 0.066 0.132 0.066 0.132	3665. 3655. 3860. 3300. 3200. 3910.	1385. 1393. 1451. 1245. 1205. 1468.	141. 141. 141. 141. 141.	0.196 0.196 0.207 0.177 0.172 0.209
3D-3A-2-7A 3D-3A-2-8A 3D-3A-2-9A 3D-3A-2-10A 3D-3A-2-11A 3D-3A-2-12A	70. 1 70. 1 70. 1 70. 1 70. 1	1.34 1.31 1.34 1.31 1.34 1.31 1.34 1.31 1.34 1.31	1.002 0.08 0.998 0.08 0.997 0.08 1.003 0.08 1.005 0.08 1.003 0.09	S S S S S S S	K L K L K L K L K L K L	0.066 0.132 0.066 0.132 0.066 0.132 0.066 0.132 0.066 0.132	3960. 3660. 3450. 3575. 3660.	1492. 1383. 1305. 1345. 1374.	141. 141. 141. 141. 141.	0.212 0.197 0.186 0.192 0.196 0.200
3D-3A-2-13H 3D-3A-2-14H 3D-3A-2-15H 3D-3A-2-17H 3D-3A-2-18H 3D-3A-2-19H	550. 1 550. 1 550. 1 550. 1	1.32 1.32 .34 1.31 .34 1.31 .33 1.31 .34 1.31	1.005 0.09 1.005 0.08 0.994 0.08 1.005 0.09 1.003 0.08 1.003 0.08	555555	K L L K L K L K L K L K L	0.066 0.132 0.066 0.132 0.066 0.132 0.066 0.132 0.066 0.132 0.066 0.132	5450. 5210. 6380. 5130. 5180. 5890.	2054. 1957. 2422. 1934. 1949. 2216.	141. 141. 141. 141. 141.	0.291 0.279 0.345 0.274 0.277 0.315
3D-4A-2-1C 3D-4A-2-2C 3D-4A-2-3C 3D-4A-2-4C 3D-4A-2-5C 3D-4A-2-6C	-250. 1 -250. 1 -250. 1 -250. 1	.32 1.31 .34 1.31 .30 1.34 .33 1.30 .32 1.31	1.006 0.11 1.002 0.08 1.005 0.09 1.002 0.09 1.006 0.10 1.001 0.09	s s s s s s s	D M D M D M D M	0.063 0.125 0.063 0.125 0.063 0.125 0.063 0.125 0.063 0.125 0.063 0.125	2880. 2340. 2410. 2420. 2545. 2615.	1089. 881. 909. 918. 962. 990.	76. 76. 76. 76. 76.	0.301 0.246 0.252 0.254 0.266 0.275
3D-4A-2-7A 3D-4A-2-8A 3D-4A-2-9A 3D-4A-2-10A 3D-4A-2-11A 3D-4A-2-12A	70. 1 70. 1 70. 1 70. 1	.32 1.34 .29 1.35 .35 1.30 .32 1.32 .33 1.30	1.006 0.09 1.006 0.08 0.994 0.09 1.004 0.09 1.006 0.09 0.997 0.09		D M D M D M D M D M	0.063 0.125 0.063 0.125 0.063 0.125 0.063 0.125 0.063 0.125 0.063 0.125	2800. 3635. 3040. 2810. 3140. 2135.	1046. 1369. 1154. 1060. 1187. 808.	76. 76. 76. 76. 76.	0.293 0.380 0.322 0.295 0.329 0.225
3D-4A-2-13H 3D-4A-2-14H 3D-4A-2-15H 3D-4A-2-16H 3D-4A-2-17H 3D-4A-2-18H	550. 1 550. 1 550. 1 550. 1	.32 1.32 .32 1.33 .29 1.34 .30 1.32 .32 1.33 .31 1.32	1:004 0.09 0.993 0.09 1:003 0.09 1:004 0.08 0:998 0.09 1:003 0.10	s s s s s s s s	D M D M D M D M D M	0.063 0.125 0.063 0.125 0.063 0.125 0.063 0.125 0.063 0.125 0.063 0.125	3180. 3490. 3070. 5000. 3560. 3490.	1200. 1327. 1164. 1901. 1347. 1322.	76. 76. 76. 76. 76.	0.333 0.370 0.322 0.524 0.376 0.366

TABLE B-2 CONTINUED

(B) US CUSTOMARY UNITS

NUMBER	TEMPERATURE	LAP LENGTHS (IN) 1 2	LAP GAP WIDTH LENGTI (IN) (IN)	CONFIG CODE*	LAYUP CODE+ 1 2	ADHEREND THICKNESSES (IN) 1 2	FAILURE LOAD (LBS)	AVERAGE JOINT STRESS (PSI)	FTU (KS1)	JOINT EFFICIENCY	
3D-5A-2-1C 3D-5A-2-2C 3D-5A-2-3C 3D-5A-2-4C 3D-5A-2-5C 3D-5A-2-6C	-250. -250. -250. -250.	1.28 1.32 1.27 1.32 1.30 1.28 1.28 1.34 1.28 1.32 1.32 1.30	1.004 0.13 1.007 0.13 0.996 0.13 0.998 0.14 1.006 0.13 1.005 0.13	\$ \$ \$ \$ \$	C N C N C N C N	0.072 0.145 0.072 0.145 0.072 0.145 0.072 0.145 0.072 0.145 0.072 0.145	3450. 3460. 3860. 3590. 3750. 3600.	1322. 1327. 1502. 1374. 1434. 1368.	76. 76. 76. 76. 76.	0.312 0.312 0.352 0.327 0.338 0.325	
3D-5A-2-7A 3D-5A-2-8A 3D-5A-2-9A 3D-5A-2-10A 3D-5A-2-11A 3D-5A-2-12A	70. 70. 70. 70.	1.31 1.29 1.30 1.29 1.28 1.33 1.29 1.32 1.33 1.28 1.33 1.27	1.007 0.14 1.002 0.13 1.005 0.13 1.004 0.13 1.008 0.14 1.005 0.14	S S S S S	C N C N C N C N C N C N	0.072 0.145 0.072 0.145 0.072 0.145 0.072 0.145 0.072 0.145 0.072 0.145	3050. 3060. 3420. 3960. 3350. 3240.	1165. 1180. 1304. 1511. 1273.	76. 76. 76. 76. 76.	0.275 0.277 0.309 0.358 0.302 0.292	
3D-5A-2-13H 3D-5A-2-14H 3D-5A-2-15H 3D-5A-2-16H 3D-5A-2-17H 3D-5A-2-18H	550. 550. 550. 550.	1.28 1.32 1.29 1.30 1.29 1.31 1.29 1.32 1.32 1.28 1.31 1.29	1.008 0.13 1.005 0.13 1.006 0.13 1.006 0.14 1.005 0.13 1.007 0.14	\$ \$ \$ \$ \$ \$	C N C N C N C N C N C N	0.072 0.145 0.072 0.145 0.072 0.145 0.072 0.145 0.072 0.145 0.072 0.145	4850. 5000. 4550. 4870. 4680. 4260.	1850. 1921. 1739. 1856. 1791. 1628.	76. 76. 76. 76. 76.	0.436 0.451 0.410 0.439 0.423 0.384	
3D-6A-2-1C 3D-6A-2-2C 3D-6A-2-3C 3D-6A-2-4C 3D-6A-2-5C 3D-6A-2-7C	-250. -250. -250. -250.	1.33 1.32 1.32 1.32 1.31 1.31 1.32 1.31 1.31 1.33 1.32 1.32	1.003 0.09 1.003 0.09 1.007 0.09 1.006 0.09 1.005 0.09 1.002 0.09	s s s s s	A G A G A G A G A G	0.068 0.091 0.068 0.091 0.068 0.091 0.068 0.091 0.068 0.091 0.068 0.091	2615. 1650. 1750. 2350. 2725. 1825.	984. 623. 664. 888. 1027. 690.	76. 76. 76. 76. 76.	0.377 0.238 0.251 0.338 0.392 0.263	
3D-6A-2-8A 3D-6A-2-9A 3D-6A-2-10A 3D-6A-2-11A 3D-6A-2-12A 3D-6A-2-13A	70. 70. 70. 70.	1.33 1.32 1.33 1.31 1.33 1.32 1.31 1.33 1.34 1.30 1.32 1.32	1.001 0.09 1.005 0.09 1.000 0.09 1.003 0.09 1.005 0.09 1.003 0.09	s s s s s	A G A G A G A G A G	0.068 0.091 0.068 0.091 0.068 0.091 0.068 0.091 0.068 0.091 0.068 0.091	1665. 1965. 1640. 1735. 2485. 2290.	627. 741. 619. 655. 937. 864.	76. 76. 76. 76. 76.	0.240 0.283 0.237 0.250 0.358 0.330	
3D-6A-14H 3D-6A-15H 3D-6A-16H 3D-6A-17H 3D-6A-18H 3D-6A-19H	550. 550. 550. 550.	1.33 1.31 1.32 1.32 1.32 1.33 1.32 1.31 1.31 1.32 1.31 1.33	1.006 0.09 1.006 0.09 0.997 0.09 1.001 0.09 0.999 0.09 1.000 0.08	. S S S S S	A G A G A G A G A G	0.068 0.091 0.068 0.091 0.068 0.091 0.068 0.091 0.068 0.091 0.068 0.091	2710. 1950. 1950. 2580. 2360. 1700.	1020. 734. 738. 980. 898. 644.	76. 76. 76. 76. 76. 76.	0.280	

TABLE B-2 CONTINUED

SPECIMEN NUMBER	TEMPERATURE (F)	LAP LENGTHS (IN) 1 2	LAP GAP WIDTH LENGT (IN) (IN)		LAYUP CODE+ 1 2	ADHEREND THICKNESSES (IN) 1 2	FAILURE LOAD (LBS)	AVERAGE JOINT STRESS (PSI)	FTU (KSI)	JOINT EFFICIENCY	
3D-7A-2-1A 3D-7A-2-2A 3D-7A-2-3A 3D-7A-2-4A 3D-7A-2-5A 3D-7A-2-6A	70. 70. 70. 70.	1.34 1.31 1.34 1.33 1.31 1.34 1.31 1.34 1.31 1.34 1.34 1.32	1.000 0.21 0.999 0.21 1.002 0.21 1.003 0.22 1.003 0.21 1.004 0.21	S S S S S S	J P J P J P P	0.130 0.261 0.130 0.261 0.130 0.261 0.130 0.261 0.130 0.261 0.130 0.261	4265. 3690. 3670. 2100. 3970. 3480.	1609. 1383. 1382. 790. 1494. 1303.	70. 76. 76. 76. 76.	0.215 0.186 0.185 0.106 0.200 0.175	
3D-7A-2-7H 3D-7A-2-8H 3D-7A-2-9H 3D-7A-2-10H 3D-7A-2-11H 3D-7A-2-12H	550. 550. i 550. i 550.	1.32 1.33 1.33 1.32 1.31 1.34 1.32 1.34 1.32 1.33 1.33 1.34	1.003 0.21 1.004 0.22 1.005 0.21 1.005 0.21 1.003 0.21 1.005 0.20	S S S S S S S	J P J P J P J	0.130 0.261 0.130 0.261 0.130 0.261 0.130 0.261 0.130 0.261 0.130 0.261	4110. 3230. 4420. 3940. 3880. 4330.	1546. 1214. 1660. 1474. 1460. 1613.	76. 76. 76. 76. 76.	0.207 0.162 0.222 0.198 0.195 0.217	
3F-1A-2-1A 3F-1A-2-2A 3F-1A-2-3A 3F-1A-2-4A 3F-1A-2-5A 3F-1A-2-6A	70. 70. 70. 70.	1.34 1.32 1.39 1.29 1.30 1.39 1.34 1.29 1.38 1.30 1.38 1.29	1.000 0.18 1.004 0.16 1.000 0.16 1.003 0.19 1.002 0.17 1.005 0.16	T T T T	J P J P J P J P	0.131 0.262 0.131 0.262 0.131 0.262 0.131 0.262 0.131 0.262 0.131 0.262	4000. 4280. 4850. 4940. 4180. 3660.	1503. 1590. 1802. 1873. 1557.	76. 76. 76. 76. 76.	0.201 0.214 0.243 0.247 0.210 0.183	
3F-1A-2-7H 3F-1A-2-8H 3F-1A-2-9H 3F-1A-2-10H 3F-1A-2-11H 3F-1A-2-12H	550. 550. 1 550. 1 550.	1.38 1.34 1.36 1.30 1.37 1.32 1.36 1.31 1.38 1.30 1.30 1.38	1.004 0.16 1.003 0.16 1.002 0.16 1.005 0.17 1.003 0.16 1.003 0.18	T T T T	J P J P J P J P	0.131 0.262 0.131 0.262 0.131 0.262 0.131 0.262 0.131 0.262 0.131 0.262	4330. 4260. 4100. 4320. 4250. 4390.	1585. 1596. 1521. 1611. 1580. 1633.	76. 76. 76. 76. 76.	0.217 0.213 0.205 0.216 0.213 0.220	
3E-1A-2-1C 3E-1A-2-2C 3E-1A-2-3C 3E-1A-2-4C 3E-1A-2-5C 3E-1A-2-6C	-250. -250. -250. -250.	0.79 0.80 0.80 0.75 0.80 0.77 0.80 0.82 0.80 0.80 0.80 0.80	0.990 0.13 0.990 0.17 1.000 0.15 0.960 0.09 0.990 0.11 0.990 0.10	S S S S S S S	A T A T A T A T A T A T	0.060 0.063 0.060 0.063 0.060 0.063 0.060 0.063 0.060 0.063	3160. 2990. 2880. 2480. 2500. 2670.	2007. 1949. 1834. 1595. 1578. 1686.	134. 134. 134. 134. 134.	0.378 0.358 0.341 0.306 0.299 0.319	
3E-1A-2-7A 3E-1A-2-8A 3E-1A-2-9A 3E-1A-2-10A 3E-1A-2-11A 3E-1A-2-12A	70. 70. 70. 70.	0.80 0.77 0.80 0.79 0.79 0.79 0.79 0.79 0.80 0.80 0.80 0.79	0.990 0.14 1.000 0.12 1.000 0.14 1.000 0.15 0.990 0.15 1.000 0.15	s s s s s	A T A T A T A T A T A T	0.060 0.063 0.060 0.063 0.060 0.063 0.060 0.063 0.060 0.063	4260. 4180. 4080. 3940. 4200. 3940.	2741. 2629. 2582. 2494. 2652. 2478.	134. 134. 134. 134. 134.	0.510 0.495 0.483 0.467 0.503 0.467	

TABLE B-2 CONTINUED

SPECIMEN TI Number		LAP ENGTHS (IN) 2	LAP WIDTH (IN)	GAP LENGTH (IN)	CONFIG CODE#		ADHERE THICKNES (IN) 1		FAILURE LOAD (LBS)	AVERAGE JOINT STRESS (PSI)	FTU (KSI)	JOINT EFFICIENCY
3E-1A-2-13H 3E-1A-2-14H 3E-1A-2-15H 3E-1A-2-16H 3E-1A-2-17H 3E-1A-2-18H	550. 0.7 550. 0.8 550. 0.7 550. 0.7 550. 0.8 550. 0.8	1 0.80 9 0.78 8 0.81 1 0.79	0.990 0.990 1.000 0.980 0.990 0.980	0.15 0.11 0.15 0.11 0.15 0.12	\$ \$ \$ \$ \$ \$	A T A T A T A T A T	0.060 0 0.060 0 0.060 0 0.060 0	.063 .063 .063 .063 .063	4070. 4030. 4110. 3770. 3870. 3780.	2602. 2528. 2618. 2419. 2443. 2411.	134. 134. 134. 134. 134.	O.487 O.482 O.487 O.456 O.463 O.457
3E-2A-2-1C 3E-2A-2-2C 3E-2A-2-3C 3E-2A-2-4C 3E-2A-2-5C 3E-2A-2-6C	-250. 1.8 -250. 1.7 -250. 1.7 -250. 1.8 -250. 1.8 -250. 1.7	9 1.79 9 1.79 0 1.80 0 1.80	0.990 1.000 0.980 1.010 1.010 0.990	0.12 0.14 0.11 0.11 0.10 0.12	s s s s s s s	C T T C T C T C T C T	0.060 0 0.060 0 0.060 0	.063 .063 .063 .063 .063	3260. 3900. 3620. 3200. 3920. 3790.	917. 1089. 1032. 880. 1078.	134. 134. 134. 134. 134.	0.390 0.462 0.438 0.375 0.460 0.453
3E-2A-2-7A 3E-2A-2-8A 3E-2A-2-9A 3E-2A-2-10A 3E-2A-2-11A 3E-2A-2-12A	70. 1.8 70. 1.7 70. 1.7 70. 1.8 70. 1.8 70. 1.7	9 1.79 8 1.79 0 1.79 1 1.79	1.000 1.000 1.000 0.990 1.000 0.990	0.12 0.14 0.11 0.12 0.13 0.11	\$ \$ \$ \$ \$ \$ \$ \$	C T C T C T C T C T	0.060 0 0.060 0 0.060 0 0.060 0	.063 .063 .063 .063 .063	3780. 3460. 4150. 3740. 4420. 3430.	1053. 966. 1162. 1052. 1228. 968.	134. 134. 134. 134. 134.	0.448 0.410 0.492 0.447 0.524 0.410
3E-2A-2-13H 3E-2A-2-14H 3E-2A-2-15H 3E-2A-2-16H 3E-2A-2-17H 3E-2A-2-18H	550. 1.8 550. 1.8 550. 1.8 550. 1.7 550. 1.8 550. 1.7	0 1.78 0 1.78 9 1.80 0 1.79	0.990 1.010 1.000 1.010 1.000	0.09 0.12 0.11 0.11 0.10 0.12	\$ . \$ \$ \$ \$ \$	C T C T C T C T C T	0.060 0 0.060 0 0.080 0 0.060 0	.063 .063 .063 .063 .063	5550. 5810. 5260. 5170. 5260. 1670.	1553. 1607. 1469. 1426. 1465. 466.	134. 134. 134. 134. 134.	0.664 0.681 0.623 0.606 0.623 0.198
3E-1B-2-1C 3E-1B-2-2C 3E-1B-2-3C 3E-1B-2-4C 3E-1B-2-5C 3E-1B-2-6C	-250. 1.7 -250. 1.7 -250. 1.7 -250. 1.8 -250. 1.7 -250. 1.8	8 1.79 9 1.79 0 1.78 9 1.80	0.980 0.990 0.990 1.000 0.990	0.11 0.13 0.11 0.10 0.12 0.10	s s s s s s	A T A T A T A T A T	0.060 0 0.060 0 0.060 0	.063 .063 .063 .063 .063	2040. 2630. 1720. 1620. 2070. 1860.	581. 744. 485. 453. 582. 523.	134. 134. 134. 134. 134.	0.247 0.315 0.206 0.192 0.248 0.223
3E-1B-2-7A 3E-1B-2-8A 3E-1B-2-9A 3E-1B-2-10A 3E-1B-2-11A 3E-1B-2-12A	70. 1.7 70. 1.7 70. 1.8 70. 1.7 70. 1.7 70. 1.8	9 1.77 1 1.80 7 1.79 9 1.79	1.000 0.990 0.980 1.010 1.000	0.12 0.12 0.07 0.12 0.11	s s s s s s	A T A T A T A T A T	0.060 0 0.060 0 0.060 0 0.060 0	.063 .063 .063 .063 .063	4180. 3010. 2920. 3250. 3400. 2590.	1171. 854. 825. 904. 950. 716.	134. 134. 134. 134. 134.	0.495 0.360 0.353 0.381 0.403 0.304

#### TABLE B-2 CONTINUED

### (B) US CUSTOMARY UNITS

SPECIMEN NUMBER	TEMPERATURE	LEN	AP GTHS N)	LAP WIDTH (IN)	GAP LENGTH (IN)	CONFIG CODE*		YUP DE+	ADHE THICKN (1		FAILURE LOAD (LBS)	AVERAGE JOINT STRESS (PSI)	FTU (KSI)	JOINT EFFICIENCY
NOMBER	117	•	4	(111)	(-1147		٠.	_	•	_	(LDS)	(1.21)	(1101)	•
3E-1B-2-13	1 550.	1.79	1.80	1.010	0.10	S	Α	T	0.060	0.063	5300.	1462.	134.	0.622
3E-18-2-14	1 550.	1.78	1.78	1.000	0.12	S	Α	Ť	0.060	0.063	5320.	1494.	134.	0.630
3E-1B-2-15	1 550.	1.77	1.81	1.000	0'.11	S	A	T	0.060	0.063	5030.	1405.	134.	0.596
3E-1B-2-16	550.	1.80	1.79	1.010	0.11	S	Α	T	0.060	0.063	5310.	1464.	134.	0.623
3E-1B-2-17	1 550.	1.78	1.78	0.990	0.12	S	A	Ť	0.060	0.063	4820.	1368.	134.	0.577
3E-18-2-18	550.	1.80	1.77	0.990	0.10	\$	A	T	0.060	0.063	5580.	1579.	134.	0.668

### \* CONFIGURATION CODE

S = STANDARD T = TAPERED ADHEREND

### + LAYUP CODE

A = [0,+/-45,90]3S	G = [0,+/-45,90]48	M = [0(3), +/-45(3), 90(3)]2S
B = [0, +/-45, 0(3)]2S	H = [0,+/-45,90]5	N = [+/-45,0,90]6S
C = [+/-45,0,90]3S	J = [0, +/-45, 90]6S	P = [0, +/-45, 90]12S
D = [0(3), +/-45(3), 0(3)]S	K = [0,+45,0(2),-45,0]2S	T = TITANIUM
E = [0. + / - 45.90128]	1 = (0 +45 0(2) -45 0145	

TABLE B-3 STEPPED LAP JOINT TEST RESULTS

(A) SI UNITS

SPECIME Number		GR/PI THICKNESS (MM)		NIUM Nesses MM) 2	WIDTH (MM)	FAILURE LOAD (KN)	AVERAGE JOINT STRESS (MPA)	FTU (MPA)	JOINT EFFICIENCY
3G-1A-2-		3.78	4.14	3.73	25.50	18.33	9.467	524.	0.364
3G-1A-2-	-2 294.	3.86	4.14	3.73	25.60	18.50	9.563	524.	0.360
3G-1A-2-	-3 294.	3.96	4.16	3.73	25.83	20.02	10.342	524.	0.380
3G-1A-2-	-4 294.	3.99	4.11	3.73	25.83	17.39	8.984	524.	0.328
3G-1A-2-	-5 294.	3.99	4.11	3.73	25.65	17.93	9.260	524.	0.338
3G-1A-2-	-6 294.	4.01	4.14	3.73	25.73	17.53	9.053	524.	0.328
3G-1A-2-	-7 561.	3.99	4.09	3.73	25.86	23.66	12.224	524.	0.446
3G-1A-2-	-8 561.	3.94	4.16	3.73	25.73	22.60	11.673	524.	0.431
3G-1A-2-		4.01	4.14	3.73	25.73	23.22	11.997	524.	0.435
3G-1A-2-	-10 561.	3.99	4.09	3.73	25.63	21.57	11.149	524.	0.406
3G-1A-2-		3.99	4.06	3.73	25.81	23.00	11.880	524.	0.433
3G-1A-2-		4.01	4.06	3.76	25.81	23.31	12.045	524.	0.436
3G-1A-2-	-13 116.	4.01	4.06	3.73	25.76	15.44	7.977	524.	0.289
3G-1A-2-		3,99	4.04	3.76	25.81	13.17	6.805	524.	0.248
3G-1A-2-		3.96	4.06	3.73	25.88	12.70	6.516	524.	0.241
3G-1A-2-		3.96	4.06	3.76	25.83	13.79	7,122	524.	
3G-1A-2-		3.99	4.03	3.76	25.88	15.66	8.088		0.261
3G-1A-2-		3.96	4.06	3.76	25.88	13.79	7.122	524. 524.	0.295 0.261

TABLE B-3 CONCLUDED
(B) US CUSTOMARY UNITS

SPECIMEN NUMBER	TEMPERATURE	GR/PI THICKNESS (IN)		IIUM IESSES In) 2	WIDTH (IN)	FAILURE LOAD (LBS)	AVERAGE JOINT STRESS (PSI)	FTU (KSI)	JOINT EFFICIENCY
3R-1A-2-1	70.	.149	.163	.147	1.004	4120.	1373.	76.	0.364
3G-1A-2-2	70.	.152	.163	.147	1.008	4160.	1387.	76.	0.360
3G-1A-2-3	70.	.156	.164	.147	1.017	4500.	1500.	76.	0.380
3G-1A-2-4	70.	.157	.162	.147	1.017	3910.	1303.	76.	0.328
3G-1A-2-5	70.	.157	.162	.147	1.010	4030.	1343.	76.	0.338
3G-1A-2 6	70.	.158	.163	.147	1.013	3940.	1313.	76.	0.328
3G-1A-2-7	550.	.157	.161	.147	1.018	5320.	1773.	76.	0.446
3G-1A-2-8	550.	.155	.164	.147	1.013	5080.	1683.	76.	0.431
3G-1A-2-9	550.	.158	.163	. 147	1.006	5220.	1740.	76.	0.435
3G-1A-2-10	550.	.157	.161	.147	1.009	4850.	1617.	76.	0.406
30-1A-2-11	550.	.157	.160	.147	1.016	5170.	1723.	76.	0.433
3G-1A-2-12		.158	.160	.148	1.016	5240.	1747.	76.	0.436
3G-1A-2-13	-250.	. 158	.160	. 147	1.014	3470.	1157.	76.	0.289
3G-1A-2-14	-250.	.157	.159	.148	1.016	2960.	987.	76.	0.248
3G-1A-2-15	-250.	.156	.160	.147	1.019	2835.	945.	76.	0.241
3G-1A-2-16		.156	.160	.148	1,017	3100.	1033.	76.	0.261
3G-1A-2-17	-250.	.157	.160	.148	1.019	3520.	1173.	76.	0.295
3G-1A-2-18	-250.	, 156	.160	.148	1.019	3100.	1033.	76.	0.261

APPENDIX C

ADVANCED BONDED JOINT
TEST RESULTS TABLES

TABLE C-1 ADVANCED SINGLE LAP JOINT TEST RESULTS - PREFORMED ADHERENDS

(A) SI UNITS

SPECIMEN Number	PREFORMED ANGLE (DEG)	TEMPERATURE (K)	LAP LENGTH (MM)	LAP WIDTH (MM)	LAYUP CODE+ 1 2	ADHEREND THICKNESSES (MM) 1 2	FAILURE LOAD (KN)	AVERAGE JOINT STRESS (MPA)	FTU (MPA)	JOINT EFFICIENCY
6-1A-2-1 6-1A-2-2 6-1A-2-3	5. 5. 5.	116. 116. 116.	25.40	25.40 25.68 25.65	A A A	1.753 1.75 1.727 1.75 1.727 1.72	3 8.696	11.700 13.333 12.492	524. 524. 524.	0.320 0.374 0.351
6-1A-2-4 6-1A-2-5 6-1A-2-6	5. 5. 5.	294. 294. 294.	25.65	25.60 25.65 25.60	A A A A	1.753 1.72 1.753 1.75 1.753 1.75	3 8.274	12.393 12.572 13.372	524. 524. 524.	0.348 0.351 0.370
6-1A-2-7 6-1A-2-8 6-1A-2-9	5. 5. 5.	561. 581. 561.	25.65	25.68 25.65 25.73	A . A A	1.727 1.75 1.753 1.75 1.727 1.75	3 7.695	12.480 11.693 9.665	524. 524. 524.	0.350 0.327 0.271
6-1B-2-1 6-1B-2-2 6-1B-2-3	5. 5. 5.	116. 116. 116.	51.31	25.55 25.60 25.58	A A A A A	1.803 1.80 1.803 1.80 1.778 1.80	3 13.367	9.217 10.175 10.405	524. 524. 524.	0.503 0.552 0.576
6-1B-2-4 6-1B-2-5 6-1B-2-6	5. 5. 5.	294. 294. 294.	51.31	25.55 25.60 25.48	A A A A A	1.778 1.80 1.778 1.80 1.778 1.75	3 14.323	10.688 10.903 11.491	524. 524. 524.	0.589 0.600 0.630
6-1B-2-7 6-1B-2-8 6-1B-2-9	5. 5. 5.	561. 561. 561.	50.80	25.50 25.48 25.48	A A A	1.778 1.80 1.778 1.77 1.803 1.77	8 11.343	8.196 8.765 10.036	524. 524. 524.	0.445 0.478 0.540
6-1C-2-1 6-1C-2-2 6-1C-2-3	5. 5. 5.	116. 116. 116.	76.96	25.50 25.37 25.86	A A A	1.702 1.75 1.727 1.72 1.727 1.70	7 16.280	8.652 8.337 8.127	524. 524. 524.	0.744 0.709 0.684
6-1C-2-4 6-1C-2-5 6-1C-2-6	5. 5. 5.	294. 294. 294.	76.96	25.40 25.45 25.40	A A A	1.753 1.75 1.727 1.70 1.753 1.75	2 15.191	8.105 7.755 7.418	524. 524. 524.	0.677 0.659 0.622
6-1C-2-7 6-1C-2-8 6-1C-2-9	5. 5. 5.	561. 561. 561.	76.96	25.45 25.45 25.65	A A A A	1.727 1.72 1.753 1.72 1.753 1.72	7 12.944	6.961 6.608 6.422	524. 524. 524.	0.590 0.554 0.540

TABLE C-1 CONTINUED

SPECIMEN NUMBER	PREFORMED ANGLE (DEG)	TEMPERATURE (K)	LAP LENGTH (MM)	LAP WIDTH (MM)	LAY! COD!		ADHE THICKN (M		FAILURE LOAD (KN)	AVERAGE JOINT STRESS (MPA)	FTU (MPA)	JOINT EFFICIENCY
6-2A-2-1	10.	116.	25.65	25.91	A	A	1.727	1.727	13.923	20.948	524.	0.594
6-2A-2-2	10.	116.	25.40	25.63	A	A	1.727	1.727	15.413	23.677	524.	0.664
6-2A-2-3	10.	116.	25.65	25.68	A	A	1.727	1.727	13.500	20.493	524.	0.581
6-2A-2-4 6-2A-2-5 6-2A-2-6	10. 10. 10.	294. 294. 294.	25.91 25.91 25.91	25.65 25.58 25.58	A A	A A A	1.727 1.727 1.727	1.727 1.727 1.727	11.899 11.098 13.011	17.903 16.748 19.634	524. 524. 524.	0.512 0.479 0.562
6-2A-2-7	10.	561.	25.91	25.58	A	A	1.702	1.727	11.387	17.184	524.	0.499
6-2A-2-8	10.	561.	25.91	25.60	A	A	1.727	1.727	9.119	13.747	524.	0.394
6-2A-2-9	10.	561.	25.91	25.55	A	A	1.753	1.727	10.920	16.496	524.	0.465
6-2B-2-1	10.	116.	51.31	25.91	A	A	1.753	1.778	18.594	13.988	524.	0.781
6-2B-2-2	10.	116.	51.31	25.58	A	A	1.778	1.778	15.769	12.016	524.	0.662
6-2B-2-3	10.	116.	51.31	25.53	A	A	1.753	1.778	11.187	8.542	524.	0.477
6-2B-2-4	10.	294.	51.31	25.58	A	A	1.778	1.778	14.835	11.304	524.	0.623
6-2B-2-5	10.	294.	51.05	25.55	A	A	1.778	1.778	17.682	13.554	524.	0.743
6-2B-2-6	10.	294.	51.05	25.58	A	A	1.778	1.753	15.591	11.939	524.	0.654
6-28-2-7	10.	561.	50.80	25.48	A	A	1.753	1.778	15.947	12.322	524.	0.682
6-28-2-8	10.	561.	50.80	25.50	A	A	1.778	1.803	14.234	10.988	524.	0.599
6-28-2-9	10.	561.	50.55	25.48	A	A	1.778	1.778	13.856	10.760	524.	0.584
6-2C-2-1	10.	116.	76.71	25.78	A	A	1.753	1.753	11.298	5.713	524.	0.477
6-2C-2-2	10.	116.	76.71	25.65	A	A	1.753	1.753	12.344	6.273	524.	0.524
6-2C-2-3	10.	116.	76.45	25.53	A	A	1.753	1.753	12.277	6.291	524.	0.524
6-2C-2-4	10.	294.	76.71	25.63	A	A	1.753	1.753	10.164	5.170	524.	0.432
6-2C-2-5	10.	294.	76.45	25.50	A	A	1.753	1.753	12.255	6.286	524.	0.523
6-2C-2-6	10.	294.	76.20	25.53	A	A	1.778	1.753	15.858	8.153	524.	0.667
6-2C-2-7	10.	561.	76.20	25.63	A	A	1.727	1.727	10.898	5.580	524.	0.470
6-2C-2-8	10.	561.	76.20	25.58	A	A	1.753	1.753	11.476	5.888	524.	0.499
6-2C-2-9	10.	561.	76.20	25.63	A	A	1.727	1.727	11.921	6.104	524.	0.514

TABLE C-1 CONTINUED

SPECIMEN Number	PREFORMED ANGLE (DEG)	TEMPERATURE (K)	LAP LENGTH (MM)	LAP WIDTH (MM)	LAYI CODI 1		ADHE THICKN (M	ESSES	FAILURE LOAD (KN)	AVERAGE JOINT STRESS (MPA)	FYU (MPA)	JOINT EFFICIENCY
6-3A-2-1	15.	116.	25.15	25.60	A	A	1.778	1.778	9.163	14.233	524.	0.384
6-3A-2-2	15.	116.	25.40	25.55	A	A	1.778	1.778	8.785	13.536	524.	0.369
6-3A-2-3	15.	116.	25.40	25.55	A	A	1.778	1.803	11.298	17.408	524.	0.475
6-3A-2-4	15.	294.	25.40	25.55	A	A	1.803	1.778	11.054	17.031	524.	0.458
6-3A-2-5	15.	294.	25.40	25.70	A	A	1.778	1.778	12.499	19.145	524.	0.522
6-3A-2-6	15.	294.	25.40	25.70	A	A	1.778	1.778	11.232	17.203	524.	0.469
6-3A-2-7	15.	561.	25.40	25.63	A	A	1.829	1.803	10.164	15.614	524.	0.414
6-3A-2-8	15.	561.	25.40	25.55	A	A	1.803	1.778	11.721	18.059	524.	0.485
6-3A-2-9	15.	561.	25.15	25.68	A	A	1.803	1.803	9.653	14.948	524.	0.398
6-3B-2-1	15.	116.	50.80	25.40	A	A	1.778	1.778	13.767	10.670	524.	0.582
6-3B-2-2	15.	116.	50.80	25.55	A	A	1.803	1.803	14.257	10.983	524.	0.590
6-3B-2-3	15.	116.	50.80	25.55	A	A	1.803	1.778	12.433	9.578	524.	0.515
6-3B-2-4	15.	294.	51.05	25.63	A	A	1.778	1.778	13.990	10.692	524.	0.586
6-3B-2-5	15.	294.	50.80	25.53	A	A	1.829	1.803	12.967	9.999	524.	0.530
6-3B-2-6	15.	294.	50.80	25.32	A	A	1.778	1.778	11.565	8.990	524.	0.490
6-3B-2-7	15.	561.	50.80	25.40	A	A	1.803	1.778	9.719	7.533	524.	0.405
6-3B-2-8	15.	561.	50.80	25.48	A	A	1.778	1.803	11.165	8.627	524.	0.470
6-3B-2-9	15.	561.	50.80	25.43	A	A	1.778	1.803	9.986	7.732	524.	0.422
6-3C-2-1	15.	116.	76.96	25.65	A	A	1.803	1.803	14.701	7.446	524.	Q.606
6-3C-2-2	15.	116.	76.96	25.53	A	A	1.829	1.803	13.767	7.008	524.	Q.563
6-3C-2-3	15.	116.	76.96	25.55	A	A	1.803	1.829	13.411	6.820	524.	Q.555
6-3C-2-4	15.	294.	76.96	25.48	A	A	1.803	1.829	15.791	8.054	524.	0.656
6-3C-2-5	15.	294.	76.96	25.53	A	A	1.803	1.803	15.413	7.845	524.	0.639
6-3C-2-6	15.	294.	76.96	25.53	A	A	1.829	1.803	14.902	7.585	524.	0.609
6-3C-2-7	15.	561.	76.71	25.53	A	A	1.803	1.778	11.654	5.952	524.	0.483
6-3C-2-8	15.	561.	76.71	25.40	A	A	1.803	1.854	13.256	6.803	524.	0.552
6-3C-2-9	15.	561.	76.20	25.58	A	A	1.829	1.803	12.188	6.253	524.	U.497

<sup>+</sup> LAYUP CODE

A = [0, +/-45, 90]3S

TABLE C-1 CONTINUED
(B) US CUSTOMARY UNITS

SPECIMEN Number	PREFORMED ANGLE (DEG)	TEMPERATURE (F)	LAP LENGTH (IN)	LAP WIDTH (IN)	LAYU CODE 1		ADHE THICKN (1	ESSES	FAILURE LOAD (LBS)	AVERAGE JOINT STRESS (PSI)	FTU (K\$1)	JOINT EFFICIENCY
6-1A-2-1 6-1A-2-2 6-1A-2-3	5. 5.	-250. -250. -250.	0.990 1.000 1.000	1.000 1.011 1.010	A A A	A A A	0.069 0.068 0.068	0.069 0.069 0.068	1680. 1955. 1830.	1697. 1934. 1812.	76. 76. 76.	0.320 0.374 0.351
6-1A-2-4	5.	70.	1.010	1.008	A	A	0.069	0.068	1830.	1798.	76.	0.346
6-1A-2-5	5.	70.	1.010	1.010	A	A	0.069	0.069	1860.	1823.	76.	0.351
6-1A-2-6	5.	70.	1.000	1.008	A	A	0.069	0.069	1955.	1939.	76.	0.370
6-1A-2-7	5.	550.	1.000	1.011	A	A	0.068	0.069	1830.	1810.	76.	0.350
6-1A-2-8	5.	550.	1.010	1.010	A	A	0.069	0.069	1730.	1696.	76.	0.327
6-1A-2-9	5.	550.	1.000	1.013	A	A	0.068	0.069	1420.	1402.	76.	0.271
6-1B-2-1	5.	-250.	2.030	1.006	A	A	0.071	0.071	2730.	1337.	76.	0.503
6-1B-2-2	5.	-250.	2.020	1.008	A	A	0.071	0.071	3005.	1476.	76.	0.552
6-1B-2-3	5.	-250.	2.030	1.007	A	A	0.070	0.071	3085.	1509.	76.	0.576
6-1B-2-4	5.	70.	2.020	1.006	A	A	0.070	0.071	3150.	1550.	76.	0.589
6-1B-2-5	5.	70.	2.020	1.008	A	A	0.070	0.071	3220.	1581.	76.	0.600
6-1B-2-6	5.	70.	2.010	1.003	A	A	0.070	0.069	3360.	1667.	76.	0.630
6-1B-2-7	5.	550.	1.990	1.004	A	AAA	0.070	0.071	2375.	1189.	76.	0.445
6-1B-2-8	5.	550.	2.000	1.003	A		0.070	0.070	2550.	1271.	76.	0.478
6-1B-2-9	5.	550.	2.000	1.003	A		0.071	0.070	2920.	1456.	76.	0.540
6-1C-2-1	5.	-250.	3.020	1.004	A	A	0.067	0.069	3805.	1255.	76.	0.744
6-1C-2-2	5.	-250.	3.030	0.999	A	A	0.068	0.068	3660.	1209.	76.	0.709
6-1C-2-3	5.	-250.	3.000	1.018	A	A	0.068	0.067	3600.	1179.	76.	0.684
6-1C-2-4	5.	70.	3.020	1.000	A	A	0.069	0.069	3550.	1175.	76.	0.677
6-1C-2-5	5.	70.	3.030	1.002	A	A	0.068	0.067	3415.	1125.	76.	0.659
6-1C-2-6	5.	70.	3.030	1.000	A	A	0.069	0.069	3260.	1076.	76.	0.622
6-1C-2-7	5.	550.	3.020	1.002	A	A	0.068	0.068	3055.	1010.	76.	0.590
6-1C-2-8	5.	550.	3.030	1.002	A	A	0.069	0.068	2910.	958.	76.	0.354
6-1C-2-9	5.	550.	3.040	1.010	A	A	0.069	0.068	2860.	931.	76.	0.540

TABLE C-1 CONTINUED

(B) US CUSTOMARY UNITS

SPECIMEN NUMBER	PREFORMED ANGLE (DEG)	TEMPERATURE (F)	LAP LENGTH (IN)	LAP WIDTH (IN)	LAYU CODE 1		ADHE THICKN (1	ESSES	FAILURE LOAD (LBS)	AVERAGE JOINT STRESS (PSI)	FTU (K\$1)	JOINT EFFICIENCY
6-2A-2-1	10.	-250.	1.010	1.020	A	A	0.068	0.068	3130.	3038.	76.	0.594
6-2A-2-2	10.	-250.	1.000	1.009		A	0.068	0.068	3465.	3434.	76.	0.664
6-2A-2-3	10.	-250.	1.010	1.011		A	0.068	0.068	3035.	2972.	76.	0.581
6-2A-2-4	10.	70.	1.020	1.010	A	A	0.068	0.068	2675.	2597.	76.	0.512
6-2A-2-5	10.	70.	1.020	1.007		A	0.068	0.068	2495.	2429.	76.	0.479
6-2A-2-6	10.	70.	1.020	1.007		A	0.068	0.068	2925.	2848.	76.	0.562
6-2A-2-7	10.	550.	1.020	1.007	Ā	A	0.067	0.068	2560.	2492.	76.	0.499
6-2A-2-8	10.	550.	1.020	1.008		A	0.068	0.068	2050.	1994.	76.	0.394
6-2A-2-9	10.	550.	1.020	1.006		A	0.069	0.068	2455.	2393.	76.	0.465
6-2B-2-1	10.	-250.	2.020	1.020	Ä	A	0.069	0.070	4180.	2029.	76.	0.781
6-2B-2-2	10.	-250.	2.020	1.007		A	0.070	0.070	3545.	1743.	76.	0.662
6-2B-2-3	10.	-250.	2.020	1.005		A	0.069	0.070	2515.	1239.	76.	0.477
6-2B-2-4	10.	70.	2.020	1.007	Ä	A	0.070	0.070	3335.	1640.	76.	0.623
6-2B-2-5	10.	70.	2.010	1.006		A	0.070	0.070	3975.	1966.	76.	0.743
6-28-2-6	10.	70.	2.010	1.007		A	0.070	0.069	3505.	1732.	76.	0.654
6-2B-2-7	10.	550.	2.000	1.003	Ä	A	0.069	0.070	3585.	1787.	76.	0.682
6-2B-2-8	10.	550.	2.000	1.004		A	0.070	0.071	3200.	1594.	76.	0.599
6-2B-2-9	10.	550.	1.990	1.003		A	0.070	0.070	3115.	1561.	76.	0.584
6-2C-2-1	10.	-250.	3.020	1.015	A	A	0.069	0.069	2540.	829.	76.	0.477
6-2C-2-2	10.	-250.	3.020	1.010		A	0.069	0.069	2775.	910.	76.	0.524
6-2C-2-3	10.	-250.	3.010	1.005		A	0.069	0.069	2760.	912.	76.	0.524
6-2C-2-4	10.	70.	3.020	1.009	Ä	A	0.069	0.069	2285.	750.	76.	0.432
6-2C-2-5	10.	70.	3.010	1.004		A	0.069	0.069	2755.	912.	76.	0.523
6-2C-2-6	10.	70.	3.000	1.005		A	0.070	0.069	3565.	1182.	76.	0.667
6-2C-2-7	10.	550.	3.000	1.009	A	A	0.068	0.068	2450.	809.	76.	0.470
6-2C-2-8	10.	550.	3.000	1.007		A	0.069	0.069	2580.	854.	76.	0.489
6-2C-2-9	10.	550.	3.000	1.009		A	0.068	0.068	2680.	885.	76.	0.514

TABLE C-1 CONCLUDED

SPECIMEN NUMBER	PREFORMED ANGLE (DEG)	TEMPERATURE (F)	LAP LENGTH (1N)	LAP WIDTH (IN)	LAYU CODE 1		ADHE THICKN (1	ESSES	FAILURE LOAD (LBS)	AVERAGE JOINT STRESS (PSI)	FTU (KSI)	JOINT EFFICIENCY
6-3A-2-1	15.	-250.	0.990	1.008	A	A	0.070	0.070	2000.	2064.	76.	0.384
6-3A-2-2	15.	-250.	1.000	1.006		A	0.070	0.070	1975.	1963.	76.	0.369
6-3A-2-3	15.	-250.	1.000	1.006		A	0.070	0.071	2540.	2525.	76.	0.475
6-3A-2-4	15.	70.	1.000	1.006	A	A	0.071	0.070	2485.	2470.	76.	0.458
6-3A-2-5	15.	70.	1.000	1.012		A	0.070	0.070	2810.	2777.	76.	0.522
6-3A-2-6	15.	70.	1.000	1.012		A	0.070	0.070	2525.	2495.	76.	0.469
6-3A-2-7 6-3A-2-8 6-3A-2-9	15. 15. 15.	550. 550. 550.	1.000 1.000 0.990	1.009 1.006 1.011	A	A A	0.072 0.071 0.071	0.071 0.070 0.071	2285. 2635. 2170.	2265. 2619. 2168.	76. 76. 76.	0.414 0.485 0.398
6-3B-2-1	15.	-250.	2.000	1.000	A	A	0.070	0.070	3095.	1548.	76.	0.582
6-3B-2-2	15.	-250.	2.000	1.006		A	0.071	0.071	3205.	1593.	76.	0.590
6-3B-2-3	15.	-250.	2.000	1.006		A	0.071	0.070	27 <b>9</b> 5.	1389.	76.	0.515
6-3B-2-4	15.	70.	2.010	1.009	A	A	0.070	0.070	3145.	1551.	76.	0.586
6-3B-2-5	15.	70.	2.000	1.005		A	0.072	0.071	2915.	1450.	76.	0.530
6-3B-2-6	15.	70.	2.000	0.997		A	0.070	0.070	2600.	1304.	76.	0.490
6-38-2-7	15.	550.	2.000	1.000	A	A	0.071	0.070	2185.	1093.	76.	0.405
6-38-2-8	15.	550.	2.000	1.003		A	0.070	0.071	2510.	1251.	76.	0.470
6-38-2-9	15.	550.	2.000	1.001		A	0.070	0.071	2245.	1121.	76.	0.422
6-3C-2-1 6-3C-2-2 6-3C-2-3	15. 15. 15.	-250. -250. -250.	3.030 3.030 3.030	1.010 1.005 1.006	A	A A	0.071 0.072 0.071	0.071 0.071 0.072	3305. 3095. 3015.	1080. 1016. 989.	76. 76. 76.	0.606 0.563 0.555
6-3C-2-4	15.	70.	3.030	1.003	A	A	0.071	0.072	3550.	1168.	76.	0.656
6-3C-2-5	15.	70.	3.030	1.005		A	0.071	0.071	3465.	1138.	76.	0.639
6-3C-2-6	15.	70.	3.030	1.005		A	0.072	0.071	3350.	1100.	76.	0.609
6-3C-2-7	15.	550.	3.020	1.005	A	A	0.071	0.070	2020.	863.	76.	0.483
6-3C-2-8	15.	550.	3.020	1.000		A	0.071	0.073	2980.	987.	76.	0.552
6-3C-2-9	15.	550.	3.000	1.007		A	0.072	0.071	2740.	907.	76.	0.497

<sup>+</sup> LAYUP CODE

A = [0, +/-45, 90]35

TABLE C-2 ADVANCED SINGLE AND DOUBLE LAP JOINT TEST RESULTS
(A) SI UNITS

SPECIMEN NUMBER	TEMPERATURE (K)	LAP LENGTH (MM)	LAP WIDTH (MM)	CONFIG CODE*	CODE		ADHEI THICKNI (MI	ESSES	FAILURE LOAD (KN)	AVERAGE JOINT STRESS (MPA)	FTU (MPA)	JOINT EFFICIENCY	
6-4A-2-1 6-4A-2-2 6-4A-2-3	294. 294. 294.	25.40 25.40 25.40	25.35 25.37 25.38	A A A	Ä	A A A	1.803 1.803 1.803	1.778 1.778 1.778	2.691 2.491 2.647	4.179 3.865 4.106	524. 524. 524.	0.112 0.104 0.110	
6-4A-2-4 6-4A-2-5 6-4A-2-6	561. 561. 561.	25.40 25.40 25.40	25.37 25.32 25.39	A A A	Ä	A A A	1.778 1.753 1.702	1.778 1.727 1.727	2.722 2.985 3.007	4.224 4.640 4.663	524. 524. 524.	0.115 0.128 0.133	
6-48-2-1 6-48-2-2 6-48-2-3 6-48-2-4	294. 294. 294. 294.	50.80 50.80 50.80 50.80	25.39 25.42 25.39 25.40	A A A	A A	A A A	1.803 1.778 1.753 1.803	1.803 1.753 1.778 1.803	5.427 5.204 5.560 5.093	4.207 4.031 4.311 3.947	524. 524. 524. 524.	0.226 0.220 0.238 0.212	
6-4B-2-5 6-4B-2-6 6-4B-2-7 6-4B-2-8	561. 561. 561. 561.	50.80 50.80 50.80 50.80	25.38 25.42 25.40 25.36	A A A	A A	A A A	1.727 1.753 1.727 1.727	1.753 1.753 1.778 1.778	6.850 4.582 5.449 5.427	5.313 3.548 4.223 4.212	524. 524. 524. 524.	0.298 0.196 0.237 0.236	
6-4C-2-1 6-4C-2-2 6-4C-2-3	294. 294. 294.	76.20 76.20 76.20	25.41 25.40 25.38	A A A	Ä	A A A	1.753 1.778 1.753	1.778 1.778 1.753	6.428 6.139 6.027	3.320 3.172 3.117	524. 524. 524.	0.275 0.259 0.259	
6-4C-2-4 6-4C-2-5 6-4C-2-6	561. 561. 561.	76.20 76.20 76.20	25.41 25.39 25.43	A A A	A	A A A	1.803 1.778 1.778	1.803 1.753 1.778	7.851 7.562 8.985	4.055 3.908 4.638	524. 524. 524.	0.327 0.320 0.379	
6-5A-2-1 6-5A-2-2 6-5A-2-3	294. 294. 294.	20.32 20.32 20.32	25.40 25.38 25.38	B · B B	B	B B B	2.388 2.438 2.388	2.362 2.413 2.438	11.943 12.411 12.989	23.138 24.062 25.184	524. 524. 524.	0.376 0.383 0.409	
6-5A-2-4 6-5A-2-5 6-5A-2-6	561. 561. 561.	20.32 20.32 20.32	25.42 25.39 25.38	B B B	В	B B 8	2.413 2.362 2.388	2.337 2.362 2.388	12.655 12.188 12.188	24.500 23.624 23.629	524. 524. 524.	0.394 0.388 0.384	
6-5B-2-1 6-5B-2-2 6-5B-2-3	294. 294. 294.	33.02 33.02 33.02	25.39 25.42 25.37	B B B	В	B B B	2.413 2.362 2.388	2.438 2.413 2.362	11.766 12.499 13.389	14.031 14.894 15.985	524. 524. 524.	0.366 0.397 0.422	
6-5B-2-4 6-5B-2-5 6-5B-2-6	561. 561. 561.	33.02 33.02 33.02	25.39 25.41 25.37	B B B	В	B B 8	2.438 2.362 2.362	2.362 2.388 2.388	16.458 14.168 13.745	19.631 16.887 16.405	524. 524. 524.	0.507 0.450 0.438	

TABLE C-2 CONTINUED

ſ	Αl	I SI	1 11	IN I	TS

SPECIMEN NUMBER	TEMPERATURE (K)	LAP LENGTH (MM)	LAP WIDTH (MM)	CONF I G CODE*			ADHE THICKN (MI	ESSES	FAILURE LOAD (KN)	AVERAGE JOINT STRESS (MPA)	FTU (MPA)	JOINT EFFICIENCY
6-5C-2-1 6-5C-2-2 6-5C-2-3	294. 294. 294.	45.72 45.72 45.72	25.43 25.45 25.38	B B B	B B B	B B	2.438 2.362 2.464	2.464 2.413 2.413	14.924 13.211 12.878	12.838 11.355 11.097	524. 524. 524.	0.459 0.419 0.393
6-5C-2-4 6-5C-2-5 6-5C-2-6	561. 561. 561.	45.72 45.72 45.72	25.41 25.38 25.37	B B B	B B	B B	2.362 2.388 2.464	2.388 2.438 2.413	17.526 19.216 18.104	15.089 16.561 15.607	524. 524. 524.	0.557 0.605 0.553
6-6A-2-1 6-6A-2-2 6-6A-2-3	294. 294. 294.	26.67 26.16 25.91	25.40 25.43 25.37	C C	A A A	A A A	1.778 1.727 1.778	1.753 1.753 1.778	3.225 4.003 3.848	4.761 6.017 5.855	524. 524. 524.	0.136 0.174 0.163
6-8A-2-4 6-6A-2-5 6-6A-2-6	561. 561. 561.	25.65 26.16 26.16	25.36. 25.39 25.38	C C	A A A	A A	1.778 1.778 1.778	1.778 1.778 1.753	3.092 2.856 2.776	4.752 4.298 4.180	524. 524. 524.	0.131 0.121 0.117
6-6B-2-1 6-6B-2-2 6-6B-2-3 6-6B-2-4	294. 294. 294. 294.	51.31 51.31 51.31 50.80	25.45 25.37 25.37 25.43	C C C	A A A	A A A	1.778 1.778 1.753 1.753	1.778 1.778 1.753 1.753	9.986 9.630 8.385 8.896	7.647 7.397 6.441 6.886	524. 524. 524. 524.	0.421 0.407 0.360 0.381
6-6B-2-5 6-6B-2-6 6-6B-2-7 6-6B-2-8	561. 561. 561.	51.05 50.80 50.80 51.05	25.40 25.39 25.41 25.43	CCCC	A A A	A A A	1.803 1.778 1.727 1.778	1.753 1.803 1.778 1.727	7.273 9.052 7.340 8.985	5.608 7.017 5.685 6.922	524. 524. 524. 524.	0.303 0.383 0.319 0.379
6-6C-2-1 6-6C-2-2 6-6C-2-3	294. 294. 294.	76.45 76.45 76.20	25.43 25.42 25.41	C C	A A A	A A A	1.753 1.778 1.753	1.753 1.778 1.778	12.055 9.719 9.986	6.200 5.001 5.158	524. 524. 524.	0.518 0.410 0.428
6-6C-2-4 6-6C-2-5 6-6C-2-6	561. 561. 561.	76.45 76.20 76.71	25.42 25.41 25.42	C C	A A A	A A A	1.803 1.727 1.778	1.803 1.778 1.778	11.143 10.653 8.429	5.733 5.503 4.323	524. 524. 524.	0.464 0.463 0.356
6-7A-2-1 6-7A-2-2 6-7A-2-3	294. 294. 294.	25.91 25.40 25.43	25.39 25.41 25.38	D D D	A A A	A A A	1.778 1.778 1.753	1.753 1.778 1.753	5.249 5.627 5.138	7.979 8.719 7.963	524. 524. 524.	0.222 0.238 0.220
6-7A-2-4 6-7A-2-5 6-7A-2-6	561. 561. 561.	25.40 25.91 25.40	25.38 25.36 25.38	D D D	A A A	A A A	1.778 1.803 1.753	1.778 1.727 1.778	5.071 5.583 5.583	7.855. 8.495 8.658	524. 524. 524.	0.214 0.233 0.239

TABLE C-2 CONTINUED

SPECIMEN NUMBER	TEMPERATURE (K)	LAP LENGTH (MM)	LAP WIDTH (MM)	CONFIG CODE*			ADHE THICKN (M	ESSES	FAILURE LOAD (KN)	AVERAGE JOINT STRESS (MPA)	FTU (MPA)	JOINT EFFICIENCY
6-78-2-1 6-78-2-2 6-78-2-3 6-78-2-4	294. 294. 294. 294.	51.31 50.80 51.31 51.31	25.42 25.38 25.39 25.43	D D D	A A A	A A A	1.803 1.829 1.753 1.803	1.753 1.778 1.778 1.778	9.008 9.008 9.141 9.497	6.906 6.986 7.017 7.279	524. 524. 524. 524.	0.375 0.370 0.392 0.395
6-7B-2-5 6-7B-2-6 6-7B-2-7 6-7B-2-8	561. 561. 561. 561.	51.05 51.31 51.31 51.31	25.40 25.38 25.37 25.40	D D D	A A A	A A A	1.778 1.753 1.778 1.803	1.803 1.803 1.829 1.753	8.919 8.919 8.207 8.407	6.878 6.848 6.305 6.451	524. 524. 524. 524.	0.377 0.383 0.347 0.350
6-7C-2-1 6-7C-2-2 6-7C-2-3	294. 294. 294.	76.20 76.96 76.71	25.45 25.39 25.42	D D D	A A A	A A	1.778 1.778 1.778	1.778 1.778 1.778	9.964 12.010 10.854	5.138 6.145 5.567	524. 524. 524.	0.420 0.508 0.458
6-7C-2-4 6-7C-2-5 6-7C-2-6	561. 561. 561.	76.71 76.96 76.45	25.43 25.37 25.37	D D D	A A A	A A A	1.803 1.778 1.803	1.753 1.803 1.803	11.143 11.276 10.587	5.713 5.775 5.457	524. 524. 524.	0.464 0.477 0.442
6-8A-2-1 6-8A-2-2 6-8A-2-3	294. 294. 294.	26.16 25.91 25.91	25.43 25.43 25.43	E E	A A A	A A A	1.778 1.778 1.803	1.753 1.778 1.753	3.514 3.092 3.336	5.283 4.692 5.064	524. 524. 524.	0.148 0.130 0.139
6-8A-2-4 6-8A-2-5 6-8A-2-6	561. 561. 561.	25.91 25.40 25.40	25.42 25.42 25.40	E E	A A A	A A A	1.778 1.778 1.803	1.753 1.753 1.778	3.314 3.092 3.047	5.031 4.789 4.723	524. 524. 524.	0.140 0.131 0.127
6-8B-2-1 6-8B-2-2 6-8B-2-3 6-8B-2-4	294. 294. 294. 294.	51.05 51.31 50.80 51.05	25.45 25.42 25.41 25.39	E E E	A A A	A A A	1.753 1.753 1.753 1.778	1.778 1.753 1.778 1.778	5.293 5.360 5.026 5.316	4.075 4.110 3.894 4.100	524. 524. 524. 524.	0.227 0.230 0.215 0.225
6-8B-2-5 6-8B-2-6 6-8B-2-7 6-8B-2-8	561. 561. 561. 561.	51.05 50.80 51.31 50.80	25.43 25.42 25.43 25.45	E E E	A A A	A A A	1.753 1.803 1.753 1.727	1.753 1.753 1.778 1.803	5.805 4.537 5.649 4.737	4.471 3.514 4.330 3.664	524. 524. 524. 524.	0.249 0.189 0.242 C.206
6-8C-2-1 6-8C-2-2 6-8C-2-3	294. 294. 294.	76.96 76.20 76.45	25.42 25.41 25.43	E E	A A A	A A A	1.803 1.753 1.778	1.702 1.803 1.803	6.761 6.850 6.339	3.456 3.538 3.261	524. 524. 524.	0.281 0.294 0.268
6-8C-2-4 6-8C-2-5 6-8C-2-6	561. 561. 561.	76.20 76.45 76.71	25.41 25.41 25.43	E	A A A	A A A	1.727 1.727 1.778	1.778 1.727 1.727	9.008 7.985 6.561	4.652 4.111 3.364	524. 524. 524.	0.392 0.347 0.277

TABLE C-2 CONTINUED

SPECIMEN NUMBER	TEMPERATURE (K)	LAP LENGTH (MM)	LAP WIDTH (MM)	CONFIG CODE*		THICKN	REND IESSES (M) 2	FAILURE LOAD (KN)	AVERAGE JOINT STRESS (MPA)	FTU (MPA)	JOINT EFFICIENCY
6-9A-2-1 6-9A-2-2 6-9A-2-3	294. 294. 294.	20.32 20.32 20.32	25.40 25.40 25.39	F F	B B B B	2.388	2.362 2.362 2.464	10.920 10.186 9.697	21.156 19.738 18.796	524. 524. 524.	0.347 0.321 0.302
6-9A-2-4 6-9A-2-5 6-9A-2-6	561. 561. 561.	20.32 20.32 20.32	25.43 25.44 25.39	F F	B B B B B	2.413 2.388 2.413	2.464 2.388 2.438	10.876 10.898 9.808	21.051 21.086 19.009	524. 524. 521.	0.338 0.342 0.305
6-9B-2-1 6-9B-2-2 6-9B-2-3	294. 294. 294.	33.02 33.02 33.02	25.43 25.45 25.43	F F	B B B B	2.464 2.388 2.388	2.489 2.388 2.413	11.632 11.543 10.676	13.854 13.734 12.714	524. 524. 524.	0.354 0.362 0.336
6-98-2-4 6-98-2-5 6-98-2-6	561. 561. 561.	33.02 33.02 33.02	25.43 25.38 25.42	F F F	B B B B	2.362 2.388 2.388	2.362 2.413 2.413	13.523 12.588 11.721	16.102 15.021 13.963	524. 524. 524.	0.430 0.396 0.369

#### \* CONFIGURATION CODE

A = SCALLOPED ADHERENDS-SINGLE LAP B = SCALLOPED ADHERENDS-DOUBLE LAP C = SOFTENING STRIP-SINGLE LAP

D = FABRIC INTERFACE-SINGLE LAP E = BASELINE SINGLE LAP F = BASELINE DOUBLE LAP

#### + LAYUP CODE

A = [0,+/-45,90]3S B = [0,+/-45,90]4S

TABLE C-2 CONTINUED
(B) US CUSTOMARY UNITS

				004510		VIIM		REND	r) unc	AVERAGE		(OLUT	
SPECIMEN NUMBER	TEMPERATURE (F)	LAP LENGTH (IN)	LAP WIDTH (IN)	CODEX			THICKN (I	N) 2	FAILURE LOAD (LBS)	JOINT STRESS (PSI)	FTU (KSI)	JOINT EFFICIENCY	
6-4A-2-1 6-4A-2-2 6-4A-2-3	70. 70. 70.	1.000 1.000 1.000	0.998 0.999 0.999	A A A	A A A	A A A	0.071 0.071 0.071	0.070 0.070 0.070	605. 560. 595.	606. 561. 595.	76. 76. 76.	0.112 0.104 0.110	
6-4A-2-4 6-4A-2-5 6-4A-2-6	550. 550. 550.	1.000 1.000 1.000	0.999 0.997 0.999	A A A	A A A	A A A	0.070 0.069 0.067	0.070 0.068 0.068	612. 671. 676.	613. 673. 676.	76. 76. 76.	0.115 0.128 0.133	
6-4B-2-1 6-4B-2-2 6-4B-2-3 6-4B-2-4	70. 70. 70. 70.	2.000 2.000 2.000 2.000	1.000 1.001 0.999 1.000	A A A	A A A	A A A	0.071 0.070 0.069 0.071	0.071 0.069 0.070 0.071	1220. 1170. 1250. 1145.	610. 585. 625. 572.	76. 76. 76. 76.	0.226 0.220 0.238 0.212	
6-4B-2-5 6-4B-2-6 6-4B-2-7 6-4B-2-8	550. 550. 550. 550.	2.000 2.000 2.000 2.000	0.999 1.001 1.000 0.999	A A A	A A A	A A A	0.068 0.069 0.068 0.068	0.069 0.069 0.070 0.070	1540. 1030. 1225. 1220.	771. 515. 613. 611.	76. 76. 76. 76.	0.298 0.196 0.237 0.236	
6-4C-2-1 6-4C-2-2 6-4C-2-3	70. 70. 70.	3.000 3.000 3.000	1.000 1.000 0.999		A A A	A A A	0.069 0.070 0.069	0.070 0.070 0.069	1445. 1380. 1355.	482. 460. 452.	76. 76. 76.	0.275 0.259 0.259	
6-4C-2-4 6-4C-2-5 6-4C-2-6	550. 550. 550.	3.000 3.000 3.000	1.000 1.000 1.001	A A A	A A A	A A A	0.071 0.070 0.070	0.071 0.069 0.070	1765. 1700. 2020.	588. 567. 673.	76. 76. 76.	0.327 0.320 0.379	
6-5A-2-1 6-5A-2-2 6-5A-2-3	70. 70. 70.	0.800 0.800 0.800	1.000 0.999 0.999	B B B	B B	B B B	0.094 0.096 0.094	0.093 0.095 0.096	2685. 2790. 2920.	3356. 3490. 3653.	76. 76. 76.	0.376 0.383 0.409	
6-5A-2-4 6-5A-2-5 6-5A-2-6	550. 550. 550.	0.800 0.800 0.800	1.001 1.000 0.999	B B	B B	8 8	0.095 0.093 0.094	0.092 0.093 0.094	2845. 2740. 2740.	3553. 3426. 3427.	76. 76. 76.	0.394 0.388 0.384	
6-5B-2-1 6-5B-2-2 6-5B-2-3	70. 70. 70.	1.300 1.300 1.300	1.000 1.001 0.999	B B	B B	B B B	0.095 0.093 0.094	0.096 0.095 0.093	2645. 2810. 3010.	2035. 2160. 2318.	76. 76. 76.	9.366 0.397 0.422	
6-5B-2-4 6-5B-2-5 6-5B-2-6	550. 550. 550.	1.300 1.300 1.300	1.000 1.000 0.999	8 8 8	B B B	<b>8</b> B	0.096 0.093 0.093	0.093 0.094 0.094	3700. 3185. 3090.	2847. 2449. 2379.	76. 76. 76.	0.507 0.450 0.438	

TABLE C-2 CONTINUED

(B) US CUSTOMARY UNITS

SPECIMEN NUMBER	TEMPERATURE (F)	LAP LENGTH (1H)	LAP WIDTH (IN)	CONFIG CODE#	CODE		ADHE THICKN (1	ESSES	FAILURE LOAD (LBS)	AVERAGE JOINT STRESS (PSI)	FTU (KSI)	JOINT EFFICIENCY	
6-5C-2-1 6-5C-2-2 6-5C-2-3	70. 70. 70.	1.800 1.800 1.800	1.001 1.002 0.999	B B B	В	B B B	0.096 0.093 0.097	0.097 0.095 0.095	3355. 2970. 2895.	1862. 1647. 1609.	76. 76. 76.	0.459 0.419 0.393	
6-5C-2-4 6-5C-2-5 6-5C-2-6	550. 550. 550.	1.800 1.800 1.800	1.000 0.999 0.999	B B B	В	B B B	0.093 0.094 0.097	0.094 0.096 0.095	3940. 4320. 4070.	2188. 2402. 2264.	76. 76. 76.	0.557 0.605 0.553	
6-6A-2-1 6-6A-2-2 6-6A-2-3	70. 70. 70.	1.050 1.030 1.020	1.000 1.001 0.999	C C	Ą	A A A	0.070 0.068 0.070	0.069 0.069 0.070	725. 900. 865.	690. 873. 849.	76. 76. 76.	0.136 0.174 0.163	
6-6A-2-4 6-6A-2-5 6-6A-2-6	550. 550. 550.	1.010 1.030 1.030	0.998 1.000 0.999	C C	A	A A A	0.070 0.070 0.070	0.070 0.070 0.069	695. 642. 624.	689. 623. 606.	76. 76. 76.	0.131 0.121 0.117	
6-6B-2-1 6-6B-2-2 6-6B-2-3 6-6B-2-4	70. 70. 70. 70.	2.020 2.020 2.020 2.000	1.002 0.999 0.999 1.001	CCCC	A	A A A	0.070 0.070 0.069 0.069	0.070 0.070 0.069 0.069	2245. 2165. 1885. 2000.	1109. 1073. 934. 999.	76. 76. 76. 76.	0.421 0.407 0.360 0.381	
6-6B-2-5 6-6B-2-6 6-6B-2-7 6-6B-2-8	550. 550. 550. 550.	2.010 2.000 2.000 2.010	1.000 1.000 1.000 1.001	CCCC	Ā	A A A	0.071 0.070 0.068 0.070	0.069 0.071 0.070 0.068	1635. 2035. 1650. 2020.	813. 1018. 825. 1004.	76. 76. 76. 76.	0.303 0.383 0.319 0.379	
6-6C-2-1 6-6C-2-2 6-6C-2-3	70. 70. 70.	3.010 3.010 3.000	1.001 1.001 1.000	CCC	Ā	A A A	0.069 0.070 0.069	0.069 0.070 0.070	2710. 2185. 2245.	899. 725. 748.	76. 76. 76.	0.516 0.410 0.428	
6-6C-2-4 6-6C-2-5 6-6C-2-6	550. 550. 550.	3.010 3.000 3.020	1.001 1.000 1.001	CCC	A	A A A	0.071 0.068 0.070	0.071 0.070 0.070	2505. 2395. 1895.	831. 798. 627.	76. 76. 76.	0.464 0.463 0.356	
6-7A-2-1 6-7A-2-2 6-7A-2-3	70. 70. 70.	1.020 1.000 1.001	1.000 1.000 0.999	D D D	A	A A A	0.070 0.070 0.069	0.069 0.070 0.069	1180. 1265. 1155.	1157. 1265. 1155.	76. 78. 76.	0.222 0.233 0.220	
6-7A-2-4 6-7A-2-5 6-7A-2-6	550. 550. 550.	1.000 1.020 1.000	0.999 0.999 0.999	D D D	A	A A A	0.070 0.071 0.069	0.070 0.068 0.070	1140. 1255. 1255.	1141. 1232. 1256.	76. 76. 76.	0.214 0.233 0.239	

TABLE C-2 CONTINUED

SPECIMEN NUMBER	TEMPERATURE (F)	LAP LENGTH (IN)	LAP WIDTH (IN)	CONFIG CODE*	CODE		THICKN	REND ESSES N) 2	FAILURE LOAD (LBS)	AVERAGE JOINT STRESS (PSI)	FTU (KSI)	JOINT EFFICIENCY
6-78-2-1 6-78-2-2 6-78-2-3 6-78-2-4	70. 70. 70. 70.	2.020 2.000 2.020 2.020	1.001 0.999 1.000 1.001	D D D	Ä A	A A A	0.071 0.072 0.069 0.071	0.069 0.070 0.070 0.070	2025. 2025. 2055. 2135.	1002. 1013. 1018. 1056.	76. 76. 76. 76.	0.375 0.370 0.392 0.395
6-7B-2-5 6-7B-2-6 6-7B-2-7 6-7B-2-8	550. 550. 550. 550.	2.010 2.020 2.020 2.020	1.000 0.999 0.999 1.000	D D D	Ā	A A A	0.070 0.069 0.070 0.071	0.071 0.071 0.072 0.069	2005. 2005. 1845. 1890.	998. 993. 914. 936.	76. 76. 76. 76.	0.377 0.383 0.347 0.350
6-7C-2-1 6-7C-2-2 6-7C-2-3	70. 70. 70.	3.000 3.030 3.020	1.002 1.000 1.001	D D D	A	A A A	0.070 0.070 0.070	0.070 0.070 0.070	2240. 2700. 2440.	745. 891. 807.	76. 76. 76.	0.420 0.508 0.458
6-7C-2-4 6-7C-2-5 6-7C-2-6	550. 550. 550.	3.020 3.030 3.010	1.001 0.999 0.999	D D	Ā	A A A	0.071 0.070 0.071	0.069 0.071 0.071	2505. 2535. 2380.	829. 838. 791.	76. 76. 76.	0.464 0.477 0.442
6-8A-2-1 6-8A-2-2 6-8A-2-3	70. 70. 70.	1.030 1.020 1.020	1.001 1.001 1.001	E	Ä	A A A	0.070 0.070 0.071	0.069 0.070 0.069	790. 695. 750.	766. 681. 734.	76. 76. 76.	0.148 0.130 0.139
6-8A-2-4 6-8A-2-5 6-8A-2-6	550. 550. 550.	1.020 1.000 1.000	1.001 1.001 1.000	E	Ä	A A	0.070 0.070 0.071	0.069 0.069 0.070	745. 695. 685.	730. 695. 685.	76. 76. 76.	0.140 0.131 0.127
6-8B-2-1 6-8B-2-2 6-8B-2-3 6-8B-2-4	70. 70. 70. 70.	2.010 2.020 2.000 2.010	1.002 1.001 1.000 1.000	EEE	A	A A A	0.069 0.069 0.069 0.070	0.070 0.069 0.070 0.070	1190. 1205. 1130. 1195.	591. 596. 565. 595.	76. 76. 76. 76.	0.227 0.230 0.215 0.225
6-8B-2-5 6-8B-2-6 6-8B-2-7 6-8B-2-8	550. 550. 550. 550.	2.010 2.000 2.020 2.000	1.001 1.001 1.001 1.002	E E E	A A	A A A	0.069 0.071 0.069 0.068	0.069 0.069 0.070 0.071	1305. 1020. 1270. 1065.	648. 510. 628. 531.	76. 76. 76. 76.	0.249 0.189 0.242 0.206
6-8C-2-1 6-8C-2-2 6-8C-2-3	70. 70. 70.	3.030 3.000 3.010	1.001 1.000 1.001	E	Ā	A A A	0.071 0.069 0.070	0.067 0.071 0.071	1520. 1540. 1425.	501. 513. 473.	76. 76. 76.	0.281 0.294 0.268
6-8C-2-4 6-8C-2-5 6-8C-2-6	550. 550. 550.	3.000 3.010 3.020	1.000 1.000 1.001	mmm	Ä	A A A	0.068 0.068 0.070	0.070 0.068 0.068	2025. 1795. 1475.	675. 596. 488.	76. 76. 76.	0.392 0.347 0.277

TAPLE C-2 CONCLUDED

SPECIMEN NUMBER	TEMPERATURE (F)	LAP LENGTH (IN)	LAP WIDTH (IN)	CONFIG CODE*	LAY! COD!		ADHE THICKN (1	ESSES	FAILURE LOAD (LBS)	AVERAGE JOINT STRESS (PSI)	FTU (KSI)	JOINT EFFICIENCY
6-9A-2-1 6-9A-2-2 6-9A-2-3	70. 70. 70.	0.800 0.800 0.800	1.000 1.000 1.000	F	B B B	B B B	0.093 0.094 0.095	0.093 0.093 0.097	2455. 2290. 2180.	3068. 2863. 2726.	76. 76. 76.	0.347 0.321 0.302
6-9A-2-4 6-9A-2-5 6-9A-2-6	550. 550. 550.	0.800 0.800 0.800	1.001 1.001 1.000	F F F	B B	B B	0.095 0.094 0.095	0.097 0.094 0.096	2445. 2450. 2205.	3053. 3058. 2757.	76. 76. 76.	0.338 0.342 0.305
6-98-2-1 6-98-2-2 6-98-2-3	70. 70. 70.	1.300 1.300 1.300	1.001 1.002 1.001	F F	B B B	8 8 8	0.097 0.094 0.094	0.098 0.094 0.095	2615. 2595. 2400.	2009. 1992. 1844.	76. 76. 75.	0.354 0.362 0.336
6-98-2-4 6-98-2-5 6-98-2-6	550. 550. 550.	1.300 1.300 1.300	1.001 0.999 1.001	F F	8 B B	B B B	0.093 0.094 0.094	0.093 0.095 0.095	3040. 2830. 2635.	2335. 2179. 2025.	76. 76. 76.	0.430 0.396 0.369

#### \* CONFIGURATION CODE

A = SCALLOPED ADHERENDS-SINGLE LAP B = SCALLOPED ADHERENDS-DOUBLE LAP

C = SOFTENING STRIP-SINGLE LAP
D = FABRIC INTERFACE-SINGLE LAP
E = BASELINE SINGLE LAP
F = BASELINE DOUBLE LAP

#### + LAYUP CODE

A = [0,+/-45,90]3S B = [0,+/-45,90]4S

#### **REFERENCES**

- Sheppard, C.H.; Hoggatt, J.T.; and Symonds, W.A.: Quality Control Developments for Graphite/PMR-15 Polyimide Composite Materials. (D180-20545-2A Boeing Aerospace Co.; NASA Contract NAS1-15009). NASA CR-159182, 1979.
- 2. St. Clair, T.L.; and Progar, B.J.: LARC-13 Polyimide Adhesive Bonding. SAMPE Series Volume 24 The Enigma of the Eighties: Environment, Economics, Energy. San Francisco. May 1979, pp. 1081-1092.
- 3. Flaggs, D.L. and Vinson, J.R.: Shear Properties of Promising Adhesive for Bonded Joints in Composite Materials Structures. AIAA Journal of Aircraft, Volume 16, No. 1, January 1979, pp. 51-54.
- 4. Cushman, J.B., and McCleskey, S.F.: Design Allowables Test Program, Celion 3000/PMR-15 and Celion 6000/PMR-15 Graphite/Polyimide Composites. (Boeing Aerospace Co.; NASA Contract NAS1-15644.) NASA CR-165840, 1982.
- 5. Sawyer, James Wayne; and Cooper, Paul A.: Analysis and Test of Bonded Single Lap Joints with Preformed Adherends. AIAA/ASME/ASCE/AHS 21st Structures, Structural Dynamics and Materials Conference. May 1980, pp. 664-673.
- Hart-Smith, L.J.: Adhesive-Bonded Single-Lap Joints. (McDonnell Douglas Corp.; NASA Contract NAS1-11234.) NASA CR-112236, January 1973.
- 7. Goland, M.; and Reissner, E.: The Stresses in Cemented Joints. Journal of Applied Mechanics, March 1944, pp. A17-A27.
- 8. Cooper, Paul A.; and Sawyer, James Wayne: A Critical Examination of Stresses in an Elastic Single Lap Joint. NASA TP 1507, 1979.
- 9. Hart-Smith, L.J.: Adhesive-Bonded Double-Lap Joints. (McDonnell Douglas Corp.; NASA Contract NAS1-11234.) NASA CR-112235, January 1973.

10. Potter, D.L.: Design Handbook for Adhesive Bonding (PABST-Primary Adhesively Bonded Structure Technology - Program). (MDC J6076, McDonnell Douglas Aircraft Co.; AF Contract F33615-75-C-3016.)
AFFDL-TR 79-3129, November 1979.

)

- 11. Air Force Advanced Composites Design Guide. Volume 2, 3rd Edition, 3rd Rev., Section 2.4.9, p. 3, January 1977.
- 12. Hart-Smith, L.J.: Adhesive-Bonded Scarf and Stepped-Lap Joints.

  (McDonnell Douglas Corp.; NASA Contract NAS1-11234.) NASA CR-112237,

  January 1973.

		•
1. Report No.	2. Government Accession No.	3. Recipient's Catalog No.
NASA_CR-165956		
4. Title and Subtitle	on 2000/DMD 15 Graphite/	5. Report Date July 1982
Test and Analysis of Celic Polyimide Bonded Composite	e Joints - Data Report	6. Performing Organization Code
7. Author(s) J. B. Cushman, S. F. McCle	eskey, S. H. Ward	8. Performing Organization Report No.
9. Performing Organization Name and Address BOEING AEROSPACE COMPANY.		10. Work Unit No.
Engineering Technology		11. Contract or Grant No.
Post Office Box 3999		NAS1-15644
Seattle, Washington 9812	4	13. Type of Report and Period Covered
2. Sponsoring Agency Name and Address		
	C Administration	Contractor Report
National Aeronautics and S Washington, D. C., 20546		14. Sponsoring Agency Code
15. Supplementary Notes		
Technical Representative:	Dr. Paul A. Cooper, NASA/Lal	RC, Hampton, VA,
Program Manager:	Jack E. Harrison, Boeing Ae	rospace Co. Seattle, WA.
6. Abstract		
metric step-lap bonded jo Composite-to-composite and (-250°F), 294K (70°F) and adherend thickness, adherend tapering. Tests establish the change in pand hybrid systems. Spec of the high temperature abonded joint tests result There were very few adhes performance trends for the	ted to evaluate standard sing ints of Celion 3000/PMR-15 grad composite-to-titanium joint 561K (550°F). Joint paramete end axial stiffness, lamina so of advanced joint concepts we erformance of preformed adherial tests were conducted to end the sive, designated A7F, used ed in interlaminar shear or prive failures. Average test relations are also provided to evarious test parameters. Reysis correlations are also provided to the side of	aphite/polyimide composite.  s were tested at 116K  ers evaluated were lap lenge tacking sequence and ere also conducted to ends, scalloped adherends stablish material properties for bonding. Most of the eel failures of the composite esults agree with expected esults of finite element

17. Key Words (Suggested by Author(s)		18. Distrib	ution Statement		
Composite, Composite Joints, Graphite/Poly	Joints, Bonded			,*	
3000/PMR-15	initially oction	Unc	lassified - Un	limited	
•			Subjec	t Category	y 39
19. Security Classif. (of this report) Unclassified	20. Security Classif. (of this Unclassified.	page)	21. No. of Pages 355	22. Price A16	

